

May 2018

# Meshless Methods for Numerically Solving Boundary Value Problems of Elliptic Type Partial Differential Equations

Minhwa Choi  
choiminhwa131@gmail.com

Follow this and additional works at: <https://digitalscholarship.unlv.edu/thesesdissertations>

 Part of the [Mathematics Commons](#)

---

## Repository Citation

Choi, Minhwa, "Meshless Methods for Numerically Solving Boundary Value Problems of Elliptic Type Partial Differential Equations" (2018). *UNLV Theses, Dissertations, Professional Papers, and Capstones*. 3232.

<https://digitalscholarship.unlv.edu/thesesdissertations/3232>

This Dissertation is protected by copyright and/or related rights. It has been brought to you by Digital Scholarship@UNLV with permission from the rights-holder(s). You are free to use this Dissertation in any way that is permitted by the copyright and related rights legislation that applies to your use. For other uses you need to obtain permission from the rights-holder(s) directly, unless additional rights are indicated by a Creative Commons license in the record and/or on the work itself.

This Dissertation has been accepted for inclusion in UNLV Theses, Dissertations, Professional Papers, and Capstones by an authorized administrator of Digital Scholarship@UNLV. For more information, please contact [digitalscholarship@unlv.edu](mailto:digitalscholarship@unlv.edu).

MESHLESS METHODS FOR NUMERICALLY SOLVING BOUNDARY VALUE  
PROBLEMS OF ELLIPTIC TYPE PARTIAL DIFFERENTIAL EQUATIONS

by

Minhwa Choi

Bachelor of Engineering - Mechanical Engineering  
Myongji University, Republic of Korea  
1997

Master of Arts - Mathematics  
University of Missouri - St. Louis, U.S.A.  
2003

A dissertation submitted in partial fulfillment of  
the requirements for the

Doctor of Philosophy - Mathematical Sciences

Department of Mathematical Sciences  
College of Sciences  
The Graduate College

University of Nevada, Las Vegas  
May 2018

Copyright © 2018 by Minhwa Choi  
All Rights Reserved

**Dissertation Approval**

The Graduate College  
The University of Nevada, Las Vegas

March 14, 2018

This dissertation prepared by

Minhwa Choi

entitled

**MESHLESS METHODS FOR NUMERICALLY SOLVING BOUNDARY VALUE  
PROBLEMS OF ELLIPTIC TYPE PARTIAL DIFFERENTIAL EQUATIONS**

is approved in partial fulfillment of the requirements for the degree of

Doctor of Philosophy - Mathematical Sciences  
Department of Mathematical Sciences

Xin Li, Ph.D.  
*Examination Committee Chair*

Kathryn Hausbeck Korgan, Ph.D.  
*Graduate College Interim Dean*

Rohan Dalpatadu, Ph.D.  
*Examination Committee Member*

Douglas Burke, Ph.D.  
*Examination Committee Member*

Woosoon Yim, Ph.D.  
*Graduate College Faculty Representative*

# ABSTRACT

## MESHLESS METHODS FOR NUMERICALLY SOLVING BOUNDARY VALUE PROBLEMS OF ELLIPTIC TYPE PARTIAL DIFFERENTIAL EQUATIONS

by

Minhwa Choi

Dr. Xin Li, Examination Committee Chair  
Associate Professor of Mathematics  
University of Nevada, Las Vegas, USA

In this dissertation we propose and examine numerical methods for solving the boundary value problems of partial differential equations (PDEs) by meshless methods. Typically, such a problem is described as

$$\mathcal{L}u(\mathbf{x}) = f(\mathbf{x}), \quad \mathbf{x} \in \Omega, \quad (0.1)$$

$$\mathcal{B}u(\mathbf{x}) = g(\mathbf{x}), \quad \mathbf{x} \in \partial\Omega, \quad (0.2)$$

where  $\Omega$  is a domain in  $\mathbb{R}^s$ ,  $s \geq 2$ ,  $\mathcal{L}$  a linear partial differential operator, and  $\mathcal{B}$  a linear operator for the boundary conditions.

First we aim at getting approximate particular solutions  $u_p$  of a nonhomogeneous equation (0.1) by radial basis methods. For instance, the collocation method by radial basis functions for finding particular solutions  $u_p$  of (0.1) is very popular in the literature. Now the particular solutions of certain important PDEs by RBF approximation are available, with the order of convergence to the exact solutions provided. Here we explore and examine the numerical performances of these particular solutions in various examples.

Once  $u_p$  is available, we then consider and solve the following boundary value problems

of the homogeneous equation

$$\mathcal{L}v(\mathbf{x}) = 0, \quad \mathbf{x} \in \Omega, \quad (0.3)$$

$$\mathcal{B}v(\mathbf{x}) = g(\mathbf{x}) - \mathcal{B}u_p(\mathbf{x}), \quad \mathbf{x} \in \partial\Omega, \quad (0.4)$$

by the methods of fundamental solutions (MFS). To be precise, let  $\Gamma$  be the fundamental solution of the differential operator  $\mathcal{L}$ . Choose a fictitious domain in  $\partial\tilde{\Omega}$  such that  $\partial\Omega \subset \partial\tilde{\Omega}$ , and choose some collocation points  $\mathbf{x}_1, \mathbf{x}_2, \dots, \mathbf{x}_M$  on  $\partial\Omega$  and some source points  $\tilde{\mathbf{x}}_1, \tilde{\mathbf{x}}_2, \dots, \tilde{\mathbf{x}}_M$ , on  $\partial\tilde{\Omega}$ . Then an approximate solution of (0.3) and (0.4) by MFS is given by

$$v_M(\mathbf{x}) = \sum_{k=1}^M c_k \Gamma(\mathbf{x}, \mathbf{x}_k), \quad (0.5)$$

where the coefficients  $\{c_k\}$  can be determined by the boundary condition (0.4) and the collocation points  $\mathbf{x}_1, \mathbf{x}_2, \dots, \mathbf{x}_M$  on  $\partial\Omega$ . Hence

$$u(\mathbf{x}) = u_p(\mathbf{x}) + v_M(\mathbf{x})$$

is considered as the numerical solution of our original problem (0.1) and (0.2).

In this dissertation, we present various examples to show the efficiencies of the above mentioned methods, especially for Poisson's, Helmholtz, and biharmonic equations of Dirichlet, or Neumann, or Robin (Mixed) boundary conditions, with numerical results provided correspondingly in tables and graphs.

# ACKNOWLEDGEMENTS

I would like to express my deepest gratitude to my advisor, Dr. Xin Li for his guidance, continuous support, helpful conversations, advice throughout the research of my Ph.D., sharing knowledge and expertise. I would never have been able to finish my dissertation without his help. I am also very grateful to my committee members Dr. Rohan Dalpatadu, Dr. Douglas Burke, and Dr. Woosoon Yim for their time, expertise and support.

My special thanks are due to my parents, my dear wife, Eun Soon Oh, and my children, Daniel and David, for their continuous love, tolerance, support, and praying during this long journey. I dedicate this dissertation to them.

# TABLE OF CONTENTS

<b>ABSTRACT</b>	<b>iii</b>
<b>ACKNOWLEDGEMENTS</b>	<b>v</b>
<b>LIST OF TABLES</b>	<b>viii</b>
<b>LIST OF FIGURES</b>	<b>xi</b>
<b>1 Method of Fundamental Solutions (MFS) for the Laplace Equations with Boundary Value Problems</b>	<b>1</b>
1.1 Description of MFS for Laplace equations . . . . .	1
1.2 Numerical Examples by using MFS . . . . .	3
1.3 MFS for Other Boundary Conditions . . . . .	10
1.4 Convergence of the method of fundamental solutions (MFS) . . . . .	16
<b>2 Dual Reciprocity Methods (DRM) for the Poisson's Equations</b>	<b>18</b>
2.1 Method of Particular Solutions (MPS) and DRM . . . . .	18
2.2 Numerical Examples by DRM . . . . .	21
2.3 On Convergence of DRM in $\mathbb{R}^2$ . . . . .	29
2.4 Numerical Examples . . . . .	39
<b>3 Dual Reciprocity Methods for the Boundary Value Problems of Helmholtz Equations</b>	<b>59</b>
3.1 Description of MFS for Helmholtz equations . . . . .	59
3.1.1 Truncated Singular Value Decomposition (TSVD) . . . . .	61
3.1.2 Tikhonov Regularization Method . . . . .	63
3.2 Numerical Examples by using MFS for Helmholtz equations . . . . .	64
3.3 DRM for boundary value problems of Helmholtz Equations . . . . .	92
3.4 Numerical Examples . . . . .	94
<b>4 Boundary Value Problems of Biharmonic Equations</b>	<b>112</b>
4.1 MFS for Biharmonic equation . . . . .	112
4.2 Numerical Examples by using MFS . . . . .	115
4.3 Method of Particular Solutions (MPS) and DRM . . . . .	127
4.4 Numerical Examples by MFS and Collocation Methods . . . . .	130
4.5 Numerical Examples by Approximate Particular Solutions . . . . .	142



<b>BIBLIOGRAPHY</b>	<b>160</b>
<b>CURRICULUM VITAE</b>	<b>163</b>

## LIST OF TABLES

1.1	Maximum Error $\ u_{exact} - u_N\ _{C(\partial\Omega)}$ . . . . .	4
1.2	Maximum Error $\ u_{exact} - u_N\ _{C(\partial\Omega)}$ . . . . .	5
1.3	Maximum Error $\ u_{exact} - u_N\ _{C(\partial\Omega)}$ . . . . .	6
1.4	Maximum Error $\ u_{exact} - u_N\ _{C(\partial\Omega)}$ . . . . .	8
1.5	Maximum Error $\ u_{exact} - u_N\ _{C(\partial\Omega)}$ . . . . .	9
1.6	Maximum Error $\ u_{exact} - u_N\ _{C(\partial\Omega)}$ . . . . .	12
1.7	Maximum Error $\ u_{exact} - u_N\ _{C(\partial\Omega)}$ . . . . .	15
2.1	Maximum Error $\ u_{exact} - u_A\ _{C(\bar{\Omega})}$ . . . . .	23
2.2	Maximum Error $\ u_{exact} - u_A\ _{C(\bar{\Omega})}$ . . . . .	24
2.3	Maximum Error $\ u_{exact} - u_A\ _{C(\bar{\Omega})}$ . . . . .	27
2.4	Maximum Error $\ u_{exact} - u_A\ _{C(\bar{\Omega})}$ with (a) the Gaussian RBFs $\phi(r^2) = \frac{c}{\pi} e^{-cr^2}$	41
2.5	Maximum Error $\ u_{exact} - u_A\ _{C(\bar{\Omega})}$ with (b) the compactly supported RBFs $\phi(r^2) = (c+1)(1-r^2)^c/\pi, 0 \leq r \leq 1$ , for $c = 3, 4, 5$ . . . . .	42
2.6	Maximum Error $\ u_{exact} - u_A\ _{C(\bar{\Omega})}$ with (c) the inverse multiquadratics RBFs $\phi(r^2) = \frac{c-1}{\pi(r^2+1)^c}$ , for $c = 3, 4, 5$ . . . . .	43
2.7	Maximum Error $\ u_{exact} - u_A\ _{C(\bar{\Omega})}$ with (a) the Gaussian RBFs $\phi(r^2) = \frac{c}{\pi} e^{-cr^2}$	46
2.8	Maximum Error $\ u_{exact} - u_A\ _{C(\bar{\Omega})}$ with (b) the compactly supported RBFs $\phi(r^2) = (c+1)(1-r^2)^c/\pi, 0 \leq r \leq 1$ , for $c = 3, 4, 5$ . . . . .	47
2.9	Maximum Error $\ u_{exact} - u_A\ _{C(\bar{\Omega})}$ with (c) the inverse multiquadratics RBFs $\phi(r^2) = \frac{c-1}{\pi(r^2+1)^c}$ , for $c = 3, 4, 5$ . . . . .	48
2.10	Maximum Error $\ u_{exact} - u_A\ _{C(\bar{\Omega})}$ with (a) the Gaussian RBFs $\phi(r^2) = \frac{c}{\pi} e^{-cr^2}$	51
2.11	Maximum Error $\ u_{exact} - u_A\ _{C(\bar{\Omega})}$ with (b) the compactly supported RBFs $\phi(r^2) = (c+1)(1-r^2)^c/\pi, 0 \leq r \leq 1$ , for $c = 3, 4, 5$ . . . . .	52
2.12	Maximum Error $\ u_{exact} - u_A\ _{C(\bar{\Omega})}$ with (c) the inverse multiquadratics RBFs $\phi(r^2) = \frac{c-1}{\pi(r^2+1)^c}$ , for $c = 3, 4, 5$ . . . . .	53
2.13	Maximum Error $\ u_{exact} - u_A\ _{C(\bar{\Omega})}$ with (a) the Gaussian RBFs $\phi(r^2) = \frac{c}{\pi} e^{-cr^2}$	56
2.14	Maximum Error $\ u_{exact} - u_A\ _{C(\bar{\Omega})}$ with (b) the compactly supported RBFs $\phi(r^2) = ((2c+3)!!)(1-r^2)^c/(4\pi(2c)!!), 0 \leq r \leq 1$ , for $c = 3, 4, 5$ . . . . .	57
2.15	Maximum Error $\ u_{exact} - u_A\ _{C(\bar{\Omega})}$ with (c) the inverse multiquadratics RBFs $\phi(r^2) = \frac{1}{2\pi^2} \frac{(2c-2)!!}{(2c-5)!!} \frac{1}{(r^2+1)^c}$ , for $c = 3, 4, 5$ . . . . .	58
3.1	Maximum Error $\ u_{exact} - u_N\ _{C(\partial\Omega)}$ . . . . .	66
3.2	Maximum Error for $u(0.25, 0.25)$ . . . . .	70
3.3	Maximum Error for $u(-0.1, 0.3)$ . . . . .	72

3.4	Maximum Error for $u(-0.3, 0.4)$ . . . . .	74
3.5	Maximum Error for $u(0.5, 0.5, 0.5)$ . . . . .	77
3.6	Maximum Error for $u(0.1, 0.5, 0.8)$ . . . . .	78
3.7	Maximum Error for $u(0.3, 0.9, 0.4)$ . . . . .	78
3.8	Maximum Error for $u(0, -0.5)$ . . . . .	82
3.9	Maximum Error for $u(-0.5, 0.5)$ . . . . .	84
3.10	Maximum Error for $u(0.5, 0.5)$ . . . . .	86
3.11	Maximum Error $\ u_{exact} - u_N\ _{C(\partial\Omega)}$ . . . . .	90
3.12	Maximum Error $\ u_{exact} - u_A\ _{C(\bar{\Omega})}$ with (a) the Gaussian RBFs $\phi(r^2) = \frac{c}{\pi} e^{-cr^2}$ for $c = 1, 3$ . . . . .	96
3.13	Maximum Error $\ u_{exact} - u_A\ _{C(\bar{\Omega})}$ with (b) the compactly supported RBFs $\phi(r^2) = (c + 1)(1 - r^2)^c/\pi$ , $0 \leq r \leq 1$ or $0, r > 1$ for $c = 3, 5$ . . . . .	97
3.14	Maximum Error $\ u_{exact} - u_A\ _{C(\bar{\Omega})}$ with (c) the inverse multiquadratics RBFs $\phi(r^2) = \frac{c-1}{\pi(r^2+1)^c}$ , for $c = 3, 5$ . . . . .	98
3.15	Maximum Error $\ u_{exact} - u_A\ _{C(\bar{\Omega})}$ with (a) the Gaussian RBFs $\phi(r^2) = \frac{c}{\pi} e^{-cr^2}$ for $c = 1, 3$ . . . . .	101
3.16	Maximum Error $\ u_{exact} - u_A\ _{C(\bar{\Omega})}$ with (b) the compactly supported RBFs $\phi(r^2) = (c + 1)(1 - r^2)^c/\pi$ , $0 \leq r \leq 1$ or $0, r > 1$ for $c = 3, 5$ . . . . .	103
3.17	Maximum Error $\ u_{exact} - u_A\ _{C(\bar{\Omega})}$ with (c) the inverse multiquadratics RBFs $\phi(r^2) = \frac{c-1}{\pi(r^2+1)^c}$ , for $c = 3, 5$ . . . . .	105
3.18	Maximum Error $\ u_{exact} - u_A\ _{C(\bar{\Omega})}$ with (a) the Gaussian RBFs $\phi(r^2) = \frac{c}{\pi} e^{-cr^2}$ for $c = 1, 3$ . . . . .	109
3.19	Maximum Error $\ u_{exact} - u_A\ _{C(\bar{\Omega})}$ with (b) the compactly supported RBFs $\phi(r^2) = ((2c + 3)!!)(1 - r^2)^c/(4\pi(2c)!!)$ , $0 \leq r \leq 1$ , or $0, r > 1$ for $c = 3, 5$ . . . . .	110
3.20	Maximum Error $\ u_{exact} - u_A\ _{C(\bar{\Omega})}$ with (c) the inverse multiquadratics RBFs $\phi(r^2) = \frac{1}{2\pi^2} \frac{(2c-2)!!}{(2c-5)!!} \frac{1}{(r^2+1)^c}$ , for $c = 3, 5$ , . . . . .	111
4.1	Maximum Error $\ u_{exact} - u_N\ _{C(\bar{\Omega})}$ . . . . .	117
4.2	Maximum Error $\ u_{exact} - u_N\ _{C(\bar{\Omega})}$ . . . . .	121
4.3	Maximum Error $\ u_{exact} - u_N\ _{C(\bar{\Omega})}$ . . . . .	125
4.4	Maximum Error $\ u_{exact} - u_A\ _{C(\bar{\Omega})}$ with the Gaussian RBF $\phi(r) = e^{-2r^2}$ . . . . .	132
4.5	Maximum Error $\ u_{exact} - u_N\ _{C(\bar{\Omega})}$ with the Gaussian RBF $\phi(r) = e^{-3r^2}$ . . . . .	136
4.6	Maximum Error $\ u_{exact} - u_N\ _{C(\bar{\Omega})}$ with the Gaussian RBF $\phi(r) = e^{-3r^2}$ . . . . .	140
4.7	Maximum Error $\ u_{exact} - u_A\ _{C(\bar{\Omega})}$ with (a) the Gaussian RBFs $\phi(r^2) = \frac{c}{\pi} e^{-cr^2}$ . . . . .	144
4.8	Maximum Error $\ u_{exact} - u_A\ _{C(\bar{\Omega})}$ with (b) the compactly supported RBFs $\phi(r^2) = (c + 1)(1 - r^2)^c/\pi$ , $0 \leq r \leq 1$ , for $c = 3, 4, 5$ . . . . .	146
4.9	Maximum Error $\ u_{exact} - u_A\ _{C(\bar{\Omega})}$ with (c) the inverse multiquadratics RBFs $\phi(r^2) = \frac{c-1}{\pi(r^2+1)^c}$ , for $c = 3, 4, 5$ . . . . .	148
4.10	Maximum Error $\ u_{exact} - u_A\ _{C(\bar{\Omega})}$ with (a) the Gaussian RBFs $\phi(r^2) = \frac{c}{\pi} e^{-cr^2}$ . . . . .	152
4.11	Maximum Error $\ u_{exact} - u_A\ _{C(\bar{\Omega})}$ with (b) the compactly supported RBFs $\phi(r^2) = (c + 1)(1 - r^2)^c/\pi$ , $0 \leq r \leq 1$ , for $c = 3, 4, 5$ . . . . .	153

4.12	Maximum Error $\ u_{exact} - u_A\ _{C(\bar{\Omega})}$ with (c) the inverse multiquadratics RBFs $\phi(r^2) = \frac{c-1}{\pi(r^2+1)^c}$ , for $c = 3, 4, 5$ . . . . .	154
4.13	Maximum Error $\ u_{exact} - u_A\ _{C(\bar{\Omega})}$ with (a) the Gaussian RBFs $\phi(r^2) = \frac{c}{\pi} e^{-cr^2}$ for $c=1, 3, 5$ . . . . .	157
4.14	Maximum Error $\ u_{exact} - u_A\ _{C(\bar{\Omega})}$ with (b) the compactly supported RBFs $\phi(r^2) = ((2c+3)!!)(1-r^2)^c/(4\pi(2c)!!)$ , $0 \leq r \leq 1$ , or $0, r > 1$ for $c = 3, 4, 5$ . . . . .	158
4.15	Maximum Error $\ u_{exact} - u_A\ _{C(\bar{\Omega})}$ with (c) the inverse multiquadratics RBFs $\phi(r^2) = \frac{1}{2\pi^2} \frac{(2c-2)!!}{(2c-5)!!} \frac{1}{(r^2+1)^c}$ , for $c = 3, 4, 5$ . . . . .	159

## LIST OF FIGURES

1.1	N collocation points on $\partial\Omega$ and N source points on $\partial\tilde{\Omega}$ . . . . .	2
1.2	Graph of $\partial\Omega$ , $\partial\tilde{\Omega}$ with $r = 1.5$ and $N = 20$ collocation points . . . . .	4
1.3	Graph of $\partial\Omega$ , $\partial\tilde{\Omega}$ with $a = 3$ , $b = 1.5$ and $N = 20$ collocation points . . . . .	5
1.4	Choose $M=20$ collocation points on the $\partial\Omega$ , and $N=20$ source points on the $\partial\tilde{\Omega}$ . . . . .	6
1.5	Choose $N=20$ collocation points on the $\partial\Omega$ , and $N=20$ source points on the $\partial\tilde{\Omega}$ . . . . .	7
1.6	Choose $N = 20$ collocation points on $\partial\Omega$ , and $N = 20$ source points on $\partial\tilde{\Omega}$ , and $r = 3.0$ . . . . .	9
1.7	Choose $M = 20$ collocation points on $\partial\Omega$ , and $N = 20$ source points on $\partial\tilde{\Omega}$ . . . . .	11
1.8	Choose $M = 20$ collocation points on $\partial\Omega = \partial\Omega_1 \cup \partial\Omega_2$ , and $N = 20$ source points on $\partial\tilde{\Omega} = \{(x, y) : x = 3 \sin(t + \sin t), y = 3 \cos(t + \cos t), 0 \leq t \leq 2\pi\}$ . . . . .	15
2.1	M points in $\Omega$ . . . . .	19
2.2	$M = 10$ , 110 points in $\bar{\Omega} = \Omega \cup \partial\Omega$ and $N = 10$ points on $\partial\tilde{\Omega}$ with $r = 1.5$ . . . . .	22
2.3	$M = 10$ , 110 points in $\bar{\Omega} = \Omega \cup \partial\Omega$ and $N = 10$ points on $\partial\tilde{\Omega}$ with $r = 2$ . . . . .	24
2.4	$M = 10$ , 1,010 points in $\bar{\Omega} = \Omega \cup \partial\Omega$ and $N = 10$ points on $\partial\tilde{\Omega}$ with $R = 2$ . . . . .	26
2.5	Maximum errors with $c = 0.5$ ( $\square$ ), $c = 1.0$ ( $\circ$ ), $c = 2.0$ ( $\triangle$ ), respectively . . . . .	28
2.6	$n = 10$ , 100 points ( $\bullet$ ) in $\Omega$ , 40 points ( $\bullet$ ) on $\partial\Omega$ and (+) on $\partial\Omega_\delta$ , respectively, and $N = 20$ points (*) on $\partial\tilde{\Omega}$ with $r = 2$ . . . . .	40
2.7	Maximum errors with $c = 1$ ( $\square$ ), $c = 3$ ( $\circ$ ), $c = 5$ ( $\triangle$ ), respectively . . . . .	41
2.8	Maximum errors with $c = 3$ ( $\square$ ), $c = 4$ ( $\circ$ ), $c = 5$ ( $\triangle$ ), respectively . . . . .	42
2.9	Maximum errors with $c = 3$ ( $\square$ ), $c = 4$ ( $\circ$ ), $c = 5$ ( $\triangle$ ), respectively . . . . .	43
2.10	$n = 20$ , 300 points ( $\bullet$ ) in $\Omega$ , 60 points ( $\bullet$ ) on $\partial\Omega$ and 35 points (+) on $\partial\Omega_\delta$ , respectively, and $N = 20$ points (*) on $\partial\tilde{\Omega}$ with $R = 2.5$ . . . . .	45
2.11	Maximum errors with $c = 1$ ( $\square$ ), $c = 3$ ( $\circ$ ), $c = 5$ ( $\triangle$ ), respectively . . . . .	46
2.12	Maximum errors with $c = 3$ ( $\square$ ), $c = 4$ ( $\circ$ ), $c = 5$ ( $\triangle$ ), respectively . . . . .	47
2.13	Maximum errors with $c = 3$ ( $\square$ ), $c = 4$ ( $\circ$ ), $c = 5$ ( $\triangle$ ), respectively . . . . .	48
2.14	$n = 20$ , 300 points ( $\bullet$ ) in $\Omega$ , 80 points ( $\bullet$ ) on $\partial\Omega$ and 40 points (+) on $\partial\Omega_\delta$ , respectively, and $N = 20$ points (*) on $\partial\tilde{\Omega}$ with $R = 2.5$ . . . . .	50
2.15	Maximum errors with $c = 1$ ( $\square$ ), $c = 3$ ( $\circ$ ), $c = 5$ ( $\triangle$ ), respectively . . . . .	51
2.16	Maximum errors with $c = 3$ ( $\square$ ), $c = 4$ ( $\circ$ ), $c = 5$ ( $\triangle$ ), respectively . . . . .	52
2.17	Maximum errors with $c = 3$ ( $\square$ ), $c = 4$ ( $\circ$ ), $c = 5$ ( $\triangle$ ), respectively . . . . .	53
2.18	$n = 10$ , 1000 points ( $\bullet$ ) in $\Omega$ , 240 points ( $\bullet$ ) on $\partial\Omega$ , and $N = 20$ points (*) on $\partial\tilde{\Omega}$ with $R = 2$ . . . . .	55
2.19	Maximum errors with $c = 1$ ( $\square$ ), $c = 3$ ( $\circ$ ), $c = 5$ ( $\triangle$ ), respectively . . . . .	56
2.20	Maximum errors with $c = 3$ ( $\square$ ), $c = 4$ ( $\circ$ ), $c = 5$ ( $\triangle$ ), respectively . . . . .	57
2.21	Maximum errors with $c = 3$ ( $\square$ ), $c = 4$ ( $\circ$ ), $c = 5$ ( $\triangle$ ), respectively . . . . .	58

3.1	Choose $M = 20$ collocation points (*) on the $\partial\Omega$ , and $N = 20$ source points (o) on the $\partial\tilde{\Omega}$ with $r = 1.5$ . . . . .	65
3.2	Maximum errors on fictitious domains $\partial\tilde{\Omega} = \{(x, y) : x^2 + y^2 = r^2, r = 1.2, 1.4, 1.6, 1.8\}$ with regularization parameters, $\mu = 10^{-3}$ ( $\square$ ), $\mu = 10^{-5}$ (o), $\mu = 10^{-7}$ ( $\triangle$ ), $\mu = 10^{-8}$ ( $\diamond$ ), respectively . . . . .	67
3.3	Choose $N=20$ collocation points (*) on the $\partial\Omega$ , and $N=20$ source points (o) on the $\partial\tilde{\Omega}$ , and three tested points (0.25, 0.25), (-0.1, 0.3), and (-0.3, 0.5) . . . . .	69
3.4	Maximum errors at a tested point (0.25, 0.25) inside $\Omega$ with singular value tolerances, $\epsilon = 10^{-1}$ ( $\square$ ), $\epsilon = 10^{-3}$ (o), $\epsilon = 10^{-7}$ ( $\triangle$ ), respectively . . . . .	71
3.5	Maximum errors at a tested point (-0.1, 0.3) inside $\Omega$ with singular value tolerances, $\epsilon = 10^{-1}$ ( $\square$ ), $\epsilon = 10^{-3}$ (o), $\epsilon = 10^{-7}$ ( $\triangle$ ), respectively . . . . .	73
3.6	Maximum errors at a tested point (-0.3, 0.4) inside $\Omega$ with singular value tolerances, $\epsilon = 10^{-1}$ ( $\square$ ), $\epsilon = 10^{-3}$ (o), $\epsilon = 10^{-7}$ ( $\triangle$ ), respectively . . . . .	75
3.7	Choose $N = 300$ collocation points on the $\partial\Omega$ , and $N = 300$ source points on the $\partial\tilde{\Omega}$ , and $r = 2.0$ . . . . .	77
3.8	Choose $M=20$ collocation points (*) on the $\partial\Omega$ , and $N=20$ source points (o) on the $\partial\tilde{\Omega}$ . . . . .	81
3.9	Maximum errors on fictitious domains, $\partial\tilde{\Omega} = \{(x, y) : x = a \cos t, y = b \sin(t + \cos t), 0 \leq t \leq 2\pi\}$ , where $a = 2, 3, 3, 4$ and $b = 2, 4, 3, 3$ with regularization parameters, $\mu = 10^{-1}$ ( $\square$ ), $\mu = 10^{-3}$ (o), $\mu = 10^{-5}$ ( $\triangle$ ), respectively . . . . .	83
3.10	Maximum errors on fictitious domains, $\partial\tilde{\Omega} = \{(x, y) : x = a \cos t, y = b \sin(t + \cos t), 0 \leq t \leq 2\pi\}$ , where $a = 2, 3, 3, 4$ and $b = 2, 4, 3, 3$ with regularization parameters, $\mu = 10^{-1}$ ( $\square$ ), $\mu = 10^{-3}$ (o), $\mu = 10^{-5}$ ( $\triangle$ ), respectively . . . . .	85
3.11	Maximum errors on fictitious domains, $\partial\tilde{\Omega} = \{(x, y) : x = a \cos t, y = b \sin(t + \cos t), 0 \leq t \leq 2\pi\}$ , where $a = 2, 3, 3, 4$ and $b = 2, 4, 3, 3$ with regularization parameters, $\mu = 10^{-1}$ ( $\square$ ), $\mu = 10^{-3}$ (o), $\mu = 10^{-5}$ ( $\triangle$ ), respectively . . . . .	87
3.12	Choose $L = 10$ collocation points (x) on the $\partial\Omega_1$ , $M = 10$ collocation points (o) on the $\partial\Omega_2$ ( $\partial\Omega = \partial\Omega_1 \cup \partial\Omega_2$ ), and $N = 20$ source points (*) on the $\partial\tilde{\Omega}$ . . . . .	89
3.13	Maximum errors on fictitious domains, $\partial\tilde{\Omega} = \{(x, y) : x = a \sin(t + \cos t), y = b \cos t, 0 \leq t \leq 2\pi\}$ , where $a = 2, 3, 4, 5$ and $b = 5, 4, 3, 3$ with singular value tolerances, $\epsilon = 10^{-1}$ ( $\square$ ), $\epsilon = 10^{-3}$ (o), $\epsilon = 10^{-7}$ ( $\triangle$ ), respectively . . . . .	91
3.14	$M = 20, 300$ points ( $\bullet$ ) in $\Omega$ , 60 points ( $\bullet$ ) on $\partial\Omega$ and 35 points (+) on $\partial\Omega_\delta$ , respectively, and $N = 20$ points (*) on $\partial\tilde{\Omega}$ with $a = 5$ and $b = 4$ . . . . .	95
3.15	Maximum errors on an evolute-of-ellipse fictitious domain, $\partial\tilde{\Omega} = \{(x, y) : x = a \cos^3(t), y = b \sin^3(t), 0 \leq t \leq 2\pi\}$ , where $a = 5, b = 4, c = 1$ , ( $\square$ ), $a = 5, b = 4, c = 3$ , (o), $a = 6, b = 5, c = 1$ , ( $\triangle$ ), and $a = 6, b = 5, c = 3$ , ( $\diamond$ ), respectively . . . . .	96
3.16	Maximum errors on an evolute-of-ellipse fictitious domain, $\partial\tilde{\Omega} = \{(x, y) : x = a \cos^3(t), y = b \sin^3(t), 0 \leq t \leq 2\pi\}$ , where $a = 5, b = 4, c = 3$ , ( $\square$ ), $a = 5, b = 4, c = 5$ , (o), $a = 6, b = 5, c = 3$ , ( $\triangle$ ), and $a = 6, b = 5, c = 5$ , ( $\diamond$ ), respectively . . . . .	97

3.17	Maximum errors on an evolute-of-ellipse fictitious domain, $\partial\tilde{\Omega} = \{(x, y) : x = a \cos^3(t), y = b \sin^3(t), 0 \leq t \leq 2\pi\}$ , where $a = 5, b = 4, c = 3$ , ( $\square$ ), $a = 5, b = 4, c = 5$ , ( $\circ$ ), $a = 6, b = 5, c = 3$ , ( $\triangle$ ), and $a = 6, b = 5, c = 5$ , ( $\diamond$ ), respectively . . . . .	98
3.18	$M = 20, 300$ points ( $\bullet$ ) in $\Omega$ , $80$ points ( $\bullet$ ) on $\partial\Omega$ and $40$ points ( $+$ ) on $\partial\Omega_\delta$ , respectively, and $N = 20$ points ( $*$ ) on $\partial\tilde{\Omega}$ with $R = 2.5$ . . . . .	100
3.19	Maximum errors on an amoeba-like fictitious domain, $\partial\tilde{\Omega} = \{(x, y) : x = r(t) \cos(t), y = r(t) \sin(t)\}$ , where $r(t) = R e^{\sin(t)} \sin^2(2t) + R e^{\cos(t)} \cos^2(2t)$ , $0 \leq t < 2\pi$ , $R = 3, 5$ , and $c = 1, 3$ with singular value tolerances, $\epsilon = 10^{-2}$ ( $\square$ ), $\epsilon = 10^{-6}$ ( $\circ$ ), $\epsilon = 10^{-10}$ ( $\triangle$ ), respectively . . . . .	102
3.20	Maximum errors on an amoeba-like fictitious domain, $\partial\tilde{\Omega} = \{(x, y) : x = r(t) \cos(t), y = r(t) \sin(t)\}$ , where $r(t) = R e^{\sin(t)} \sin^2(2t) + R e^{\cos(t)} \cos^2(2t)$ , $0 \leq t < 2\pi$ , $R = 3, 5$ , and $c = 1, 3$ with singular value tolerances, $\epsilon = 10^{-2}$ ( $\square$ ), $\epsilon = 10^{-6}$ ( $\circ$ ), $\epsilon = 10^{-10}$ ( $\triangle$ ), respectively . . . . .	104
3.21	Maximum errors on an amoeba-like fictitious domain, $\partial\tilde{\Omega} = \{(x, y) : x = r(t) \cos(t), y = r(t) \sin(t)\}$ , where $r(t) = R e^{\sin(t)} \sin^2(2t) + R e^{\cos(t)} \cos^2(2t)$ , $0 \leq t < 2\pi$ , $R = 3, 5$ , and $c = 1, 3$ with singular value tolerances, $\epsilon = 10^{-2}$ ( $\square$ ), $\epsilon = 10^{-6}$ ( $\circ$ ), $\epsilon = 10^{-10}$ ( $\triangle$ ), respectively . . . . .	106
3.22	$M = 10, 1000$ points ( $\bullet$ ) in $\Omega$ , $240$ points ( $\bullet$ ) on $\partial\Omega$ , and $N = 800$ points ( $*$ ) on a bumpy sphere $\partial\tilde{\Omega}$ with $R = 3$ . . . . .	108
3.23	Maximum errors on a bumpy spherical fictitious domain $\tilde{\Omega} = \{(x, y, z) : \rho \sin(\theta) \cos(\phi), \rho \sin(\theta) \sin(\phi), \rho \cos(\theta), 0 \leq \theta \leq 2\pi, 0 \leq \phi \leq \pi\}$ , where $\rho(\theta, \phi) = R + \frac{1}{6} \sin(6\theta) \sin(7\phi)$ with $R = 3, c = 1$ , ( $\square$ ), $R = 3, c = 3$ , ( $\circ$ ), $R = 5, c = 1$ , ( $\triangle$ ), and $R = 5, c = 3$ , ( $\diamond$ ), respectively . . . . .	109
3.24	Maximum errors on a bumpy spherical fictitious domain $\tilde{\Omega} = \{(x, y, z) : \rho \sin(\theta) \cos(\phi), \rho \sin(\theta) \sin(\phi), \rho \cos(\theta), 0 \leq \theta \leq 2\pi, 0 \leq \phi \leq \pi\}$ , where $\rho(\theta, \phi) = R + \frac{1}{6} \sin(6\theta) \sin(7\phi)$ with $R = 3, c = 3$ , ( $\square$ ), $R = 3, c = 4$ , ( $\circ$ ), $R = 5, c = 3$ , ( $\triangle$ ), and $R = 5, c = 4$ , ( $\diamond$ ), respectively . . . . .	110
3.25	Maximum errors on a bumpy spherical fictitious domain $\tilde{\Omega} = \{(x, y, z) : \rho \sin(\theta) \cos(\phi), \rho \sin(\theta) \sin(\phi), \rho \cos(\theta), 0 \leq \theta \leq 2\pi, 0 \leq \phi \leq \pi\}$ , where $\rho(\theta, \phi) = R + \frac{1}{6} \sin(6\theta) \sin(7\phi)$ with $R = 3, c = 3$ , ( $\square$ ), $R = 3, c = 4$ , ( $\circ$ ), $R = 5, c = 3$ , ( $\triangle$ ), and $R = 5, c = 4$ , ( $\diamond$ ), respectively . . . . .	111
4.1	Choose collocation points in $\bar{\Omega} = \Omega \cup \partial\Omega$ where $\partial\Omega = \partial\Omega_1 \cup \partial\Omega_2$ , and $N = 20$ source points on the $\partial\tilde{\Omega} = \{(x, y) : x = 3 \cos t, y = 3 \sin(t + \sin t), 0 \leq t < 2\pi\}$	116
4.2	Maximum errors in a domain $\bar{\Omega}$ with singular value tolerances, $\epsilon = 10^{-3}$ ( $\square$ ), $\epsilon = 10^{-5}$ ( $\circ$ ), $\epsilon = 10^{-7}$ ( $\triangle$ ), respectively . . . . .	118
4.3	Choose collocation points on the $\bar{\Omega} = \Omega \cup \partial\Omega$ and $N = 20$ source points on the $\partial\tilde{\Omega} = \{(x, y) : x = a \sin t, y = b \cos(t + \cos t), 0 \leq t < 2\pi\}$ . . . . .	120
4.4	Maximum errors in a domain $\bar{\Omega}$ with regularization parameters, $\mu = 10^{-3}$ ( $\square$ ), $\mu = 10^{-5}$ ( $\circ$ ), $\mu = 10^{-7}$ ( $\triangle$ ), respectively . . . . .	122
4.5	Choose collocation points on $\bar{\Omega} = \Omega \cup \partial\Omega$ and $N = 100$ source points on the bumpy spherical fictitious domain $\partial\tilde{\Omega}$ . . . . .	124

4.6	Maximum errors in a domain $\overline{\Omega}$ with singular value tolerances, $\epsilon = 10^{-3}$ ( $\square$ ), $\epsilon = 10^{-5}$ ( $\circ$ ), $\epsilon = 10^{-7}$ ( $\triangle$ ), respectively . . . . .	126
4.7	Choose collocation points in $\overline{\Omega} = \Omega \cup \partial\Omega$ and $N = 20$ source points on the $\partial\tilde{\Omega} = \{(x, y) : x = 4 \cos^3(t), y = 4 \sin^3(t), 0 \leq t < 2\pi\}$ . . . . .	131
4.8	Maximum errors in a domain $\overline{\Omega}$ with singular value tolerances, $\epsilon = 10^{-3}$ ( $\square$ ), $\epsilon = 10^{-5}$ ( $\circ$ ), $\epsilon = 10^{-7}$ ( $\triangle$ ), respectively . . . . .	133
4.9	Choose collocation points on the $\overline{\Omega} = \Omega \cup \partial\Omega$ and $N = 20$ source points on the $\partial\tilde{\Omega} = \{(x, y) : x = a \sin t, y = b \cos(t + \cos t), 0 \leq t < 2\pi\}$ . . . . .	135
4.10	Maximum errors in a domain $\overline{\Omega}$ with regularization parameters, $\mu = 10^{-1}$ ( $\square$ ), $\mu = 10^{-3}$ ( $\circ$ ), $\mu = 10^{-5}$ ( $\triangle$ ), respectively . . . . .	137
4.11	Choose collocation points on $\overline{\Omega} = \Omega \cup \partial\Omega$ and $N = 100$ source points on the ellipsoid fictitious domain $\partial\tilde{\Omega}$ with $a = 5$ , $b = 3$ , and $c = 3$ . . . . .	139
4.12	Maximum errors in domain $\overline{\Omega}$ with singular value tolerances, $\epsilon = 10^{-1}$ ( $\square$ ), $\epsilon = 10^{-3}$ ( $\circ$ ), $\epsilon = 10^{-5}$ ( $\triangle$ ), respectively . . . . .	141
4.13	Choose collocation points in $\overline{\Omega} = \Omega \cup \partial\Omega$ and $N = 20$ source points on the $\partial\tilde{\Omega} = \{(x, y) : x = 3 \sin(t), y = 3 \cos(t + \cos(t)), 0 \leq t \leq 2\pi\}$ . . . . .	143
4.14	Maximum errors with $c = 1$ ( $\square$ ), $c = 3$ ( $\circ$ ), $c = 5$ ( $\triangle$ ), respectively . . . . .	145
4.15	Maximum errors with $c = 3$ ( $\square$ ), $c = 4$ ( $\circ$ ), $c = 5$ ( $\triangle$ ), respectively . . . . .	147
4.16	Maximum errors with $c = 3$ ( $\square$ ), $c = 4$ ( $\circ$ ), $c = 5$ ( $\triangle$ ), respectively . . . . .	149
4.17	Choose collocation points on the $\overline{\Omega} = \Omega \cup \partial\Omega$ and $N = 20$ source points on the amoeba-like fictitious domain $\partial\tilde{\Omega}$ . . . . .	151
4.18	Maximum errors with $c = 1$ ( $\square$ ), $c = 3$ ( $\circ$ ), $c = 5$ ( $\triangle$ ), respectively . . . . .	152
4.19	Maximum errors with $c = 3$ ( $\square$ ), $c = 4$ ( $\circ$ ), $c = 5$ ( $\triangle$ ), respectively . . . . .	153
4.20	Maximum errors with $c = 3$ ( $\square$ ), $c = 4$ ( $\circ$ ), $c = 5$ ( $\triangle$ ), respectively . . . . .	154
4.21	Choose collocation points on $\overline{\Omega} = \Omega \cup \partial\Omega$ and $N = 100$ source points on the bumpy spherical fictitious domain $\partial\tilde{\Omega}$ with $R = 3, 5$ . . . . .	156
4.22	Maximum errors on a bumpy spherical fictitious domain $\tilde{\Omega} = \{(x, y, z) : \rho \sin(\theta) \cos(\phi), \rho \sin(\theta) \sin(\phi), \rho \cos(\phi), 0 \leq \theta \leq 2\pi, 0 \leq \phi \leq \pi\}$ , where $\rho(\theta, \phi) = R + \frac{1}{6} \sin(6\theta) \sin(7\phi)$ with $R = 3, 5$ and $c = 1$ , ( $\square$ ), $c = 3$ , ( $\circ$ ), $c = 5$ , ( $\triangle$ ), respectively . . . . .	157
4.23	Maximum errors on a bumpy spherical fictitious domain $\tilde{\Omega} = \{(x, y, z) : \rho \sin(\theta) \cos(\phi), \rho \sin(\theta) \sin(\phi), \rho \cos(\phi), 0 \leq \theta \leq 2\pi, 0 \leq \phi \leq \pi\}$ , where $\rho(\theta, \phi) = R + \frac{1}{6} \sin(6\theta) \sin(7\phi)$ with $R = 3, 5$ and $c = 3$ , ( $\square$ ), $c = 4$ , ( $\circ$ ), $c = 5$ , ( $\triangle$ ), respectively . . . . .	158
4.24	Maximum errors on a bumpy spherical fictitious domain $\tilde{\Omega} = \{(x, y, z) : \rho \sin(\theta) \cos(\phi), \rho \sin(\theta) \sin(\phi), \rho \cos(\phi), 0 \leq \theta \leq 2\pi, 0 \leq \phi \leq \pi\}$ , where $\rho(\theta, \phi) = R + \frac{1}{6} \sin(6\theta) \sin(7\phi)$ with $R = 3, 5$ and $c = 3$ , ( $\square$ ), $c = 4$ , ( $\circ$ ), $c = 5$ , ( $\triangle$ ), respectively . . . . .	159



# CHAPTER 1

## METHOD OF FUNDAMENTAL SOLUTIONS (MFS) FOR THE LAPLACE EQUATIONS WITH BOUNDARY VALUE PROBLEMS

### 1.1 Description of MFS for Laplace equations

For a general linear partial differential operator  $\mathcal{L} = \sum_{|\alpha| \leq m} a_\alpha D^\alpha$  of order  $m$  with constant coefficients, its fundamental solution with singularity at  $\mathbf{y}$  is a distribution  $\Gamma(\mathbf{x}, \mathbf{y})$  satisfying  $\mathcal{L}(\Gamma(\mathbf{x}, \mathbf{y})) = \delta((\mathbf{x} - \mathbf{y}))$ , where  $\delta$  is the Dirac delta function.

Consider the Dirichlet boundary problem for the Laplace equation

$$\Delta u(\mathbf{x}) = 0, \quad \mathbf{x} \in \Omega, \quad (1.1)$$

$$u(\mathbf{x}) = f(\mathbf{x}), \quad \mathbf{x} \in \partial\Omega, \quad (1.2)$$

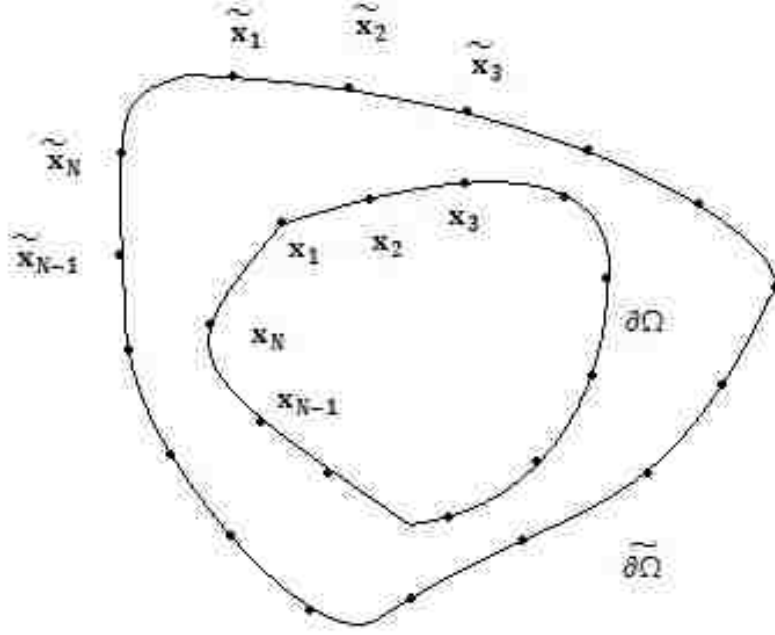
where  $\Omega$  is a domain in  $\mathbb{R}^2$  or  $\mathbb{R}^3$ . The fundamental solution for  $\mathcal{L} = -\Delta$ , where  $\Delta = \frac{\partial^2}{\partial x_1^2} + \frac{\partial^2}{\partial x_2^2}$  in  $\mathbb{R}^2$  or  $\Delta = \frac{\partial^2}{\partial x_1^2} + \frac{\partial^2}{\partial x_2^2} + \frac{\partial^2}{\partial x_3^2}$  in  $\mathbb{R}^3$  is given by

$$\Gamma(\mathbf{x}, \mathbf{y}) = \begin{cases} -\frac{1}{2\pi} \log \|\mathbf{x} - \mathbf{y}\|, & \text{for all } \mathbf{x}, \mathbf{y} \in \mathbb{R}^2, \\ \frac{1}{4\pi} \frac{1}{\|\mathbf{x} - \mathbf{y}\|}, & \text{for all } \mathbf{x}, \mathbf{y} \in \mathbb{R}^3. \end{cases} \quad (1.3)$$

To use the method of fundamental solutions (MFS), we choose a fictitious domain  $\partial\tilde{\Omega}$  such that  $\bar{\Omega} \subset \tilde{\Omega}$ . Then choose  $N$  points on  $\partial\tilde{\Omega}$  listed as  $\tilde{\mathbf{x}}_1, \tilde{\mathbf{x}}_2, \dots, \tilde{\mathbf{x}}_N$ , and form

$$u_N(\mathbf{x}) = \sum_{k=1}^N c_k \Gamma(\mathbf{x}, \tilde{\mathbf{x}}_k). \quad (1.4)$$

Figure 1.1:  $N$  collocation points on  $\partial\Omega$  and  $N$  source points on  $\partial\tilde{\Omega}$



Clearly,  $u_N(\mathbf{x})$  satisfies the Laplace equation (1.1) since  $\Gamma(\mathbf{x}, \tilde{\mathbf{x}}_k)$  is the fundamental solution. For  $u_N(\mathbf{x})$  to satisfy the Dirichlet boundary condition (1.2) as much as possible, we choose  $N$  points  $\mathbf{x}_1, \mathbf{x}_2, \dots, \mathbf{x}_N$  on  $\partial\Omega$  and set up

$$u_N(\mathbf{x}_k) = f(\mathbf{x}_k), \quad 1 \leq k \leq N,$$

namely,

$$\sum_{k=1}^N c_k \Gamma(\mathbf{x}_m, \tilde{\mathbf{x}}_k) = f(\mathbf{x}_m), \quad 1 \leq m \leq N,$$

which leads to the following system

$$\begin{bmatrix} \Gamma(\mathbf{x}_1, \tilde{\mathbf{x}}_1) & \Gamma(\mathbf{x}_1, \tilde{\mathbf{x}}_2) & \Gamma(\mathbf{x}_1, \tilde{\mathbf{x}}_3) & \dots & \Gamma(\mathbf{x}_1, \tilde{\mathbf{x}}_N) \\ \Gamma(\mathbf{x}_2, \tilde{\mathbf{x}}_1) & \Gamma(\mathbf{x}_2, \tilde{\mathbf{x}}_2) & \Gamma(\mathbf{x}_2, \tilde{\mathbf{x}}_3) & \dots & \Gamma(\mathbf{x}_2, \tilde{\mathbf{x}}_N) \\ \vdots & \vdots & \vdots & \ddots & \vdots \\ \Gamma(\mathbf{x}_N, \tilde{\mathbf{x}}_1) & \Gamma(\mathbf{x}_N, \tilde{\mathbf{x}}_2) & \Gamma(\mathbf{x}_N, \tilde{\mathbf{x}}_3) & \dots & \Gamma(\mathbf{x}_N, \tilde{\mathbf{x}}_N) \end{bmatrix} \begin{bmatrix} c_1 \\ c_2 \\ \vdots \\ c_N \end{bmatrix} = \begin{bmatrix} f(\mathbf{x}_1) \\ f(\mathbf{x}_2) \\ \vdots \\ f(\mathbf{x}_N) \end{bmatrix}. \quad (1.5)$$

Once the coefficient matrix is invertible, the coefficients  $c_k$ ,  $1 \leq k \leq N$ , can be deter-

mined by the above system (1.5) and  $u_N(\mathbf{x})$  in (1.4) is considered as an approximate solution of the Dirichlet boundary value problem (1.1)-(1.2).

To show the efficiency of such a numerical method, we let  $u_{exact}$  be the exact solution of (1.1)-(1.2), and calculate the approximation error  $|u_{exact}(\mathbf{x}) - u_N(\mathbf{x})|$ ,  $\mathbf{x} \in \Omega$ . From the maximal principal for Laplace equation

$$\max_{\mathbf{x} \in \Omega} |u_{exact}(\mathbf{x}) - u_N(\mathbf{x})| = \max_{\mathbf{x} \in \partial\Omega} |u_{exact}(\mathbf{x}) - u_N(\mathbf{x})|, \quad (1.6)$$

we only need to consider the approximation error on  $\partial\Omega$ .

## 1.2 Numerical Examples by using MFS

In this section we present some numerical examples in which fictitious domains are chosen arbitrarily and we compare the numerical results by using MFS in various situations.

**Example 1.1.** Consider the Dirichlet boundary problem for the Laplace equation

$$\begin{aligned} \Delta u(x, y) &= 0, & (x, y) &\in \Omega, \\ u(x, y) &= e^x \cos(y), & (x, y) &\in \partial\Omega, \end{aligned}$$

where  $\Omega = \{(x, y) : x^2 + y^2 \leq 1\}$  is the unit disc. The exact solution of the above problem is  $u_{exact} = e^x \cos(y)$ . To use the MFS, we choose  $N$  points equally distributed on  $\partial\Omega$ , namely:  $\mathbf{x}_k = (\cos \frac{2\pi k}{N}, \sin \frac{2\pi k}{N})$ ,  $0 \leq k \leq N - 1$ .

**a)** First, we use a fictitious domain  $\tilde{\Omega} = \{(x, y) : x^2 + y^2 \leq r^2\}$ , where  $r = 1.5, 3, 10$ , respectively, as shown in Figure 1.2 for  $r = 1.5$ . Choose  $\tilde{\mathbf{x}}_k = r(\cos \frac{2\pi k}{N}, \sin \frac{2\pi k}{N})$ ,  $0 \leq k \leq N - 1$  on  $\partial\tilde{\Omega}$ . Then the approximate solution can be obtained through (1.3)-(1.4). To estimate

the maximum error (1.5), we use equally spaced  $N = 100$  points  $\mathbf{z}_k$ ,  $1 \leq k \leq 100$ , on  $\partial\Omega$  to get the numerical infinity norm

$$\max_{1 \leq k \leq 100} |u_{exact}(\mathbf{z}_k) - u_N(\mathbf{z}_k)|.$$

Then our numerical approximation errors are presented in the following table with various  $r$  and  $N$ :

Figure 1.2: Graph of  $\partial\Omega$ ,  $\partial\tilde{\Omega}$  with  $r = 1.5$  and  $N = 20$  collocation points

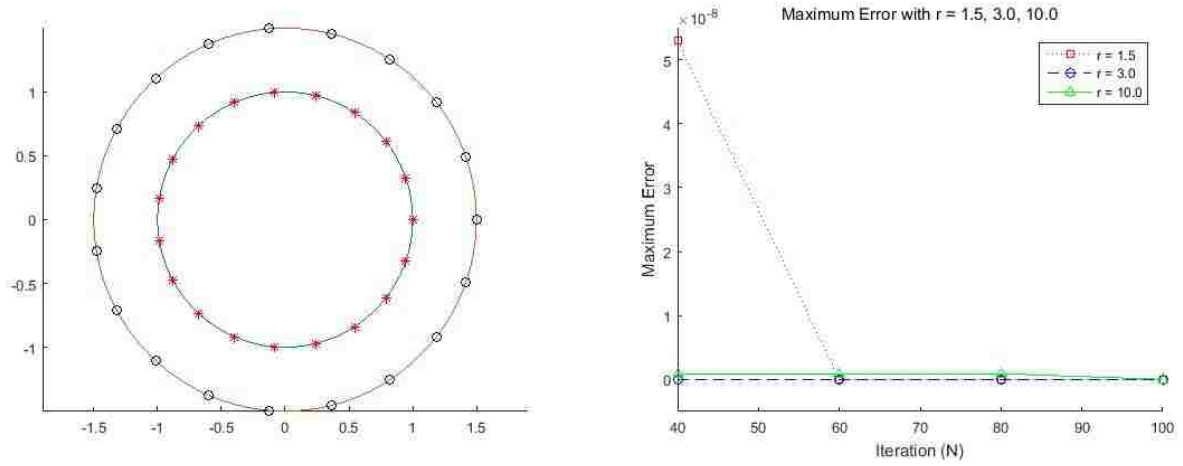


Table 1.1: Maximum Error  $\|u_{exact} - u_N\|_{C(\partial\Omega)}$

	N = 40	N = 60	N = 80	N = 100
r = 1.5	5.2904e-08	1.0313e-11	1.7764e-15	1.7764e-15
r = 3.0	1.5543e-15	1.5543e-15	1.5543e-15	3.4861e-14
r = 10.0	9.1854e-10	9.1854e-10	9.1854e-10	2.3353e-11

b) Next we use a fictitious domain  $\tilde{\Omega} = \{(x, y) : \frac{x^2}{a^2} + \frac{y^2}{b^2} \leq 1\}$ , where  $a = 7, 2, 10, 3$  and  $b = 2, 7, 3, 10$ , respectively. We choose  $\tilde{\mathbf{x}}_k = (a \cos \frac{2\pi k}{N}, b \sin \frac{2\pi k}{N})$ ,  $0 \leq k \leq N - 1$  on  $\partial\tilde{\Omega}$ , (see Figure 1.3). Then we have the following numerical results with various  $a$  and  $b$ :

Figure 1.3: Graph of  $\partial\Omega$ ,  $\partial\tilde{\Omega}$  with  $a = 3$ ,  $b = 1.5$  and  $N = 20$  collocation points

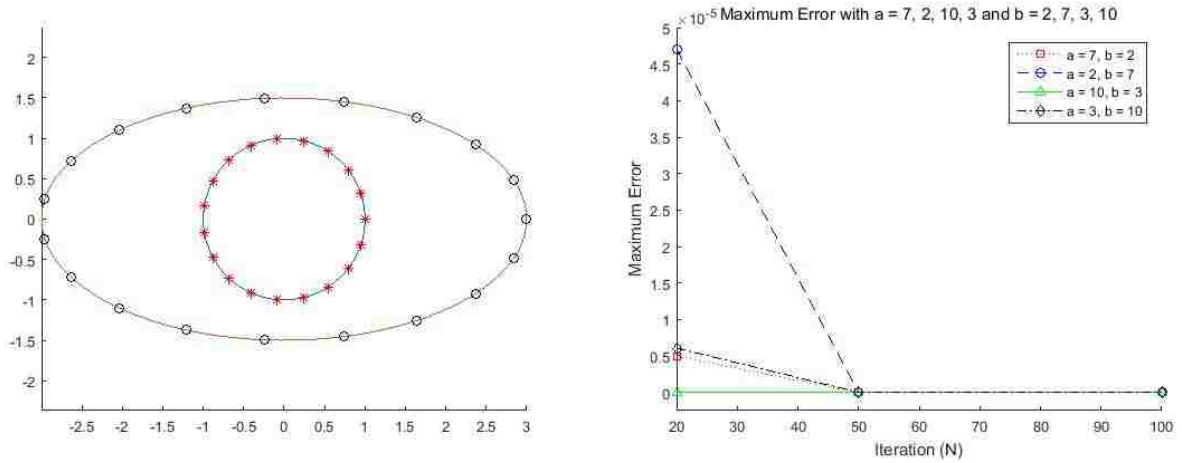


Table 1.2: Maximum Error  $\|u_{exact} - u_N\|_{C(\partial\Omega)}$

	$N = 20$	$N = 50$	$N = 100$
$a = 7, b = 2$	4.9695e-06	1.9748e-09	9.4712e-11
$a = 2, b = 7$	4.7048e-05	9.1681e-09	5.8001e-10
$a = 10, b = 3$	5.8001e-10	7.0755e-11	9.5451e-13
$a = 3, b = 10$	6.0709e-06	4.5870e-09	5.8106e-12

c) Finally, we use an arbitrarily fictitious domain  $\tilde{\Omega} = \{(x, y) : x = a \sin t + b \cos t - 3, y = c(\cos t)^2 - 2, 0 \leq t \leq 2\pi\}$ , where  $a = 4, 7, 10$ ,  $b = 3, 4, 7$ , and  $c = 4, 5, 6$ , respectively. We choose  $\tilde{\mathbf{x}}_{\mathbf{k}} = (a \sin \frac{2\pi k}{N} + b \cos \frac{2\pi k}{N} - 3, c(\cos \frac{2\pi k}{N})^2 - 2)$ ,  $0 \leq k \leq N - 1$  on  $\partial\tilde{\Omega}$ , (see Figure 1.4). Then we have the following numerical results:

Figure 1.4: Choose  $M=20$  collocation points on the  $\partial\Omega$ , and  $N=20$  source points on the  $\partial\tilde{\Omega}$

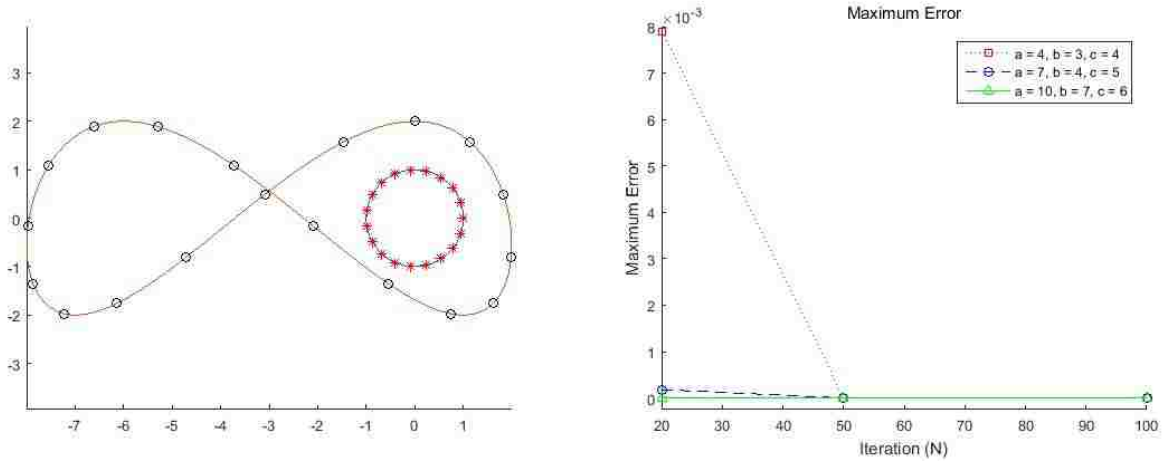


Table 1.3: Maximum Error  $\|u_{exact} - u_N\|_{C(\partial\Omega)}$

	N = 20	N = 50	N = 100
a = 4, b = 3, c = 4	0.0079	1.0900e-05	2.6453e-08
a = 7, b = 4, c = 5	1.8106e-04	1.0849e-09	2.1551e-10
a = 10, b = 7, c = 6	1.0123e-05	1.7959e-08	2.4932e-10

Next, we present examples about an arbitrary domain  $\Omega \subset \mathbb{R}^2$  and a three-dimensional domain  $\Omega \subset \mathbb{R}^3$ .

**Example 1.2.** Consider the Dirichlet boundary problem for the Laplace equation

$$\Delta u(x, y) = 0, \quad (x, y) \in \Omega,$$

$$u(x, y) = e^x \cos(y), \quad (x, y) \in \partial\Omega,$$

where  $\Omega = \{(x, y) : x = \sin(t + \sin t), y = \cos(t + \cos t), 0 \leq t \leq 2\pi\}$ . The exact solution of the above problem is  $u_{exact} = e^x \cos(y)$ . We use a fictitious domain  $\tilde{\Omega} = \{(x, y) : x = a \cos t, y = b \sin(t + \cos t), 0 \leq t \leq 2\pi\}$ , where  $a = 2, 3, 2$  and  $b = 1.5, 4, 2$ , respectively. We choose  $\tilde{\mathbf{x}}_k = (a \cos \frac{2\pi k}{N}, b \sin(\frac{2\pi k}{N} + \cos \frac{2\pi k}{N}))$ ,  $0 \leq k \leq N - 1$  on  $\partial\tilde{\Omega}$ . To use the MFS, we choose  $N$  points on  $\partial\Omega$  corresponding to  $t_k = \frac{2\pi k}{N}$ ,  $0 \leq k \leq N - 1$ , (see Figure 1.5). Then the approximate solution can be obtained through (1.3)-(1.4). Our maximum error is also estimated by using points on  $\partial\Omega$  corresponding to 100 even spaced points in  $[0, 2\pi]$ . We have the following numerical results:

Figure 1.5: Choose  $N=20$  collocation points on the  $\partial\Omega$ , and  $N=20$  source points on the  $\partial\tilde{\Omega}$

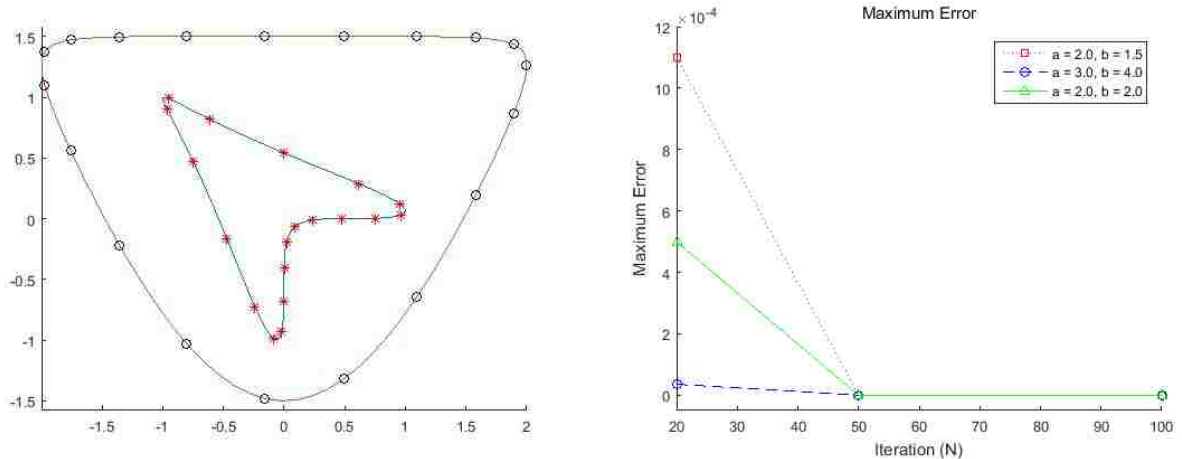


Table 1.4: Maximum Error  $\|u_{exact} - u_N\|_{C(\partial\Omega)}$

	N = 20	N = 50	N = 100
a = 2.0, b = 1.5	0.0011	2.1269e-08	9.4311e-12
a = 3.0, b = 4.0	3.5269e-05	8.0126e-10	3.3815e-12
a = 2.0, b = 2.0	4.9950e-04	2.7468e-08	6.0702e-11

**Example 1.3.** Consider the Dirichlet boundary problem for the Laplace equation

$$\Delta u(x, y, z) = 0, \quad (x, y, z) \in \Omega,$$

$$u(x, y, z) = x e^y \cos(z), \quad (x, y, z) \in \partial\Omega,$$

where  $\Omega = \{(x, y, z) : x^2 + y^2 + z^2 < 1\}$  is the unit ball. The exact solution of the above problem is  $u_{exact} = x e^y \cos(z)$ . To use the MFS, we choose  $N$  points on  $\partial\Omega$  corresponding to  $t_k = \frac{2\pi k}{N}$ ,  $s_k = \frac{\pi k}{N}$ ,  $0 \leq k \leq N - 1$ . We use a fictitious domain  $\tilde{\Omega} = \{(x, y, z) : x^2 + y^2 + z^2 \leq r^2\}$ , where  $r = 1.5, 2, 3$ . We choose  $\tilde{\mathbf{x}}_{\mathbf{k}} = (r \cos \frac{2\pi k}{N} \sin \frac{\pi k}{N}, r \sin \frac{2\pi k}{N} \sin \frac{\pi k}{N}, r \cos \frac{\pi k}{N})$ ,  $0 \leq k \leq N - 1$ ,  $r = 1.5, 2, 3$  on  $\partial\tilde{\Omega}$ , (see Figure 1.6). Then the approximate solution can be obtained through (1.3)-(1.4). Our maximum error is also estimated by using points on  $\partial\Omega$  corresponding to 100 evenly spaced points in  $[0, 2\pi]$ . We have the following numerical results:



Figure 1.6: Choose  $N = 20$  collocation points on  $\partial\Omega$ , and  $N = 20$  source points on  $\partial\tilde{\Omega}$ , and  $r = 3.0$

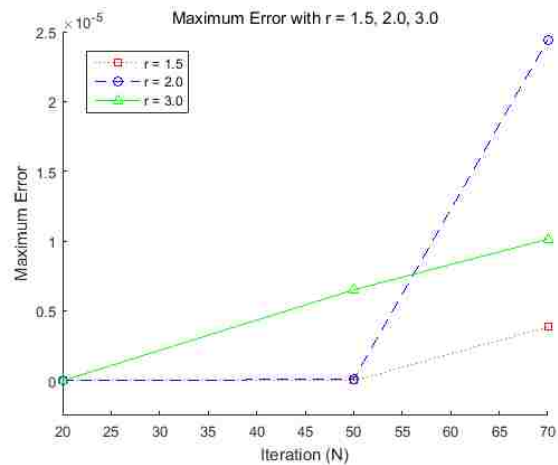
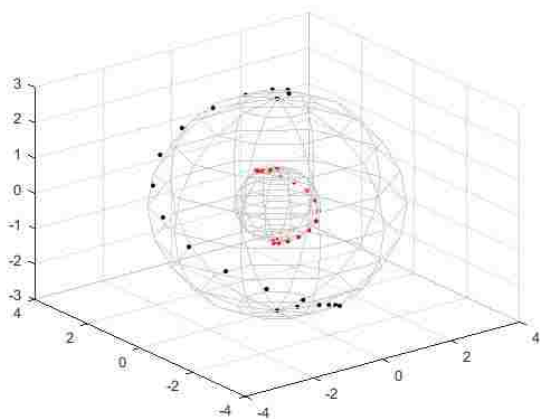


Table 1.5: Maximum Error  $\|u_{exact} - u_N\|_{C(\partial\Omega)}$

	N = 20	N = 50	N = 70
r = 1.5	3.3959e-14	1.1642e-10	3.8503e-06
r = 2.0	1.1007e-12	1.0357e-07	2.4414e-05
r = 3.0	5.8208e-11	6.5000e-06	1.0138e-05

### 1.3 MFS for Other Boundary Conditions

Similarly the MFS can be applied to the Newmann boundary problem as follows:

$$\Delta u(\mathbf{x}) = 0, \quad \mathbf{x} \in \Omega, \quad (1.7)$$

$$\frac{\partial u}{\partial \mathbf{n}}(\mathbf{x}) = g(\mathbf{x}), \quad \mathbf{x} \in \partial\Omega, \quad (1.8)$$

where  $\Omega$  is a domain in  $\mathbb{R}^2$  and  $\mathbf{n} = (n_1, n_2)$  is the unit exterior normal vector on  $\partial\Omega$ . As in Section 1, an approximate solution is formed in (1.4). For the Newmann boundary condition (1.8), we use the collocation method, namely, choose  $N$  points  $\mathbf{x}_1, \mathbf{x}_2, \dots, \mathbf{x}_N$  on  $\partial\Omega$  and set up

$$\nabla u \cdot \mathbf{n} = \frac{\partial u_N}{\partial \mathbf{n}}(\mathbf{x}_k) = g(\mathbf{x}_k), \quad 1 \leq k \leq N.$$

Or

$$\sum_{m=1}^N c_k \frac{\partial \Gamma}{\partial \mathbf{n}}(\mathbf{x}_k, \tilde{\mathbf{x}}_m) = g(\mathbf{x}_k), \quad 1 \leq k \leq N,$$

which can be expressed as

$$\begin{bmatrix} \frac{\partial \Gamma}{\partial \mathbf{n}}(\mathbf{x}_1, \tilde{\mathbf{x}}_1) & \frac{\partial \Gamma}{\partial \mathbf{n}}(\mathbf{x}_1, \tilde{\mathbf{x}}_2) & \frac{\partial \Gamma}{\partial \mathbf{n}}(\mathbf{x}_1, \tilde{\mathbf{x}}_3) & \dots & \frac{\partial \Gamma}{\partial \mathbf{n}}(\mathbf{x}_1, \tilde{\mathbf{x}}_N) \\ \frac{\partial \Gamma}{\partial \mathbf{n}}(\mathbf{x}_2, \tilde{\mathbf{x}}_1) & \frac{\partial \Gamma}{\partial \mathbf{n}}(\mathbf{x}_2, \tilde{\mathbf{x}}_2) & \frac{\partial \Gamma}{\partial \mathbf{n}}(\mathbf{x}_2, \tilde{\mathbf{x}}_3) & \dots & \frac{\partial \Gamma}{\partial \mathbf{n}}(\mathbf{x}_2, \tilde{\mathbf{x}}_N) \\ \vdots & \vdots & \vdots & \ddots & \vdots \\ \frac{\partial \Gamma}{\partial \mathbf{n}}(\mathbf{x}_N, \tilde{\mathbf{x}}_1) & \frac{\partial \Gamma}{\partial \mathbf{n}}(\mathbf{x}_N, \tilde{\mathbf{x}}_2) & \frac{\partial \Gamma}{\partial \mathbf{n}}(\mathbf{x}_N, \tilde{\mathbf{x}}_3) & \dots & \frac{\partial \Gamma}{\partial \mathbf{n}}(\mathbf{x}_N, \tilde{\mathbf{x}}_N) \end{bmatrix} \begin{bmatrix} c_1 \\ c_2 \\ \vdots \\ c_N \end{bmatrix} = \begin{bmatrix} g(\mathbf{x}_1) \\ g(\mathbf{x}_2) \\ \vdots \\ g(\mathbf{x}_N) \end{bmatrix}. \quad (1.9)$$

The coefficients  $c_k$ ,  $1 \leq m \leq N$ , can then be determined by the above system (1.9) and  $u_N(\mathbf{x})$  in (1.4) is considered as an approximate solution of the Newmann boundary value problem (1.7)-(1.8).

Below we present some examples to solve the Newmann boundary value problems by MFS.

**Example 1.4.** Consider the Neumann boundary problem for the Laplace equation

$$\begin{aligned} \Delta u(x, y) &= 0, & (x, y) \in \Omega, \\ \frac{\partial u}{\partial \mathbf{n}}(x, y) &= 3x^3 - 9xy^2, & (x, y) \in \partial\Omega, \end{aligned}$$

where  $\Omega = \{(x, y) : x^2 + y^2 < 1\}$ . The exact solution of the above problem is  $u_{exact} = x^3 - 3xy^2$ . To use the MFS, we choose  $M$  points on  $\partial\Omega$  as in Example 1.2. We use a fictitious domain  $\tilde{\Omega} = \{(x, y) : x = a \cos t, y = b \sin(t + \cos t), 0 \leq t \leq 2\pi\}$ , where  $a = 2, 3, 4, 4$  and  $b = 2, 4, 2, 3$ , respectively. We choose  $\tilde{\mathbf{x}}_k = (a \cos \frac{2\pi k}{N}, b \sin(\frac{2\pi k}{N} + \cos \frac{2\pi k}{N}))$ ,  $0 \leq k \leq N - 1$  on  $\partial\tilde{\Omega}$ , (see Figure 1.7). Then we have the following numerical results:

Figure 1.7: Choose  $M = 20$  collocation points on  $\partial\Omega$ , and  $N = 20$  source points on  $\partial\tilde{\Omega}$

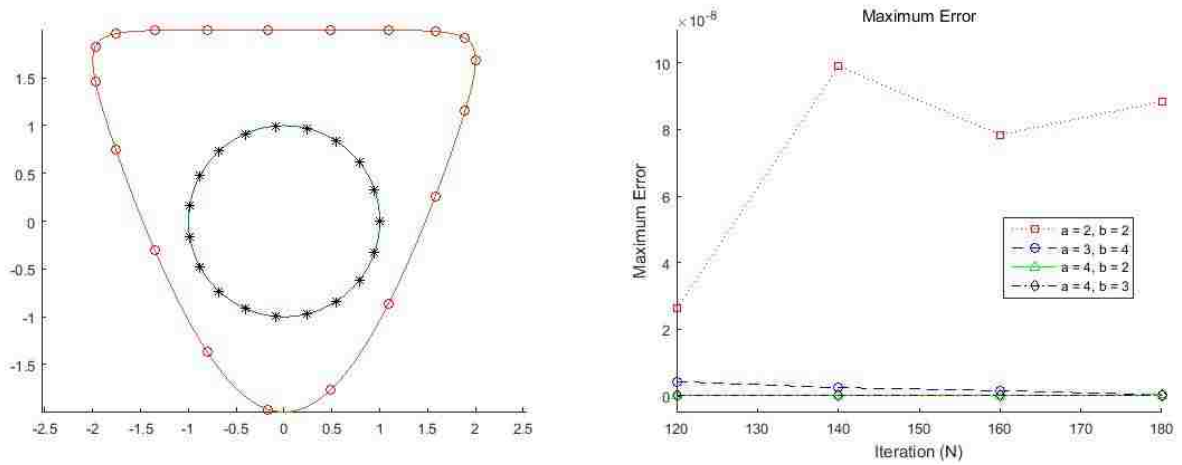


Table 1.6: Maximum Error  $\|u_{exact} - u_N\|_{C(\partial\Omega)}$

	N = 120	N = 140	N = 160	N = 180
a = 2, b = 2	2.6338e-08	9.9064e-08	7.8426e-08	8.8402e-08
a = 3, b = 4	4.3082e-09	2.5001e-09	1.5980e-09	3.3865e-10
a = 4, b = 2	3.0100e-10	3.1147e-10	9.5455e-11	3.9710e-10
a = 4, b = 3	2.4490e-10	2.7728e-10	3.5139e-10	3.0854e-10

Next we consider the Robin boundary problem

$$\Delta u(\mathbf{x}) = 0, \quad \mathbf{x} \in \Omega, \quad (1.10)$$

$$u(\mathbf{x}) = f(\mathbf{x}), \quad \mathbf{x} \in \partial\Omega_1, \quad (1.11)$$

$$\frac{\partial u}{\partial \mathbf{n}}(\mathbf{x}) = g(\mathbf{x}), \quad \mathbf{x} \in \partial\Omega_2, \quad (1.12)$$

where  $\partial\Omega = \partial\Omega_1 \cup \partial\Omega_2$  and  $\mathbf{n} = (n_1, n_2)$  is the unit exterior normal vector on  $\partial\Omega_2$ . As in Section 1, an approximate solution is formed in (1.4). For the Robin (Mixed) boundary condition (1.11)-(1.12), we choose M points  $\mathbf{x}_1, \mathbf{x}_2, \dots, \mathbf{x}_M$  on  $\partial\Omega_1$  and N-M points  $\mathbf{x}_{M+1}, \mathbf{x}_{M+2}, \dots, \mathbf{x}_N$  on  $\partial\Omega_2$  and set up

$$u_N(\mathbf{x}_k) = f(\mathbf{x}_k), \quad 1 \leq k \leq M,$$

and

$$\nabla u \cdot \mathbf{n} = \frac{\partial u_N}{\partial \mathbf{n}}(\tilde{\mathbf{x}}_k) = g(\tilde{\mathbf{x}}_k), \quad M+1 \leq k \leq N.$$

Or

$$\sum_{m=1}^N c_k \Gamma(\mathbf{x}_k, \tilde{\mathbf{x}}_m) = f(\mathbf{x}_k), \quad 1 \leq k \leq M,$$

and

$$\sum_{m=1}^N c_k \frac{\partial \Gamma}{\partial \mathbf{n}}(\mathbf{x}_k, \tilde{\mathbf{x}}_m) = g(\mathbf{x}_k), \quad M+1 \leq k \leq N.$$

It is expressed as follows:

$$\begin{bmatrix} \Gamma(\mathbf{x}_1, \tilde{\mathbf{x}}_1) & \dots & \Gamma(\mathbf{x}_1, \tilde{\mathbf{x}}_M) & \dots & \Gamma(\mathbf{x}_1, \tilde{\mathbf{x}}_N) \\ \Gamma(\mathbf{x}_2, \tilde{\mathbf{x}}_1) & \dots & \Gamma(\mathbf{x}_2, \tilde{\mathbf{x}}_M) & \dots & \Gamma(\mathbf{x}_2, \tilde{\mathbf{x}}_N) \\ \vdots & \ddots & \vdots & \ddots & \vdots \\ \Gamma(\mathbf{x}_M, \tilde{\mathbf{x}}_1) & \dots & \Gamma(\mathbf{x}_M, \tilde{\mathbf{x}}_M) & \dots & \Gamma(\mathbf{x}_M, \tilde{\mathbf{x}}_N) \\ \frac{\partial \Gamma}{\partial \mathbf{n}}(\mathbf{x}_{M+1}, \tilde{\mathbf{x}}_1) & \dots & \frac{\partial \Gamma}{\partial \mathbf{n}}(\mathbf{x}_{M+1}, \tilde{\mathbf{x}}_M) & \dots & \frac{\partial \Gamma}{\partial \mathbf{n}}(\mathbf{x}_{M+1}, \tilde{\mathbf{x}}_N) \\ \vdots & \ddots & \vdots & \ddots & \vdots \\ \frac{\partial \Gamma}{\partial \mathbf{n}}(\mathbf{x}_N, \tilde{\mathbf{x}}_1) & \dots & \frac{\partial \Gamma}{\partial \mathbf{n}}(\mathbf{x}_N, \tilde{\mathbf{x}}_M) & \dots & \frac{\partial \Gamma}{\partial \mathbf{n}}(\mathbf{x}_N, \tilde{\mathbf{x}}_N) \end{bmatrix} \begin{bmatrix} c_1 \\ c_2 \\ \vdots \\ c_M \\ c_{M+1} \\ \vdots \\ c_N \end{bmatrix} = \begin{bmatrix} f(\mathbf{x}_1) \\ f(\mathbf{x}_2) \\ \vdots \\ f(\mathbf{x}_M) \\ g(\mathbf{x}_{M+1}) \\ \vdots \\ g(\mathbf{x}_N) \end{bmatrix}. \quad (1.13)$$

Hence, the coefficients  $c_k$ ,  $1 \leq m \leq N$ , can be determined by the above system (1.13)

and an approximate solution  $u_N(\mathbf{x})$  in (1.4) can be obtained.

**Example 1.5.** Consider the Robin (Mixed) boundary problem for the Laplace equation

$$\begin{aligned}\Delta u(x, y) &= 0, & (x, y) \in \Omega, \\ u(x, y) &= \ln(x^2 + y^2), & (x, y) \in \partial\Omega_1, \\ \frac{\partial u}{\partial \mathbf{n}}(x, y) &= -\frac{2y}{x^2 + y^2}, & (x, y) \in \partial\Omega_2,\end{aligned}$$

where  $\partial\Omega = \partial\Omega_1 \cup \partial\Omega_2$  such that  $\partial\Omega_1 = \{(x, y) : x = \cos(t), y = \frac{1}{8} + \sin(t), 0 \leq t < \pi\}$  and  $\partial\Omega_2 = \{(x, \frac{1}{8}) : x = t, -1 \leq t \leq 1\}$ . The exact solution of the above problem is  $u_{exact} = \ln(x^2 + y^2)$ . To use the MFS, we choose  $N$  points on  $\partial\Omega = \partial\Omega_1 \cup \partial\Omega_2$ , where  $\mathbf{x}_k = (\cos(\frac{2\pi k}{N}), \sin(\frac{2\pi k}{N}))$ ,  $0 \leq k \leq N - 1$ . We use a fictitious domain  $\tilde{\Omega} = \{(x, y) : x = a \sin(t + \sin t), y = b \cos(t + \cos t), 0 \leq t \leq 2\pi\}$ , where  $a = 3, 4, 4, 5$  and  $b = 3, 3, 4, 4$ , respectively. We choose  $\tilde{\mathbf{x}}_k = (a \sin(\frac{2\pi k}{N} + \cos \frac{2\pi k}{N}), b \cos \frac{2\pi k}{N})$ ,  $0 \leq k \leq N - 1$  on  $\partial\tilde{\Omega}$  corresponding to  $N$  equally spaced points in  $[0, 2\pi]$ , (see Figure 1.8). Then the approximate solution can be obtained by (1.4) and (1.13). To estimate the maximum error (1.6), we choose equally spaced  $M = 50$  points  $\mathbf{z}_k$ ,  $1 \leq k \leq 50$ , on  $\partial\Omega_1$  and  $N-M = 50$  points  $\mathbf{z}_k$ ,  $51 \leq k \leq 100$ , on  $\partial\Omega_2$  which implies that  $\mathbf{z}_k$ ,  $1 \leq k \leq 100$ , on  $\partial\Omega = \partial\Omega_1 \cup \partial\Omega_2$  to get the numerical infinity norm

$$\max_{1 \leq k \leq 100} |u_{exact}(\mathbf{z}_k) - u_N(\mathbf{z}_k)|.$$

Then we have the following numerical results:

Figure 1.8: Choose  $M = 20$  collocation points on  $\partial\Omega = \partial\Omega_1 \cup \partial\Omega_2$ , and  $N = 20$  source points on  $\partial\tilde{\Omega} = \{(x, y) : x = 3 \sin(t + \sin t), y = 3 \cos(t + \cos t), 0 \leq t \leq 2\pi\}$

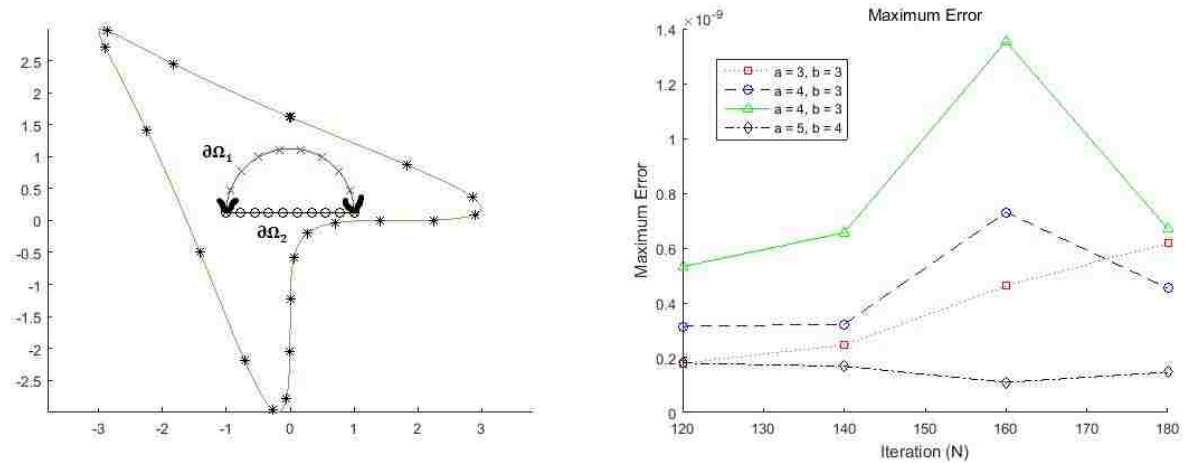


Table 1.7: Maximum Error  $\|u_{exact} - u_N\|_{C(\partial\Omega)}$

	$N = 120$	$N = 140$	$N = 160$	$N = 180$
$a = 3, b = 3$	1.7955e-10	2.4638e-10	4.6182e-10	6.1806e-10
$a = 4, b = 3$	3.1412e-10	3.2222e-10	7.3061e-10	4.5347e-10
$a = 4, b = 4$	5.3191e-10	6.5618e-10	1.3543e-09	6.7015e-10
$a = 5, b = 4$	1.8034e-10	1.6841e-10	1.0995e-10	1.4699e-10

## 1.4 Convergence of the method of fundamental solutions (MFS)

The numerical efficiency of MFS has been well reported in the literature (cf. [10]). However, the convergence rates of MFS with respect to arbitrary domains and fictitious domains, and arbitrary choices of source and collocation points, largely remain unanswered. In certain special cases that  $\partial\Omega$  and  $\partial\tilde{\Omega}$  are concentric circles, the rates of convergence of MFS are derived by several authors (cf. [23]). Here we quote a constructive method by the fundamental solution and a result of the rate of convergence derived in [23].

For a  $2\pi$ -periodic function  $f(t) \in L^2([-\pi, \pi])$ , its Fourier series expansion is given by

$$f(t) = \sum_{n=-\infty}^{\infty} c_n(f) e^{int}, \quad (1.14)$$

where

$$c_n(f) := \frac{1}{2\pi} \int_0^{2\pi} f(t) e^{-int} dt, \quad n \in \mathbb{Z}.$$

For the sake of argument, we identify  $\mathbb{R}^2$  with a complex plane  $\mathbb{C}$ , and write

$$\partial\Omega := \{re^{it} : -\pi \leq t < \pi\} \quad \text{and} \quad \partial\tilde{\Omega} := \{Re^{it} : -\pi \leq t < \pi\},$$

where  $R > r$ . Associated with the fundamental solution  $\Gamma$ , we introduce

$$g(t) = -\frac{1}{4\pi} \ln ||re^{it} - R||^2.$$

It is known from [11] (formula 1.514, p.45) that

$$\begin{aligned} g(t) &= -\frac{1}{4\pi} \ln[r^2 - 2rR \cos t + R^2] \\ &= -\frac{1}{2\pi} \ln R + \frac{1}{4\pi} \sum_{n \in \mathbb{Z} \setminus \{0\}} \frac{1}{|n|} \left(\frac{r}{R}\right)^{|n|} e^{int}, \end{aligned}$$



namely:

$$c_n(g) = \begin{cases} -\frac{1}{2\pi} \ln R, & n = 0, \\ \frac{1}{4\pi|n|} \left(\frac{r}{R}\right)^{|n|}, & n \neq 0. \end{cases} \quad (1.15)$$

Assume  $R \neq 1$  so that  $c_n(g) \neq 0$ . Since  $\partial\tilde{\Omega}$  is a fictitious boundary, it would not impose any practical difficulty.

Now for the boundary value problem (1.1)-(1.2), we let

$$f(t) = f(re^{it}), \quad -\pi \leq t < \pi.$$

Denote by  $C^j([-\pi, \pi])$  the set of all functions with  $j$ th order continuous derivatives in  $[-\pi, \pi]$ .

Assume  $f(t) \in C^j([-\pi, \pi])$  for some  $j \geq 2$ . With  $\tilde{\mathbf{x}}_k = Re^{ik\pi/N}$ ,  $-N \leq k \leq N-1$ , we introduce

$$u_{N,k}(\mathbf{x}) = \sum_{l=-N}^{N-1} a_l(k) \Gamma(\mathbf{x}, \tilde{\mathbf{x}}_k), \quad (1.16)$$

where

$$a_l(k) := \sum_{n=-k}^k \frac{c_n(f)}{2Nc_n(g)} e^{i\frac{ln\pi}{N}}, \quad -N \leq l \leq N-1.$$

Then the following theorem is derived in [23].

**Theorem 1.1.** *Suppose that  $u$  is the exact solution of (1.1) and (1.2), and  $f(t) = f(re^{it}) \in C^j([-\pi, \pi])$  for some  $j \geq 2$ . Let  $u_{N,k}$  be constructed above in (1.16), where  $R > r$  and  $R \neq 1$ .*

*Then*

$$\|u - u_{N,k}\|_{L^\infty(\Omega)} \leq c \|f^{(j)}\|_{L^\infty([-\pi, \pi])} \left( \frac{1}{k^{j-1}} + \frac{(r/R)^{2(N-k)}}{1 - (r/R)^{2N}} \right),$$

*where  $c$  is a constant independent of  $f(t)$ ,  $k$ , and  $N$ .*

## CHAPTER 2

# DUAL RECIPROCITY METHODS (DRM) FOR THE POISSON'S EQUATIONS

## 2.1 Method of Particular Solutions (MPS) and DRM

First we describe the method of particular solutions to find an approximate particular solution of a Poisson's equation

$$\Delta u(\mathbf{x}) = f(\mathbf{x}) \quad \text{in } \Omega. \quad (2.1)$$

For this purpose, we use a radial basis functions (RBF)

$$\phi(\mathbf{x}) = \phi(\|\mathbf{x}\|),$$

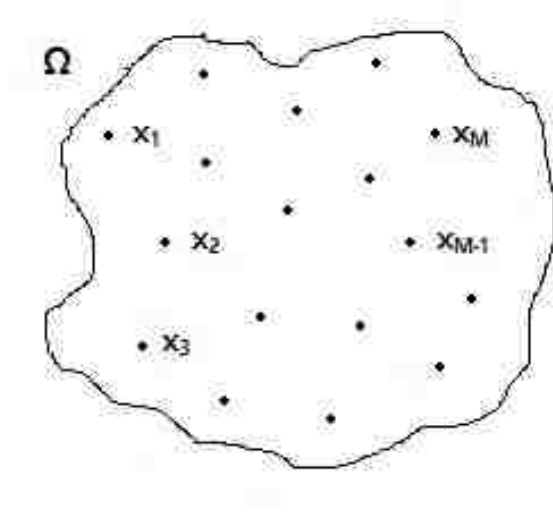
where  $\phi(\cdot)$  is a univariate function. Approximate  $f(\mathbf{x})$  by the collocation method. To be specific, we choose  $\mathbf{x}_1, \mathbf{x}_2, \dots, \mathbf{x}_M$  in  $\Omega$ , (see Figure 2.1) and consider a linear combination of  $\phi(\|\mathbf{x} - \mathbf{x}_k\|)$ ,  $1 \leq k \leq M$ , or

$$\sum_{k=1}^M c_k \phi(\|\mathbf{x} - \mathbf{x}_k\|),$$

where  $c_k$ ,  $1 \leq k \leq M$ , so chosen that

$$\sum_{k=1}^M c_k \phi(\|\mathbf{x}_m - \mathbf{x}_k\|) = f(\mathbf{x}_m), \quad 1 \leq m \leq M.$$

Figure 2.1: M points in  $\Omega$



The above equation yields

$$\begin{bmatrix} \phi(0) & \phi(\|\mathbf{x}_1 - \mathbf{x}_2\|) & \dots & \phi(\|\mathbf{x}_1 - \mathbf{x}_M\|) \\ \phi(\|\mathbf{x}_2 - \mathbf{x}_1\|) & \phi(0) & \dots & \phi(\|\mathbf{x}_2 - \mathbf{x}_M\|) \\ \vdots & \vdots & \ddots & \vdots \\ \phi(\|\mathbf{x}_M - \mathbf{x}_1\|) & \phi(\|\mathbf{x}_M - \mathbf{x}_2\|) & \dots & \phi(0) \end{bmatrix} \begin{bmatrix} c_1 \\ c_2 \\ \vdots \\ c_M \end{bmatrix} = \begin{bmatrix} f(\mathbf{x}_1) \\ f(\mathbf{x}_2) \\ \vdots \\ f(\mathbf{x}_M) \end{bmatrix}. \quad (2.2)$$

It is known in [25] that for Gaussian  $e^{-c\|\mathbf{x}\|^2}$ , or multiquadratic  $\sqrt{\|\mathbf{x}\|^2 + c^2}$ , where  $c > 0$  is a constant, the above coefficient matrix is always invertible. Hence  $\{c_k\}_{k=1}^M$  can be found. However, the above matrix may not be invertible for other RBFs, e.g.  $\phi(\mathbf{x}) = \|\mathbf{x}\|^2 \ln \|\mathbf{x}\|$ , thin plate splines.

Suppose that  $\{c_k\}_{k=1}^M$  is determined (e.g. using  $e^{-c\|\mathbf{x}\|^2}$  or  $\sqrt{\|\mathbf{x}\|^2 + c^2}$ ). Then

$$\sum_{k=1}^M c_k \phi(\|\mathbf{x} - \mathbf{x}_k\|)$$

is considered as an approximation of  $f(\mathbf{x})$ , and hence we turn to study the following Poisson's equation

$$\Delta u(\mathbf{x}) = \sum_{k=1}^M c_k \phi(\|\mathbf{x} - \mathbf{x}_k\|), \quad \mathbf{x} \in \Omega.$$

If  $\psi$  is a RBF solution of  $\Delta\psi(\|\mathbf{x}\|) = \phi(\|\mathbf{x}\|)$ , then

$$u(\mathbf{x}) = \sum_{k=1}^M c_k \psi(\|\mathbf{x} - \mathbf{x}_k\|)$$

is an approximate solution of the Poisson's equation (2.1).

For  $\Omega \in \mathbb{R}^2$ , it follows from Lemma 2.1 in Section 2.3 that

$$\psi(r) = \left( \int_0^r t \phi(t) dt \right) \ln r - \int_0^r t \phi(t) \ln t dt, \quad (2.3)$$

where we choose  $A = B = 0$ . Let  $\phi(r) = e^{-cr^2}$  or  $\sqrt{r^2 + c^2}$ , then substitute  $\phi(r)$  into (1.15)

to get  $\psi(r)$  as follows:

$$\psi(r) = \left( \int_0^r t e^{-ct^2} dt \right) \ln r - \int_0^r t e^{-ct^2} \ln t dt,$$

or

$$\psi(r) = \left( \int_0^r t \sqrt{t^2 + c^2} dt \right) \ln r - \int_0^r t \sqrt{t^2 + c^2} \ln t dt,$$

respectively.

Hence, the numerical particular solution of the Poisson's equation (2.1) is

$$u_p(\mathbf{x}) = \sum_{k=1}^M c_k \left[ \left( \int_0^{\|\mathbf{x} - \mathbf{x}_k\|} t \phi(t) dt \right) \ln \|\mathbf{x} - \mathbf{x}_k\| - \int_0^{\|\mathbf{x} - \mathbf{x}_k\|} t \phi(t) \ln t dt \right]. \quad (2.4)$$

Now for a Dirichlet problem of the Poisson's equation

$$\Delta u(\mathbf{x}) = f(\mathbf{x}), \quad \mathbf{x} \in \Omega, \quad (2.5)$$

$$u(\mathbf{x}) = h(\mathbf{x}), \quad \mathbf{x} \in \partial\Omega, \quad (2.6)$$

first, we use the MPS to get an approximate solution of the Poisson's equations. Namely, choose a RBF  $\phi(r)$  to interpolate  $f$  on  $\Omega$ . Then we get an approximate solution  $u_p$  of  $\Delta u(\mathbf{x}) = f(\mathbf{x})$ , as discussed above in (2.5). Next we consider the Dirichlet boundary problem of the Laplace equation

$$\Delta u(\mathbf{x}) = 0, \quad \mathbf{x} \in \Omega, \quad (2.7)$$

$$u(\mathbf{x}) = h(\mathbf{x}) - u_p(\mathbf{x}), \quad \mathbf{x} \in \partial\Omega. \quad (2.8)$$

The MFS can be applied to obtain an approximate solution  $u_N$  of (2.7)-(2.8). Then

$$u_A(\mathbf{x}) = u_N(\mathbf{x}) + u_p(\mathbf{x}).$$

is considered as an approximate solution of (2.5)-(2.6). Such a combination of MPS and MFS is called the dual reciprocity method (DRM).

## 2.2 Numerical Examples by DRM

**Example 2.1.** Consider the Dirichlet boundary problem for the Poisson's equation

$$\Delta u(x, y) = 4e^{2x} + 6y, \quad (x, y) \in \Omega,$$

$$u(x, y) = e^{2x} + y^3, \quad (x, y) \in \partial\Omega,$$

where  $\Omega = \{(x, y) : x^2 + y^2 \leq 1\}$  is the unit disc. The exact solution of the above problem is  $u_{exact} = e^{2x} + y^3$ . Choose  $\phi(r) = \sqrt{r^2 + c^2}$ , where  $r = \|\mathbf{x}\|$  and  $c = 0.5, 1, 2$ , respectively, and use  $\mathbf{x}_k = (r_k \cos \frac{2\pi k}{M}, r_k \sin \frac{2\pi k}{M})$ ,  $r_k = \frac{k}{M}$ ,  $1 \leq k \leq M$ , in  $\Omega$  to get  $u_p$  in (2.4). Next, we use the MFS to obtain  $u_N$ , as discussed in section by using  $N$  points equally spaced on  $\partial\Omega$  and choosing a fictitious domain  $\tilde{\Omega} = \{(x, y) : x^2 + y^2 \leq 3^2\}$ . Let  $\tilde{\mathbf{x}}_k = 3(\cos \frac{2\pi k}{N}, \sin \frac{2\pi k}{N})$ ,  $0 \leq$

$k \leq N - 1$  on  $\partial\tilde{\Omega}$ . Then the approximate solution  $u_N$  of the BVP (2.7)-(2.8) can be obtained.

To estimate the maximum error (1.6), we use  $M^2$  points  $\mathbf{z}_{k,m} = (r_k \cos \frac{2\pi m}{M}, r_k \sin \frac{2\pi m}{M})$ ,  $r_k = \frac{k}{M}$ ,  $1 \leq k, m \leq M$ , in  $\Omega$  and  $\mathbf{z}_k = (\cos \frac{2\pi k}{N}, \sin \frac{2\pi k}{N})$ ,  $0 \leq k \leq N - 1$  on  $\partial\Omega$ , where  $\bar{\Omega} = \Omega \cup \partial\Omega$ , to get the numerical estimate for

$$\max |u_{exact}(\mathbf{z}_k) - u_A(\mathbf{z}_k)|_{C(\bar{\Omega})}.$$

Then our numerical approximation errors are presented in the following table with various  $c$ ,  $M$ , and  $N$ :

Figure 2.2:  $M = 10, 110$  points in  $\bar{\Omega} = \Omega \cup \partial\Omega$  and  $N = 10$  points on  $\partial\tilde{\Omega}$  with  $r = 1.5$

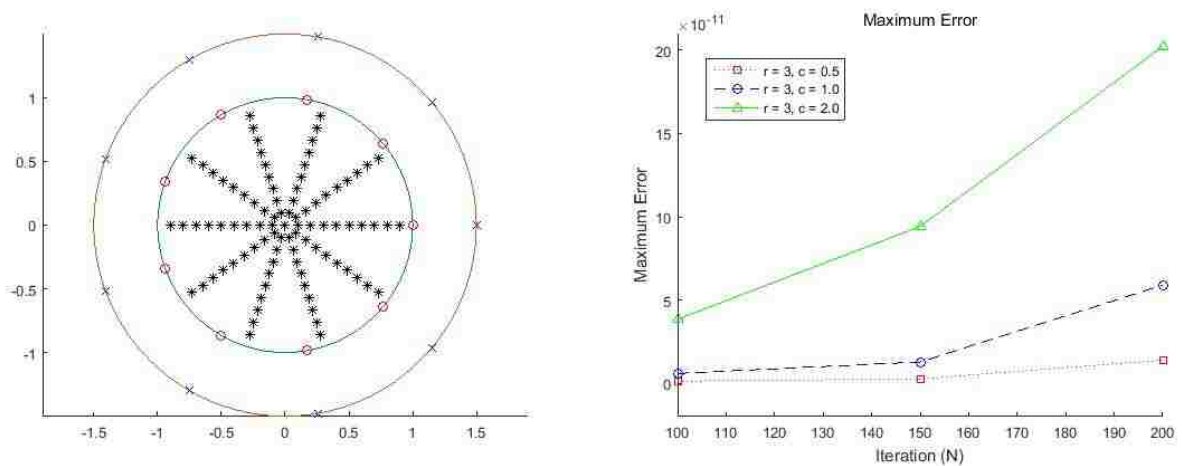


Table 2.1: Maximum Error  $\|u_{exact} - u_A\|_{C(\bar{\Omega})}$

	M = 70 N = 30	M = 100 N = 50	M = 150 N = 50
r = 3, c = 0.5	1.3281e-12	2.6550e-12	1.3975e-11
r = 3, c = 1.0	5.9295e-12	1.2833e-11	5.8940e-11
r = 3, c = 2.0	3.8501e-11	9.4205e-11	2.0234e-10

**Example 2.2.** Consider the Dirichlet boundary problem for the Poisson's equation

$$\Delta u(x, y) = e^x \tan(y)(1 + 2 \sec^2(y)), \quad (x, y) \in \Omega,$$

$$u(x, y) = e^x \tan(y), \quad (x, y) \in \partial\Omega,$$

where  $\partial\Omega = \{(x, y) : x = \cos(t + \sin t), y = \sin(t + \cos t), 0 \leq t \leq 2\pi\}$ . The exact solution of the above problem is  $u_{exact} = e^x \tan(y)$ . Choose  $\phi(r) = \sqrt{r^2 + c^2}$ , where  $r = \|\mathbf{x}\|$  and  $c = 0.5, 1, 2$ , respectively, and use  $\mathbf{x}_k = (r_k \cos(\frac{2\pi k}{M} + \sin \frac{2\pi k}{M}), r_k \sin(\frac{2\pi k}{M} + \cos \frac{2\pi k}{M}))$ ,  $r_k = \frac{k}{M}$ ,  $1 \leq k \leq M$ , in  $\Omega$  to get  $u_p$  in (2.4). Then the approximate solution  $u_N$  of the BVP (2.7)-(2.8) can be obtained and our maximum error is also estimated as in Example 2.1. We use a fictitious domain  $\tilde{\Omega} = \{(x, y) : x = 2 \cos t, y = 2 \sin(t + \cos t), 0 \leq t \leq 2\pi\}$ . We choose  $\tilde{\mathbf{x}}_k = (2 \cos \frac{2\pi k}{N}, 2 \sin(\frac{2\pi k}{N} + \cos \frac{2\pi k}{N}))$ ,  $0 \leq k \leq N - 1$  on  $\partial\tilde{\Omega}$ . To estimate the maximum error (1.6), we use  $M^2$  points  $\mathbf{z}_{k,m} = (r_k \cos(\frac{2\pi m}{M} + \sin \frac{2\pi m}{M}), r_k \sin(\frac{2\pi m}{M} + \cos \frac{2\pi m}{M}))$ ,  $r_k = \frac{k}{M}$ ,  $1 \leq k, m \leq M$ , in  $\Omega$  and  $\mathbf{z}_k = (\cos(\frac{2\pi k}{N} + \sin \frac{2\pi k}{N}), \sin(\frac{2\pi k}{N} + \cos \frac{2\pi k}{N}))$ ,  $0 \leq k \leq N - 1$  on  $\partial\Omega$ ,

where  $\bar{\Omega} = \Omega \cup \partial\Omega$ , to get the numerical infinity norm as in Example 2.1. Then our numerical approximation errors are presented in the following table with various  $c$ ,  $M$ , and  $N$ :

Figure 2.3:  $M = 10$ , 110 points in  $\bar{\Omega} = \Omega \cup \partial\Omega$  and  $N = 10$  points on  $\partial\tilde{\Omega}$  with  $r = 2$

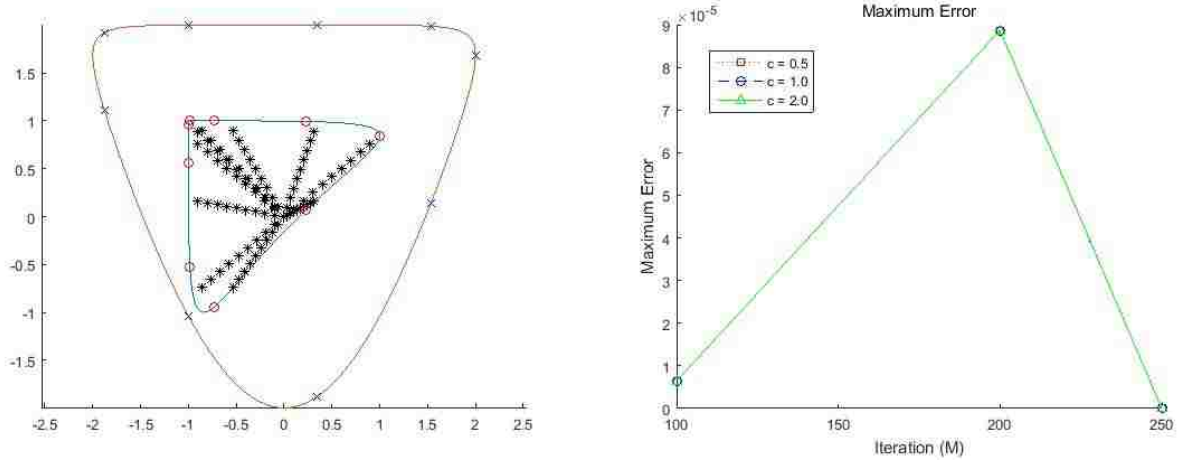


Table 2.2: Maximum Error  $\|u_{exact} - u_A\|_{C(\bar{\Omega})}$

	M = 70 N = 30	M = 140 N = 60	M = 150 N = 100
$c = 0.5$	6.4842e-06	8.8665e-05	5.2443e-12
$c = 1.0$	6.4842e-06	8.8665e-05	3.1248e-10
$c = 2.0$	6.4842e-06	8.8665e-05	7.4231e-09



**Example 2.3.** Consider the Dirichlet boundary problem for the Poisson's equation

$$\Delta u(x, y, z) = e^{x-y} \cos(z), \quad (x, y, z) \in \Omega,$$

$$u(x, y, z) = e^{x-y} \cos(z), \quad (x, y, z) \in \partial\Omega,$$

where  $\Omega = \{(x, y, z) : x^2 + y^2 + z^2 \leq 1\}$ . The exact solution of the above problem is  $u_{exact} = e^{x-y} \cos(z)$ . Choose  $\phi(r) = \sqrt{r^2 + c^2}$ , where  $r = \|\mathbf{x}\|$  and  $c = 0.5, 1, 2$ , respectively, and use  $\mathbf{x}_k = (r_k \cos \frac{2\pi k}{M} \sin \frac{\pi k}{M}, r_k \sin \frac{2\pi k}{M} \sin \frac{\pi k}{M}, r_k \cos \frac{\pi k}{M})$ ,  $r_k = \frac{k}{M}$ ,  $1 \leq k \leq M$ , in  $\Omega$  to get  $u_p$  in (2.4). Then the approximate solution  $u_N$  of the BVP (2.7)-(2.8) can be obtained and our maximum error is also estimated as in Example 2.1. We use a fictitious domain  $\tilde{\Omega} = \{(x, y, z) : x^2 + y^2 + z^2 \leq R^2\}$ , where  $R = 1.5, 2, 3, 3.5$ . We choose  $\tilde{\mathbf{x}}_k = (R \cos \frac{2\pi k}{M} \sin \frac{\pi k}{M}, R \sin \frac{2\pi k}{M} \sin \frac{\pi k}{M}, R \cos \frac{\pi k}{M})$ ,  $R = \{1.5, 2, 3, 3.5\}$ ,  $1 \leq k \leq M$ , on  $\partial\tilde{\Omega}$ . To estimate the maximum error (1.6), we use  $M^3$  points  $\mathbf{z}_{k,l,m} = (r_k \cos \frac{2\pi l}{M} \sin \frac{\pi m}{M}, r_k \sin \frac{2\pi l}{M} \sin \frac{\pi m}{M}, r_k \cos \frac{\pi m}{M})$ ,  $r_k = \frac{k}{M}$ ,  $1 \leq k, l, m \leq M$ , in  $\Omega$  and  $\mathbf{z}_k = (\cos \frac{2\pi k}{N} \sin \frac{\pi k}{N}, \sin \frac{2\pi k}{N} \sin \frac{\pi k}{N}, \cos \frac{\pi k}{N})$ ,  $0 \leq k \leq N-1$  on  $\partial\Omega$ , where  $\bar{\Omega} = \Omega \cup \partial\Omega$ , to get the numerical infinity norm in Example 2.1. Then our numerical approximation errors are presented in the following table with various  $R, c, M$ , and  $N$ :

Figure 2.4:  $M = 10, 1,010$  points in  $\bar{\Omega} = \Omega \cup \partial\Omega$  and  $N = 10$  points on  $\partial\tilde{\Omega}$  with  $R = 2$

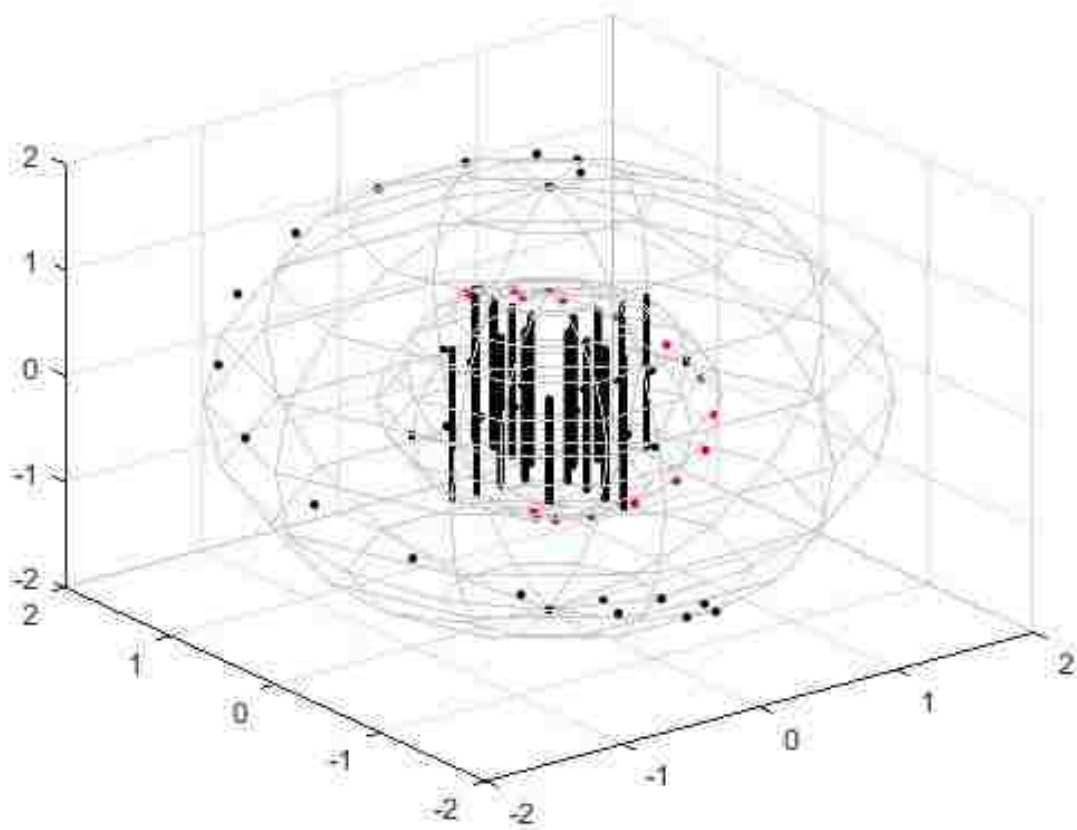
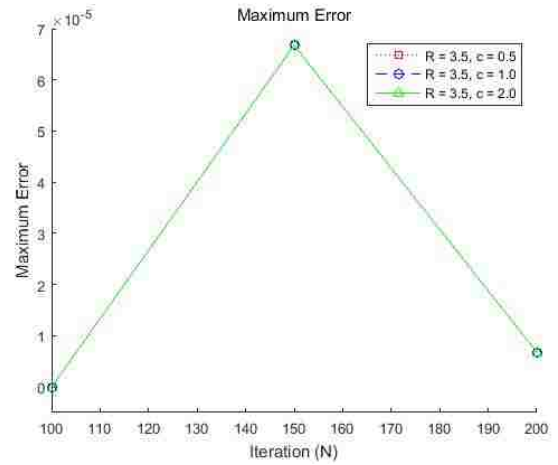
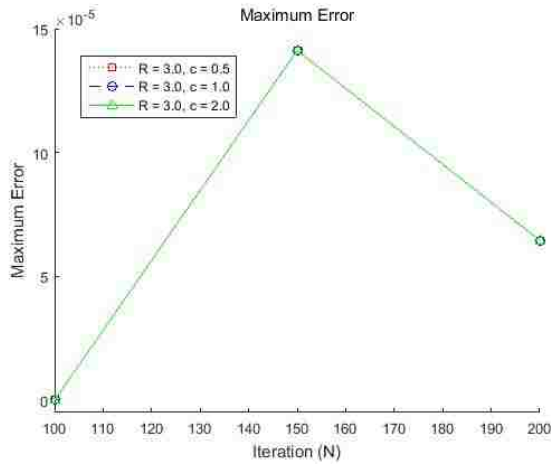
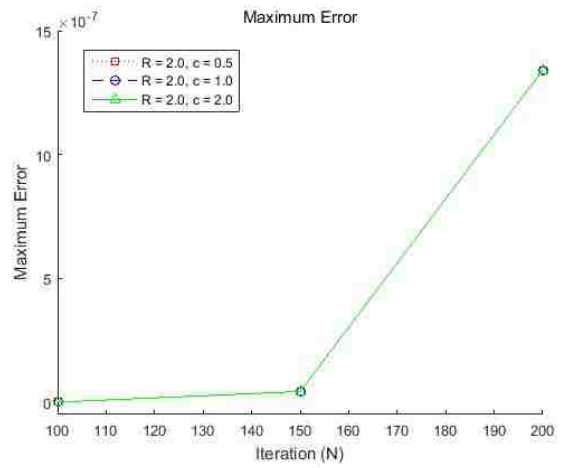
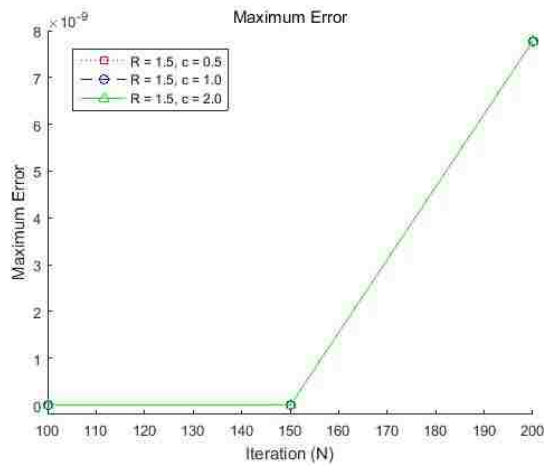


Table 2.3: Maximum Error  $\|u_{exact} - u_A\|_{C(\bar{\Omega})}$

	M = 70 N = 30	M = 90 N = 60	M = 120 N = 80
R = 1.5, c = 0.5	3.1612e-12	1.8190e-12	7.7796e-09
R = 1.5, c = 1.0	3.1612e-12	1.8190e-12	7.7796e-09
R = 1.5, c = 2.0	3.8769e-12	2.8000e-12	7.7796e-09
R = 2.0, c = 0.5	3.1446e-11	4.2837e-08	1.3402e-06
R = 2.0, c = 1.0	3.1446e-11	4.2837e-08	1.3402e-06
R = 2.0, c = 2.0	3.1446e-11	4.2837e-08	1.3402e-06
R = 3.0, c = 0.5	4.9695e-11	1.4119e-04	6.4563e-05
R = 3.0, c = 1.0	4.9695e-11	1.4119e-04	6.4563e-05
R = 3.0, c = 2.0	4.9695e-11	1.4119e-04	6.4563e-05
R = 3.5, c = 0.5	3.3019e-10	6.6754e-05	6.8057e-06
R = 3.5, c = 1.0	3.3019e-10	6.6754e-05	6.8057e-06
R = 3.5, c = 2.0	3.3019e-10	6.6754e-05	6.8057e-06

Figure 2.5: Maximum errors with  $c = 0.5$  ( $\square$ ),  $c = 1.0$  ( $\circ$ ),  $c = 2.0$  ( $\triangle$ ), respectively



## 2.3 On Convergence of DRM in $\mathbb{R}^2$

The convergence of DRM was discussed in [25], where the boundary value problems are solved by integral equations with double layer potentials. Here by using the convergence results of MFS described in section 1.4, we will describe the rate of convergence of DRM by using RBF approximation in [16].

For  $\delta > 0$ , let  $\Omega_\delta = \Omega + \delta I := \{\mathbf{x} + \mathbf{y} : \mathbf{x} \in \Omega, \mathbf{y} \in \delta I\}$ , where  $I = [-1, 1]^s$ . For any integer  $n$ , set

$$I_n(\Omega_\delta) = \left\{ \mathbf{j} \in \mathbb{Z}^s : \left[ \frac{\mathbf{j}}{n}, \frac{\mathbf{j} + \mathbf{1}}{n} \right]^s \cap \Omega_\delta \neq \emptyset \right\},$$

where  $\mathbf{1} = (1, \dots, 1) \in \mathbb{Z}^s$ . For  $1 \leq p \leq \infty$ , denote by  $\mathcal{W}^{1,p}(\Omega)$  the space of all functions  $f$  whose gradient is in  $\mathcal{L}^p(\Omega)$  with the usual Sobolev norm

$$\|f\|_{\mathcal{W}^{1,p}(\Omega)} = \|f\|_{\mathcal{L}^p(\Omega)} + \sum_{k=1}^s \left\| \frac{\partial f}{\partial x_k} \right\|_{\mathcal{L}^p(\Omega)}.$$

For a function  $f \in \mathcal{W}^{1,p}(\Omega_\delta)$ , one can choose a smooth function  $\chi$  such that  $\chi$  is identical to 1 on the closure  $\bar{\Omega}$ , and vanishes outside of  $\Omega_\delta$ . Let  $f_\chi = f \cdot \chi$ , then  $f_\chi \in \mathcal{W}^{1,p}(R^s)$  and it is compactly supported in  $\bar{\Omega}_\delta$ . Denote by  $\mathcal{W}_0^{1,p}(\Omega_\delta)$  the subspace of functions in  $\mathcal{W}^{1,p}(R^s)$  which vanish outside of  $\Omega_\delta$ . We then consider the approximation of functions in  $\mathcal{W}_0^{1,p}(\Omega_\delta)$  over the domain  $\Omega$ . Suppose that  $\phi \in \mathcal{L}^1(R^s)$  is given with the property

$$\int_{R^s} \phi(\mathbf{x}) \, d\mathbf{x} = 1. \quad (2.9)$$

Choose  $\gamma$  such that  $0 < \gamma \leq 1$ . For every  $f \in \mathcal{W}_0^{1,p}(\Omega_\delta)$  and an integer  $n \geq 1$ , let

$$\mathcal{B}_{n,\gamma} f(\mathbf{x}) = \frac{1}{n^{s(1-\gamma)}} \sum_{\mathbf{j} \in I_n(\Omega_\delta)} f\left(\frac{\mathbf{j}}{n}\right) \phi(n^\gamma \mathbf{x} - \mathbf{j}n^{\gamma-1}). \quad (2.10)$$

Let  $q$  satisfy  $\frac{1}{p} + \frac{1}{q} = 1$ . If  $p = \infty$ , we consider  $q = 1$ . For  $\alpha > 0$ , let  $\mathcal{S}^\alpha(R^s)$  be the set consisting of all functions  $\phi$  satisfying

$$|\phi(\mathbf{x})| \leq c(1 + \|\mathbf{x}\|)^{-\alpha}. \quad (2.11)$$

The following result holds and a more general result can be found in [17].

**Theorem 2.1.** *Let  $m \geq 0$ . Suppose that  $\phi \in \mathcal{S}^{m+1,\alpha}(R^s)$  for some  $\alpha > s + 1$ . Then for any  $f \in \mathcal{C}_0^{m+1}(\Omega_\delta)$ , and an integer  $n$ , the inequality*

$$\|\mathcal{B}_{n,\frac{1}{m+2}}f - f\|_{\mathcal{C}^m(\Omega)} \leq \frac{c}{m+2\sqrt[m]{n}}\|f\|_{\mathcal{C}^{m+1}(\Omega_\delta)},$$

holds and when  $\alpha = s + 1$ ,

$$\|\mathcal{B}_{n,\frac{1}{m+2}}f - f\|_{\mathcal{C}^m(\Omega)} \leq \frac{c \ln n}{m+2\sqrt[m]{n}}\|f\|_{\mathcal{C}^{m+1}(\Omega_\delta)}.$$

Choose  $\phi$  to be a radial basis function, i.e.  $\phi(\mathbf{x}) = \phi(r)$ , where  $r = \|\mathbf{x}\|$ . Then the condition (2.9) becomes

$$\int_0^\infty r^{s-1}\phi(r) dr = \frac{1}{\omega_s}, \quad s \geq 2, \quad (2.12)$$

where  $\omega_s = \frac{2\pi^{s/2}}{\Gamma(s/2)}$  is the surface area of the unit sphere in  $\mathbb{R}^s$ .

**Lemma 2.1.** *For a RBF  $\phi(r)$ , a radially particular solution of  $\Delta\psi = \phi$  is given by*

$$\psi(r) = -\frac{1}{(s-2)r^{s-2}} \int_0^r t^{s-1}\phi(t) dt + \frac{1}{s-2} \int_0^r t\phi(t) dt + \frac{A}{r^{s-2}} + B, \quad s \geq 3, \quad (2.13)$$

or

$$\psi(r) = \left( \int_0^r t \phi(t) dt \right) \ln r - \int_0^r t \phi(t) \ln t dt + A \ln r + B, \quad s = 2, \quad (2.14)$$

where  $A$  and  $B$  are constants.

For clarity, we present the proof in the following.

*Proof.* A radial solution of  $\Delta\psi = \phi$  satisfies

$$\frac{\partial^2\psi}{\partial r^2} + \frac{s-1}{r} \frac{\partial\psi}{\partial r} = \phi(r),$$

which can be written as

$$\frac{1}{r^{s-1}} \frac{\partial}{\partial r} \left( r^{s-1} \frac{\partial\psi}{\partial r} \right) = \phi(r).$$

Hence,

$$\frac{\partial\psi}{\partial r} = \frac{1}{r^{s-1}} \int_0^r t^{s-1} \phi(t) dt + \frac{c_1}{r^{s-1}}.$$

For  $s \geq 3$ , we have

$$\begin{aligned} \psi(r) &= \int_1^r \left( \frac{1}{\tau^{s-1}} \int_0^\tau t^{s-1} \phi(t) dt \right) d\tau + \frac{c_2}{r^{s-2}} + c_3 \\ &= \int_1^r \left( \frac{d}{d\tau} \left( -\frac{1}{(s-2)\tau^{s-2}} \right) \int_0^\tau t^{s-1} \phi(t) dt \right) d\tau + \frac{c_2}{r^{s-2}} + c_3 \\ &= -\frac{1}{(s-2)r^{s-2}} \int_0^r t^{s-1} \phi(t) dt + \frac{1}{s-2} \int_1^r \tau \phi(\tau) d\tau + \frac{c_2}{r^{s-2}} + c_4 \\ &= -\frac{1}{(s-2)r^{s-2}} \int_0^r t^{s-1} \phi(t) dt + \frac{1}{s-2} \int_0^r t \phi(t) dt + \frac{A}{r^{s-2}} + B. \end{aligned}$$

If  $s = 2$ , then

$$\begin{aligned} \psi(r) &= \int_1^r \left( \frac{1}{r} \int_0^r t \phi(t) dt + \frac{A}{r} \right) dr + c \\ &= \left( \int_0^r t \phi(t) dt \right) \ln r - \int_0^r t \phi(t) \ln t dt + A \ln r + B. \end{aligned}$$

This lemma is proved.  $\square$

To ensure that  $\psi$  is differentiable at 0, we choose  $A = 0$ , and also set  $B = 0$  for the simplicity of discussion. Assume that  $f$  is compactly supported in  $\Omega_\delta$ . Choose a radial basis

$\phi$  satisfying the conditions in Theorem 2.1, and let  $\psi$  be the corresponding solution given by (2.13) or (2.14). Set

$$\tilde{u}_n(\mathbf{x}) = \frac{1}{n^{s(1-\gamma)}} \sum_{\mathbf{j} \in I_n(\Omega_\delta)} f\left(\frac{\mathbf{j}}{n}\right) n^{2\gamma} \psi(n^\gamma(\mathbf{x} - \mathbf{j}/n)). \quad (2.15)$$

Then

$$\Delta \tilde{u}_n(\mathbf{x}) = \mathcal{B}_{n,\gamma} f(\mathbf{x}).$$

The following result is shown in [16].

**Proposition 2.1.** *Suppose that a radial basis function  $\phi \in \mathcal{W}^{1,p}(R^s) \cap \mathcal{S}^\alpha(R^s)$  where  $\alpha > s$ . Let  $\tilde{u}_n$  be given by (2.15). Then, for any  $f \in \mathcal{W}_0^{1,p}(\Omega_\delta)$  and large  $n$ ,*

$$\|\Delta \tilde{u}_n - f\|_{\mathcal{L}^p(R^s)} \leq \frac{c}{n^\tau} \|f\|_{\mathcal{W}^{1,p}(\Omega_\delta)}, \quad (2.16)$$

where  $\tau = \min\{\gamma(\alpha - s), \gamma\}$ . Moreover, for sufficiently large  $\mathbf{x}$ ,

$$|\Delta \tilde{u}_n(\mathbf{x})| \leq \frac{c}{\|\mathbf{x}\|^\alpha} \|f\|_{\mathcal{L}^\infty(\Omega_\delta)}.$$

For a given bounded domain  $\Omega$  in  $\mathbb{R}^2$ , choose  $\mathbf{x}_0$  such that  $\mathcal{B}(\mathbf{x}_0, \delta) \cap \Omega_\delta = \emptyset$ , where  $\mathcal{B}(\mathbf{x}_0, \delta) = \{\mathbf{x} \in \mathbb{R}^2, \|\mathbf{x} - \mathbf{x}_0\| < \delta\}$ . Let  $\tilde{u}_n$  be given by (2.15), which is expressed as

$$\tilde{u}_n(\mathbf{x}) = \frac{1}{n^2} \sum_{\mathbf{j} \in I_n(\Omega_\delta)} f\left(\frac{\mathbf{j}}{n}\right) \left[ \left( \int_0^{n^\gamma \|\mathbf{x} - \mathbf{j}/n\|} t \phi(t) dt \right) \ln(n^\gamma \|\mathbf{x} - \mathbf{j}/n\|) - \int_0^{n^\gamma \|\mathbf{x} - \mathbf{j}/n\|} t \phi(t) \ln(t) dt \right].$$

Set

$$a_n := \left[ \frac{1}{n^2} \sum_{\mathbf{j} \in I_n(\Omega_\delta)} f\left(\frac{\mathbf{j}}{n}\right) \right] \int_0^\infty t \phi(t) dt,$$

$$b_n := \left[ \frac{1}{n^2} \sum_{\mathbf{j} \in I_n(\Omega_\delta)} f\left(\frac{\mathbf{j}}{n}\right) \right] \int_0^\infty t \phi(t) \ln(t) dt.$$



Let

$$\bar{u}_n(\mathbf{x}) = a_n \ln(n^\gamma \|\mathbf{x} - \mathbf{x}_0\|) - b_n,$$

and

$$u_n(\mathbf{x}) = \tilde{u}_n(\mathbf{x}) - \bar{u}_n(\mathbf{x}). \quad (2.17)$$

A particular solution of (2.5) is known and given by the classical Newtonian potential

$$u(\mathbf{x}) = \frac{1}{2\pi} \int_{\Omega} f(\mathbf{y}) \ln \|\mathbf{x} - \mathbf{y}\| d\mathbf{y}, \quad (2.18)$$

in  $\mathbb{R}^2$  and in view of (2.18), we define

$$u_p(\mathbf{x}) = \frac{1}{2\pi} \int_{\Omega_\delta} f(\mathbf{y}) \ln \|\mathbf{x} - \mathbf{y}\| d\mathbf{y} - a_0 \ln(\|\mathbf{x} - \mathbf{x}_0\|), \quad (2.19)$$

where

$$a_0 = \frac{1}{2\pi} \int_{\Omega_\delta} f(\mathbf{y}) d\mathbf{y}.$$

Then obviously  $u_p(\mathbf{x})$  satisfies  $\Delta u_p(\mathbf{x}) = f(\mathbf{x})$  in  $\Omega$ . And for sufficiently large  $\mathbf{x}$  we have

$$\begin{aligned} |u_p(\mathbf{x})| &= \frac{1}{2\pi} \left| \int_{\Omega_\delta} f(\mathbf{y}) \ln \frac{\|\mathbf{x} - \mathbf{y}\|}{\|\mathbf{x} - \mathbf{x}_0\|} d\mathbf{y} \right| \\ &\leq \frac{1}{2\pi} \int_{\Omega_\delta} |f(\mathbf{y})| \ln \frac{\|\mathbf{x}\| + \rho}{\|\mathbf{x}\| - \rho} d\mathbf{y} \\ &\leq \frac{1}{2\pi} \int_{\Omega_\delta} |f(\mathbf{y})| \ln \left( 1 + \frac{2\rho}{\|\mathbf{x}\| - \rho} \right) d\mathbf{y} \\ &\leq \left( \frac{1}{2\pi} \int_{\Omega_\delta} |f(\mathbf{y})| d\mathbf{y} \right) \frac{2\rho}{\|\mathbf{x}\| - \rho} \\ &\leq \frac{c}{\|\mathbf{x}\|} \|f\|_{\mathcal{L}^1(\Omega_\delta)}. \end{aligned}$$

Let  $\mathcal{D} = \mathcal{B}(\mathbf{x}_0, \delta)^c$ , the complement of  $\mathcal{B}(\mathbf{x}_0, \delta)$ , and

$$\mathcal{O}_{s,\alpha}(n) := \begin{cases} \frac{1}{n^\tau}, & \alpha \neq s + 2, \\ \frac{\ln n}{n^\tau}, & \alpha = s + 2. \end{cases} \quad (2.20)$$

where  $\tau := \min\{\gamma(\alpha - s), 2\gamma\}$ .

The following result is derived in [16].

**Theorem 2.2.** *Suppose that a radial basis function  $\phi \in \mathcal{W}^{1,\infty}(\mathbb{R}^2) \cap \mathcal{S}^\alpha(\mathbb{R}^2)$  for some  $\alpha > 2$ . Let  $u_n, u_p$  be given by (2.17) and (2.19), respectively. Then*

$$\|u_n - u_p\|_{\mathcal{L}^\infty(\mathcal{D})} \leq c \mathcal{O}_{2,\alpha}(n) \ln(n) \|f\|_{\mathcal{L}^\infty(\Omega_\delta)} + \frac{c}{n} \|f\|_{\mathcal{W}_0^{1,\infty}(\Omega_\delta)},$$

where  $\mathcal{O}_{2,\alpha}(n)$  is given by (2.20) with  $s = 2$ . And moreover for sufficiently large  $\mathbf{x}$ ,

$$|u_n(\mathbf{x})| \leq \frac{c \ln \|\mathbf{x}\|}{\|\mathbf{x}\|^\beta} \|f\|_{\mathcal{W}_0^{1,\infty}(\Omega_\delta)},$$

where  $\beta := \min\{\alpha - 2, 1\}$ .

Now we consider the approximation for the Newtonian potentials in  $\mathbb{R}^s$ ,  $s \geq 3$ . Let  $\tilde{u}_n$  be given by (2.15). From Lemma 2.1, we have

$$\begin{aligned} \tilde{u}_n(\mathbf{x}) &= -\frac{1}{n^{s(1-\gamma)+2\gamma}} \sum_{\mathbf{j} \in I_n(\Omega_\delta)} f\left(\frac{\mathbf{j}}{n}\right) \frac{1}{(s-2)(n^\gamma \|\mathbf{x} - \mathbf{j}/n\|)^{s-2}} \int_0^{n^\gamma \|\mathbf{x} - \mathbf{j}/n\|} t^{s-1} \phi(t) dt \\ &\quad + \frac{1}{n^{s(1-\gamma)+2\gamma}} \sum_{\mathbf{j} \in I_n(\Omega_\delta)} f\left(\frac{\mathbf{j}}{n}\right) \frac{1}{s-2} \int_0^{n^\gamma \|\mathbf{x} - \mathbf{j}/n\|} t \phi(t) dt \end{aligned} \quad (2.21)$$

Introduce a constant

$$C_n = \frac{1}{(s-2)n^{s(1-\gamma)+2\gamma}} \sum_{\mathbf{j} \in I_n(\Omega_\delta)} f\left(\frac{\mathbf{j}}{n}\right) \int_0^\infty t \phi(t) dt. \quad (2.22)$$

Set

$$u_n(\mathbf{x}) = \tilde{u}_n(\mathbf{x}) - C_n. \quad (2.23)$$

Denote by  $u_p$  the Newtonian potential of  $f$  over  $\Omega_\delta$ , i.e.

$$u_p(\mathbf{x}) = -\frac{1}{(s-2)\omega_s} \int_{\Omega_\delta} f(\mathbf{y}) \frac{1}{\|\mathbf{x} - \mathbf{y}\|^{(s-2)}} d\mathbf{y}. \quad (2.24)$$

As before assume that  $\Omega$  is bounded. Then the next result is shown in [16].

**Theorem 2.3.** *Suppose that  $\phi \in \mathcal{W}^{1,\infty}(R^s) \cap \mathcal{S}^\alpha(R^s)$  for some  $\alpha > s$  and  $f \in \mathcal{W}_0^{1,\infty}(\Omega_\delta)$ .*

*Let  $u_n, u_p$  be given by (2.23), (2.24), respectively. Then*

$$\|u_n - u_p\|_{\mathcal{L}^\infty(R^s)} \leq c\mathcal{O}_{s,\alpha}(n)\|f\|_{\mathcal{L}^\infty(\Omega_\delta)} + \frac{c}{n}\|f\|_{\mathcal{W}_0^{1,\infty}(\Omega_\delta)},$$

*And for sufficiently large  $\mathbf{x}$ ,*

$$|u_n(\mathbf{x})| \leq \frac{c}{\|\mathbf{x}\|^{s-2}}\|f\|_{\mathcal{L}^\infty(\Omega_\delta)}. \quad (2.25)$$

For the sake of discussion, we consider radial basis functions of the form  $\phi(r^2)$  with the property that

$$\int_{R^s} \phi(r^2) d\mathbf{x} = 1, \quad (2.26)$$

and moreover we require that  $\phi$  is  $l$  times continuously differentiable and its derivatives decay in the following order

$$\frac{d^i \phi}{dx^i}(r^2) = O(x^{-i}), \quad x \rightarrow \infty, \quad (2.27)$$

for  $0 \leq i \leq l$ . The following example shows that several commonly used radial basis functions satisfy the conditions (2.26) and (2.27).

**Example 2.4.** 1: The Gaussian function

$$\phi(r^2) = \left(\frac{c}{\pi}\right)^{s/2} e^{-cr^2}, \quad c > 0.$$

2: The following compactly supported radial basis functions

$$\phi(r^2) = \begin{cases} (k+1)(1-r^2)^k/\pi, & 0 \leq r \leq 1, \\ 0, & r > 1, \end{cases}$$

for  $k \geq l+1$  in  $\mathbb{R}^2$ , or

$$\phi(r^2) = \begin{cases} ((2n+3)!!)(1-r^2)^n/(4\pi(2n)!!), & 0 \leq r \leq 1, \\ 0, & r > 1, \end{cases}$$

in  $\mathbb{R}^3$ , where

$$n!! = \begin{cases} 1 \cdot 3 \cdots n, & \text{if } n \text{ is an odd number,} \\ 2 \cdot 4 \cdots n, & \text{if } n \text{ is an even number.} \end{cases}$$

3: The inverse multiquadratics

$$\phi(r^2) = \frac{k-1}{\pi(r^2+1)^k}, \quad k > 2,$$

in  $\mathbb{R}^2$ , or

$$\phi(r^2) = \frac{1}{2\pi^2} \frac{(2n-2)!!}{(2n-5)!!} \frac{1}{(r^2+1)^n}, \quad n \geq 3$$

in  $\mathbb{R}^3$ .

Suppose that  $\phi$  satisfies (2.26) and (2.27), and  $\psi$  is the solution of  $\Delta\psi = \phi$ . Let  $\tilde{u}_n$  be the approximate particular solution given by (2.15) or (2.21). Then it is shown in the Proposition 4.4 of [25] that

$$\|\tilde{u}_n\|_{\mathcal{W}^{l,p}(\partial\Omega)} \leq c n^{(l+s)\tau}, \quad (2.28)$$

for any  $p$ ,  $1 \leq p \leq \infty$ . Now if  $u_n$  is given by (2.15) or (2.21), then obviously

$$\|u_n\|_{\mathcal{W}^{l,p}(\partial\Omega)} \leq c n^{(l+s)\tau}. \quad (2.29)$$

Next we establish the convergent result of MPS and MFS for solving the Dirichlet problem of Poisson's equation in  $\mathbb{R}^2$ .

Assume  $\Omega = \{\mathbf{x} \in \mathbb{R}^2 : \|\mathbf{x}\|_2 < r\}$ . Without loss of generality, assume  $r < \pi$ , otherwise a simple scaling transformation can be used to transform  $\Omega$  inside  $[-\pi, \pi]^2$ .

**Theorem 2.4.** *Let  $u$  be the exact solution of*

$$\begin{aligned}\Delta u(\mathbf{x}) &= f(\mathbf{x}), & \mathbf{x} \in \Omega, \\ u(\mathbf{x}) &= h(\mathbf{x}), & \mathbf{x} \in \partial\Omega,\end{aligned}$$

where  $\Omega = \{\mathbf{x} \in \mathbb{R}^2 : \|\mathbf{x}\|_2 < r\}$ . Suppose  $h(t) := h(r \cos t, r \sin t) \in C^j([-\pi, \pi])$  for some  $j$ ,  $2 \leq j \leq l-1$ . Let  $u_p$  be an approximate particular solution given in (2.4) and  $v_{n,N,k}$  the numerical solution of

$$\begin{aligned}\Delta v(\mathbf{x}) &= 0, & \|\mathbf{x}\|_2 < r, \\ v(\mathbf{x}) &= h(\mathbf{x}) - u_p(\mathbf{x}), & \|\mathbf{x}\|_2 = r,\end{aligned}$$

given by MFS (cf. (1.16)). Let

$$u_{n,N,k} = u_p + v_{n,N,k}$$

then

$$\|u_{n,N,k} - u\|_{\mathcal{L}^2(\Omega)} \leq \frac{c}{n^\tau} \|f\|_{\mathcal{W}^{1,2}(\Omega_\delta)} + c n^{(j+2)\gamma} \left( \frac{1}{k^{j-1}} + \frac{(r/R)^{2(N-k)}}{1 - (r/R)^{2N}} \right),$$

for any  $R > r$  and  $R \neq 1$ , where  $k < N - 1$ ,  $\tau := \min\{\gamma(\alpha - s), 2\gamma\}$ , and  $c$  is a constant independent of  $f$ ,  $N$ ,  $n$ ,  $k$ .

*Proof.* Let  $v_n$  be the exact solution of

$$\begin{aligned}\Delta v(\mathbf{x}) &= 0, & \mathbf{x} \in \Omega, \\ v(\mathbf{x}) &= h(\mathbf{x}) - u_p(\mathbf{x}), & \mathbf{x} \in \partial\Omega.\end{aligned}$$

Set

$$\tilde{u}_n(\mathbf{x}) = u_p(\mathbf{x}) + v_n(\mathbf{x}).$$

Then

$$\|u_{n,N,k} - u\|_{\mathcal{L}^2(\Omega)} \leq \|u_{n,N,k} - \tilde{u}_n\|_{\mathcal{L}^2(\Omega)} + \|\tilde{u}_n - u\|_{\mathcal{L}^2(\Omega)}. \quad (2.30)$$

From Theorem 1.1 and (2.29),

$$\begin{aligned}\|u_{n,N,k} - \tilde{u}_n\|_{\mathcal{L}^2(\Omega)} &= \|v_n - v_{n,N,k}\|_{\mathcal{L}^2(\Omega)} \\ &\leq c \|(h - u_p)^{(j)}\|_{\mathcal{L}^\infty([-\pi, \pi])} \left( \frac{1}{k^{j-1}} + \frac{(r/R)^{2(N-k)}}{1 - (r/R)^{2N}} \right) \\ &\leq c n^{(j+2)\gamma} \left( \frac{1}{k^{j-1}} + \frac{(r/R)^{2(N-k)}}{1 - (r/R)^{2N}} \right).\end{aligned} \quad (2.31)$$

Note that for  $\mathbf{x} \in \Omega$ ,

$$\Delta(\tilde{u}_n - u) = \Delta u_p + \Delta v_n - \Delta u = \mathcal{B}_{n,\gamma} f - f,$$

and thus from Proposition 2.1,

$$\|\Delta(\tilde{u}_n - u)\|_{\mathcal{L}^2(\Omega)} \leq \frac{c}{n^\tau} \|f\|_{\mathcal{W}^{1,2}(\Omega_\delta)}, \quad (2.32)$$

When  $\mathbf{x} \in \partial\Omega$ ,

$$\tilde{u}_n(\mathbf{x}) - u(\mathbf{x}) = u_p(\mathbf{x}) + h(\mathbf{x}) - u_p(\mathbf{x}) - h(\mathbf{x}) = 0. \quad (2.33)$$

It follows from (2.32) and (2.33) and a-priori estimate (cf. [29]) that

$$\|\tilde{u}_n - u\|_{\mathcal{L}^2(\Omega)} \leq \frac{c}{n^\tau} \|f\|_{\mathcal{W}^{1,2}(\Omega_\delta)}. \quad (2.34)$$

Hence the conclusion of the theorem follows from (2.30), (2.31) and (2.34).

## 2.4 Numerical Examples

In this section, we use the approximate particular solutions described in section 2.3 with MFS to present some numerical examples.

**Example 2.5.** Consider the Dirichlet boundary problem for the Poisson's equation

$$\begin{aligned} \Delta u(x, y) &= e^x + 2, & (x, y) \in \Omega, \\ u(x, y) &= e^x + y^2, & (x, y) \in \partial\Omega, \end{aligned}$$

where  $\Omega = \{(x, y) : -1 \leq x \leq 1, -1 \leq y \leq 0 \text{ or } -1 \leq x \leq 0, 0 \leq y \leq 1\}$  is the L-shaped domain. The exact solution of the above problem is  $u_{exact} = e^x + y^2$ . Choose three different radial basis functions in Example 2.4:

- (a)  $\phi(r^2) = \frac{c}{\pi} e^{-cr^2}$ , where  $r = \|\mathbf{x}\|$  and  $c = 1, 3, 5$ , respectively,
- (b)  $\phi(r^2) = \begin{cases} (c+1)(1-r^2)^c/\pi, & 0 \leq r \leq 1, \\ 0, & r > 1, \end{cases}$  for  $c = 3, 4, 5$ , respectively,
- (c)  $\phi(r^2) = \frac{c-1}{\pi(r^2+1)^c}$ , for  $c = 3, 4, 5$ , respectively,

and use  $\mathbf{x}_0 = (1, 1)$  and  $\mathbf{x}_{k,m} = (\frac{k}{n}, \frac{m}{n})$ ,  $-1.1n \leq k \leq 1.1n$  and  $-1.1n \leq m \leq 0.1n$ , or  $-1.1n \leq k \leq 0.1n$  and  $-0.1n \leq m \leq 1.1n$ , in  $\Omega_\delta$  with  $\delta = 0.1$  to get  $u_n$  in (2.17). Next, we use the MFS to obtain  $u_N$ , as discussed in section by using  $N$  points equally spaced on  $\partial\Omega$

and choosing a fictitious domain  $\tilde{\Omega} = \{(x, y) : x^2 + y^2 \leq R^2\}$ , where  $R = 1.5, 3$ , respectively. Let  $\tilde{\mathbf{x}}_k = (R \cos \frac{2\pi k}{N}, R \sin \frac{2\pi k}{N})$ ,  $R = 1.5, 3$ ,  $0 \leq k \leq N - 1$  on  $\partial\tilde{\Omega}$ . Then the approximate solution  $u_N$  of the BVP (2.7)-(2.8) can be obtained. To estimate the maximum error (1.6), we use  $M^2$  points  $\mathbf{z}_{k,m} = (\frac{k}{M}, \frac{m}{M})$ ,  $1 \leq k, m \leq M$ , with  $M = 100$  in  $\bar{\Omega} = \Omega \cup \partial\Omega$  to get the numerical infinity norm

$$\max_{\bar{\Omega}} |u_{exact}(\mathbf{z}_{k,m}) - u_A(\mathbf{z}_{k,m})|.$$

Then our numerical approximation errors are presented in the following table with various  $R, c, n$ , and  $N$ :

Figure 2.6:  $n = 10, 100$  points ( $\bullet$ ) in  $\Omega$ , 40 points ( $\bullet$ ) on  $\partial\Omega$  and ( $+$ ) on  $\partial\Omega_\delta$ , respectively, and  $N = 20$  points ( $*$ ) on  $\partial\tilde{\Omega}$  with  $r = 2$

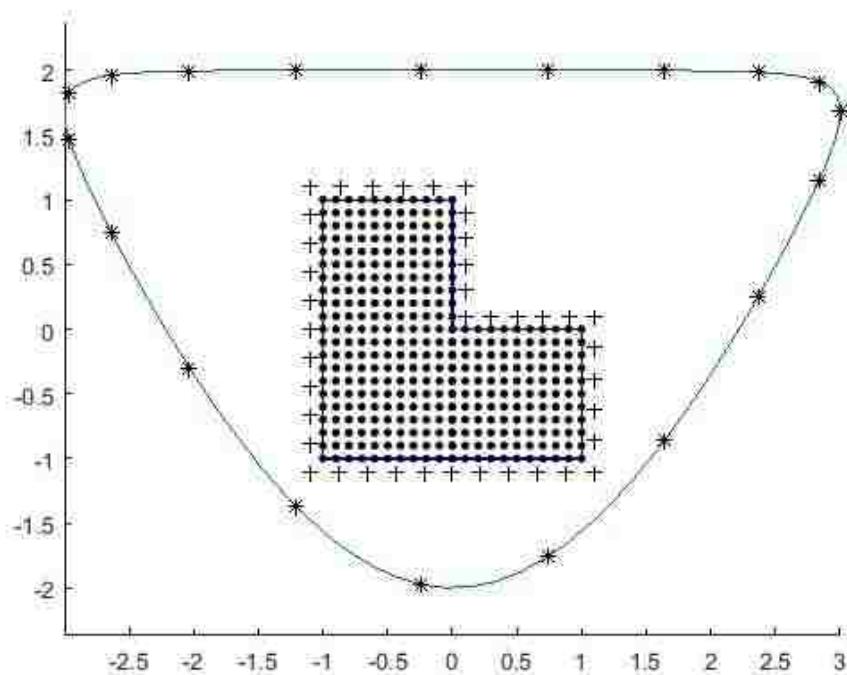




Table 2.4: Maximum Error  $\|u_{exact} - u_A\|_{C(\bar{\Omega})}$  with (a) the Gaussian RBFs  $\phi(r^2) = \frac{c}{\pi} e^{-cr^2}$

	n = 40 N = 30	n = 100 N = 50	n = 120 N = 80
R = 1.5, c = 1	7.3348e-08	3.6730e-07	4.8013e-07
R = 1.5, c = 3	2.5898e-05	7.7863e-06	5.3581e-06
R = 1.5, c = 5	2.2344e-05	1.3413e-05	1.6347e-05
R = 3.0, c = 1	7.3348e-08	3.6730e-07	4.8013e-07
R = 3.0, c = 3	2.5898e-05	7.7863e-06	5.3581e-06
R = 3.0, c = 5	2.2344e-05	1.3413e-05	1.6347e-05

Figure 2.7: Maximum errors with  $c = 1$  ( $\square$ ),  $c = 3$  ( $\circ$ ),  $c = 5$  ( $\triangle$ ), respectively

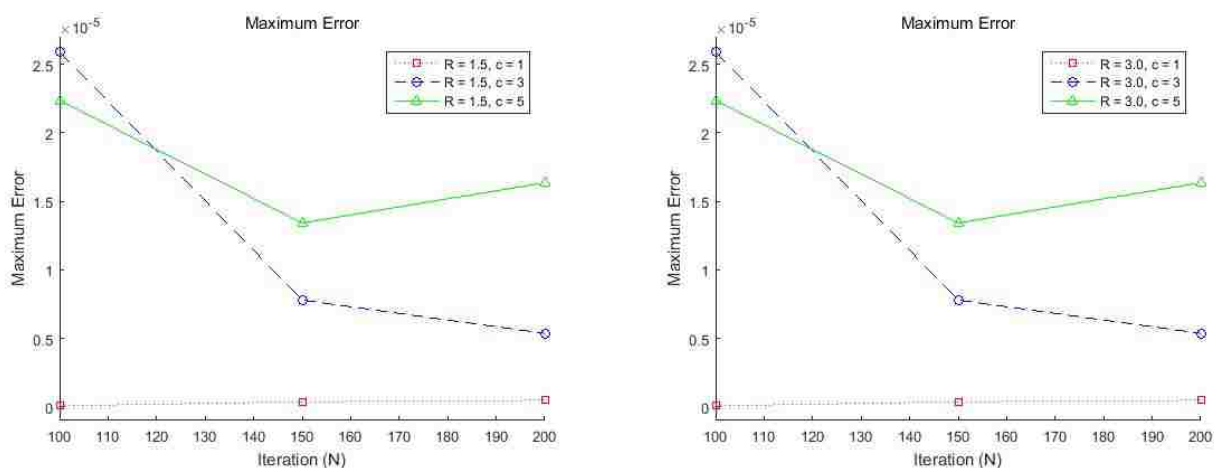


Table 2.5: Maximum Error  $\|u_{exact} - u_A\|_{C(\bar{\Omega})}$  with (b) the compactly supported RBFs  $\phi(r^2) = (c+1)(1-r^2)^c/\pi, 0 \leq r \leq 1$ , for  $c = 3, 4, 5$ .

	n = 40 N = 30	n = 50 N = 50	n = 40 N = 80
R = 1.5, c = 3	3.7748e-15	7.5495e-15	1.2212e-14
R = 1.5, c = 4	2.6645e-15	6.6613e-15	1.8430e-14
R = 1.5, c = 5	1.3323e-15	9.1038e-15	1.7097e-14
R = 3.0, c = 3	3.7748e-15	3.3529e-14	3.4417e-14
R = 3.0, c = 4	3.1086e-15	3.3529e-14	3.4417e-14
R = 3.0, c = 5	3.1086e-15	3.3529e-14	3.4417e-14

Figure 2.8: Maximum errors with  $c = 3$  ( $\square$ ),  $c = 4$  ( $\circ$ ),  $c = 5$  ( $\triangle$ ), respectively

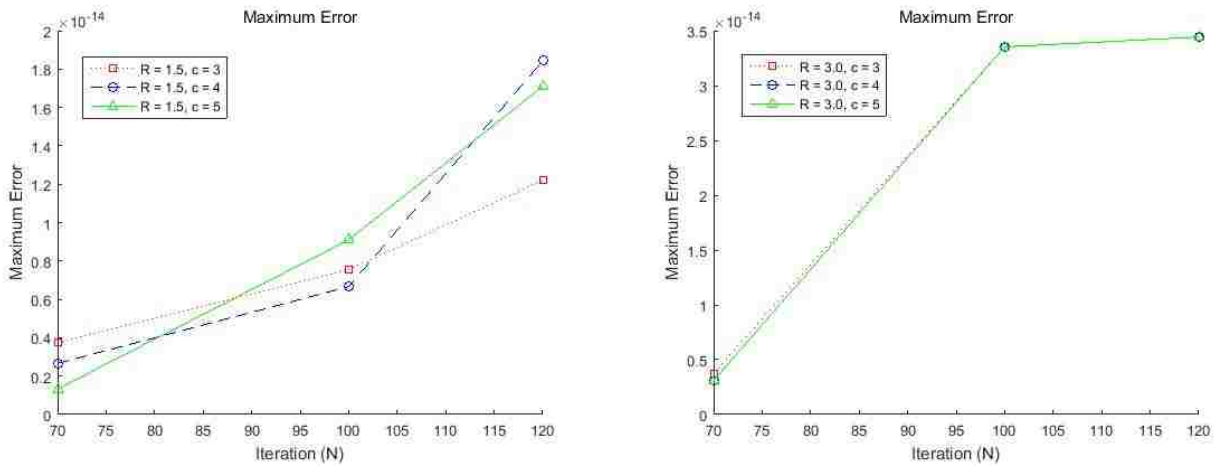
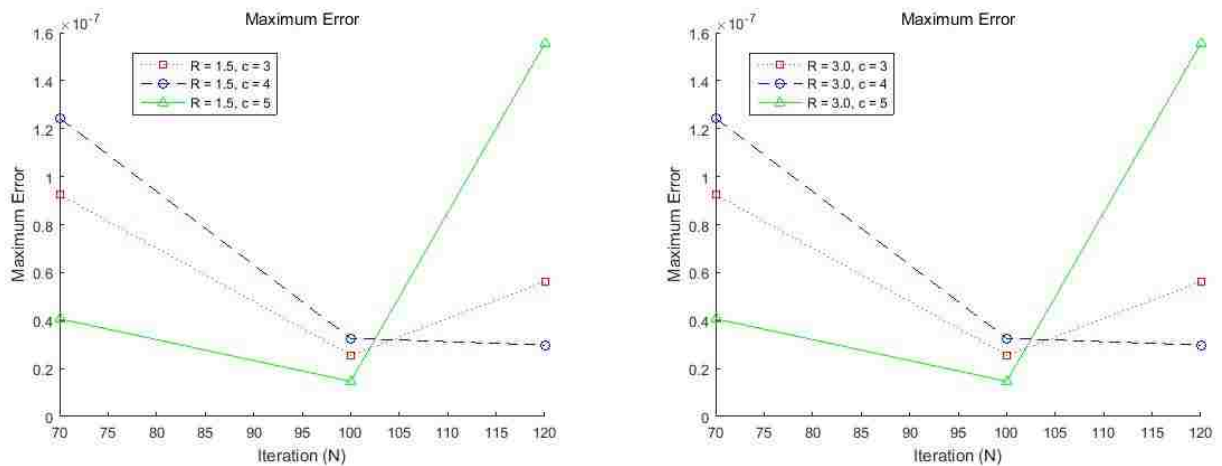


Table 2.6: Maximum Error  $\|u_{exact} - u_A\|_{C(\bar{\Omega})}$  with (c) the inverse multiquadratics RBFs  $\phi(r^2) = \frac{c-1}{\pi(r^2+1)^c}$ , for  $c = 3, 4, 5$ .

	n = 40 N = 30	n = 50 N = 50	n = 40 N = 80
R = 1.5, c = 3	9.2459e-08	2.5582e-08	5.6170e-08
R = 1.5, c = 4	1.2439e-07	3.2560e-08	2.9810e-08
R = 1.5, c = 5	4.0713e-08	1.4644e-08	1.5542e-07
R = 3.0, c = 3	9.2459e-08	2.5582e-08	5.6170e-08
R = 3.0, c = 4	1.2439e-07	3.2560e-08	2.9810e-08
R = 3.0, c = 5	4.0713e-08	1.4644e-08	1.5542e-07

Figure 2.9: Maximum errors with  $c = 3$  ( $\square$ ),  $c = 4$  ( $\circ$ ),  $c = 5$  ( $\triangle$ ), respectively



**Example 2.6.** Consider the Dirichlet boundary problem on a L-shaped domain with a gear-shaped fictitious domain for the Poisson's equation

$$\begin{aligned}\Delta u(x, y) &= (x^2 + 2) e^y, & (x, y) \in \Omega, \\ u(x, y) &= (\sin x + x^2) e^y, & (x, y) \in \partial\Omega,\end{aligned}$$

where  $\Omega = \{(x, y) : -1 \leq x \leq 1, -1 \leq y \leq 0 \text{ or } -1 \leq x \leq 0, 0 \leq y \leq 1\}$  is the L-shaped domain. The exact solution of the above problem is  $u_{exact} = (\sin x + x^2) e^y$ . Choose three different radial basis functions as in Example 2.4 and use  $\mathbf{x}_0 = (1, 1)$  and  $\mathbf{x}_{k,m} = (\frac{k}{n}, \frac{m}{n})$ ,  $-1.1n \leq k \leq 1.1n$  and  $-1.1n \leq m \leq 0.1n$ , or  $-1.1n \leq k \leq 0.1n$  and  $-0.1n \leq m \leq 1.1n$ , in  $\Omega_\delta$  with  $\delta = 0.1$  to get  $u_n$  in (2.17). Next, we use the MFS to obtain  $u_N$ , as discussed in section by using  $N$  points equally spaced on  $\partial\Omega$  and choosing a gear-shaped fictitious domain  $\tilde{\Omega} = \{(x, y) : x = (R + \frac{1}{2} \sin(7t)) \cos(t + \frac{1}{2} \sin(7t)), y = (R + \frac{1}{2} \sin(7t)) \cos(t + \frac{1}{2} \sin(7t)), 0 \leq t < 2\pi\}$ ,  $R = 2, 3$ , respectively. Let  $\tilde{\mathbf{x}}_k = ((R + \frac{1}{2} \sin(7\frac{2\pi k}{N})) \cos(\frac{2\pi k}{N} + \frac{1}{2} \sin(7\frac{2\pi k}{N})), (R + \frac{1}{2} \sin(7\frac{2\pi k}{N})) \sin(\frac{2\pi k}{N} + \frac{1}{2} \sin(7\frac{2\pi k}{N})))$ ,  $0 \leq k \leq N - 1$  on  $\partial\tilde{\Omega}$ . Then the approximate solution  $u_N$  of the BVP (2.7)-(2.8) can be obtained. To estimate the maximum error (1.6), we use  $M^2$  points  $\mathbf{z}_{k,m} = (\frac{k}{M}, \frac{m}{M})$ ,  $-M \leq k \leq M$  and  $-M \leq m \leq 0$  or  $-M \leq k \leq 0$  and  $0 \leq m \leq M$  with  $M = 100$  in  $\bar{\Omega} = \Omega \cup \partial\Omega$  to get the numerical infinity norm in Example 2.4. Then our numerical approximation errors are presented in the following table with various  $R$ ,  $c$ ,  $n$ , and  $N$ :

Figure 2.10:  $n = 20$ , 300 points ( $\bullet$ ) in  $\Omega$ , 60 points ( $\bullet$ ) on  $\partial\Omega$  and 35 points ( $+$ ) on  $\partial\Omega_\delta$ , respectively, and  $N = 20$  points ( $*$ ) on  $\partial\tilde{\Omega}$  with  $R = 2.5$

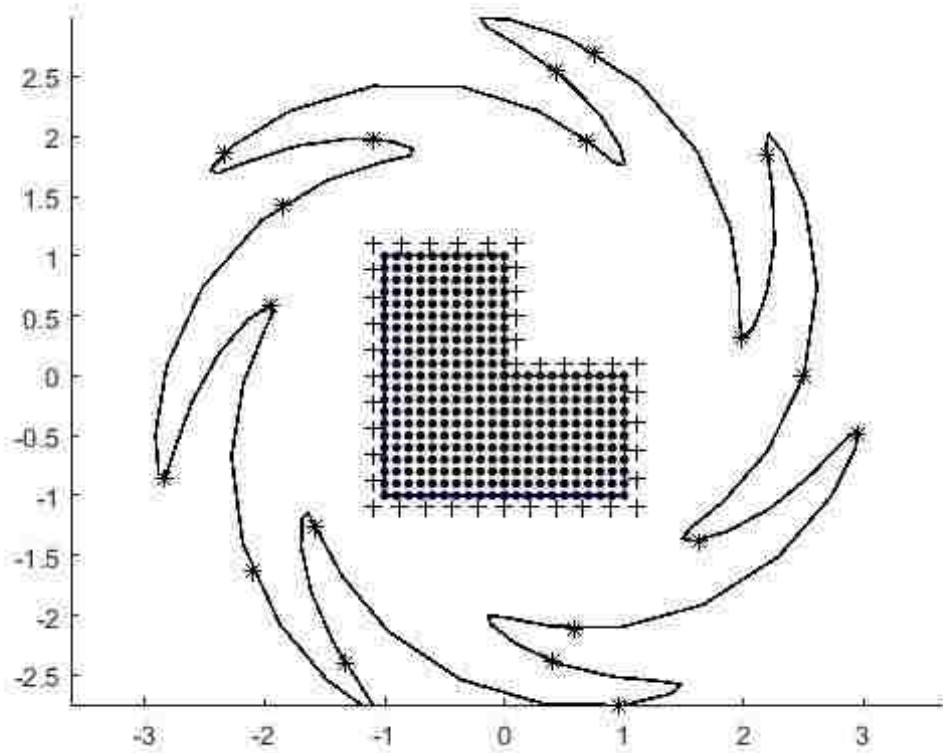


Table 2.7: Maximum Error  $\|u_{exact} - u_A\|_{C(\bar{\Omega})}$  with (a) the Gaussian RBFs  $\phi(r^2) = \frac{c}{\pi} e^{-cr^2}$

	n = 20 N = 30	n = 40 N = 40	n = 50 N = 50
R = 2, c = 1	6.1979e-06	4.2870e-07	6.1780e-06
R = 2, c = 3	3.7903e-05	1.8962e-06	2.0928e-06
R = 2, c = 5	2.9046e-08	1.3116e-06	9.2832e-07
R = 3, c = 1	6.1979e-06	4.2870e-07	6.1780e-06
R = 3, c = 3	3.7903e-05	1.8962e-06	2.0928e-06
R = 3, c = 5	2.9046e-08	1.3116e-06	9.2832e-07

Figure 2.11: Maximum errors with  $c = 1$  ( $\square$ ),  $c = 3$  ( $\circ$ ),  $c = 5$  ( $\triangle$ ), respectively

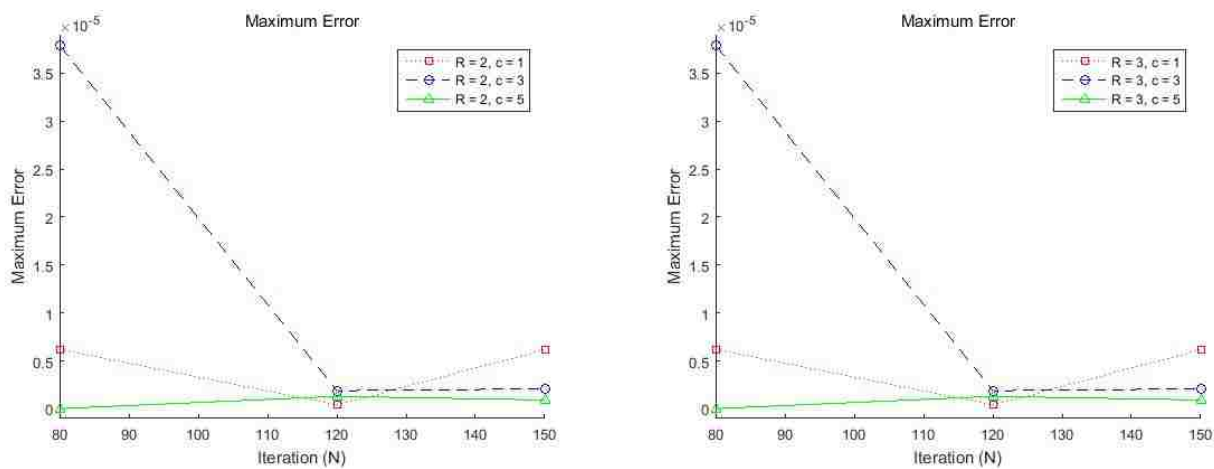


Table 2.8: Maximum Error  $\|u_{exact} - u_A\|_{C(\bar{\Omega})}$  with (b) the compactly supported RBFs  $\phi(r^2) = (c+1)(1-r^2)^c/\pi$ ,  $0 \leq r \leq 1$ , for  $c = 3, 4, 5$ .

	n = 20 N = 30	n = 40 N = 40	n = 50 N = 50
R = 2, c = 3	2.2204e-15	5.0238e-15	1.1248e-14
R = 2, c = 4	2.2204e-15	5.0238e-15	1.1248e-14
R = 2, c = 5	2.2204e-15	5.0238e-15	1.1248e-14
R = 3, c = 3	3.9094e-14	2.7686e-14	1.3536e-13
R = 3, c = 4	3.9094e-14	2.7686e-14	1.3536e-13
R = 3, c = 5	3.9094e-14	2.7686e-14	1.3536e-13

Figure 2.12: Maximum errors with  $c = 3$  ( $\square$ ),  $c = 4$  ( $\circ$ ),  $c = 5$  ( $\triangle$ ), respectively

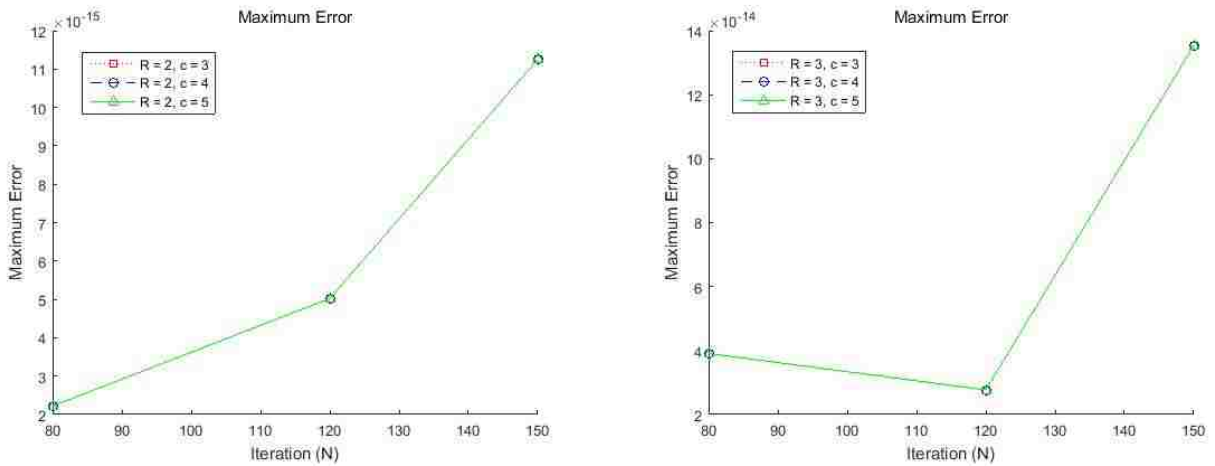
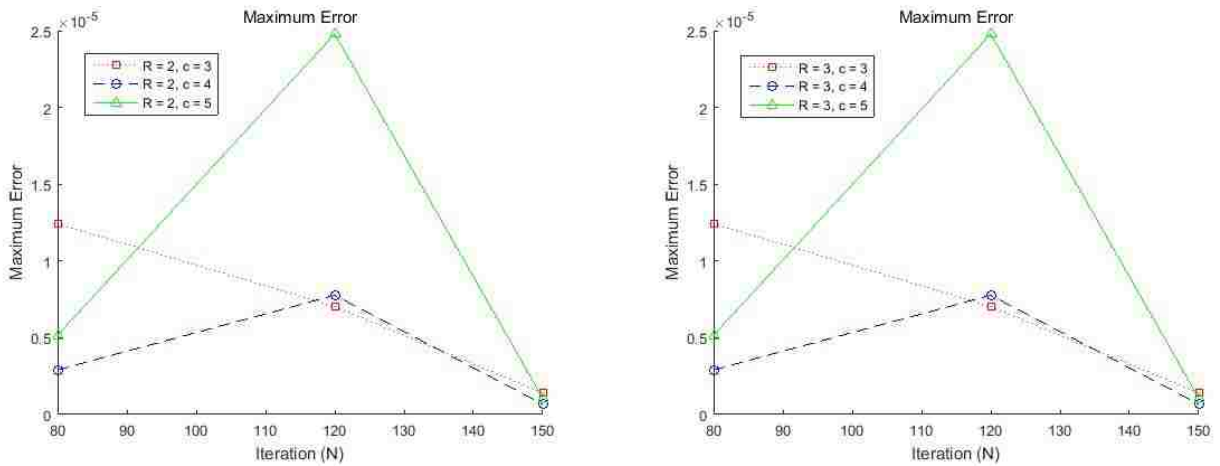


Table 2.9: Maximum Error  $\|u_{exact} - u_A\|_{C(\bar{\Omega})}$  with (c) the inverse multiquadratics RBFs  $\phi(r^2) = \frac{c-1}{\pi(r^2+1)^c}$ , for  $c = 3, 4, 5$ .

	n = 20 N = 30	n = 40 N = 40	n = 50 N = 50
R = 2, c = 3	1.2424e-05	7.0323e-06	1.3949e-06
R = 2, c = 4	2.9106e-06	7.7640e-06	6.7156e-07
R = 2, c = 5	5.1589e-06	2.4789e-05	1.0574e-06
R = 3, c = 3	1.2424e-05	7.0323e-06	1.3949e-06
R = 3, c = 4	2.9106e-06	7.7640e-06	6.7156e-07
R = 3, c = 5	5.1589e-06	2.4789e-05	1.0574e-06

Figure 2.13: Maximum errors with  $c = 3$  ( $\square$ ),  $c = 4$  ( $\circ$ ),  $c = 5$  ( $\triangle$ ), respectively





**Example 2.7.** Consider the Dirichlet boundary problem for the Poisson's equation

$$\Delta u(x, y) = -\frac{17}{16} \sin\left(x + \frac{y}{4}\right) - y^2 e^x \sin(e^x) + (2 - y^2 e^{2x}) \cos(e^x), \quad (x, y) \in \Omega,$$

$$u(x, y) = \sin\left(x + \frac{y}{4}\right) + y^2 \cos(e^x), \quad (x, y) \in \partial\Omega,$$

where  $\Omega = \{(x, y) : 0 \leq x \leq 1, 0 \leq y \leq 0.5 \text{ or } 0 \leq x \leq 0.5, 0.5 \leq y \leq 1\}$  is the L-shaped domain. The exact solution of the above problem is  $u_{exact} = \sin\left(x + \frac{y}{4}\right) + y^2 \cos(e^x)$ . Choose three different radial basis functions as in Example 2.4 and use  $\mathbf{x}_0 = (1, 1)$  and  $\mathbf{x}_{k,m} = \left(\frac{k}{n}, \frac{m}{n}\right)$ ,  $-1.1n \leq k \leq 1.1n$  and  $-1.1n \leq m \leq 0.1n$ , or  $-1.1n \leq k \leq 0.1n$  and  $-0.1n \leq m \leq 1.1n$ , in  $\Omega_\delta$  with  $\delta = 0.1$  to get  $u_n$  in (2.17). Next, we use the MFS to obtain  $u_N$ , as discussed in section by using  $N$  points equally spaced on  $\partial\Omega$  and choosing an amoeba-like fictitious domain  $\tilde{\Omega} = \{(x, y) : x = r(t) \cos(t), y = r(t) \sin(t), \text{ where } r(t) = R e^{\sin(t)} \sin^2(2t) + R e^{\cos(t)} \cos^2(2t), 0 \leq t < 2\pi, R = 3, 5, \text{ respectively. Let } \tilde{\mathbf{x}}_k = ((R e^{\sin(\frac{2\pi k}{N})} \sin^2(2\frac{2\pi k}{N}) + R e^{\cos(\frac{2\pi k}{N})} \cos^2(2\frac{2\pi k}{N})) \cos(\frac{2\pi k}{N}), (R e^{\sin(\frac{2\pi k}{N})} \sin^2(2\frac{2\pi k}{N}) + R e^{\cos(\frac{2\pi k}{N})} \cos^2(2\frac{2\pi k}{N})) \sin(\frac{2\pi k}{N}), 0 \leq t < 2\pi, 0 \leq k \leq N-1 \text{ on } \partial\tilde{\Omega}. \text{ Then the approximate solution } u_N \text{ of the BVP (2.7)-(2.8) can be obtained. To estimate the maximum error (1.6), we use } M^2 \text{ points } \mathbf{z}_{k,m} = \left(\frac{k}{M}, \frac{m}{M}\right), -M \leq k \leq M \text{ and } -M \leq m \leq 0 \text{ or } -M \leq k \leq 0 \text{ and } 0 \leq m \leq M \text{ with } M = 100 \text{ in } \bar{\Omega} = \Omega \cup \partial\Omega \text{ to get the numerical infinity norm in Example 2.4. Then our numerical approximation errors are presented in the following table with various } R, c, n, \text{ and } N:$

Figure 2.14:  $n = 20$ , 300 points ( $\bullet$ ) in  $\Omega$ , 80 points ( $\bullet$ ) on  $\partial\Omega$  and 40 points ( $+$ ) on  $\partial\Omega_\delta$ , respectively, and  $N = 20$  points ( $*$ ) on  $\partial\tilde{\Omega}$  with  $R = 2.5$

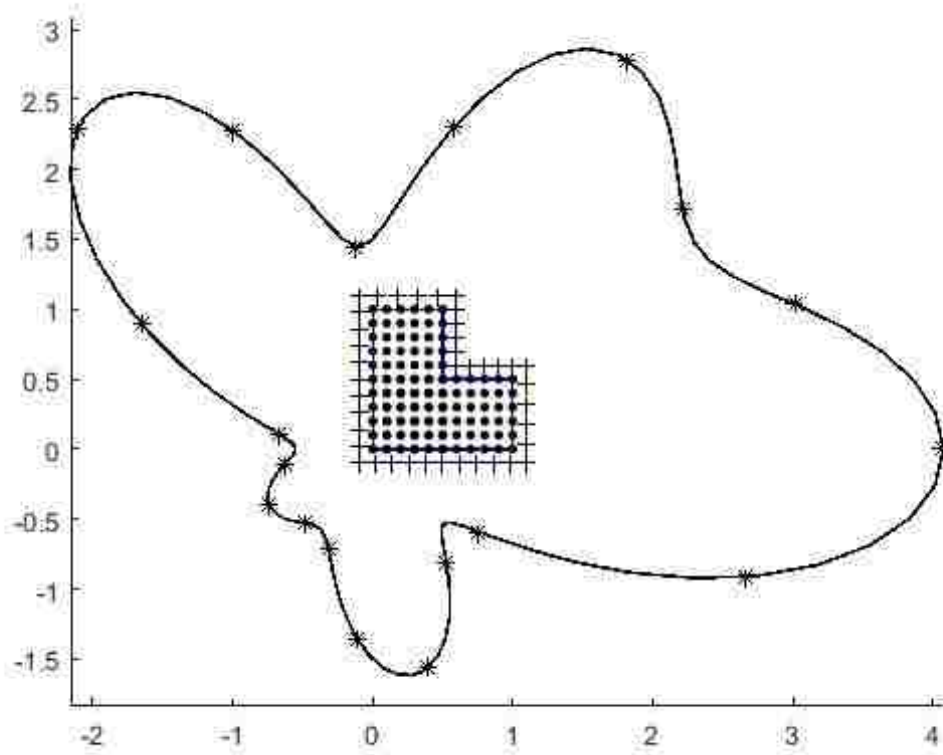


Table 2.10: Maximum Error  $\|u_{exact} - u_A\|_{C(\bar{\Omega})}$  with (a) the Gaussian RBFs  $\phi(r^2) = \frac{c}{\pi} e^{-cr^2}$

	n = 20 N = 30	n = 40 N = 40	n = 50 N = 50
R = 3, c = 1	0.0167	0.0131	0.0146
R = 3, c = 3	0.0160	0.0114	0.0071
R = 3, c = 5	0.0206	0.0045	0.0123
R = 5, c = 1	0.0167	0.0131	0.0146
R = 5, c = 3	0.0160	0.0114	0.0071
R = 5, c = 5	0.0206	0.0045	0.0123

Figure 2.15: Maximum errors with  $c = 1$  ( $\square$ ),  $c = 3$  ( $\circ$ ),  $c = 5$  ( $\triangle$ ), respectively

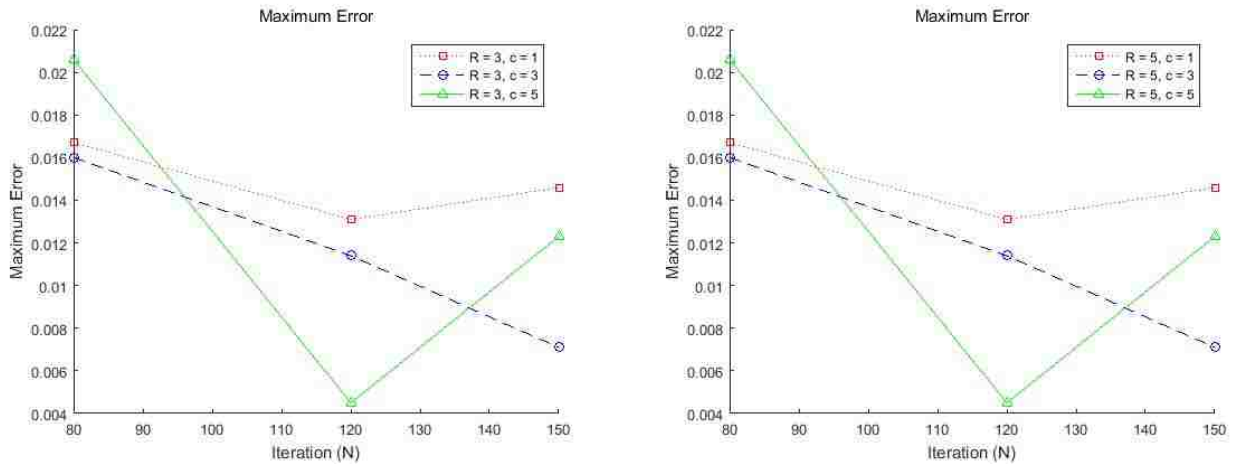


Table 2.11: Maximum Error  $\|u_{exact} - u_A\|_{C(\bar{\Omega})}$  with (b) the compactly supported RBFs  $\phi(r^2) = (c + 1)(1 - r^2)^c/\pi, 0 \leq r \leq 1$ , for  $c = 3, 4, 5$ .

	n = 20 N = 30	n = 40 N = 40	n = 50 N = 50
R = 3, c = 3	7.4094e-14	4.0935e-13	1.4341e-13
R = 3, c = 4	7.4094e-14	4.0935e-13	1.4341e-13
R = 3, c = 5	7.4094e-14	4.0935e-13	1.4341e-13
R = 5, c = 3	7.6299e-13	4.8181e-13	1.1156e-12
R = 5, c = 4	7.6299e-13	4.8181e-13	1.1156e-12
R = 5, c = 5	7.6299e-13	4.8181e-13	1.1156e-12

Figure 2.16: Maximum errors with  $c = 3$  ( $\square$ ),  $c = 4$  ( $\circ$ ),  $c = 5$  ( $\triangle$ ), respectively

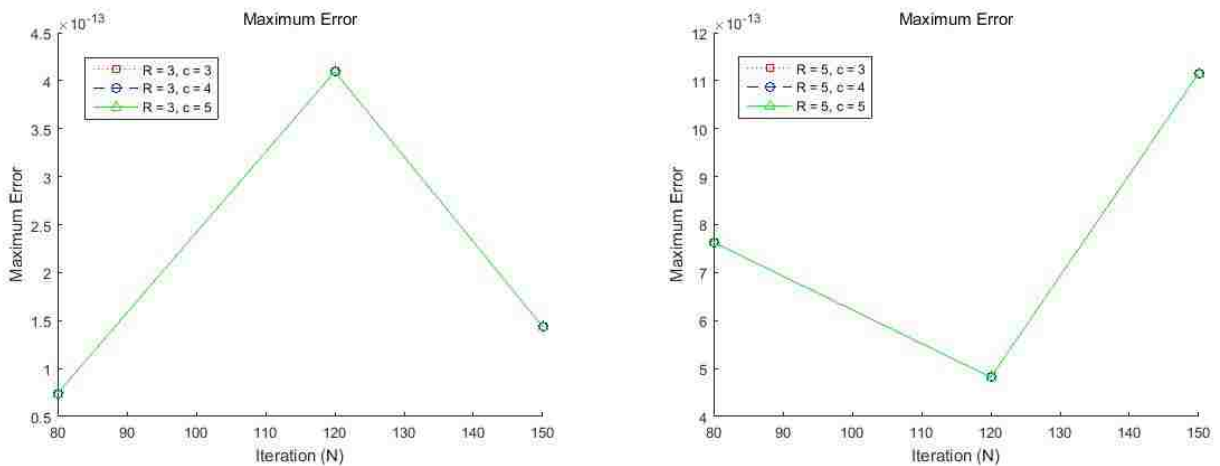
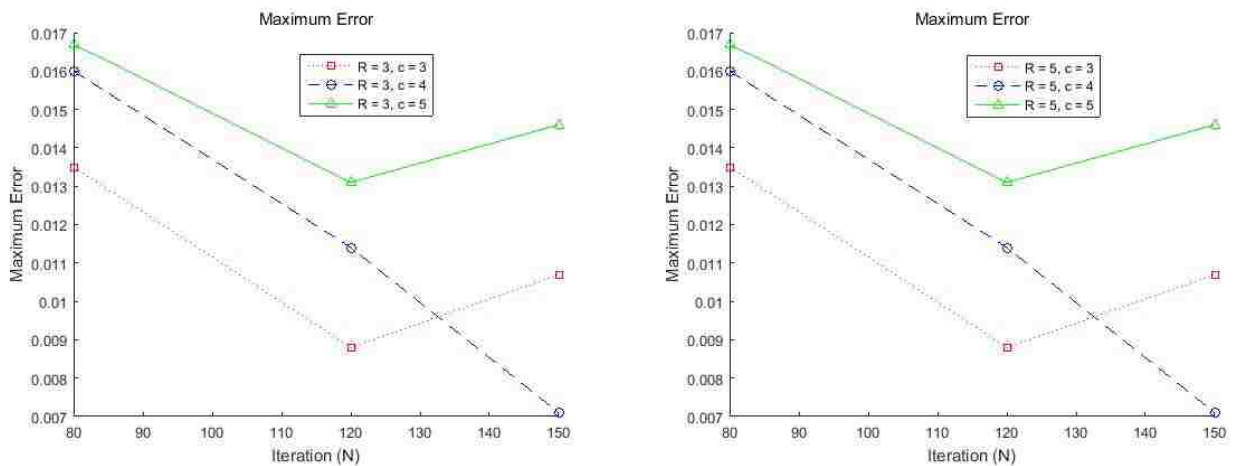


Table 2.12: Maximum Error  $\|u_{exact} - u_A\|_{C(\bar{\Omega})}$  with (c) the inverse multiquadratics RBFs  $\phi(r^2) = \frac{c-1}{\pi(r^2+1)^c}$ , for  $c = 3, 4, 5$ .

	n = 20 N = 30	n = 40 N = 40	n = 50 N = 50
R = 3, c = 3	0.0135	0.0088	0.0107
R = 3, c = 4	0.0160	0.0114	0.0071
R = 3, c = 5	0.0167	0.0131	0.0146
R = 5, c = 3	0.0135	0.0088	0.0107
R = 5, c = 4	0.0160	0.0114	0.0071
R = 5, c = 5	0.0167	0.0131	0.0146

Figure 2.17: Maximum errors with  $c = 3$  ( $\square$ ),  $c = 4$  ( $\circ$ ),  $c = 5$  ( $\triangle$ ), respectively



**Example 2.8.** Consider the Dirichlet boundary problem for the Poisson's equation

$$\Delta u(x, y, z) = e^{x-y} \cos(z), \quad (x, y, z) \in \Omega,$$

$$u(x, y, z) = e^{x-y} \cos(z), \quad (x, y, z) \in \partial\Omega,$$

where  $\Omega = \{(x, y, z) : -1 \leq x \leq 1, -1 \leq y \leq 1, -1 \leq z \leq 1\}$ . The exact solution of the above problem is  $u_{exact} = e^{x-y} \cos(z)$ . Choose three different radial basis functions in

Example 2.4:

$$(a) \phi(r^2) = \frac{c}{\pi} e^{-cr^2}, \text{ where } r = |\mathbf{0x}| \text{ and } c = 1, 3, 5, \text{ respectively,}$$

$$(b) \phi(r^2) = \begin{cases} ((2c+3)!!)(1-r^2)^c / (4\pi(2c)!!), & 0 \leq r \leq 1, \\ 0, & r > 1, \end{cases} \text{ for } c = 3, 4, 5, \text{ respectively,}$$

$$(c) \phi(r^2) = \frac{1}{2\pi^2} \frac{(2c-2)!!}{(2c-5)!!} \frac{1}{(r^2+1)^c}, \text{ for } c = 3, 4, 5, \text{ respectively,}$$

$$\text{where } n!! = \begin{cases} 1 \cdot 3 \cdot \dots \cdot n, & \text{if } n \text{ is an odd number,} \\ 2 \cdot 4 \cdot \dots \cdot n, & \text{if } n \text{ is an even number,} \end{cases}$$

and use  $\mathbf{x}_0 = (-1.5, -1.5, -1.5)$  and  $\mathbf{x}_{k,l,m} = (\frac{k}{n}, \frac{l}{n}, \frac{m}{n})$ ,  $-1.1n \leq k, l, m \leq 1.1n$ , in  $\Omega_\delta =$

$[-1.1, 1.1]^3$  to get  $u_n$  in (2.21). Then the approximate solution  $u_N$  of the BVP (2.7)-(2.8)

can be obtained and our maximum error is also estimated as in Example 2.4. We use

a fictitious domain  $\tilde{\Omega} = \{(x, y, z) : x^2 + y^2 + z^2 \leq R^2\}$ , where  $R = 3, 5$ . We choose

$\tilde{\mathbf{x}}_k = (R \cos \frac{2\pi k}{M} \sin \frac{\pi k}{M}, R \sin \frac{2\pi k}{M} \sin \frac{\pi k}{M}, R \cos \frac{\pi k}{M})$ ,  $R = 3, 5$ ,  $1 \leq k \leq M$ , on  $\partial\tilde{\Omega}$ . To

estimate the maximum error (1.6), we use  $M^3$  points  $\mathbf{z}_{k,l,m} = (\frac{k}{M}, \frac{l}{M}, \frac{m}{M})$ ,  $-M \leq k, l, m \leq$

$M$ , with  $M = 40$  in  $\bar{\Omega} = \Omega \cup \partial\Omega$ , to get the numerical infinity norm in Example 2.4. Then

our numerical approximation errors are presented in the following table with various  $R, c,$

$n$ , and  $N$ :

Figure 2.18:  $n = 10$ , 1000 points ( $\bullet$ ) in  $\Omega$ , 240 points ( $\bullet$ ) on  $\partial\Omega$ , and  $N = 20$  points ( $*$ ) on  $\partial\tilde{\Omega}$  with  $R = 2$

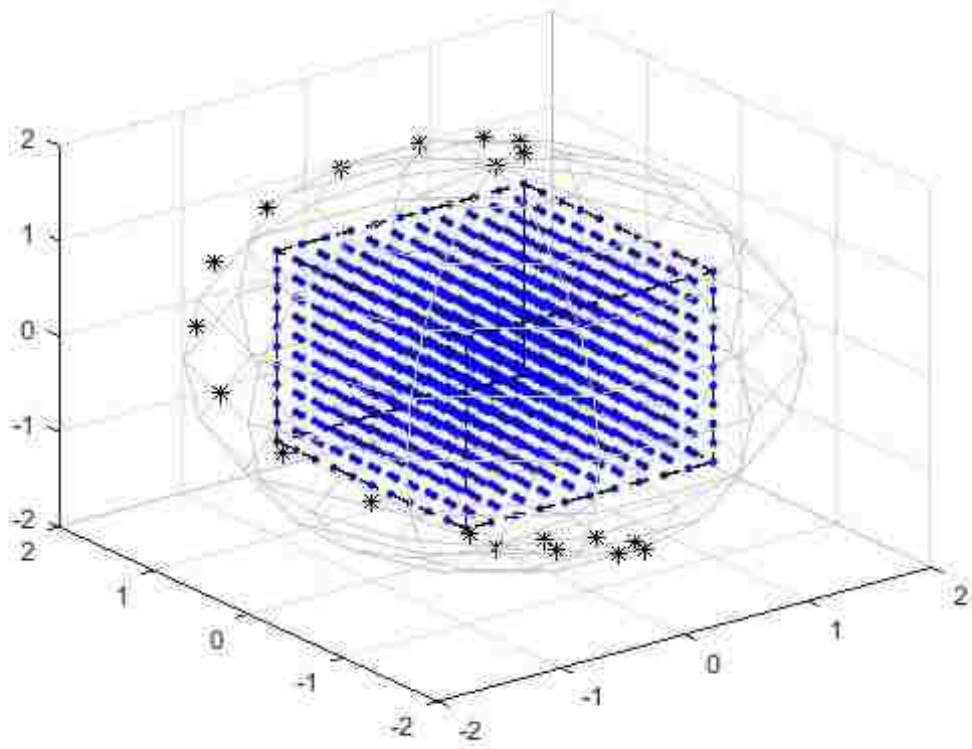


Table 2.13: Maximum Error  $\|u_{exact} - u_A\|_{C(\bar{\Omega})}$  with (a) the Gaussian RBFs  $\phi(r^2) = \frac{c}{\pi} e^{-cr^2}$

	n = 10 N = 20	n = 20 N = 30	n = 30 N = 50
R = 3, c = 1	2.4676e-04	0.0020	1.7414e-04
R = 3, c = 3	9.8249e-04	5.5944e-04	8.7610e-05
R = 3, c = 5	1.3205e-04	2.6556e-05	5.2635e-05
R = 5, c = 1	2.4676e-04	0.0020	1.7414e-04
R = 5, c = 3	9.8249e-04	5.5944e-04	8.7610e-05
R = 5, c = 5	1.3205e-04	2.6556e-05	5.2635e-05

Figure 2.19: Maximum errors with  $c = 1$  ( $\square$ ),  $c = 3$  ( $\circ$ ),  $c = 5$  ( $\triangle$ ), respectively

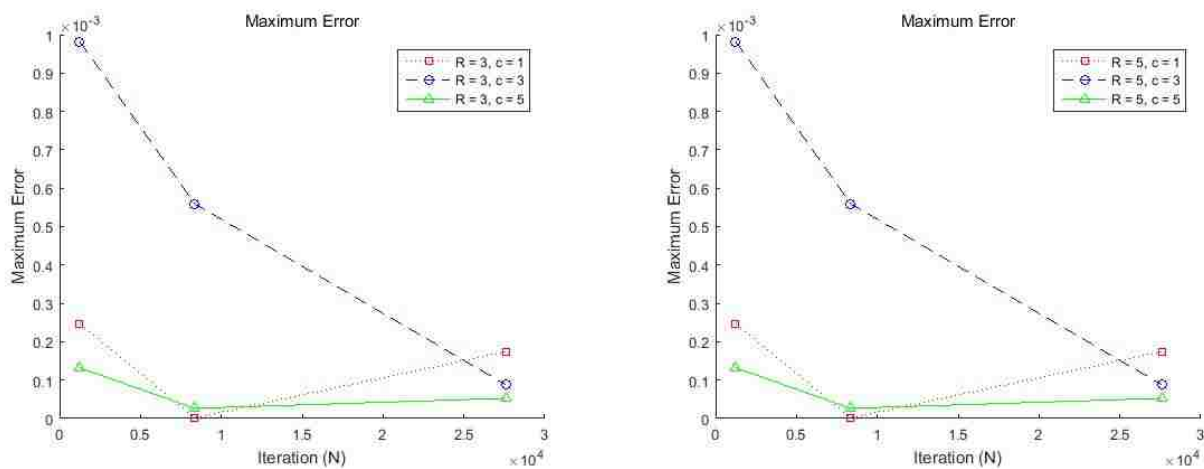




Table 2.14: Maximum Error  $\|u_{exact} - u_A\|_{C(\bar{\Omega})}$  with (b) the compactly supported RBFs  $\phi(r^2) = ((2c + 3)!!)(1 - r^2)^c / (4\pi(2c)!!)$ ,  $0 \leq r \leq 1$ , for  $c = 3, 4, 5$ .

	n = 10 N = 20	n = 20 N = 30	n = 30 N = 50
R = 3, c = 3	1.6653e-15	1.9984e-15	6.9944e-15
R = 3, c = 4	1.6653e-15	1.9984e-15	2.5535e-15
R = 3, c = 5	1.6653e-15	1.9984e-15	8.7708e-15
R = 5, c = 3	9.9920e-16	7.7716e-16	6.9944e-15
R = 5, c = 4	9.9920e-16	6.6613e-16	2.5535e-15
R = 5, c = 5	9.9920e-16	4.4409e-16	8.7708e-15

Figure 2.20: Maximum errors with  $c = 3$  ( $\square$ ),  $c = 4$  ( $\circ$ ),  $c = 5$  ( $\triangle$ ), respectively

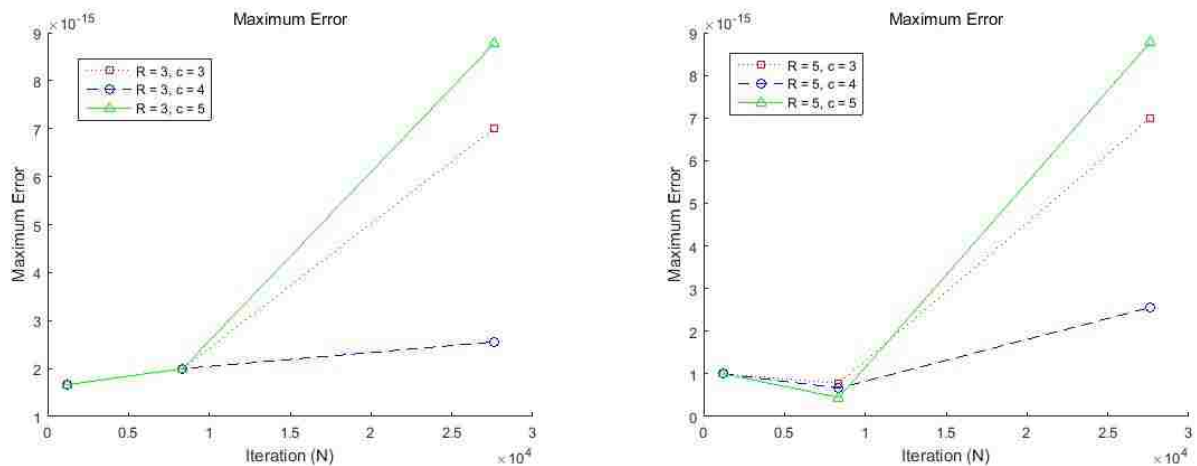
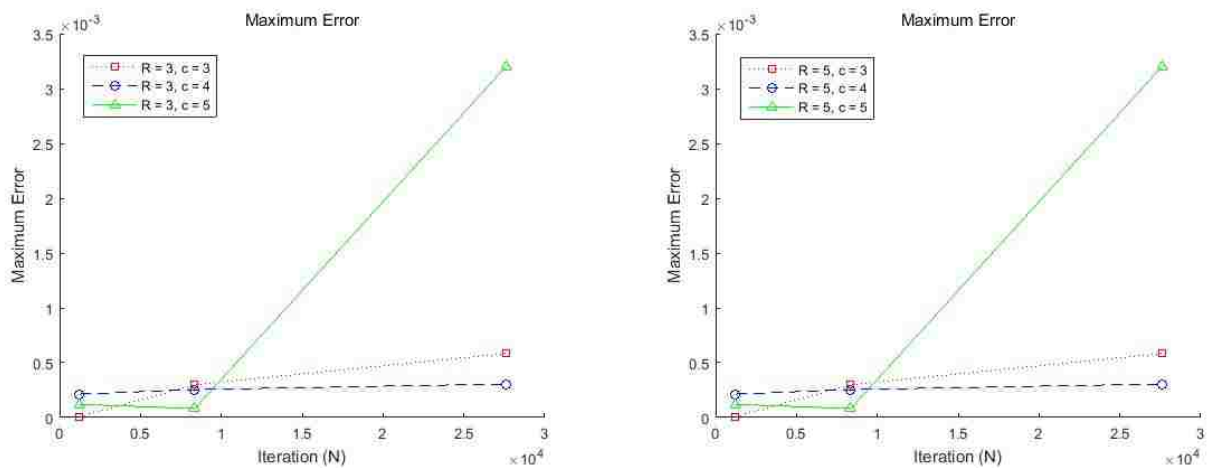


Table 2.15: Maximum Error  $\|u_{exact} - u_A\|_{C(\bar{\Omega})}$  with (c) the inverse multiquadratics RBFs  $\phi(r^2) = \frac{1}{2\pi^2} \frac{(2c-2)!!}{(2c-5)!!} \frac{1}{(r^2+1)^c}$ , for  $c = 3, 4, 5$ .

	n = 10 N = 20	n = 20 N = 30	n = 30 N = 50
R = 3, c = 3	7.3079e-06	2.9932e-04	5.8447e-04
R = 3, c = 4	2.1399e-04	2.5427e-04	3.0569e-04
R = 3, c = 5	1.2014e-04	8.1775e-05	0.0032
R = 5, c = 3	7.3079e-06	2.9932e-04	5.8447e-04
R = 5, c = 4	2.1399e-04	2.5427e-04	3.0569e-04
R = 5, c = 5	1.2014e-04	8.1775e-05	0.0032

Figure 2.21: Maximum errors with  $c = 3$  ( $\square$ ),  $c = 4$  ( $\circ$ ),  $c = 5$  ( $\triangle$ ), respectively



## CHAPTER 3

# DUAL RECIPROCITY METHODS FOR THE BOUNDARY VALUE PROBLEMS OF HELMHOLTZ EQUATIONS

### 3.1 Description of MFS for Helmholtz equations

Consider the Dirichlet boundary problem for a homogeneous Helmholtz equation

$$\Delta u(\mathbf{x}) + \kappa^2 u(\mathbf{x}) = 0, \quad \mathbf{x} \in \Omega, \quad (3.1)$$

$$u(\mathbf{x}) = h(\mathbf{x}), \quad \mathbf{x} \in \partial\Omega, \quad (3.2)$$

where  $\Omega$  is a bounded domain in  $\mathbb{R}^s$ ,  $s \geq 2$  and  $\kappa = a + bi$  is a complex number with  $b = \text{Im}(\kappa) \geq 0$ . The fundamental solution of the Helmholtz equation (3.1) with the differential operator,  $\mathcal{L} = -(\Delta + \kappa^2 \mathbf{I})$ , is given by

$$\Gamma(\mathbf{x}) = \frac{i}{4} \left( \frac{\kappa}{2\pi r} \right)^{s/2-1} H_{s/2-1}^{(1)}(\kappa r), \quad s \geq 2, \quad (3.3)$$

where  $r = \|\mathbf{x}\|$  and  $H_{s/2-1}^{(1)}$  is a Hankel function (cf. [18]). Especially, when  $s = 3, 2$ ,

$$H_{1/2}^{(1)}(\mathbf{z}) = -i \left( \frac{2}{\pi z} \right)^{1/2} e^{iz}, \quad H_0^{(1)}(\mathbf{z}) = J_0(\mathbf{z}) + iY_0(\mathbf{z}), \quad (3.4)$$

where  $J_k$  is the Bessel functions of the first kind of order  $k$  and  $Y_k$  is the Bessel functions of the second kind of order  $k$ .

The method of fundamental solutions (MFS) for the boundary value problems of Helmholtz equations is similar to the MFS for the Laplace equation. Namely, we choose a fictitious domain  $\partial\tilde{\Omega}$  such that  $\bar{\Omega} \subset \tilde{\Omega}$ . Then choose  $N$  points on  $\partial\tilde{\Omega}$  listed as  $\tilde{\mathbf{x}}_1, \tilde{\mathbf{x}}_2, \dots, \tilde{\mathbf{x}}_N$ , and form

$$u_N(\mathbf{x}) = \sum_{k=1}^N c_k \Gamma(\mathbf{x}, \tilde{\mathbf{x}}_k). \quad (3.5)$$

Clearly,  $u_N(\mathbf{x})$  satisfies the Helmholtz equation (3.1) since  $\Gamma(\mathbf{x}, \tilde{\mathbf{x}}_k)$  is the fundamental solution. For  $u_N(\mathbf{x})$  to satisfy the Dirichlet boundary condition as much as possible, we choose  $N$  points  $\mathbf{x}_1, \mathbf{x}_2, \dots, \mathbf{x}_N$  on  $\partial\Omega$  and set up

$$u_N(\mathbf{x}_k) = f(\mathbf{x}_k), \quad 1 \leq k \leq N,$$

namely,

$$\sum_{k=1}^N c_k \Gamma(\mathbf{x}_m, \tilde{\mathbf{x}}_k) = f(\mathbf{x}_m), \quad 1 \leq m \leq N,$$

which leads to the following system

$$\begin{bmatrix} \Gamma(\mathbf{x}_1, \tilde{\mathbf{x}}_1) & \Gamma(\mathbf{x}_1, \tilde{\mathbf{x}}_2) & \Gamma(\mathbf{x}_1, \tilde{\mathbf{x}}_3) & \dots & \Gamma(\mathbf{x}_1, \tilde{\mathbf{x}}_N) \\ \Gamma(\mathbf{x}_2, \tilde{\mathbf{x}}_1) & \Gamma(\mathbf{x}_2, \tilde{\mathbf{x}}_2) & \Gamma(\mathbf{x}_2, \tilde{\mathbf{x}}_3) & \dots & \Gamma(\mathbf{x}_2, \tilde{\mathbf{x}}_N) \\ \vdots & \vdots & \vdots & \ddots & \vdots \\ \Gamma(\mathbf{x}_N, \tilde{\mathbf{x}}_1) & \Gamma(\mathbf{x}_N, \tilde{\mathbf{x}}_2) & \Gamma(\mathbf{x}_N, \tilde{\mathbf{x}}_3) & \dots & \Gamma(\mathbf{x}_N, \tilde{\mathbf{x}}_N) \end{bmatrix} \begin{bmatrix} c_1 \\ c_2 \\ \vdots \\ c_N \end{bmatrix} = \begin{bmatrix} f(\mathbf{x}_1) \\ f(\mathbf{x}_2) \\ \vdots \\ f(\mathbf{x}_N) \end{bmatrix}. \quad (3.6)$$

Once the coefficient matrix is invertible, the coefficients  $c_k$ ,  $1 \leq m \leq N$ , can be determined by the above system (3.6) and  $u_N(\mathbf{x})$  in (3.5) is considered as an approximate solution of the Dirichlet boundary value problem (3.1)-(3.2).

However, where  $N$  is very large, the system (3.6) may be ill-conditioned, or finding the inverse of the coefficient matrix could be numerically unstable.

Furthermore, we may choose a different number of collocation points, say  $x_m$ ,  $1 \leq m \leq M$ . In this case, the coefficients  $\{c_k\}$  in (3.5) can not be determined by solving (3.6). Instead,

we let

$$A = \begin{bmatrix} \Gamma(\mathbf{x}_1, \tilde{\mathbf{x}}_1) & \Gamma(\mathbf{x}_1, \tilde{\mathbf{x}}_2) & \Gamma(\mathbf{x}_1, \tilde{\mathbf{x}}_3) & \dots & \Gamma(\mathbf{x}_1, \tilde{\mathbf{x}}_N) \\ \Gamma(\mathbf{x}_2, \tilde{\mathbf{x}}_1) & \Gamma(\mathbf{x}_2, \tilde{\mathbf{x}}_2) & \Gamma(\mathbf{x}_2, \tilde{\mathbf{x}}_3) & \dots & \Gamma(\mathbf{x}_2, \tilde{\mathbf{x}}_N) \\ \vdots & \vdots & \vdots & \ddots & \vdots \\ \Gamma(\mathbf{x}_M, \tilde{\mathbf{x}}_1) & \Gamma(\mathbf{x}_M, \tilde{\mathbf{x}}_2) & \Gamma(\mathbf{x}_M, \tilde{\mathbf{x}}_3) & \dots & \Gamma(\mathbf{x}_M, \tilde{\mathbf{x}}_N) \end{bmatrix}, \quad \mathbf{b} = \begin{bmatrix} f(\mathbf{x}_1) \\ f(\mathbf{x}_2) \\ \vdots \\ f(\mathbf{x}_M) \end{bmatrix},$$

where  $A$  is an  $M \times N$  matrix. And we choose or determine  $\mathbf{c} = [c_1 \ c_2 \ \dots \ c_N]^T$  to be the solution of the following minimization problem

$$\min_{\mathbf{x} \in \mathbb{R}^N} \|A\mathbf{x} - \mathbf{b}\|. \quad (3.7)$$

To overcome the ill-conditioning issue or find the stable solution of the minimization problem, we sometimes need to use the singular value decomposition of a matrix or regularization, described below (cf. [2]).

### 3.1.1 Truncated Singular Value Decomposition (TSVD)

The singular value decomposition (SVD) of an  $M \times N$  matrix  $A$  is given by

$$A = USV^T \quad (3.8)$$

where  $U = [\mathbf{u}_1, \mathbf{u}_2, \dots, \mathbf{u}_M] \in \mathbb{R}^{M \times M}$  and  $V = [\mathbf{v}_1, \mathbf{v}_2, \dots, \mathbf{v}_N] \in \mathbb{R}^{N \times N}$  are orthogonal matrices, and  $S$  is a diagonal matrix containing the singular values  $(s_i)_{i=1}^N$  such that

$$s_1 \geq s_2 \geq \dots \geq s_N > 0.$$

Let  $A$  be of rank  $l$ . Then (3.8) can be expressed as

$$A = \sum_{j=1}^l s_j \mathbf{u}_j \mathbf{v}_j^T \quad (3.9)$$

with  $s_1 \geq s_2 \geq \dots \geq s_l > 0$ . Now, we consider the Moore-Penrose pseudoinverse of  $A$ , given by

$$A^+ = \sum_{j=1}^l s_j^{-1} \mathbf{v}_j \mathbf{u}_j^T. \quad (3.10)$$

The small positive singular values of the matrix  $A$  may cause the numerical instability in finding the solution of the minimization problem (3.7). In order to overcome the difficulty, we use the truncated singular value decomposition (TSVD) or ignore the small singular values of  $A$ . Namely, we use

$$A_\epsilon = \sum_{j=1}^k s_j \mathbf{u}_j \mathbf{v}_j^T,$$

for some preassigned  $\epsilon > 0$ , where  $s_k > \epsilon \geq s_{k+1}$ , with Moore-Penrose pseudoinverse

$$A_\epsilon^+ = \sum_{j=1}^k s_j^{-1} \mathbf{v}_j \mathbf{u}_j^T.$$

Using the TSVD method we get approximate solutions of (3.10) of the form

$$\mathbf{x}_\epsilon = A_\epsilon^+ \mathbf{b} = \sum_{j=1}^k \frac{\mathbf{u}_j^T \mathbf{b}}{s_j} \mathbf{v}_j, \quad k = 1, 2, \dots, l. \quad (3.11)$$

It is easy to apply the quantities

$$\tilde{\mathbf{x}}_\epsilon = V^T \mathbf{x}_\epsilon, \quad \tilde{\mathbf{b}} = [\tilde{b}_1, \tilde{b}_2, \dots, \tilde{b}_m]^T = U^T \mathbf{b}.$$

Thus, we get

$$\tilde{\mathbf{x}}_\epsilon = \left[ \frac{\tilde{b}_1}{s_1}, \frac{\tilde{b}_2}{s_2}, \dots, \frac{\tilde{b}_k}{s_k}, 0, \dots, 0 \right]^T \quad (3.12)$$

for  $1 \leq k \leq l$  and then determine the approximate solution  $\mathbf{x}_\epsilon = V \tilde{\mathbf{x}}_\epsilon$  of (3.10).

### 3.1.2 Tikhonov Regularization Method

The details of the Tikhonov regularization theory can be formed in [8]. Here we just quote the procedure for the purposes of numerical computations. The solution of the system of  $A\mathbf{x} = \mathbf{b}$  by the regularization method with respect to a parameter  $\mu$  is denoted by  $\mathbf{x}_\mu$ , which solves the following minimization problem

$$\min_{\mathbf{x} \in \mathbb{R}^N} \{ \|A\mathbf{x} - \mathbf{b}\|^2 + \mu \|T_k \mathbf{x}\|^2 \}, \quad (3.13)$$

where the matrix  $T_k \in \mathbb{R}^{(N-k) \times N}$ ,  $k = 0, 1, 2$ , induces a  $C^k$ -constraint on the solution  $\mathbf{x}$  and the scalar  $\mu > 0$  is known as the regularization parameter. If  $\mu = 0$  in (3.13), then it reduces to the ordinary least-squares method which is usually unstable. The matrix  $T_k$ ,  $k = 0, 1, 2$ , is given by (cf. [2]),

$$\begin{aligned} T_0 &= \mathbb{I} \in \mathbb{R}^{N \times N}, \\ T_1 &= \begin{bmatrix} -1 & 1 & 0 & \dots & 0 \\ 0 & -1 & 1 & \dots & 0 \\ \vdots & \vdots & \vdots & \ddots & \vdots \\ 0 & 0 & 0 & \dots & 1 \end{bmatrix} \in \mathbb{R}^{(N-1) \times N}, \\ T_2 &= \begin{bmatrix} 1 & -2 & 1 & 0 & \dots & 0 \\ 0 & 1 & -2 & 1 & \dots & 0 \\ \vdots & \vdots & \vdots & \vdots & \ddots & \vdots \\ 0 & 0 & 0 & 0 & \dots & 1 \end{bmatrix} \in \mathbb{R}^{(N-2) \times N}. \end{aligned}$$

For the minimization of  $\|A\mathbf{x} - \mathbf{b}\|^2 + \mu \|\mathbf{x}\|^2$ , the solution (3.13) becomes

$$\mathbf{x}_\mu = (A^T A + \mu T_k^T T_k)^{-1} A^T \mathbf{b}. \quad (3.14)$$

The applications of TSVD and Tikhonov regularization methods will be illustrated in the examples presented in the next section.

## 3.2 Numerical Examples by using MFS for Helmholtz equations

**Example 3.1.** Consider the Dirichlet boundary problem for the following so-called modified Helmholtz equation

$$\begin{aligned}\Delta u(x, y) - 5u(x, y) &= 0, & (x, y) \in \Omega, \\ u(x, y) &= e^{3x} \cos(2y), & (x, y) \in \partial\Omega,\end{aligned}$$

where  $\kappa = \sqrt{5}$  and  $\Omega = \{(x, y) : x^2 + y^2 \leq 1\}$  is the unit disc. The exact solution of the above problem is  $u_{exact} = e^{3x} \cos(2y)$ . To use the MFS, we choose  $M$  points equally distributed on  $\partial\Omega$ , namely:  $\mathbf{x}_k = (\cos \frac{2\pi k}{M}, \sin \frac{2\pi k}{M})$ ,  $0 \leq k \leq M - 1$ . We use a fictitious domain  $\tilde{\Omega} = \{(x, y) : x^2 + y^2 \leq r^2\}$ , where  $r = 1.2, 1.4, 1.6, 1.8$ , respectively, as shown in Figure 3.1 for  $r = 1.5$ . Choose equally distributed  $N = \{100, 150, 200, 250\}$  points  $\tilde{\mathbf{x}}_k = R(\cos \frac{2\pi k}{N}, \sin \frac{2\pi k}{N})$ ,  $0 \leq k \leq N - 1$  on  $\partial\tilde{\Omega}$ . Then the varying number of collocation points on  $\partial\Omega$  and source points on  $\partial\tilde{\Omega}$  cause the ill-condition system (3.6) and hence in order to resolve the unstable results, we use the Tikhonov regularization with regularization parameters,  $\mu = \{10^{-3}, 10^{-5}, 10^{-7}, 10^{-8}\}$ , respectively to obtain the approximate solution through (3.13)-(3.14). To estimate the maximum error, we use equally spaced  $N = 100$  points  $\mathbf{z}_k$ ,  $1 \leq k \leq 100$ , on  $\partial\Omega$  to get the numerical infinity norm

$$\max_{1 \leq k \leq 100} |u_{exact}(\mathbf{z}_k) - u_N(\mathbf{z}_k)|,$$

since the maximal principal holds for the modified Helmholtz equation. Then our numerical approximation errors are presented in the following table with various  $r$  and  $N$ :



Figure 3.1: Choose  $M = 20$  collocation points (\*) on the  $\partial\Omega$ , and  $N = 20$  source points (o) on the  $\partial\tilde{\Omega}$  with  $r = 1.5$

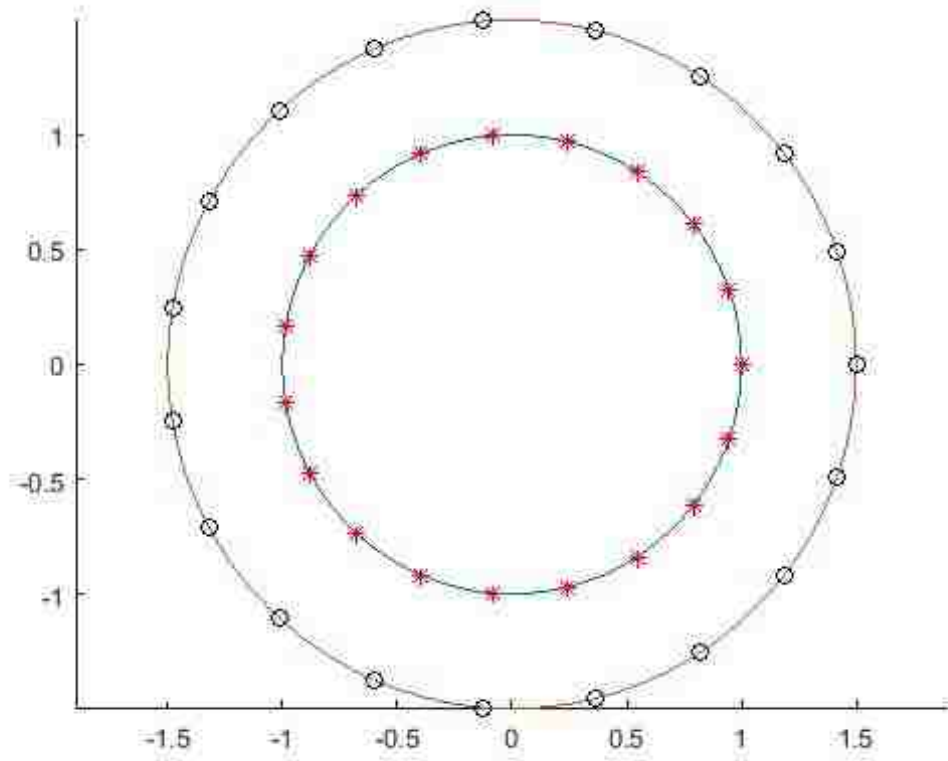
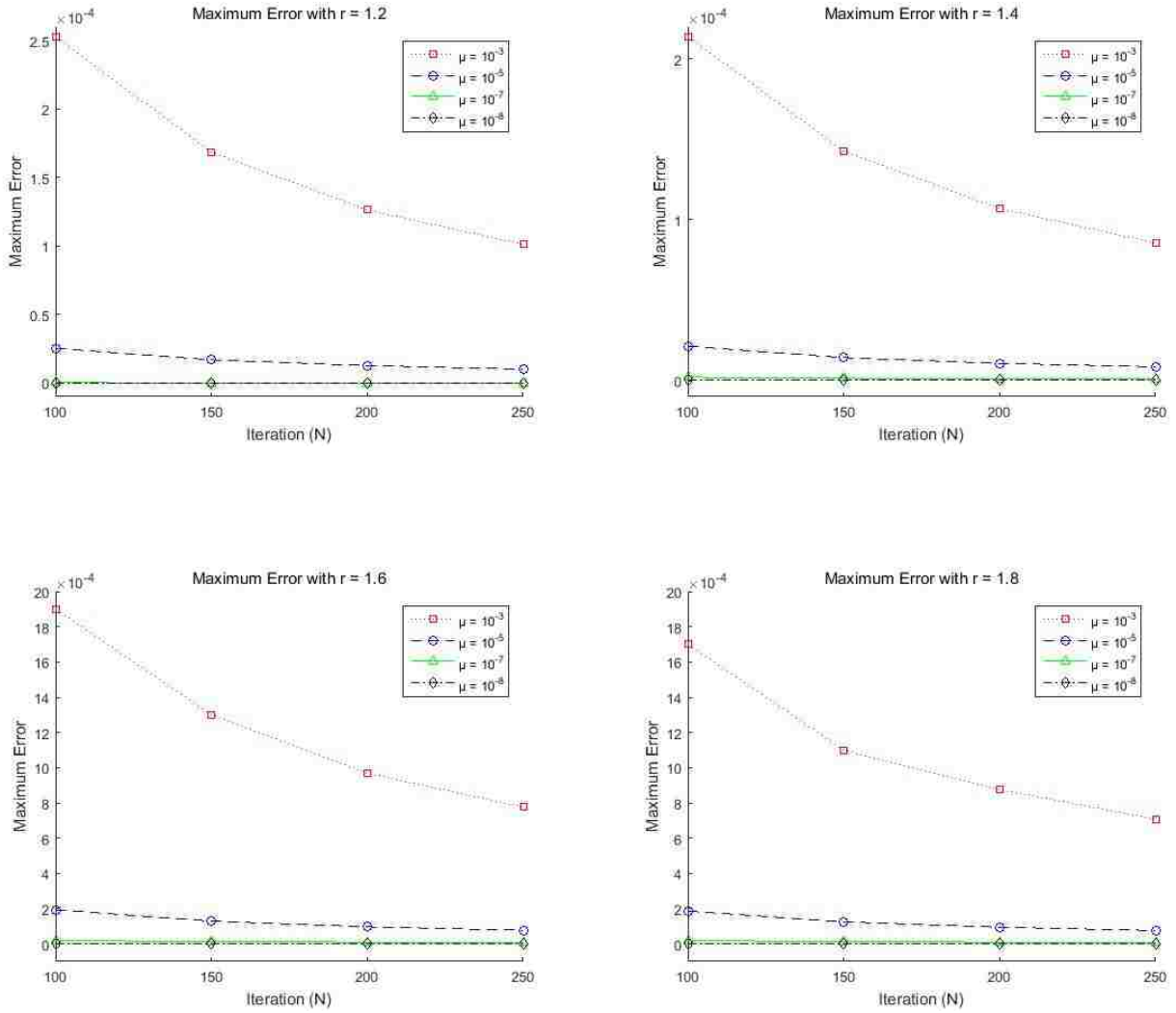


Table 3.1: Maximum Error  $\|u_{exact} - u_N\|_{C(\partial\Omega)}$ 

	M = 300 N = 100	M = 300 N = 150	M = 300 N = 200	M = 300 N = 250
$r = 1.2, \mu = 10^{-3}$	2.5252e-04	1.6834e-04	1.2626e-04	1.0101e-04
$r = 1.2, \mu = 10^{-5}$	2.5262e-05	1.6835e-05	1.2626e-05	1.0101e-05
$r = 1.2, \mu = 10^{-7}$	2.6218e-07	1.6835e-07	1.2626e-07	1.0102e-07
$r = 1.2, \mu = 10^{-8}$	3.4904e-08	1.6847e-08	1.2663e-08	1.0157e-08
$r = 1.4, \mu = 10^{-3}$	2.1389e-04	1.4253e-04	1.0687e-04	8.5481e-05
$r = 1.4, \mu = 10^{-5}$	2.1360e-05	1.4239e-05	1.0679e-05	8.5433e-06
$r = 1.4, \mu = 10^{-7}$	2.1357e-06	1.4238e-06	1.0679e-06	8.5429e-07
$r = 1.4, \mu = 10^{-8}$	2.1357e-07	1.4238e-07	1.0680e-07	8.5447e-08
$r = 1.6, \mu = 10^{-3}$	0.0019	0.0013	9.6849e-04	7.7560e-04
$r = 1.6, \mu = 10^{-5}$	1.9332e-04	1.2859e-04	9.6335e-05	7.7020e-05
$r = 1.6, \mu = 10^{-7}$	1.9177e-05	1.2772e-05	9.5736e-06	7.6557e-06
$r = 1.6, \mu = 10^{-8}$	1.9108e-06	1.2736e-06	9.5503e-07	7.6396e-07
$r = 1.8, \mu = 10^{-3}$	0.0017	0.0011	8.7517e-04	7.0747e-04
$r = 1.8, \mu = 10^{-5}$	1.8555e-04	1.2482e-04	9.4055e-05	7.5455e-05
$r = 1.8, \mu = 10^{-7}$	1.8969e-05	1.2648e-05	9.4938e-06	7.5977e-06
$r = 1.8, \mu = 10^{-8}$	1.8969e-06	1.2633e-06	9.4680e-07	7.5702e-07

Figure 3.2: Maximum errors on fictitious domains  $\partial\tilde{\Omega} = \{(x, y) : x^2 + y^2 = r^2, r = 1.2, 1.4, 1.6, 1.8\}$  with regularization parameters,  $\mu = 10^{-3}$  ( $\square$ ),  $\mu = 10^{-5}$  ( $\circ$ ),  $\mu = 10^{-7}$  ( $\triangle$ ),  $\mu = 10^{-8}$  ( $\diamond$ ), respectively



**Example 3.2.** Consider the Dirichlet boundary problem for the Helmholtz equation

$$\Delta u(x, y) + 3u(x, y) = 0, \quad (x, y) \in \Omega,$$

$$u(x, y) = e^x \sin(2y), \quad (x, y) \in \partial\Omega,$$

where  $\kappa = \sqrt{3}$  and  $\Omega = \{(x, y) : x = \sin(t + \sin t), y = \cos(t + \cos t), 0 \leq t \leq 2\pi\}$ .

The exact solution of the above problem is  $u_{exact} = e^x \sin(2y)$ . We use a fictitious domain

$\tilde{\Omega} = \{(x, y) : x = a \cos t, y = b \sin(t + \cos t), 0 \leq t \leq 2\pi\}$ , where  $a = 2, 3, 4$  and  $b = 2,$

$4, 2$ , respectively. We choose  $\tilde{\mathbf{x}}_{\mathbf{k}} = (a \cos \frac{2\pi k}{N}, b \sin(\frac{2\pi k}{N} + \cos \frac{2\pi k}{N}))$ ,  $0 \leq k \leq N - 1$  on  $\partial\tilde{\Omega}$ .

To use the MFS, we choose  $N$  points on  $\partial\Omega$  corresponding to  $t_k = \frac{2\pi k}{N}$ ,  $0 \leq k \leq N - 1$ , (see

Figure 3.3). Here we test our numerical results for points  $(0.25, 0.25)$ ,  $(-0.1, 0.3)$ , and  $(-0.3,$

$0.5)$  inside  $\Omega$  with  $N = 150, 200, 250, 300$  and  $a = 2, 3, 4$  and  $b = 2, 4, 2$ , respectively. Then

in order to resolve the difficulty due to the unstable result, we use the TSVD with singular

value tolerances,  $\epsilon = \{10^{-1}, 10^{-3}, 10^{-7}\}$ , respectively to obtain the approximate solution

through (3.5)-(3.6). The results are presented in the following tables:

Figure 3.3: Choose  $N=20$  collocation points (\*) on the  $\partial\Omega$ , and  $N=20$  source points (o) on the  $\partial\tilde{\Omega}$ , and three tested points  $(0.25, 0.25)$ ,  $(-0.1, 0.3)$ , and  $(-0.3, 0.5)$

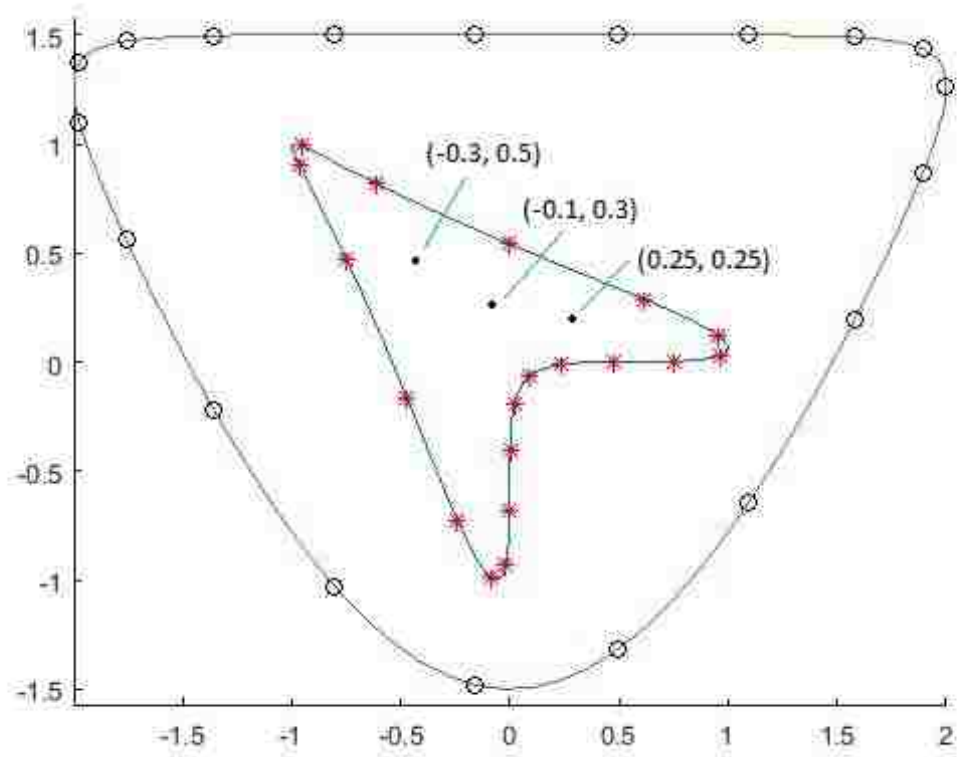


Table 3.2: Maximum Error for  $u(0.25, 0.25)$ 

	M = 300 N = 150	M = 300 N = 200	M = 300 N = 250	M = 300 N = 300
a = 2, b = 2 $\epsilon = 10^{-1}$	2.1438e-15 (k = 1)	1.2718e-15 (k = 1)	1.9754e-15 (k = 1)	1.5079e-16 (k = 1)
a = 2, b = 2 $\epsilon = 10^{-3}$	2.1438e-15 (k = 7)	1.2652e-15 (k = 7)	1.9795e-15 (k = 7)	1.5536e-16 (k = 7)
a = 2, b = 2 $\epsilon = 10^{-7}$	2.1334e-15 (k = 150)	1.2678e-15 (k = 199)	1.9951e-15 (k = 249)	1.5908e-16 (k = 299)
a = 3, b = 4 $\epsilon = 10^{-1}$	2.7566e-15 (k = 1)	5.8370e-16 (k = 1)	8.1430e-16 (k = 1)	1.2429e-15 (k = 1)
a = 3, b = 4 $\epsilon = 10^{-3}$	1.5400e-13 (k = 1)	3.4410e-14 (k = 6)	4.6313e-14 (k = 6)	7.0444e-14 (k = 7)
a = 3, b = 4 $\epsilon = 10^{-7}$	1.5369e-13 (k = 149)	3.2953e-14 (k = 199)	4.4814e-14 (k = 249)	7.0064e-14 (k = 299)
a = 4, b = 2 $\epsilon = 10^{-1}$	3.4914e-15 (k = 1)	8.1888e-16 (k = 1)	1.0354e-15 (k = 1)	1.8038e-15 (k = 1)
a = 4, b = 2 $\epsilon = 10^{-3}$	1.9322e-13 (k = 1)	4.4064e-14 (k = 6)	5.7993e-14 (k = 7)	1.0079e-13 (k = 7)
a = 4, b = 2 $\epsilon = 10^{-7}$	1.9371e-13 (k = 149)	4.4462e-14 (k = 199)	5.7653e-14 (k = 249)	1.0178e-13 (k = 299)
a = 4, b = 3 $\epsilon = 10^{-1}$	2.7766e-15 (k = 1)	1.4698e-15 (k = 1)	5.5405e-16 (k = 1)	1.4090e-15 (k = 1)
a = 4, b = 3 $\epsilon = 10^{-3}$	1.5407e-13 (k = 1)	8.0714e-14 (k = 6)	3.0036e-14 (k = 6)	7.8086e-14 (k = 7)
a = 4, b = 3 $\epsilon = 10^{-7}$	1.5399e-13 (k = 149)	8.1380e-14 (k = 199)	3.1246e-14 (k = 249)	7.6771e-14 (k = 299)

Figure 3.4: Maximum errors at a tested point (0.25, 0.25) inside  $\Omega$  with singular value tolerances,  $\epsilon = 10^{-1}$  ( $\square$ ),  $\epsilon = 10^{-3}$  ( $\circ$ ),  $\epsilon = 10^{-7}$  ( $\triangle$ ), respectively

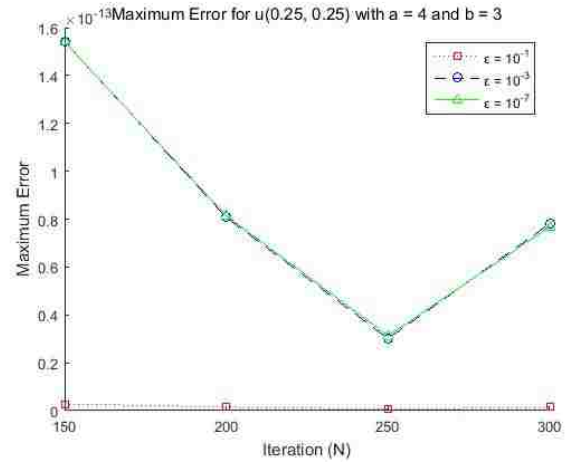
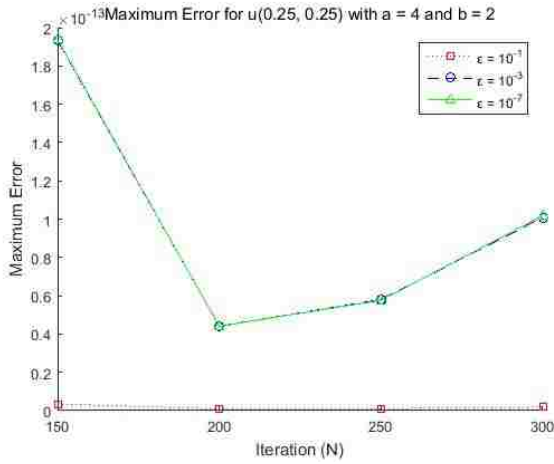
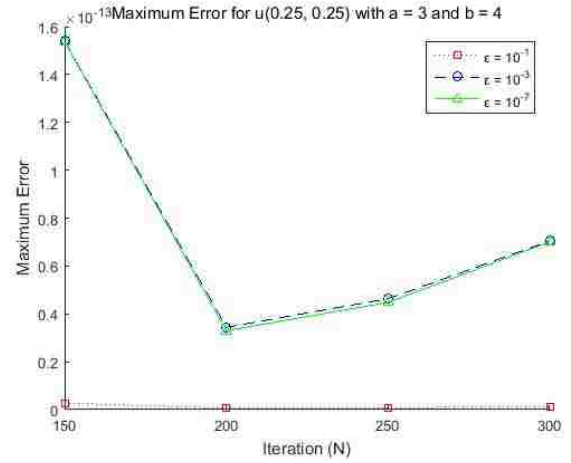
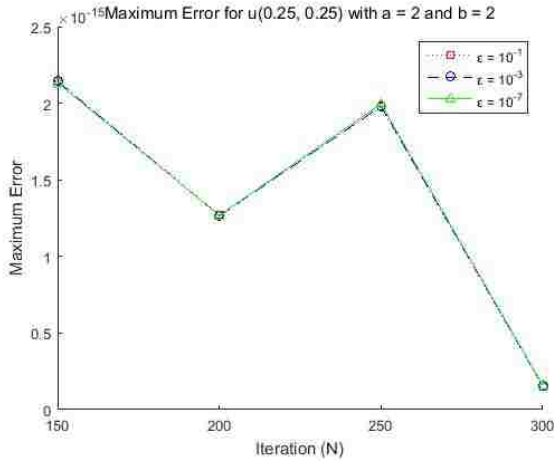


Table 3.3: Maximum Error for  $u(-0.1, 0.3)$ 

	M = 300 N = 150	M = 300 N = 200	M = 300 N = 250	M = 300 N = 300
a = 2, b = 2 $\epsilon = 10^{-1}$	5.6286e-16 (k = 1)	2.2879e-16 (k = 1)	3.2760e-16 (k = 1)	3.3526e-16 (k = 1)
a = 2, b = 2 $\epsilon = 10^{-3}$	9.7318e-14 (k = 2)	3.8999e-14 (k = 7)	5.7074e-14 (k = 7)	5.7684e-14 (k = 7)
a = 2, b = 2 $\epsilon = 10^{-7}$	9.7058e-14 (k = 149)	3.9054e-14 (k = 199)	5.6641e-14 (k = 249)	5.7924e-14 (k = 299)
a = 3, b = 4 $\epsilon = 10^{-1}$	8.3914e-14 (k = 1)	3.9264e-14 (k = 1)	3.2507e-14 (k = 1)	4.2169e-14 (k = 1)
a = 3, b = 4 $\epsilon = 10^{-3}$	8.3914e-14 (k = 6)	3.8853e-14 (k = 6)	3.3487e-14 (k = 6)	4.2086e-14 (k = 6)
a = 3, b = 4 $\epsilon = 10^{-7}$	8.3877e-14 (k = 149)	3.9159e-14 (k = 199)	3.3151e-14 (k = 249)	4.2390e-14 (k = 299)
a = 4, b = 2 $\epsilon = 10^{-1}$	7.3569e-14 (k = 1)	2.0651e-14 (k = 1)	1.4421e-15 (k = 1)	3.8017e-14 (k = 1)
a = 4, b = 2 $\epsilon = 10^{-3}$	7.3569e-14 (k = 1)	2.0539e-14 (k = 6)	1.0965e-15 (k = 7)	3.6803e-14 (k = 7)
a = 4, b = 2 $\epsilon = 10^{-7}$	7.3906e-14 (k = 149)	2.0652e-14 (k = 199)	1.0774e-15 (k = 249)	3.7358e-14 (k = 299)
a = 4, b = 3 $\epsilon = 10^{-1}$	9.4201e-14 (k = 1)	1.0281e-14 (k = 1)	4.0873e-14 (k = 1)	6.0280e-14 (k = 1)
a = 4, b = 3 $\epsilon = 10^{-3}$	9.4201e-14 (k = 6)	9.1901e-15 (k = 6)	4.0774e-14 (k = 6)	6.1221e-14 (k = 7)
a = 4, b = 3 $\epsilon = 10^{-7}$	9.4384e-14 (k = 149)	1.0817e-14 (k = 199)	4.1577e-14 (k = 249)	6.1424e-14 (k = 299)



Figure 3.5: Maximum errors at a tested point  $(-0.1, 0.3)$  inside  $\Omega$  with singular value tolerances,  $\epsilon = 10^{-1}$  ( $\square$ ),  $\epsilon = 10^{-3}$  ( $\circ$ ),  $\epsilon = 10^{-7}$  ( $\triangle$ ), respectively

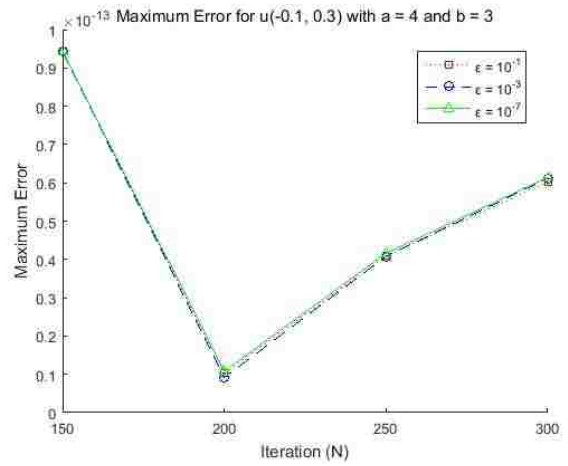
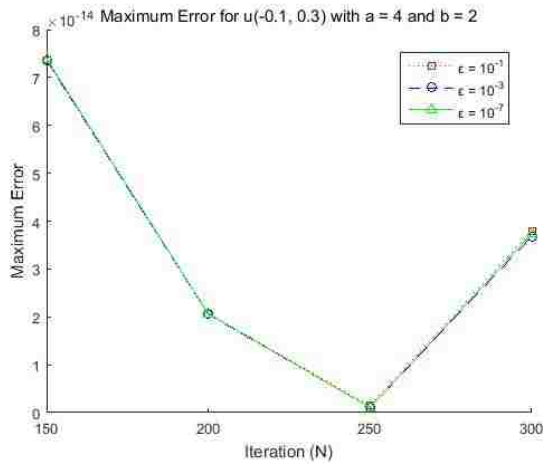
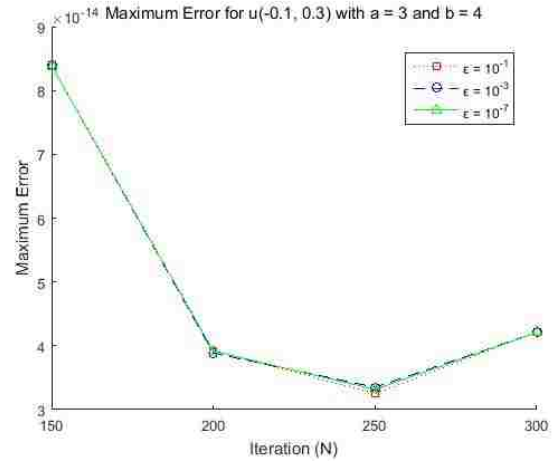
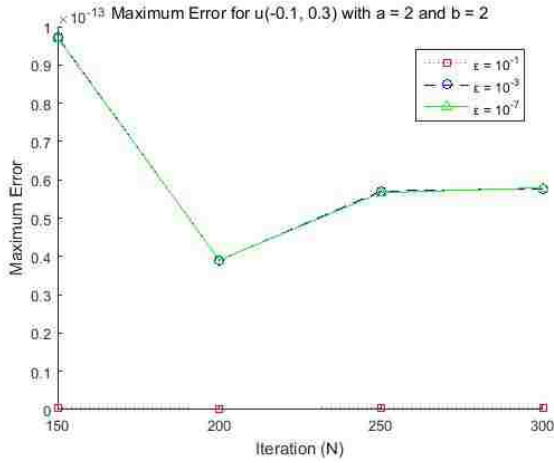
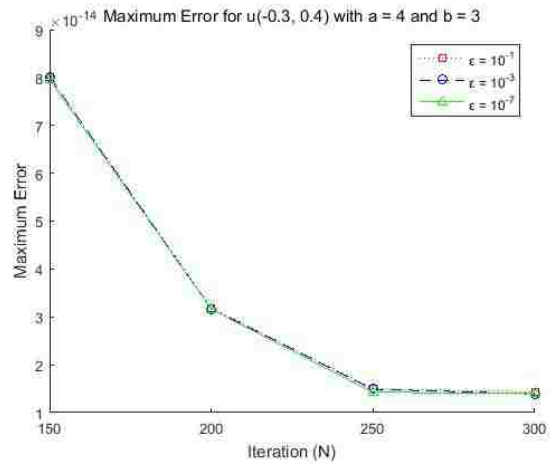
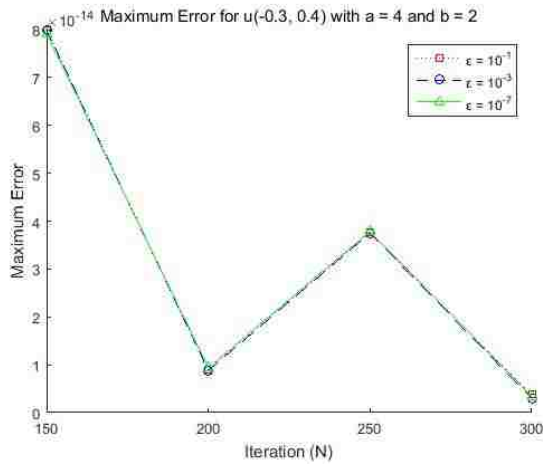
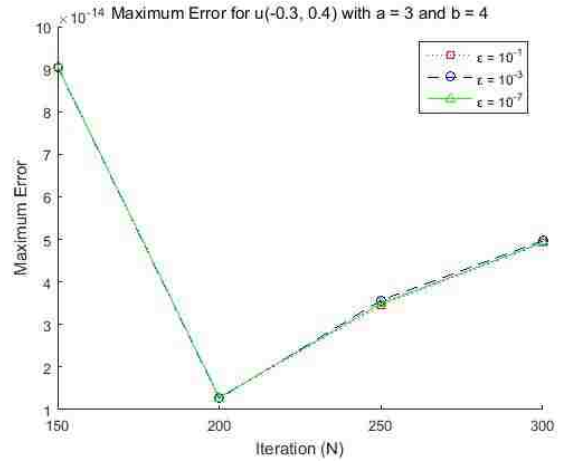
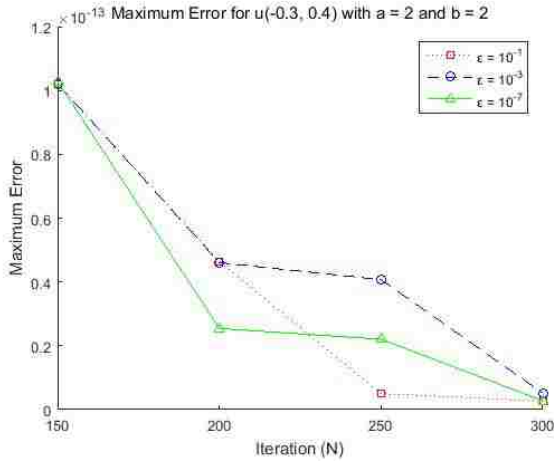


Table 3.4: Maximum Error for  $u(-0.3, 0.4)$ 

	M = 300 N = 150	M = 300 N = 200	M = 300 N = 250	M = 300 N = 300
a = 2, b = 2 $\epsilon = 10^{-1}$	1.0213e-13 (k = 1)	4.6447e-14 (k = 1)	5.0229e-15 (k = 1)	2.6757e-15 (k = 1)
a = 2, b = 2 $\epsilon = 10^{-3}$	1.0213e-13 (k = 1)	4.6062e-14 (k = 7)	4.0722e-14 (k = 7)	5.1481e-15 (k = 7)
a = 2, b = 2 $\epsilon = 10^{-7}$	1.0284e-13 (k = 149)	2.5439e-14 (k = 199)	2.2066e-14 (k = 249)	2.7971e-15 (k = 299)
a = 3, b = 4 $\epsilon = 10^{-1}$	9.0552e-14 (k = 1)	1.2859e-14 (k = 1)	3.4508e-14 (k = 1)	4.9189e-14 (k = 1)
a = 3, b = 4 $\epsilon = 10^{-3}$	9.0552e-14 (k = 1)	1.2628e-14 (k = 6)	3.5696e-14 (k = 7)	4.9667e-14 (k = 7)
a = 3, b = 4 $\epsilon = 10^{-7}$	9.0738e-14 (k = 149)	1.2865e-14 (k = 199)	3.4968e-14 (k = 249)	4.9233e-14 (k = 299)
a = 4, b = 2 $\epsilon = 10^{-1}$	7.9908e-14 (k = 1)	9.0141e-15 (k = 1)	3.7597e-14 (k = 1)	3.7726e-15 (k = 1)
a = 4, b = 2 $\epsilon = 10^{-3}$	7.9908e-14 (k = 1)	8.8085e-15 (k = 6)	3.7504e-14 (k = 7)	2.9795e-15 (k = 7)
a = 4, b = 2 $\epsilon = 10^{-7}$	7.9237e-14 (k = 149)	9.3523e-15 (k = 199)	3.7836e-14 (k = 249)	3.3494e-15 (k = 299)
a = 4, b = 3 $\epsilon = 10^{-1}$	8.0163e-14 (k = 1)	3.1870e-14 (k = 1)	1.4948e-14 (k = 1)	1.4347e-14 (k = 1)
a = 4, b = 3 $\epsilon = 10^{-3}$	8.0163e-14 (k = 1)	3.1662e-14 (k = 6)	1.4907e-14 (k = 7)	1.3900e-14 (k = 7)
a = 4, b = 3 $\epsilon = 10^{-7}$	7.9556e-14 (k = 149)	3.1604e-14 (k = 199)	1.4264e-14 (k = 249)	1.3986e-14 (k = 299)

Figure 3.6: Maximum errors at a tested point  $(-0.3, 0.4)$  inside  $\Omega$  with singular value tolerances,  $\epsilon = 10^{-1}$  ( $\square$ ),  $\epsilon = 10^{-3}$  ( $\circ$ ),  $\epsilon = 10^{-7}$  ( $\triangle$ ), respectively



**Example 3.3.** Consider the Dirichlet boundary problem for the Helmholtz equation

$$\Delta u(x, y, z) + 3u(x, y, z) = 0, \quad (x, y, z) \in \Omega,$$

$$u(x, y, z) = x e^y \cos(2z), \quad (x, y, z) \in \partial\Omega,$$

where  $\kappa = \sqrt{3}$  and  $\Omega = \{(x, y, z) : x^2 + y^2 + z^2 < 1\}$  is the unit ball. The exact solution of the above problem is  $u_{exact} = x e^y \cos(2z)$ . To use the MFS, we choose  $N$  points on  $\partial\Omega$  corresponding to spherical coordinates  $x = r \sin \theta \cos \phi$ ,  $y = r \sin \theta \sin \phi$ ,  $z = r \cos \theta$ , where  $0 \leq \theta \leq \pi$ ,  $0 \leq \phi \leq 2\pi$ , with respect to  $\theta_k = \frac{\pi(k+0.5)}{M_\theta}$ ,  $0 \leq k \leq M_\theta - 1$ , with  $M_\theta = \frac{\sqrt{\pi N}}{2r}$  ( $r = 1$  for the unit sphere), and  $\phi_{k,m} = \frac{2\pi m}{M_k}$ ,  $0 \leq m \leq M_k - 1$ , with  $M_k = \sqrt{\pi N \sin \theta_k}$ . We use a fictitious domain  $\tilde{\Omega} = \{(x, y, z) : x^2 + y^2 + z^2 \leq r^2\}$ , where  $r = 1.5, 2, 3$ . We choose  $\tilde{\mathbf{x}}_{\mathbf{k},\mathbf{m}} = (\sin \theta_k \cos \phi_{k,m}, \sin \theta_k \sin \phi_{k,m}, \cos \phi_{k,m})$ ,  $0 \leq k \leq M_\theta - 1$ ,  $0 \leq m \leq M_k - 1$ , where  $M_\theta = \frac{\sqrt{\pi N}}{2r}$  and  $M_k = \frac{\sqrt{\pi N \sin \theta_k}}{r}$  with  $r = 1.5, 2, 3$  on  $\partial\tilde{\Omega}$ , (cf. [3]), (see Figure 3.7). Then the approximate solution for  $u(0.5, 0.5, 0.5)$ ,  $u(0.1, 0.5, 0.8)$ , and  $u(0.3, 0.9, 0.4)$  in  $\Omega$  can be obtained with  $N = 150, 200, 250, 300$  and  $r = 1.5, 2, 3$  in Table 27, 28, and 29, respectively. We have the following numerical results:

Figure 3.7: Choose  $N = 300$  collocation points on the  $\partial\Omega$ , and  $N = 300$  source points on the  $\partial\Omega$ , and  $r = 2.0$

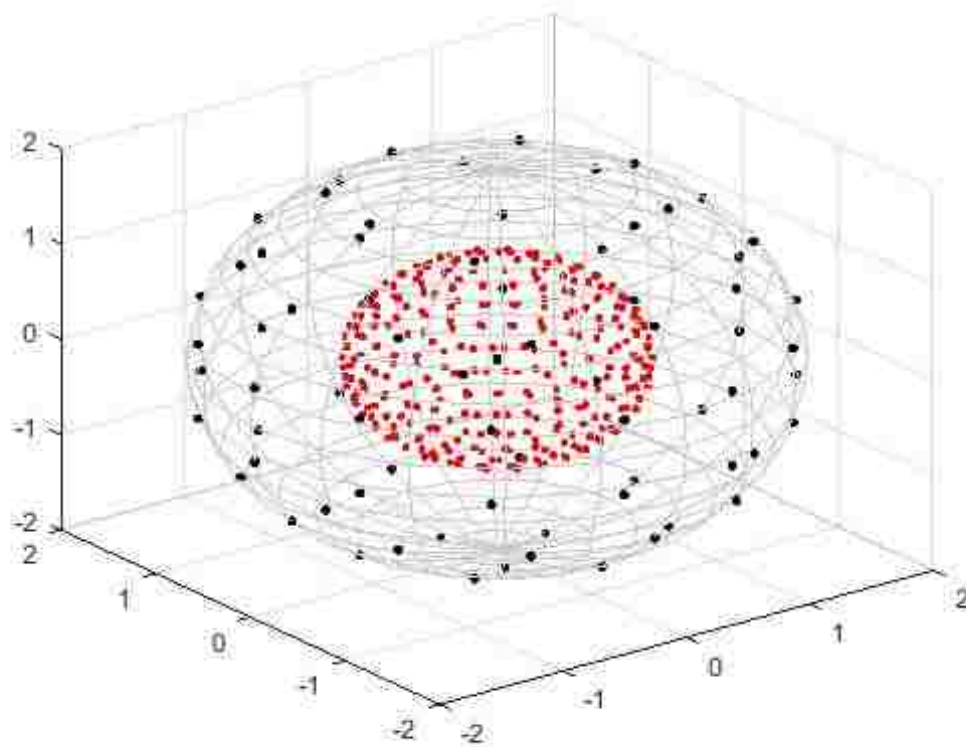


Table 3.5: Maximum Error for  $u(0.5, 0.5, 0.5)$

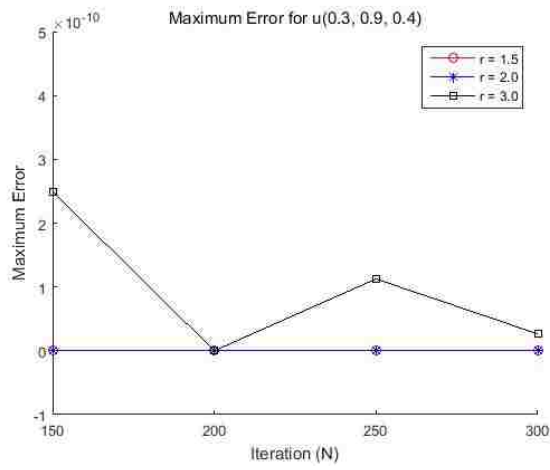
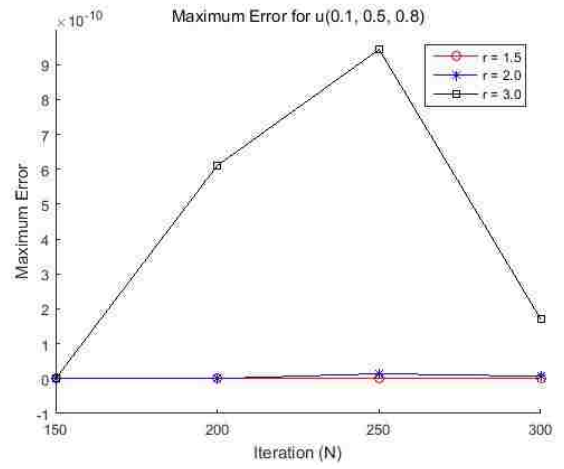
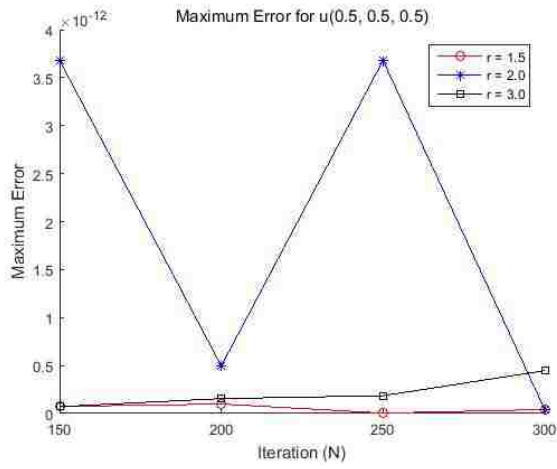
	$N = 150$	$N = 200$	$N = 250$	$N = 300$
$r = 1.5$	$7.3608e-14$	$9.8477e-14$	$4.5519e-15$	$4.1633e-14$
$r = 2.0$	$3.6796e-12$	$4.9638e-13$	$3.6796e-12$	$4.1633e-14$
$r = 3.0$	$7.2053e-14$	$1.5532e-13$	$1.8574e-13$	$4.4642e-13$

Table 3.6: Maximum Error for  $u(0.1, 0.5, 0.8)$

	N = 150	N = 200	N = 250	N = 300
r = 1.5	1.1935e-15	8.4127e-14	3.4592e-13	3.4592e-13
r = 2.0	1.3461e-14	3.0423e-13	1.3988e-11	6.7124e-12
r = 3.0	8.0408e-14	6.1062e-10	9.4327e-10	1.7090e-10

Table 3.7: Maximum Error for  $u(0.3, 0.9, 0.4)$

	N = 150	N = 200	N = 250	N = 300
r = 1.5	2.2204e-15	4.7740e-15	4.5519e-15	8.9928e-15
r = 2.0	2.5868e-14	6.3283e-15	1.6098e-14	4.6962e-14
r = 3.0	2.4956e-10	1.5210e-14	1.1257e-10	2.6547e-11



Similarly, the MFS can be applied to other boundary value problems for Helmholtz equations. Below we present the examples for Newmann and Robin (Mixed) conditions.

**Example 3.4.** Consider the Newmann boundary problem for the Helmholtz equation

$$\begin{aligned}\Delta u(x, y) + 6u(x, y) &= 0, & (x, y) \in \Omega, \\ \frac{\partial u}{\partial \mathbf{n}}(x, y) &= (x + y)e^{x+y} \cos(2x - 2y) - 2(x - y)e^{x+y} \sin(2x - 2y), & (x, y) \in \partial\Omega,\end{aligned}$$

where  $\kappa = \sqrt{6}$  and  $\Omega = \{(x, y) : x^2 + y^2 < 1\}$ . The exact solution of the above problem is  $u_{exact} = e^{x+y} \cos(2x - 2y)$ . We use a fictitious domain  $\tilde{\Omega} = \{(x, y) : x = a \cos t, y = b \sin(t + \cos t), 0 \leq t \leq 2\pi\}$ , where  $a = 2, 3, 3, 4$  and  $b = 2, 4, 3, 3$ , respectively. We choose  $N = \{120, 140, 160, 180\}$  points  $\tilde{\mathbf{x}}_{\mathbf{k}} = (a \cos \frac{2\pi k}{N}, b \sin(\frac{2\pi k}{N} + \cos \frac{2\pi k}{N}))$ ,  $0 \leq k \leq N - 1$  on  $\partial\tilde{\Omega}$ . To use the MFS, we choose  $M$  points on  $\partial\Omega$  corresponding to  $t_k = \frac{2\pi k}{M}$ ,  $0 \leq k \leq M - 1$ , (see Figure 3.8). Here we test our numerical results for points  $(0, -0.5)$ ,  $(-0.5, 0.5)$ , and  $(0.5, 0.5)$  inside  $\Omega$  with  $N = 120, 140, 160, 180$  and  $a = 2, 3, 3, 4$  and  $b = 2, 4, 3, 3$ , respectively. Then the varying number of collocation points on  $\partial\Omega$  and source points on  $\partial\tilde{\Omega}$  cause the ill-condition system (3.6) and hence in order to resolve the unstable results, we use the Tikhonov regularization with regularization parameters,  $\mu = \{10^{-1}, 10^{-3}, 10^{-5}\}$ , respectively to obtain the approximate solution through (3.5)-(3.6). The results are presented in the following tables:



Figure 3.8: Choose  $M=20$  collocation points (\*) on the  $\partial\Omega$ , and  $N=20$  source points (o) on the  $\partial\tilde{\Omega}$

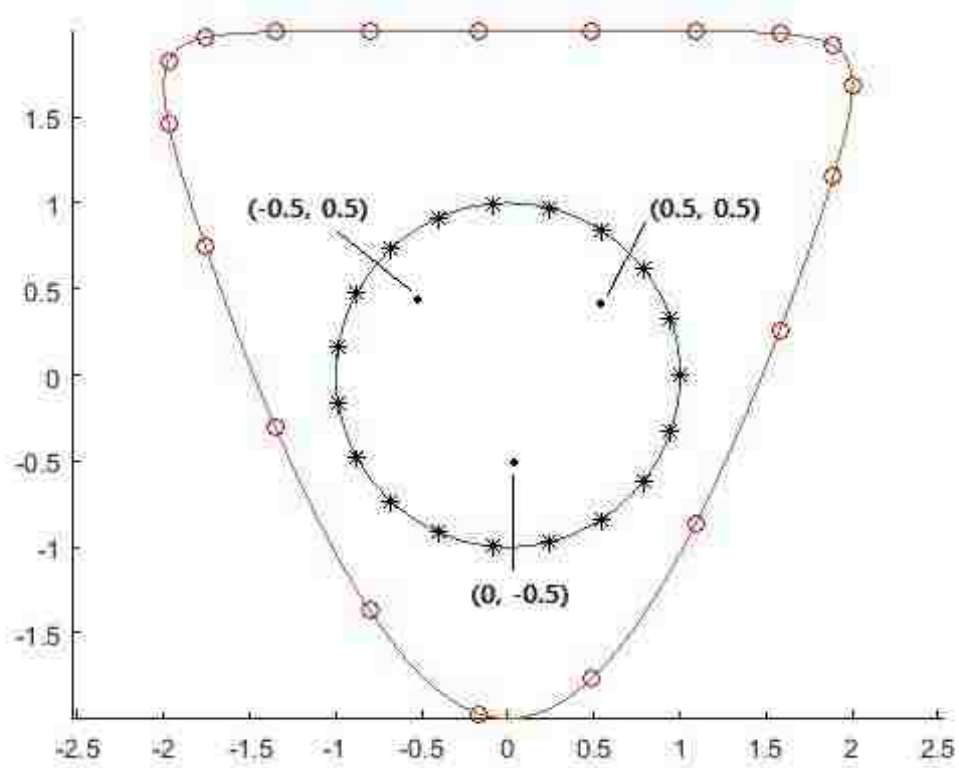


Table 3.8: Maximum Error for  $u(0, -0.5)$

	M = 200 N = 120	M = 200 N = 140	M = 200 N = 160	M = 200 N = 180
$a = 2, b = 2, \mu = 10^{-1}$	2.3472e-04	2.0117e-04	1.7601e-04	1.5645e-04
$a = 2, b = 2, \mu = 10^{-3}$	2.3457e-06	2.0106e-06	1.7593e-06	1.5638e-06
$a = 2, b = 2, \mu = 10^{-5}$	2.3457e-08	2.0106e-08	1.7593e-08	1.5638e-08
$a = 3, b = 4, \mu = 10^{-1}$	3.2508e-04	2.7861e-04	2.4376e-04	2.1666e-04
$a = 3, b = 4, \mu = 10^{-3}$	3.2480e-06	2.7840e-06	2.4360e-06	2.1653e-06
$a = 3, b = 4, \mu = 10^{-5}$	3.2480e-08	2.7840e-08	2.4360e-08	2.1653e-08
$a = 3, b = 3, \mu = 10^{-1}$	0.0011	9.2497e-04	8.0927e-04	7.1930e-04
$a = 3, b = 3, \mu = 10^{-3}$	1.0783e-05	9.2426e-06	8.0873e-06	7.1887e-06
$a = 3, b = 3, \mu = 10^{-5}$	1.0783e-07	9.2425e-08	8.0872e-08	7.1886e-08
$a = 4, b = 3, \mu = 10^{-1}$	6.4393e-04	5.5179e-04	4.8272e-04	4.2901e-04
$a = 4, b = 3, \mu = 10^{-3}$	6.4271e-06	5.5089e-06	4.8203e-06	4.2847e-06
$a = 4, b = 3, \mu = 10^{-5}$	6.4270e-08	5.5088e-08	4.8202e-08	4.2847e-08

Figure 3.9: Maximum errors on fictitious domains,  $\partial\tilde{\Omega} = \{(x, y) : x = a \cos t, y = b \sin(t + \cos t), 0 \leq t \leq 2\pi\}$ , where  $a = 2, 3, 3, 4$  and  $b = 2, 4, 3, 3$  with regularization parameters,  $\mu = 10^{-1}$  ( $\square$ ),  $\mu = 10^{-3}$  ( $\circ$ ),  $\mu = 10^{-5}$  ( $\triangle$ ), respectively

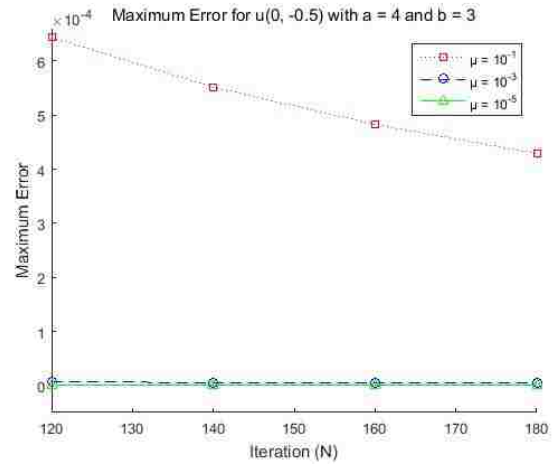
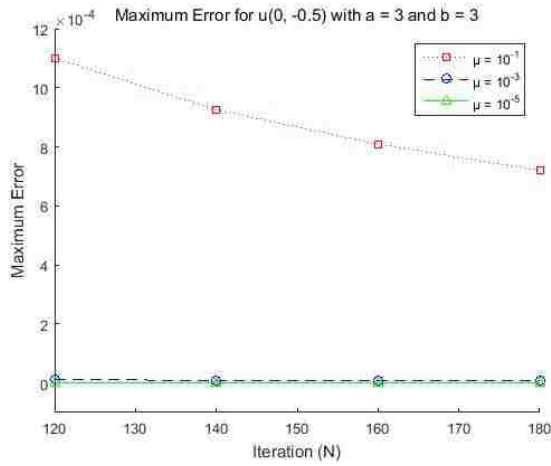
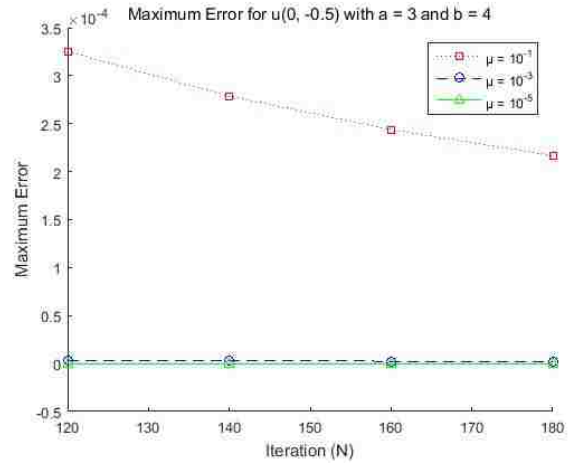
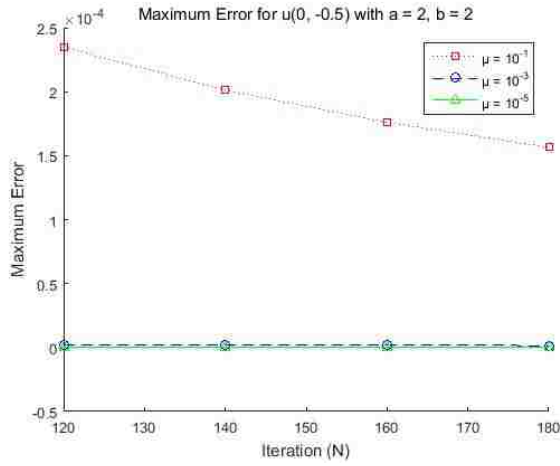


Table 3.9: Maximum Error for  $u(-0.5, 0.5)$

	M = 200 N = 120	M = 200 N = 140	M = 200 N = 160	M = 200 N = 180
$a = 2, b = 2, \mu = 10^{-1}$	1.1169e-04	9.5733e-05	8.3765e-05	7.4456e-05
$a = 2, b = 2, \mu = 10^{-3}$	1.1167e-06	9.5715e-07	8.3751e-07	7.4445e-07
$a = 2, b = 2, \mu = 10^{-5}$	1.1167e-08	9.5715e-09	8.3750e-09	7.4445e-09
$a = 3, b = 4, \mu = 10^{-1}$	4.8254e-04	4.1367e-04	3.6201e-04	3.2182e-04
$a = 3, b = 4, \mu = 10^{-3}$	4.8309e-06	4.1408e-06	3.6232e-06	3.2206e-06
$a = 3, b = 4, \mu = 10^{-5}$	4.8310e-08	4.1409e-08	3.6233e-08	3.2207e-08
$a = 3, b = 3, \mu = 10^{-1}$	2.4509e-04	2.1008e-04	1.8381e-04	1.6339e-04
$a = 3, b = 3, \mu = 10^{-3}$	2.4507e-06	2.1006e-06	1.8380e-06	1.6338e-06
$a = 3, b = 3, \mu = 10^{-5}$	2.4507e-08	2.1006e-08	1.8380e-08	1.6338e-08
$a = 4, b = 3, \mu = 10^{-1}$	3.9661e-04	3.3997e-04	2.9748e-04	2.6444e-04
$a = 4, b = 3, \mu = 10^{-3}$	3.9675e-06	3.4007e-06	2.9756e-06	2.6450e-06
$a = 4, b = 3, \mu = 10^{-5}$	3.9675e-08	3.4007e-08	2.9756e-08	2.6450e-08

Figure 3.10: Maximum errors on fictitious domains,  $\partial\tilde{\Omega} = \{(x, y) : x = a \cos t, y = b \sin(t + \cos t), 0 \leq t \leq 2\pi\}$ , where  $a = 2, 3, 3, 4$  and  $b = 2, 4, 3, 3$  with regularization parameters,  $\mu = 10^{-1}$  ( $\square$ ),  $\mu = 10^{-3}$  ( $\circ$ ),  $\mu = 10^{-5}$  ( $\triangle$ ), respectively

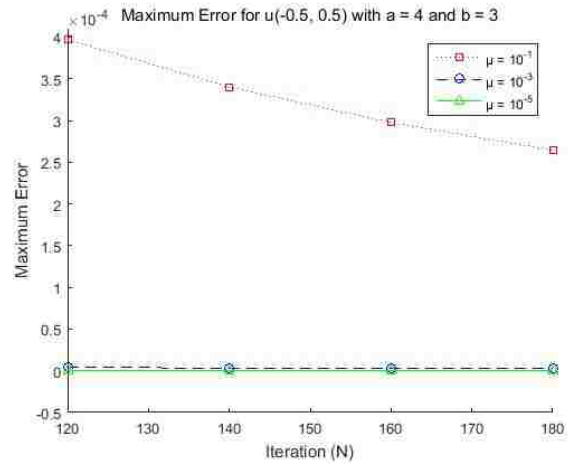
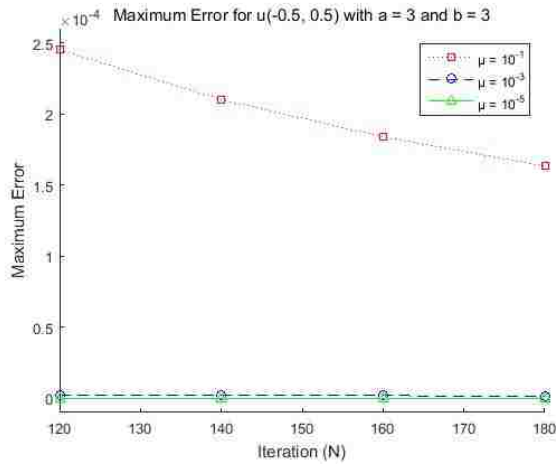
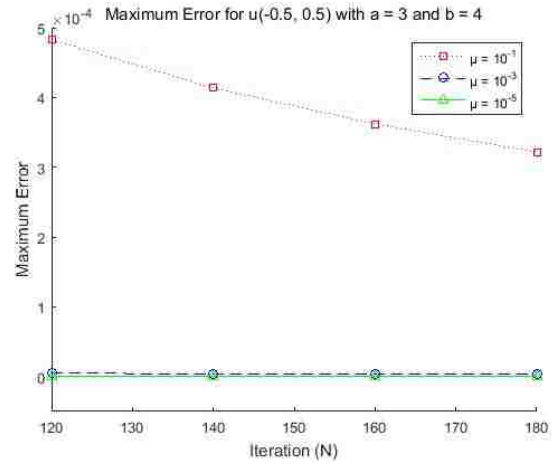
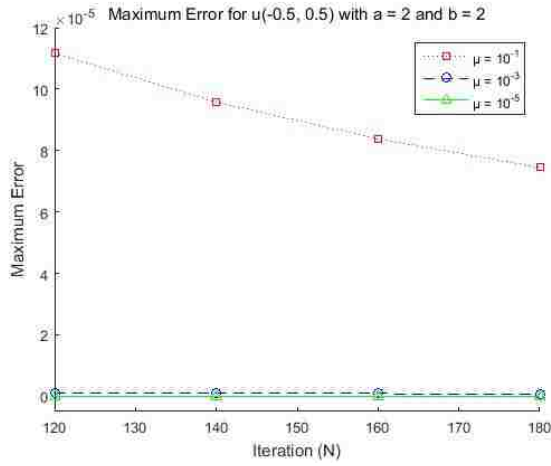
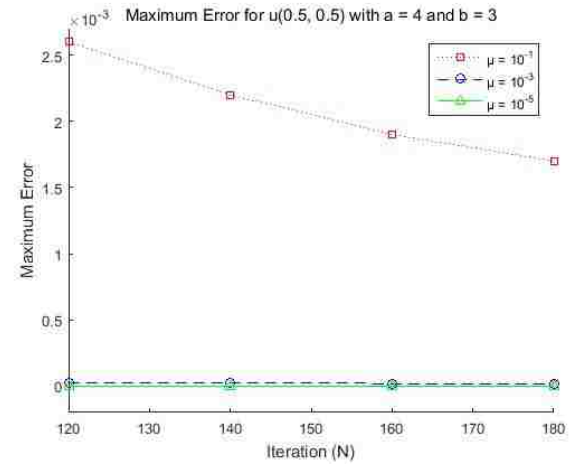
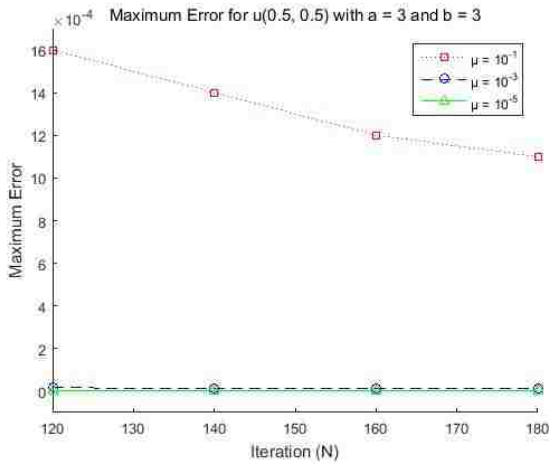
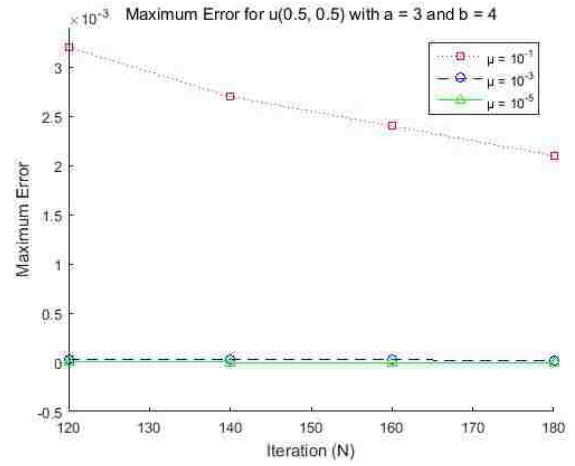
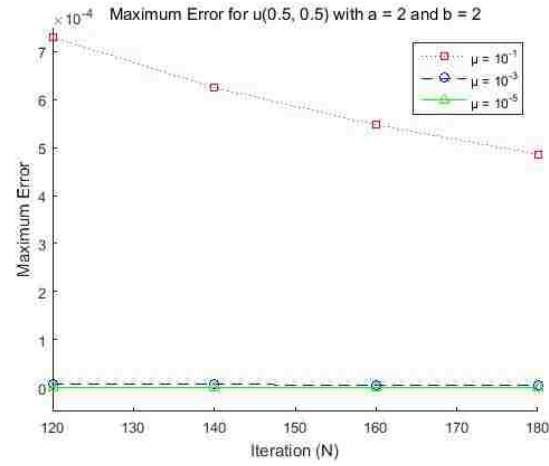


Table 3.10: Maximum Error for  $u(0.5, 0.5)$ 

	M = 200 N = 120	M = 200 N = 140	M = 200 N = 160	M = 200 N = 180
a = 2, b = 2, $\mu = 10^{-1}$	7.2958e-04	6.2533e-04	5.4715e-04	4.8635e-04
a = 2, b = 2, $\mu = 10^{-3}$	7.2941e-06	6.2521e-06	5.4706e-06	4.8628e-06
a = 2, b = 2, $\mu = 10^{-5}$	7.2941e-08	6.2521e-08	5.4706e-08	4.8628e-08
a = 3, b = 4, $\mu = 10^{-1}$	0.0032	0.0027	0.0024	0.0021
a = 3, b = 4, $\mu = 10^{-3}$	3.1556e-05	2.7048e-05	2.3667e-05	2.1037e-05
a = 3, b = 4, $\mu = 10^{-5}$	3.1556e-07	2.7048e-07	2.3667e-07	2.1037e-07
a = 3, b = 3, $\mu = 10^{-1}$	0.0016	0.0014	0.0012	0.0011
a = 3, b = 3, $\mu = 10^{-3}$	1.6008e-05	1.3721e-05	1.2006e-05	1.0672e-05
a = 3, b = 3, $\mu = 10^{-5}$	1.6008e-07	1.3721e-07	1.2006e-07	1.0672e-07
a = 4, b = 3, $\mu = 10^{-1}$	0.0026	0.0022	0.0019	0.0017
a = 4, b = 3, $\mu = 10^{-3}$	2.5916e-05	2.2214e-05	1.9437e-05	1.7277e-05
a = 4, b = 3, $\mu = 10^{-5}$	2.5916e-07	2.2214e-07	1.9437e-07	1.7277e-07

Figure 3.11: Maximum errors on fictitious domains,  $\partial\tilde{\Omega} = \{(x, y) : x = a \cos t, y = b \sin(t + \cos t), 0 \leq t \leq 2\pi\}$ , where  $a = 2, 3, 3, 4$  and  $b = 2, 4, 3, 3$  with regularization parameters,  $\mu = 10^{-1}$  ( $\square$ ),  $\mu = 10^{-3}$  ( $\circ$ ),  $\mu = 10^{-5}$  ( $\triangle$ ), respectively



**Example 3.5.** Consider the Robin (Mixed) boundary problem for the modified Helmholtz equation

$$\begin{aligned}\Delta u(x, y) - 3u(x, y) &= 0, & (x, y) \in \Omega, \\ u(x, y) &= e^{2x} \cos(y), & (x, y) \in \partial\Omega_1, \\ \frac{\partial u}{\partial \mathbf{n}}(x, y) &= e^{2x} \sin(y), & (x, y) \in \partial\Omega_2,\end{aligned}$$

where  $\kappa = \sqrt{3}$  and  $\partial\Omega = \partial\Omega_1 \cup \partial\Omega_2$  such that  $\partial\Omega_1 = \{(x, y) : x = \cos(t), y = \sin(t), 0 \leq t < \pi\}$  and  $\partial\Omega_2 = \{(x, 0) : x = t, -1 \leq t \leq 1\}$ . The exact solution of the above problem is  $u_{exact} = e^{2x} \cos(y)$ . To use the MFS, we choose  $N$  points on  $\partial\Omega = \partial\Omega_1 \cup \partial\Omega_2$ , where  $\mathbf{x}_k = (\cos(\frac{2\pi k}{N} + \cos \frac{2\pi k}{N}), \sin(\frac{2\pi k}{N} + \sin \frac{2\pi k}{N}))$ ,  $0 \leq k \leq N - 1$ . We use a fictitious domain  $\tilde{\Omega} = \{(x, y) : x = a \sin(t + \cos t), y = b \cos t, 0 \leq t \leq 2\pi\}$ , where  $a = 2, 3, 4, 5$  and  $b = 5, 4, 3, 3$ , respectively. We choose  $\tilde{\mathbf{x}}_k = (a \sin(\frac{2\pi k}{N} + \cos \frac{2\pi k}{N}), b \cos \frac{2\pi k}{N})$ ,  $0 \leq k \leq N - 1$  on  $\partial\tilde{\Omega}$  corresponding to  $N$  equally spaced points in  $[0, 2\pi]$ , (see Figure 3.12). Then in order to resolve the difficulty due to the unstable result as example 3.2, we apply the TSVD with singular value tolerances,  $\epsilon = \{10^{-1}, 10^{-3}, 10^{-7}\}$ , respectively to obtain the approximate solution by the system (1.13) in section 1.3 and  $u_N$  (3.5) in section 3.1. To estimate the maximum error (1.6), we choose equally spaced  $L = 50$  points  $\mathbf{z}_k$ ,  $1 \leq k \leq 50$ , on  $\partial\Omega_1$  and  $M = 50$  points  $\mathbf{z}_k$ ,  $51 \leq k \leq 100$ , on  $\partial\Omega_2$  which implies that  $\mathbf{z}_k$ ,  $1 \leq k \leq 100$ , on  $\partial\Omega = \partial\Omega_1 \cup \partial\Omega_2$  to get the numerical infinity norm in example 3.4. Then we have the following numerical results:



Figure 3.12: Choose  $L = 10$  collocation points (x) on the  $\partial\Omega_1$ ,  $M = 10$  collocation points (o) on the  $\partial\Omega_2$  ( $\partial\Omega = \partial\Omega_1 \cup \partial\Omega_2$ ), and  $N = 20$  source points (\*) on the  $\partial\tilde{\Omega}$

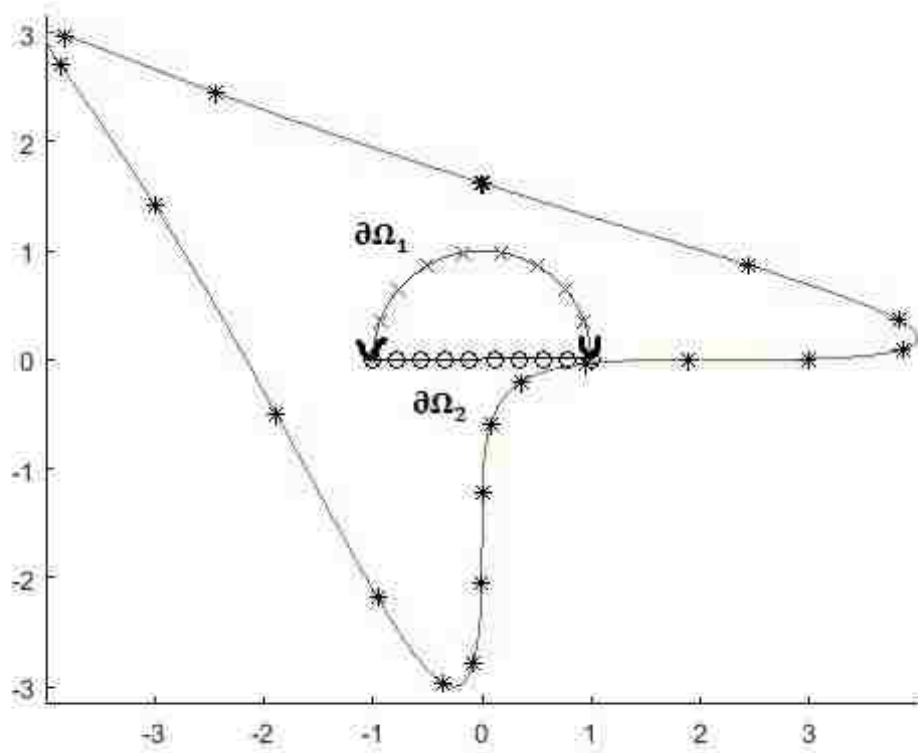
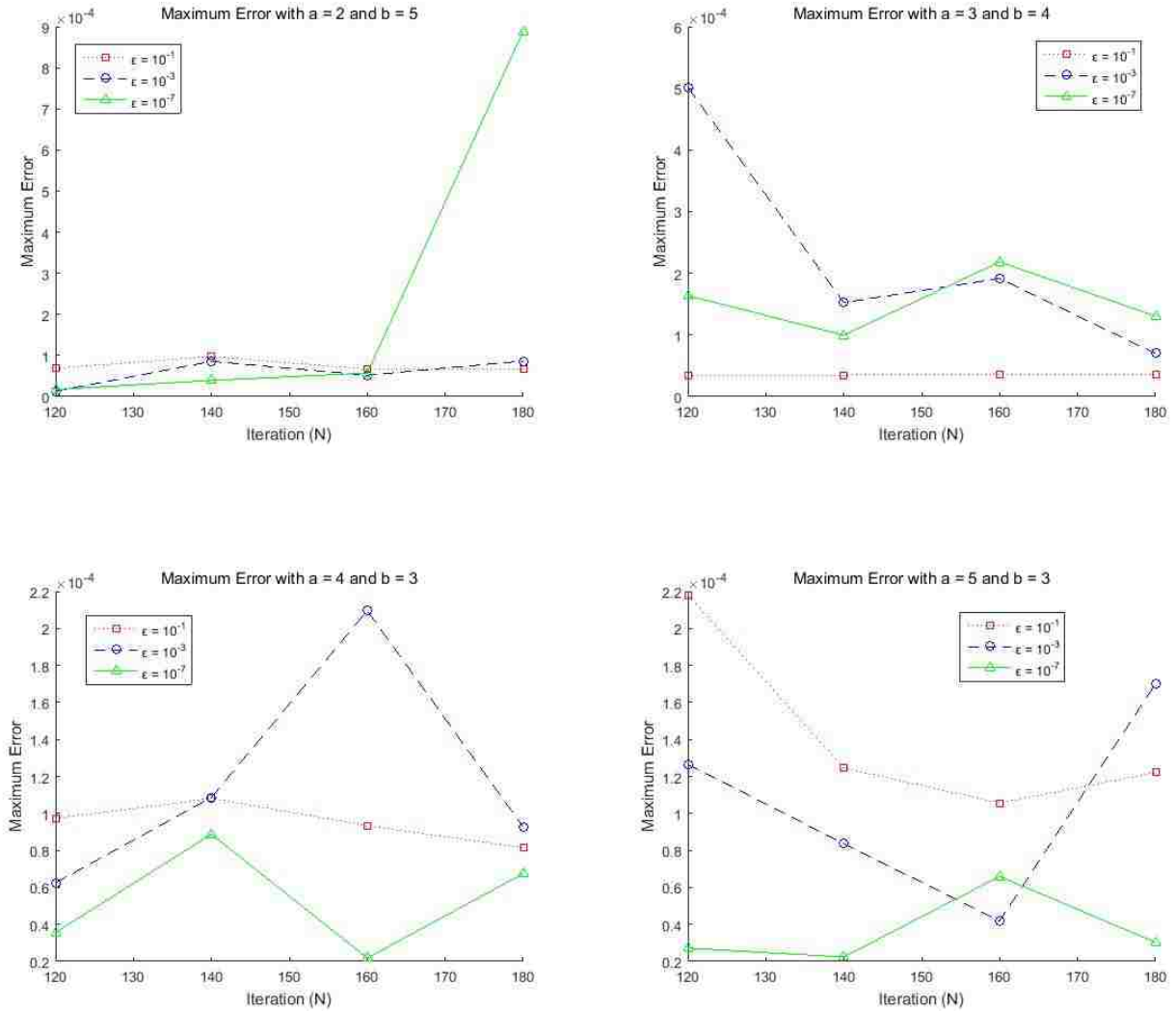


Table 3.11: Maximum Error  $\|u_{exact} - u_N\|_{C(\partial\Omega)}$ 

	L = 100 M = 100 N = 120	L = 100 M = 100 N = 140	L = 100 M = 100 N = 160	L = 100 M = 100 N = 180
a = 2, b = 5 $\epsilon = 10^{-1}$	6.9162e-05 (k = 19)	9.7574e-05 (k = 19)	6.6513e-05 (k = 19)	6.6813e-05 (k = 19)
a = 2, b = 5 $\epsilon = 10^{-3}$	1.2879e-05 (k = 198)	8.5751e-05 (k = 198)	5.1969e-05 (k = 198)	8.6498e-05 (k = 198)
a = 2, b = 5 $\epsilon = 10^{-7}$	1.7120e-05 (k = 200)	3.9487e-05 (k = 200)	5.7199e-05 (k = 200)	8.8919e-04 (k = 200)
a = 3, b = 4 $\epsilon = 10^{-1}$	3.3653e-05 (k = 19)	3.4899e-05 (k = 19)	3.6728e-05 (k = 19)	3.6190e-05 (k = 19)
a = 3, b = 4 $\epsilon = 10^{-3}$	5.0181e-04 (k = 198)	1.5255e-04 (k = 198)	1.9149e-04 (k = 198)	6.9974e-05 (k = 198)
a = 3, b = 4 $\epsilon = 10^{-7}$	1.6378e-04 (k = 200)	9.9596e-05 (k = 200)	2.1852e-04 (k = 200)	1.3058e-04 (k = 200)
a = 4, b = 3 $\epsilon = 10^{-1}$	9.7282e-05 (k = 19)	1.0810e-04 (k = 19)	9.3353e-05 (k = 19)	8.1409e-05 (k = 19)
a = 4, b = 3 $\epsilon = 10^{-3}$	6.2492e-05 (k = 198)	1.0862e-04 (k = 198)	2.0962e-04 (k = 198)	9.2714e-05 (k = 198)
a = 4, b = 3 $\epsilon = 10^{-7}$	3.5619e-05 (k = 200)	8.8765e-05 (k = 200)	2.1796e-05 (k = 200)	6.7458e-05 (k = 200)
a = 5, b = 3 $\epsilon = 10^{-1}$	2.1821e-04 (k = 50)	1.2450e-04 (k = 52)	1.0570e-04 (k = 54)	1.2215e-04 (k = 55)
a = 5, b = 3 $\epsilon = 10^{-3}$	1.2656e-04 (k = 198)	8.3628e-05 (k = 198)	4.1858e-05 (k = 198)	1.7004e-04 (k = 198)
a = 5, b = 3 $\epsilon = 10^{-7}$	2.7168e-05 (k = 200)	2.2366e-05 (k = 200)	6.5958e-05 (k = 200)	3.0312e-05 (k = 200)

Figure 3.13: Maximum errors on fictitious domains,  $\partial\tilde{\Omega} = \{(x, y) : x = a \sin(t + \cos t), y = b \cos t, 0 \leq t \leq 2\pi\}$ , where  $a = 2, 3, 4, 5$  and  $b = 5, 4, 3, 3$  with singular value tolerances,  $\epsilon = 10^{-1}$  ( $\square$ ),  $\epsilon = 10^{-3}$  ( $\circ$ ),  $\epsilon = 10^{-7}$  ( $\triangle$ ), respectively



**Remark 3.1.** It is worthy to mention that the convergence of the MFS for the modified Helmholtz equations has been discussed in [24].

### 3.3 DRM for boundary value problems of Helmholtz Equations

Consider the Dirichlet problem of a non-homogeneous Helmholtz equation

$$\Delta u(\mathbf{x}) + \kappa^2 u(\mathbf{x}) = f(\mathbf{x}) \quad \mathbf{x} \in \Omega, \quad (3.15)$$

$$u(\mathbf{x}) = h(\mathbf{x}) \quad \mathbf{x} \in \partial\Omega, \quad (3.16)$$

where  $\Omega$  is a bounded domain in  $\mathcal{R}^s$ ,  $s \geq 2$ . To use the DRM for the above problem, we first find a particular solution  $u_p$  of (3.15), namely

$$\Delta u_p(\mathbf{x}) + \kappa^2 u_p(\mathbf{x}) = f(\mathbf{x}) \quad \mathbf{x} \in \Omega. \quad (3.17)$$

Then we turn to solve the following boundary problem of a homogeneous Helmholtz equation

$$\Delta v(\mathbf{x}) + \kappa^2 v(\mathbf{x}) = 0 \quad \mathbf{x} \in \Omega,$$

$$v(\mathbf{x}) = g(\mathbf{x}) - u_p(\mathbf{x}) \quad \mathbf{x} \in \partial\Omega,$$

which we use  $v_\epsilon$  for the exact solution. Hence,

$$u(\mathbf{x}) = u_p(\mathbf{x}) + v_\epsilon(\mathbf{x}),$$

will be the exact solution of the original boundary problem.

However, as in many cases, the exact solutions of PDEs or boundary problems are rarely available in general. Therefore some numerical methods or approximation methods are needed to get approximate solutions.

Here we first like to get approximate particular solutions of (3.15). For this purpose, we use the approximation schemes described in section 2.3, namely: Choose a RBF  $\phi$  such that

$$\int_{\mathcal{R}^s} \phi(\mathbf{x}) d\mathbf{x} = 1,$$

and the approximate  $f$  by

$$\mathcal{B}_{n,\gamma}f(\mathbf{x}) = \frac{1}{n^{s(1-\gamma)}} \sum_{\mathbf{j} \in I_n(\Omega_\delta)} f\left(\frac{\mathbf{j}}{n}\right) \phi(n^\gamma \mathbf{x} - \mathbf{j} n^{\gamma-1}),$$

as in (2.10).

The exact solution of

$$\Delta u(\mathbf{x}) + \kappa^2 u(\mathbf{x}) = \mathcal{B}_{n,\gamma}f(\mathbf{x}),$$

is derived in [Li], given by

$$\begin{aligned} u_n(\mathbf{x}) &= -\frac{i\pi}{2} \frac{1}{n^s} \sum_{\mathbf{j} \in I_n(\Omega_\delta)} f\left(\frac{\mathbf{j}}{n}\right) n^{-\gamma+\gamma s/2} \\ &\times \left[ \frac{H_{s/2-1}^{(1)}(\kappa \|\mathbf{x} - \mathbf{j}/n\|)}{\|\mathbf{x} - \mathbf{j}/n\|^{s/2-1}} \int_0^{n^\gamma \|\mathbf{x} - \mathbf{j}/n\|} t^{s/2} \phi(t) J_{s/2-1}(\kappa n^{-\gamma} t) dt \right. \\ &\left. + \frac{J_{s/2-1}(\kappa \|\mathbf{x} - \mathbf{j}/n\|)}{\|\mathbf{x} - \mathbf{j}/n\|^{s/2-1}} \int_{n^\gamma \|\mathbf{x} - \mathbf{j}/n\|}^\infty t^{s/2} \phi(t) H_{s/2-1}^{(1)}(\kappa n^{-\gamma} t) dt \right]. \end{aligned} \quad (3.18)$$

For  $s = 2$ ,

$$\begin{aligned} u_n(\mathbf{x}) &= -\frac{i\pi}{2} H_0^{(1)}(\kappa n^{-\gamma} r) \int_0^r t \phi(t) J_0(\kappa n^{-\gamma} t) dt \\ &\quad - \frac{i\pi}{2} J_0(\kappa n^{-\gamma} r) \int_r^\infty t \phi(t) H_0^{(1)}(\kappa n^{-\gamma} t) dt, \end{aligned}$$

and for  $s = 3$ ,

$$\begin{aligned} u_n(\mathbf{x}) &= -\frac{e^{i\kappa n^{-\gamma} r}}{\kappa n^{-\gamma} r} \int_0^r t \phi(t) \sin(\kappa n^{-\gamma} t) dt \\ &\quad - \frac{\sin(\kappa n^{-\gamma} r)}{\kappa n^{-\gamma} r} \int_r^\infty t \phi(t) e^{i\kappa n^{-\gamma} t} dt. \end{aligned}$$

The convergence of  $u_n$  to the exact solution of (3.18) is also derived in [18].

The method of fundamental solution can be used to solve the following boundary problem

$$\Delta v(\mathbf{x}) + \kappa^2 v(\mathbf{x}) = 0 \quad \mathbf{x} \in \Omega,$$

$$v(\mathbf{x}) = g(\mathbf{x}) - u_n(\mathbf{x}) \quad \mathbf{x} \in \partial\Omega.$$

where we denote by  $v_{MFS}$  the numerical solution. Hence

$$u_A(\mathbf{x}) = u_p(\mathbf{x}) + v_{MFS}(\mathbf{x}),$$

is considered as a numerical solution of the original problem (3.15)-(3.16).

### 3.4 Numerical Examples

**Example 3.6.** Consider the Dirichlet boundary problem on a L-shaped domain with an evolute-of-ellipse fictitious domain for the Helmholtz equation

$$\begin{aligned} \Delta u(x, y) + u(x, y) &= (\sin x + 2x^2 + 2) e^y, & (x, y) \in \Omega, \\ u(x, y) &= (x^2 + 2) e^y, & (x, y) \in \partial\Omega, \end{aligned}$$

where  $\Omega = \{(x, y) : -1 \leq x \leq 1, -1 \leq y \leq 0 \text{ or } -1 \leq x \leq 0, 0 \leq y \leq 1\}$  is the L-shaped domain. The exact solution of the above problem is  $u_{exact} = (\sin x + x^2) e^y$ . Choose three different radial basis functions in Example 2.4:

- (a)  $\phi(r^2) = \frac{c}{\pi} e^{-cr^2}$ , where  $r = \|\mathbf{x}\|$  and  $c = 1, 3$ , respectively,
- (b)  $\phi(r^2) = \begin{cases} (c+1)(1-r^2)^c/\pi, & 0 \leq r \leq 1, \\ 0, & r > 1, \end{cases}$  for  $c = 3, 5$ , respectively,
- (c)  $\phi(r^2) = \frac{c-1}{\pi(r^2+1)^c}$ , for  $c = 3, 5$ , respectively,

and use  $\mathbf{x}_{k,m} = (\frac{k}{n}, \frac{m}{n})$ ,  $-1.1n \leq k \leq 1.1n$  and  $-1.1n \leq m \leq 0.1n$ , or  $-1.1n \leq k \leq 0.1n$  and  $-0.1n \leq m \leq 1.1n$ , in  $\Omega_\delta$  with  $\delta = 0.1$  to get  $u_n$  in (3.18). Next, we use the MFS to obtain  $u_N$ , as discussed in section by using  $N$  points equally spaced on  $\partial\Omega$  and choosing an evolute-of-ellipse fictitious domain  $\tilde{\Omega} = \{(x, y) : x = a \cos^3(t), y = b \sin^3(t), 0 \leq t < 2\pi\}$ ,  $a = 5, 6$ ,  $b = 4, 5$ , respectively. Let  $\tilde{\mathbf{x}}_k = (\cos^3(\frac{2\pi k}{N}), \sin^3(\frac{2\pi k}{N}))$ ,  $0 \leq k \leq N-1$  on  $\partial\tilde{\Omega}$ .

To estimate the maximum error, we use  $M^2$  points  $\mathbf{z}_{k,m} = (\frac{k}{M}, \frac{m}{M})$ ,  $-M \leq k \leq M$  and  $-M \leq m \leq 0$  or  $-M \leq k \leq 0$  and  $0 \leq m \leq M$  with  $M = 100$  in  $\bar{\Omega} = \Omega \cup \partial\Omega$  to get the numerical infinity norm in example 2.5. Then our numerical approximation errors are presented in the following table with various a, b, c, n, and N:

Figure 3.14:  $M = 20$ , 300 points ( $\bullet$ ) in  $\Omega$ , 60 points ( $\bullet$ ) on  $\partial\Omega$  and 35 points ( $+$ ) on  $\partial\Omega_\delta$ , respectively, and  $N = 20$  points ( $*$ ) on  $\partial\tilde{\Omega}$  with a = 5 and b = 4

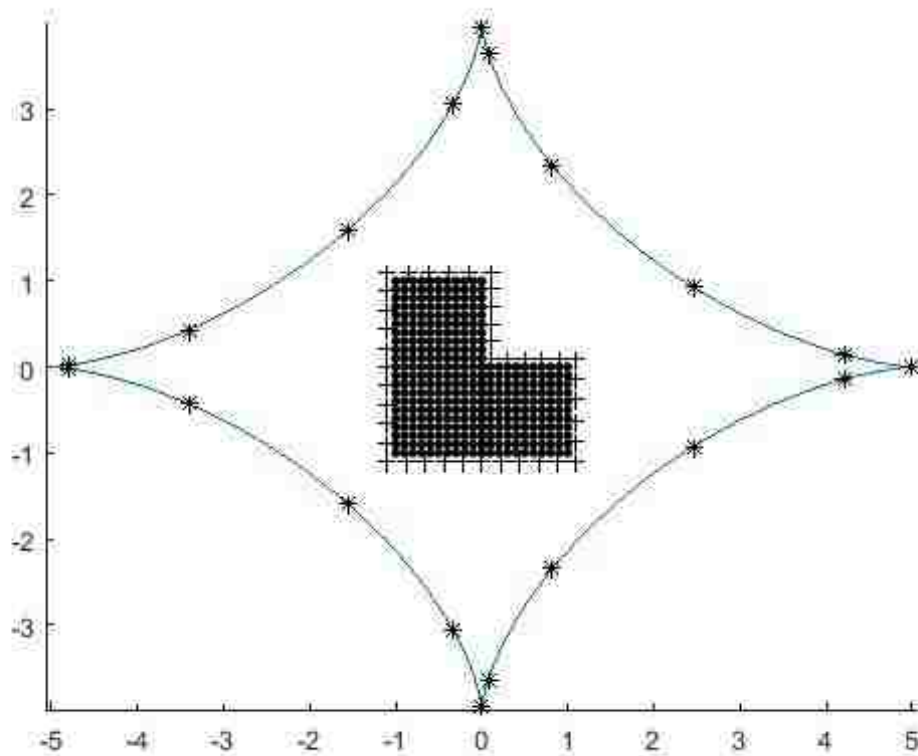


Table 3.12: Maximum Error  $\|u_{exact} - u_A\|_{C(\bar{\Omega})}$  with (a) the Gaussian RBFs  $\phi(r^2) = \frac{c}{\pi} e^{-cr^2}$  for  $c = 1, 3$ .

	M = 20 N = 200	M = 30 N = 200	M = 40 N = 200	M = 50 N = 200
a = 5, b = 4, c = 1	8.4799e-11	1.9734e-11	2.3871e-10	3.8704e-10
a = 5, b = 4, c = 3	8.4799e-11	1.9734e-11	2.3871e-10	3.8704e-10
a = 6, b = 5, c = 1	6.2305e-10	4.9483e-10	4.4148e-10	1.8323e-10
a = 6, b = 5, c = 3	6.2305e-10	4.9483e-10	4.4148e-10	1.8323e-10

Figure 3.15: Maximum errors on an evolute-of-ellipse fictitious domain,  $\partial\tilde{\Omega} = \{(x, y) : x = a \cos^3(t), y = b \sin^3(t), 0 \leq t \leq 2\pi\}$ , where a = 5, b = 4, c = 1, ( $\square$ ), a = 5, b = 4, c = 3, ( $\circ$ ), a = 6, b = 5, c = 1, ( $\triangle$ ), and a = 6, b = 5, c = 3, ( $\diamond$ ), respectively

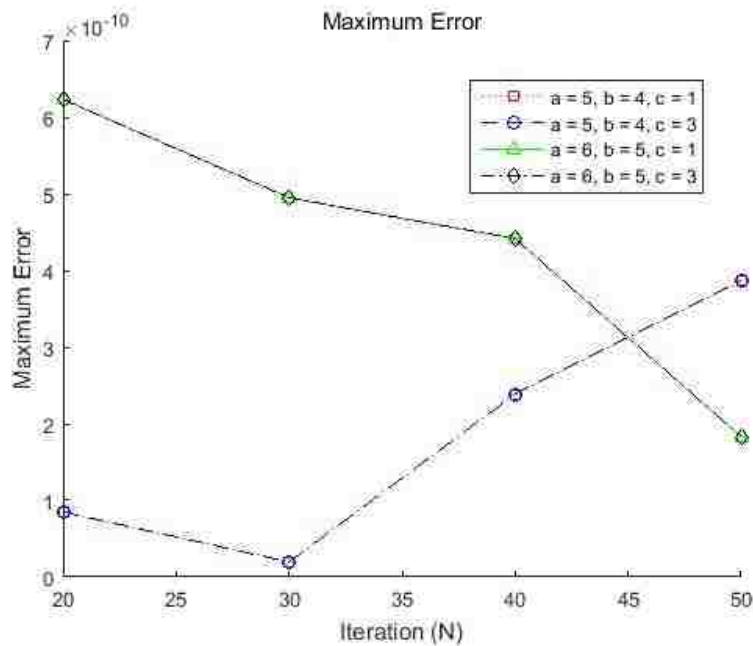




Table 3.13: Maximum Error  $\|u_{exact} - u_A\|_{C(\bar{\Omega})}$  with (b) the compactly supported RBFs  $\phi(r^2) = (c + 1)(1 - r^2)^c/\pi$ ,  $0 \leq r \leq 1$  or  $0, r > 1$  for  $c = 3, 5$ .

	M = 20 N = 200	M = 30 N = 200	M = 40 N = 200	M = 50 N = 200
a = 5, b = 4, c = 3	1.1100e-08	1.3158e-08	1.1110e-10	1.0941e-10
a = 5, b = 4, c = 5	1.0195e-05	1.1432e-05	1.5757e-08	1.9091e-08
a = 6, b = 5, c = 3	1.1105e-08	1.3165e-08	1.6674e-10	1.7428e-10
a = 6, b = 5, c = 5	1.0196e-05	1.1433e-05	1.5768e-08	1.9107e-08

Figure 3.16: Maximum errors on an evolute-of-ellipse fictitious domain,  $\partial\tilde{\Omega} = \{(x, y) : x = a \cos^3(t), y = b \sin^3(t), 0 \leq t \leq 2\pi\}$ , where a = 5, b = 4, c = 3, ( $\square$ ), a = 5, b = 4, c = 5, ( $\circ$ ), a = 6, b = 5, c = 3, ( $\triangle$ ), and a = 6, b = 5, c = 5, ( $\diamond$ ), respectively

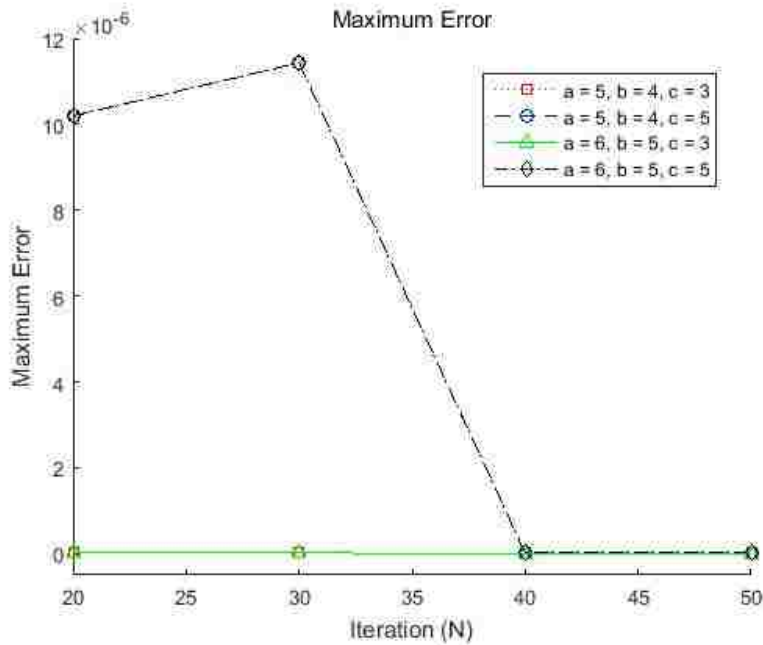
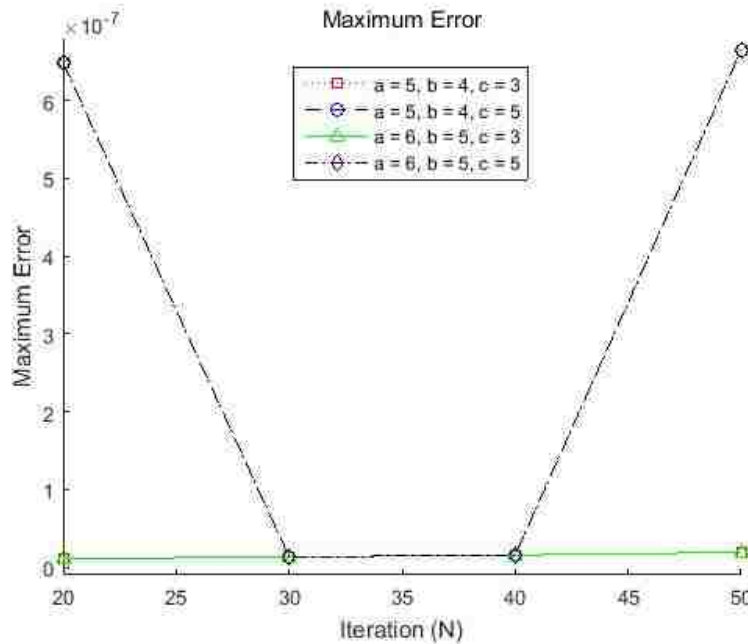


Table 3.14: Maximum Error  $\|u_{exact} - u_A\|_{C(\bar{\Omega})}$  with (c) the inverse multiquadratics RBFs  $\phi(r^2) = \frac{c-1}{\pi(r^2+1)^c}$ , for  $c = 3, 5$ .

	M = 20 N = 200	M = 30 N = 200	M = 40 N = 200	M = 50 N = 200
a = 5, b = 4, c = 3	1.1100e-08	1.3158e-08	1.5757e-08	1.9091e-08
a = 5, b = 4, c = 5	6.4904e-07	1.3158e-08	1.5757e-08	6.6510e-07
a = 6, b = 5, c = 3	1.1105e-08	1.3165e-08	1.5768e-08	1.9107e-08
a = 6, b = 5, c = 5	6.4904e-07	1.3165e-08	1.5768e-08	6.6510e-07

Figure 3.17: Maximum errors on an evolute-of-ellipse fictitious domain,  $\partial\tilde{\Omega} = \{(x, y) : x = a \cos^3(t), y = b \sin^3(t), 0 \leq t \leq 2\pi\}$ , where a = 5, b = 4, c = 3, ( $\square$ ), a = 5, b = 4, c = 5, ( $\circ$ ), a = 6, b = 5, c = 3, ( $\triangle$ ), and a = 6, b = 5, c = 5, ( $\diamond$ ), respectively



**Example 3.7.** Consider the Dirichlet boundary problem for the Helmholtz equation

$$\begin{aligned}\Delta u(x, y) + u(x, y) &= \left(\frac{x^2 + y^2}{4}\right) e^{\frac{x^2 - y^2}{4}}, & (x, y) \in \Omega, \\ u(x, y) &= e^{\frac{x^2 - y^2}{4}}, & (x, y) \in \partial\Omega,\end{aligned}$$

where  $\Omega = \{(x, y) : 0 \leq x \leq 1, 0 \leq y \leq 0.5 \text{ or } 0 \leq x \leq 0.5, 0.5 \leq y \leq 1\}$  is the L-shaped domain. The exact solution of the above problem is  $u_{exact} = e^{\frac{x^2 - y^2}{4}}$ . Choose three different radial basis functions as in Example 3.6 and use  $\mathbf{x}_{k,m} = (\frac{k}{n}, \frac{m}{n})$ ,  $-1.1n \leq k \leq 1.1n$  and  $-1.1n \leq m \leq 0.1n$ , or  $-1.1n \leq k \leq 0.1n$  and  $-0.1n \leq m \leq 1.1n$ , in  $\Omega_\delta$  with  $\delta = 0.1$  to get  $u_n$  in (3.18). Next, we use the MFS to obtain  $u_N$ , as discussed in section by using  $N$  points equally spaced on  $\partial\Omega$  and choosing an amoeba-like fictitious domain  $\tilde{\Omega} = \{(x, y) : x = r(t) \cos(t), y = r(t) \sin(t)\}$ , where  $r(t) = R e^{\sin(t)} \sin^2(2t) + R e^{\cos(t)} \cos^2(2t)$ ,  $0 \leq t < 2\pi$ ,  $R = 3, 4, 5$ , respectively. Let  $\tilde{\mathbf{x}}_k = ((R e^{\sin(\frac{2\pi k}{N})} \sin^2(2\frac{2\pi k}{N}) + R e^{\cos(\frac{2\pi k}{N})} \cos^2(2\frac{2\pi k}{N})) \cos(\frac{2\pi k}{N}), (R e^{\sin(\frac{2\pi k}{N})} \sin^2(2\frac{2\pi k}{N}) + R e^{\cos(\frac{2\pi k}{N})} \cos^2(2\frac{2\pi k}{N})) \sin(\frac{2\pi k}{N}))$ ,  $0 \leq t < 2\pi$ ,  $0 \leq k \leq N - 1$  on  $\partial\tilde{\Omega}$ . Then in order to resolve the difficulty due to the unstable result, we apply the TSVD with singular value tolerances,  $\epsilon = \{10^{-2}, 10^{-6}, 10^{-10}\}$ , respectively to obtain the approximate solution through (3.5)-(3.6). To estimate the maximum error, we use points  $\mathbf{z}_{k,m} = (\frac{k}{M}, \frac{m}{M})$ ,  $-M \leq k \leq M$  and  $-M \leq m \leq 0$  or  $-M \leq k \leq 0$  and  $0 \leq m \leq M$  with  $M = 100$  in  $\bar{\Omega} = \Omega \cup \partial\Omega$  to get the numerical infinity norm in Example 3.6. Then our numerical approximation errors are presented in the following table with various  $R$ ,  $c$ ,  $n$ , and  $N$ :

Figure 3.18:  $M = 20$ , 300 points ( $\bullet$ ) in  $\Omega$ , 80 points ( $\bullet$ ) on  $\partial\Omega$  and 40 points ( $+$ ) on  $\partial\Omega_\delta$ , respectively, and  $N = 20$  points ( $*$ ) on  $\partial\tilde{\Omega}$  with  $R = 2.5$

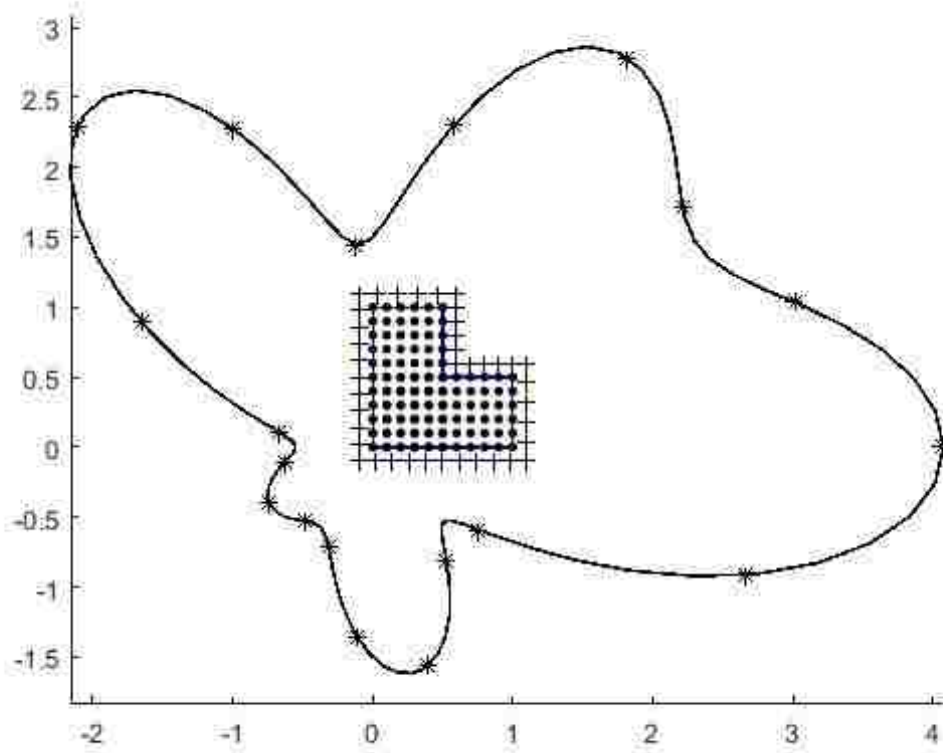


Table 3.15: Maximum Error  $\|u_{exact} - u_A\|_{C(\bar{\Omega})}$  with (a) the Gaussian RBFs  $\phi(r^2) = \frac{c}{\pi} e^{-cr^2}$  for  $c = 1, 3$ .

	M = 20 N = 200	M = 30 N = 200	M = 40 N = 200	M = 50 N = 200
R = 3, c = 1 $\epsilon = 10^{-2}$	5.8258e-09 (k = 2)	6.5228e-09 (k = 2)	7.3519e-09 (k = 2)	8.3486e-09 (k = 2)
R = 3, c = 1 $\epsilon = 10^{-6}$	6.2872e-12 (k = 3)	2.0413e-12 (k = 3)	3.0138e-11 (k = 3)	1.2075e-11 (k = 3)
R = 3, c = 1 $\epsilon = 10^{-10}$	1.0053e-08 (k = 4)	5.6569e-09 (k = 4)	6.2683e-09 (k = 4)	4.6383e-09 (k = 4)
R = 3, c = 3 $\epsilon = 10^{-2}$	5.8258e-09 (k = 2)	6.5228e-09 (k = 2)	7.3519e-09 (k = 3)	8.3486e-09 (k = 2)
R = 3, c = 3 $\epsilon = 10^{-6}$	1.0053e-08 (k = 4)	5.6569e-09 (k = 4)	6.2683e-09 (k = 4)	4.6383e-09 (k = 4)
R = 3, c = 3 $\epsilon = 10^{-10}$	2.5055e-06 (k = 199)	6.8148e-06 (k = 199)	1.3302e-05 (k = 199)	3.9563e-07 (k = 199)
R = 5, c = 1 $\epsilon = 10^{-2}$	3.0970e-09 (k = 2)	3.4658e-09 (k = 2)	3.9043e-09 (k = 2)	4.4313e-09 (k = 2)
R = 5, c = 1 $\epsilon = 10^{-6}$	9.2145e-11 (k = 3)	3.1448e-11 (k = 3)	5.6557e-12 (k = 3)	4.3416e-11 (k = 3)
R = 5, c = 1 $\epsilon = 10^{-10}$	1.8226e-08 (k = 4)	1.3441e-09 (k = 4)	2.2221e-08 (k = 4)	6.3689e-08 (k = 4)
R = 5, c = 3 $\epsilon = 10^{-2}$	3.0970e-09 (k = 2)	3.4658e-09 (k = 2)	3.9043e-09 (k = 2)	4.4313e-09 (k = 2)
R = 5, c = 3 $\epsilon = 10^{-6}$	4.0773e-08 (k = 11)	5.9070e-08 (k = 6)	2.2957e-08 (k = 7)	4.5252e-08 (k = 12)
R = 5, c = 3 $\epsilon = 10^{-10}$	1.1058e-07 (k = 199)	9.0139e-08 (k = 199)	1.8541e-08 (k = 199)	2.3637e-08 (k = 199)

Figure 3.19: Maximum errors on an amoeba-like fictitious domain,  $\partial\tilde{\Omega} = \{(x, y) : x = r(t) \cos(t), y = r(t) \sin(t)\}$ , where  $r(t) = R e^{\sin(t)} \sin^2(2t) + R e^{\cos(t)} \cos^2(2t)$ ,  $0 \leq t < 2\pi$ ,  $R = 3, 5$ , and  $c = 1, 3$  with singular value tolerances,  $\epsilon = 10^{-2}$  ( $\square$ ),  $\epsilon = 10^{-6}$  ( $\circ$ ),  $\epsilon = 10^{-10}$  ( $\triangle$ ), respectively

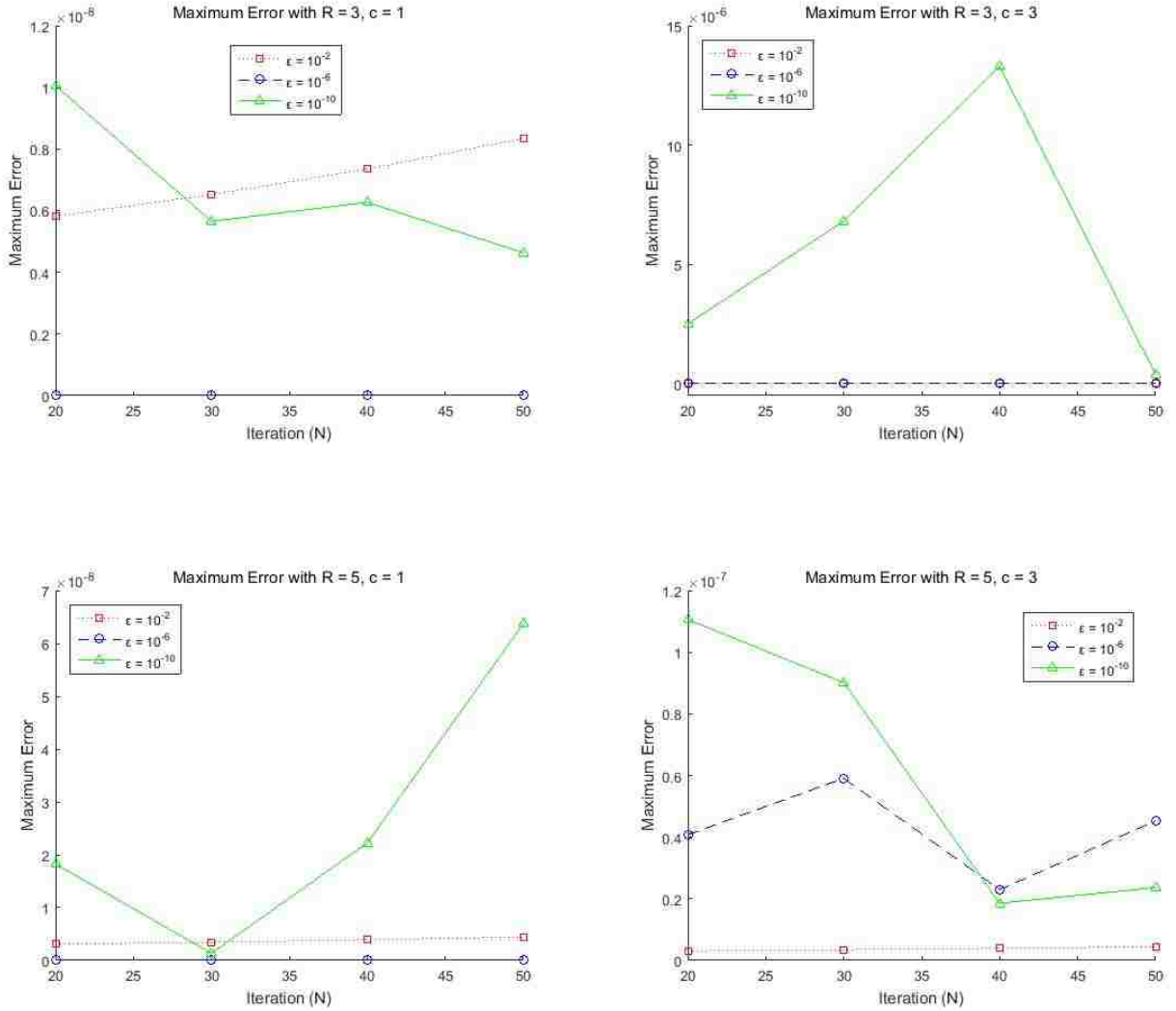


Table 3.16: Maximum Error  $\|u_{exact} - u_A\|_{C(\bar{\Omega})}$  with (b) the compactly supported RBFs  $\phi(r^2) = (c + 1)(1 - r^2)^c/\pi$ ,  $0 \leq r \leq 1$  or  $0, r > 1$  for  $c = 3, 5$ .

	M = 20 N = 200	M = 30 N = 200	M = 40 N = 200	M = 50 N = 200
R = 3, c = 3 $\epsilon = 10^{-2}$	1.3776e-13 (k = 3)	4.0927e-14 (k = 3)	2.9498e-12 (k = 4)	2.3617e-13 (k = 4)
R = 3, c = 3 $\epsilon = 10^{-6}$	3.2282e-14 (k = 13)	2.3093e-13 (k = 14)	1.9291e-13 (k = 14)	1.5343e-13 (k = 15)
R = 3, c = 3 $\epsilon = 10^{-10}$	4.4126e-14 (k = 190)	5.5542e-13 (k = 190)	7.7609e-14 (k = 190)	3.3442e-12 (k = 190)
R = 3, c = 5 $\epsilon = 10^{-2}$	8.6570e-13 (k = 4)	1.7521e-12 (k = 4)	5.2458e-12 (k = 4)	1.6271e-12 (k = 4)
R = 3, c = 5 $\epsilon = 10^{-6}$	1.4231e-12 (k = 11)	9.7948e-13 (k = 11)	5.3077e-12 (k = 12)	8.5781e-11 (k = 13)
R = 3, c = 5 $\epsilon = 10^{-10}$	9.6468e-13 (k = 60)	1.5841e-12 (k = 70)	9.4312e-11 (k = 80)	1.4930e-12 (k = 90)
R = 5, c = 3 $\epsilon = 10^{-2}$	1.3776e-13 (k = 4)	4.0927e-14 (k = 4)	2.9498e-12 (k = 4)	2.3617e-13 (k = 4)
R = 5, c = 3 $\epsilon = 10^{-6}$	3.2282e-14 (k = 13)	2.3093e-13 (k = 13)	1.9291e-13 (k = 13)	1.5343e-13 (k = 13)
R = 5, c = 3 $\epsilon = 10^{-10}$	1.9679e-13 (k = 84)	4.4126e-14 (k = 89)	5.5542e-13 (k = 94)	7.7609e-14 (k = 104)
R = 5, c = 5 $\epsilon = 10^{-2}$	8.6570e-13 (k = 2)	1.7521e-12 (k = 2)	5.2458e-12 (k = 2)	1.6271e-12 (k = 2)
R = 5, c = 5 $\epsilon = 10^{-6}$	1.4231e-12 (k = 11)	9.7948e-13 (k = 11)	5.3077e-12 (k = 12)	8.5781e-11 (k = 12)
R = 5, c = 5 $\epsilon = 10^{-10}$	9.6468e-13 (k = 90)	1.5841e-12 (k = 110)	9.4312e-11 (k = 120)	1.4930e-12 (k = 120)

Figure 3.20: Maximum errors on an amoeba-like fictitious domain,  $\partial\tilde{\Omega} = \{(x, y) : x = r(t) \cos(t), y = r(t) \sin(t)\}$ , where  $r(t) = R e^{\sin(t)} \sin^2(2t) + R e^{\cos(t)} \cos^2(2t)$ ,  $0 \leq t < 2\pi$ ,  $R = 3, 5$ , and  $c = 1, 3$  with singular value tolerances,  $\epsilon = 10^{-2}$  ( $\square$ ),  $\epsilon = 10^{-6}$  ( $\circ$ ),  $\epsilon = 10^{-10}$  ( $\triangle$ ), respectively

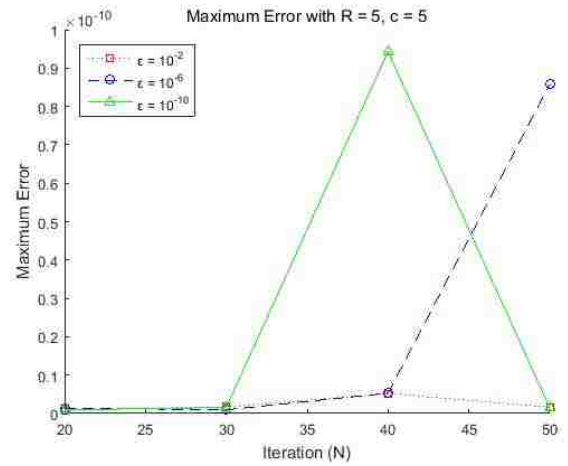
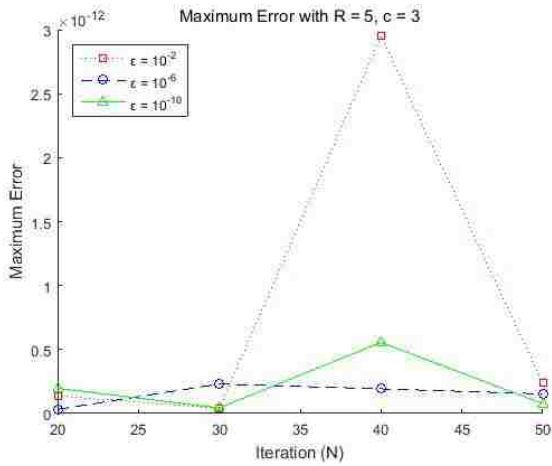
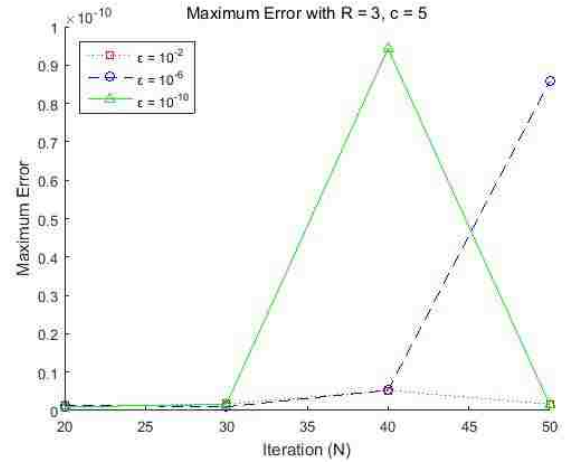
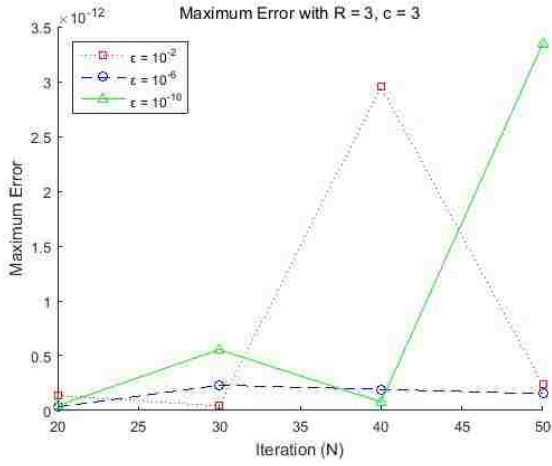
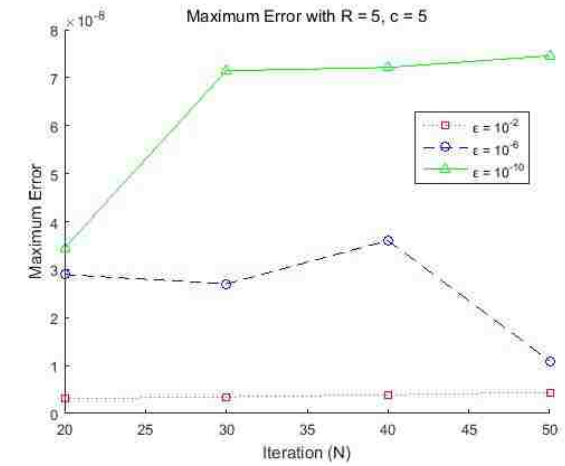
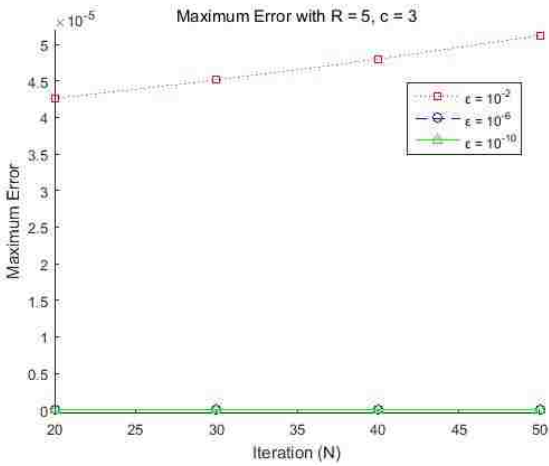
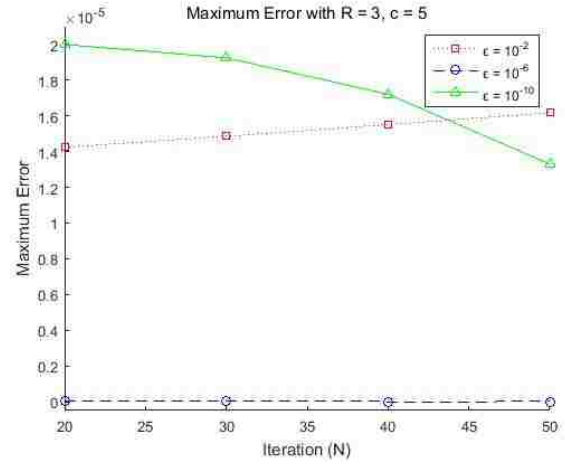
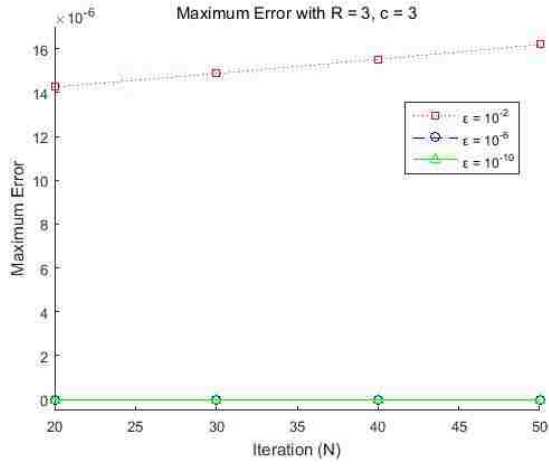




Table 3.17: Maximum Error  $\|u_{exact} - u_A\|_{C(\bar{\Omega})}$  with (c) the inverse multiquadratics RBFs  $\phi(r^2) = \frac{c-1}{\pi(r^2+1)^c}$ , for  $c = 3, 5$ .

	M = 20 N = 200	M = 30 N = 200	M = 40 N = 200	M = 50 N = 200
R = 3, c = 3 $\epsilon = 10^{-2}$	1.4246e-05 (k = 3)	1.4866e-05 (k = 3)	1.5515e-05 (k = 4)	1.6184e-05 (k = 4)
R = 3, c = 3 $\epsilon = 10^{-6}$	5.8258e-09 (k = 13)	6.5228e-09 (k = 14)	7.3519e-09 (k = 14)	8.3486e-09 (k = 15)
R = 3, c = 3 $\epsilon = 10^{-10}$	1.3312e-11 (k = 190)	2.3606e-11 (k = 190)	9.6714e-12 (k = 190)	7.3461e-12 (k = 190)
R = 3, c = 5 $\epsilon = 10^{-2}$	1.4246e-05 (k = 4)	1.4866e-05 (k = 4)	1.5515e-05 (k = 4)	1.6184e-05 (k = 4)
R = 3, c = 5 $\epsilon = 10^{-6}$	3.5740e-09 (k = 11)	1.5421e-08 (k = 11)	8.9900e-10 (k = 12)	1.4249e-09 (k = 13)
R = 3, c = 5 $\epsilon = 10^{-10}$	2.0002e-05 (k = 60)	1.9255e-05 (k = 70)	1.7213e-05 (k = 80)	1.3308e-05 (k = 90)
R = 5, c = 3 $\epsilon = 10^{-2}$	4.2601e-05 (k = 4)	4.5127e-05 (k = 4)	4.7975e-05 (k = 4)	5.1211e-05 (k = 4)
R = 5, c = 3 $\epsilon = 10^{-6}$	3.0969e-09 (k = 13)	3.4658e-09 (k = 13)	3.9043e-09 (k = 13)	4.4313e-09 (k = 13)
R = 5, c = 3 $\epsilon = 10^{-10}$	2.3497e-12 (k = 199)	8.3265e-12 (k = 199)	1.1181e-11 (k = 199)	6.5103e-12 (k = 199)
R = 5, c = 5 $\epsilon = 10^{-2}$	3.0970e-09 (k = 2)	3.4658e-09 (k = 2)	3.9043e-09 (k = 2)	4.4313e-09 (k = 2)
R = 5, c = 5 $\epsilon = 10^{-6}$	2.8955e-08 (k = 4)	2.7007e-08 (k = 4)	3.6047e-08 (k = 4)	1.0924e-08 (k = 4)
R = 5, c = 5 $\epsilon = 10^{-10}$	3.4517e-08 (k = 199)	7.1434e-08 (k = 199)	7.2123e-08 (k = 199)	7.4562e-08 (k = 199)

Figure 3.21: Maximum errors on an amoeba-like fictitious domain,  $\partial\tilde{\Omega} = \{(x, y) : x = r(t) \cos(t), y = r(t) \sin(t)\}$ , where  $r(t) = R e^{\sin(t)} \sin^2(2t) + R e^{\cos(t)} \cos^2(2t)$ ,  $0 \leq t < 2\pi$ ,  $R = 3, 5$ , and  $c = 1, 3$  with singular value tolerances,  $\epsilon = 10^{-2}$  ( $\square$ ),  $\epsilon = 10^{-6}$  ( $\circ$ ),  $\epsilon = 10^{-10}$  ( $\triangle$ ), respectively



**Example 3.8.** Consider the Dirichlet boundary problem for the Helmholtz equation

$$\Delta u(x, y, z) + u(x, y, z) = 2 e^{x-y} \cos(z), \quad (x, y, z) \in \Omega,$$

$$u(x, y, z) = e^{x-y} \cos(z), \quad (x, y, z) \in \partial\Omega,$$

where  $\Omega = \{(x, y, z) : -1 \leq x \leq 1, -1 \leq y \leq 1, -1 \leq z \leq 1\}$ . The exact solution of the above problem is  $u_{exact} = e^{x-y} \cos(z)$ . Choose three different radial basis functions in

Example 2.4:

$$(a) \phi(r^2) = \frac{c}{\pi} e^{-cr^2}, \text{ where } r = \|\mathbf{x}\| \text{ and } c = 1, 3, 5, \text{ respectively,}$$

$$(b) \phi(r^2) = \begin{cases} ((2c+3)!!)(1-r^2)^c/(4\pi(2c)!!), & 0 \leq r \leq 1, \\ 0, & r > 1, \end{cases} \text{ for } c = 3, 4, 5, \text{ respectively,}$$

$$(c) \phi(r^2) = \frac{1}{2\pi^2} \frac{(2c-2)!!}{(2c-5)!!} \frac{1}{(r^2+1)^c}, \text{ for } c = 3, 4, 5, \text{ respectively,}$$

$$\text{where } n!! = \begin{cases} 1 \cdot 3 \cdot \dots \cdot n, & \text{if } n \text{ is an odd number,} \\ 2 \cdot 4 \cdot \dots \cdot n, & \text{if } n \text{ is an even number,} \end{cases}$$

and use  $\mathbf{x}_{k,l,m} = (\frac{k}{n}, \frac{l}{n}, \frac{m}{n})$ ,  $-1.1n \leq k, l, m \leq 1.1n$ , in  $\Omega_\delta = [-1.1, 1.1]^3$  to get  $u_n$  in (2.21).

Then the approximate solution  $u_N$  of the BVP can be obtained and our maximum error is also

estimated as in example 3.6. We use a bumpy spherical fictitious domain  $\tilde{\Omega} = \{(x, y, z) :$

$\rho \sin(\theta) \cos(\phi), \rho \sin(\theta) \sin(\phi), \rho \cos(\theta), 0 \leq \theta \leq \pi, 0 \leq \phi \leq 2\pi\}$ , where  $\rho(\phi, \theta) =$

$R + \frac{1}{6} \sin(6\phi) \sin(7\theta)$ ,  $R = 3, 5$ . We choose  $\tilde{\mathbf{x}}_{k,m} = (\rho \sin(\theta_k) \cos(\phi_{k,m}), \rho \sin(\theta_k) \sin(\phi_{k,m}),$

$\rho \cos(\theta_k))$ , where  $\rho = R + \frac{1}{6} \sin(6\theta_k) \sin(7\phi_{k,m})$ ,  $R = 2, 3, 4, 5$ , and  $\theta_k = \frac{\pi(k+0.5)}{M_\theta}$ ,  $0 \leq$

$k \leq M_\theta - 1$ , with  $M_\theta = \frac{\sqrt{\pi N}}{2r}$ , and  $\phi_{k,m} = \frac{2\pi m}{M_k}$ ,  $0 \leq m \leq M_k - 1$ , with  $M_k =$

$\sqrt{\pi N \sin \theta_k}$ , on  $\partial\tilde{\Omega}$ . To estimate the maximum error, we use  $M^3$  points  $\mathbf{z}_{k,l,m} = (\frac{k}{M}, \frac{l}{M}, \frac{m}{M})$ ,

$-M \leq k, l, m \leq M$ , with  $M = 40$  in  $\bar{\Omega} = \Omega \cup \partial\Omega$ , to get the numerical infinity norm in

example 3.6. Then our numerical approximation errors are presented in the following table

with various R, c, M, and N:

Figure 3.22:  $M = 10, 1000$  points ( $\bullet$ ) in  $\Omega$ ,  $240$  points ( $\bullet$ ) on  $\partial\Omega$ , and  $N = 800$  points ( $*$ ) on a bumpy sphere  $\partial\tilde{\Omega}$  with  $R = 3$

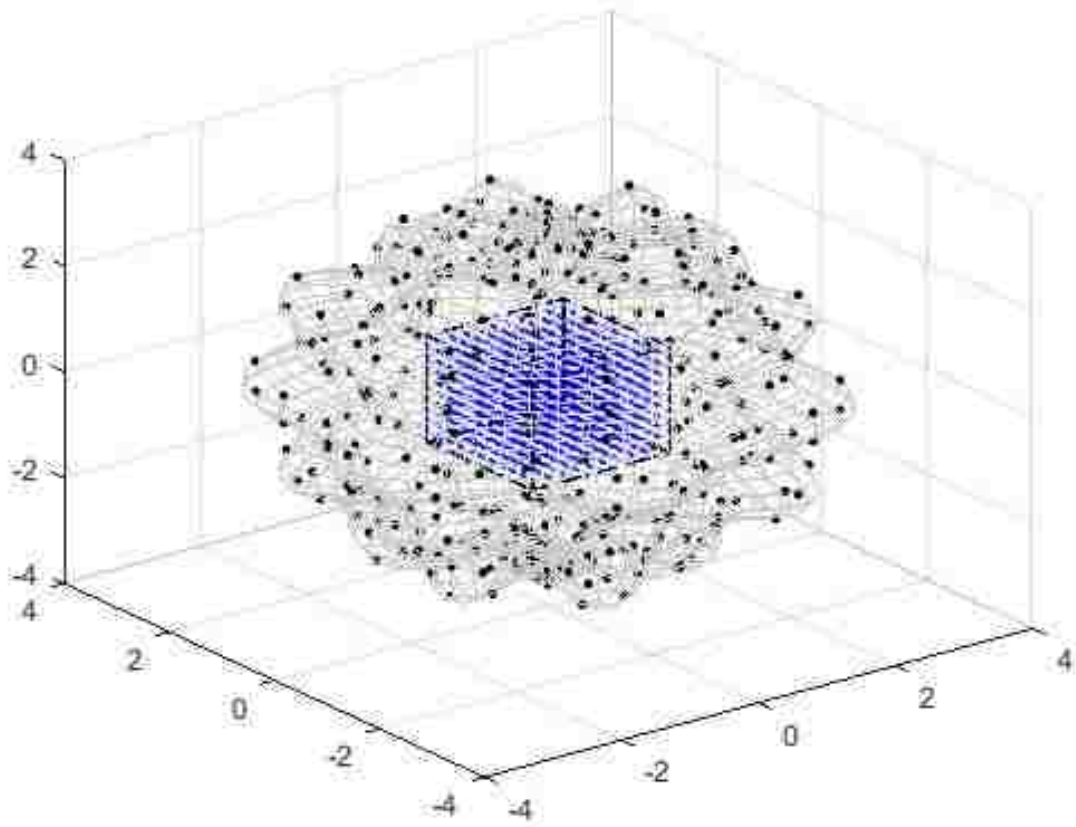


Table 3.18: Maximum Error  $\|u_{exact} - u_A\|_{C(\bar{\Omega})}$  with (a) the Gaussian RBFs  $\phi(r^2) = \frac{c}{\pi} e^{-cr^2}$  for  $c = 1, 3$ .

	M = 10 N = 200	M = 12 N = 200	M = 14 N = 200	M = 16 N = 200
R = 3, c = 1	2.7985e-11	2.8678e-11	3.5562e-11	3.7931e-11
R = 3, c = 3	2.7985e-11	2.8678e-11	3.5562e-11	3.7931e-11
R = 5, c = 1	4.8631e-11	5.2541e-11	5.8593e-11	5.3589e-11
R = 5, c = 3	4.8631e-11	5.2541e-11	5.8593e-11	5.3589e-11

Figure 3.23: Maximum errors on a bumpy spherical fictitious domain  $\tilde{\Omega} = \{(x, y, z) : \rho \sin(\theta) \cos(\phi), \rho \sin(\theta) \sin(\phi), \rho \cos(\theta), 0 \leq \theta \leq 2\pi, 0 \leq \phi \leq \pi\}$ , where  $\rho(\theta, \phi) = R + \frac{1}{6} \sin(6\theta) \sin(7\phi)$  with R = 3, c = 1, ( $\square$ ), R = 3, c = 3, ( $\circ$ ), R = 5, c = 1, ( $\triangle$ ), and R = 5, c = 3, ( $\diamond$ ), respectively

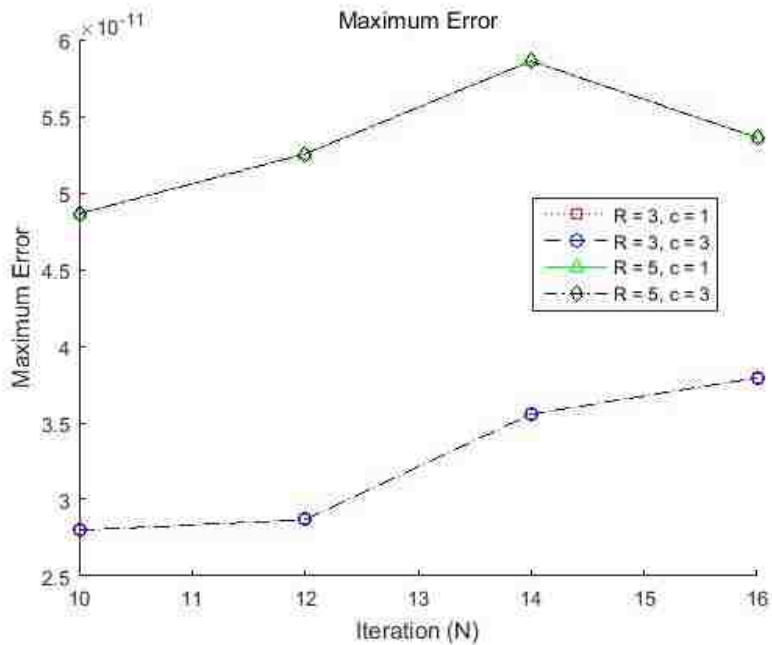


Table 3.19: Maximum Error  $\|u_{exact} - u_A\|_{C(\bar{\Omega})}$  with (b) the compactly supported RBFs  $\phi(r^2) = ((2c + 3)!!)(1 - r^2)^c / (4\pi(2c)!!)$ ,  $0 \leq r \leq 1$ , or  $0$ ,  $r > 1$  for  $c = 3, 5$ .

	M = 10 N = 200	M = 12 N = 200	M = 14 N = 200	M = 16 N = 200
R = 3, c = 3	1.4163e-07	1.1111e-07	3.2973e-08	1.0304e-07
R = 3, c = 4	1.9122e-08	1.4438e-08	1.3430e-08	9.7797e-08
R = 5, c = 3	3.6532e-08	9.7335e-09	1.3148e-08	3.3851e-08
R = 5, c = 4	7.2813e-09	6.5098e-09	4.4031e-09	1.7557e-08

Figure 3.24: Maximum errors on a bumpy spherical fictitious domain  $\tilde{\Omega} = \{(x, y, z) : \rho \sin(\theta) \cos(\phi), \rho \sin(\theta) \sin(\phi), \rho \cos(\phi), 0 \leq \theta \leq 2\pi, 0 \leq \phi \leq \pi\}$ , where  $\rho(\theta, \phi) = R + \frac{1}{6} \sin(6\theta) \sin(7\phi)$  with  $R = 3, c = 3$ , ( $\square$ ),  $R = 3, c = 4$ , ( $\circ$ ),  $R = 5, c = 3$ , ( $\triangle$ ), and  $R = 5, c = 4$ , ( $\diamond$ ), respectively

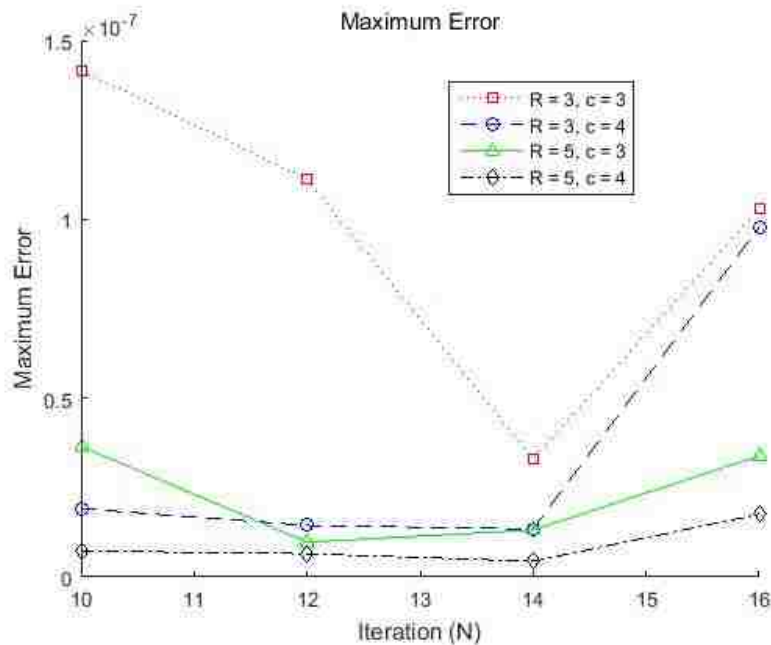
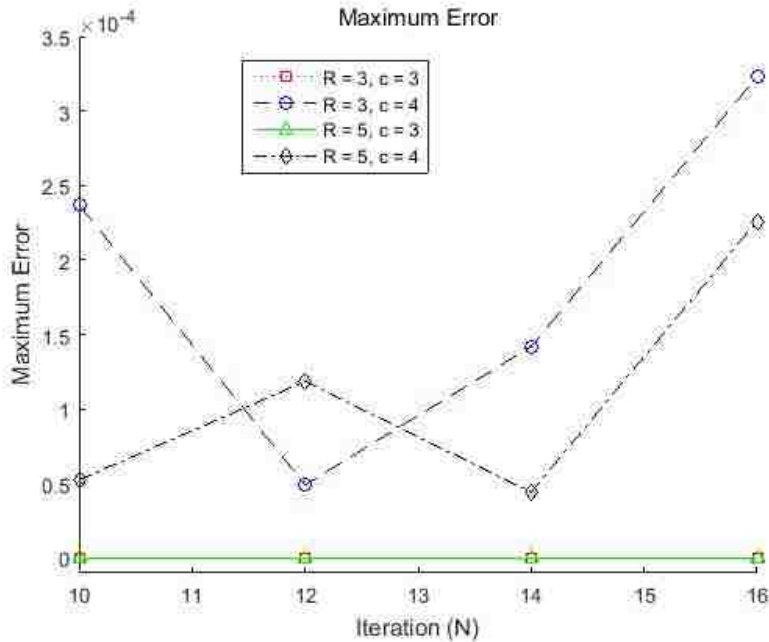


Table 3.20: Maximum Error  $\|u_{exact} - u_A\|_{C(\bar{\Omega})}$  with (c) the inverse multiquadratics RBFs  $\phi(r^2) = \frac{1}{2\pi^2} \frac{(2c-2)!!}{(2c-5)!!} \frac{1}{(r^2+1)^c}$ , for  $c = 3, 5$ ,

	M = 10 N = 200	M = 12 N = 200	M = 14 N = 200	M = 16 N = 200
R = 3, c = 3	4.4195e-08	6.1029e-08	2.5682e-07	4.0217e-08
R = 3, c = 4	2.3709e-04	4.9233e-05	1.4192e-04	3.2298e-04
R = 5, c = 3	3.3052e-07	6.2125e-08	3.0242e-07	4.7039e-08
R = 5, c = 4	5.2491e-05	1.1849e-04	4.4205e-05	2.2612e-04

Figure 3.25: Maximum errors on a bumpy spherical fictitious domain  $\tilde{\Omega} = \{(x, y, z) : \rho \sin(\theta) \cos(\phi), \rho \sin(\theta) \sin(\phi), \rho \cos(\phi), 0 \leq \theta \leq 2\pi, 0 \leq \phi \leq \pi\}$ , where  $\rho(\theta, \phi) = R + \frac{1}{6} \sin(6\theta) \sin(7\phi)$  with R = 3, c = 3, ( $\square$ ), R = 3, c = 4, ( $\circ$ ), R = 5, c = 3, ( $\triangle$ ), and R = 5, c = 4, ( $\diamond$ ), respectively



## CHAPTER 4

# BOUNDARY VALUE PROBLEMS OF BIHARMONIC EQUATIONS

### 4.1 MFS for Biharmonic equation

Consider the general Robin boundary value problem for a biharmonic equation

$$\Delta^2 u(\mathbf{x}) = 0 \quad \mathbf{x} \in \Omega, \quad (4.1)$$

$$u(\mathbf{x}) = f_1(\mathbf{x}) \quad \text{and} \quad \Delta u(\mathbf{x}) = f_2(\mathbf{x}) \quad \mathbf{x} \in \partial\Omega_1, \quad (4.2)$$

$$\frac{\partial u}{\partial \mathbf{n}}(\mathbf{x}) = g_1(\mathbf{x}) \quad \text{and} \quad \frac{\partial \Delta u}{\partial \mathbf{n}}(\mathbf{x}) = g_2(\mathbf{x}) \quad \mathbf{x} \in \partial\Omega_2, \quad (4.3)$$

where  $\Omega$  is a domain in  $\mathbb{R}^2$  or in  $\mathbb{R}^3$ ,  $\partial\Omega = \partial\Omega_1 \cup \partial\Omega_2$ , and  $\Delta^2 = \frac{\partial^4}{\partial x_1^4} + 2 \frac{\partial^4}{\partial x_1^2 \partial x_2^2} + \frac{\partial^4}{\partial x_2^4}$  in  $\mathbb{R}^2$  or  $\Delta^2 = \frac{\partial^4}{\partial x_1^4} + \frac{\partial^4}{\partial x_2^4} + \frac{\partial^4}{\partial x_3^4} + 2 \frac{\partial^4}{\partial x_1^2 \partial x_2^2} + 2 \frac{\partial^4}{\partial x_2^2 \partial x_3^2} + 2 \frac{\partial^4}{\partial x_3^2 \partial x_1^2}$  in  $\mathbb{R}^3$ . To use MFS for the above problem, we need use the fundamental solutions of both Laplace equation and biharmonic equation (cf. [17]). The fundamental solution  $\Gamma_1$  of Laplace equation (1.1) is given by

$$\Gamma_1(\mathbf{x}, \mathbf{y}) = \begin{cases} -\frac{1}{2\pi} \log \|\mathbf{x} - \mathbf{y}\|, & \text{for all } \mathbf{x}, \mathbf{y} \in \mathbb{R}^2, \\ \frac{1}{4\pi} \frac{1}{\|\mathbf{x} - \mathbf{y}\|}, & \text{for all } \mathbf{x}, \mathbf{y} \in \mathbb{R}^3. \end{cases} \quad (4.4)$$

And the fundamental solution  $\Gamma_2$  of biharmonic equation (4.1) is expressed as

$$\Gamma_2(\mathbf{x}, \mathbf{y}) = \begin{cases} -\frac{1}{8\pi} \|\mathbf{x} - \mathbf{y}\|^2 \log \|\mathbf{x} - \mathbf{y}\|, & \text{for all } \mathbf{x}, \mathbf{y} \in \mathbb{R}^2, \\ \frac{1}{8\pi} \|\mathbf{x} - \mathbf{y}\|, & \text{for all } \mathbf{x}, \mathbf{y} \in \mathbb{R}^3. \end{cases} \quad (4.5)$$



To use the MFS, we choose a fictitious domain  $\partial\tilde{\Omega}$  such that  $\bar{\Omega} \subset \tilde{\Omega}$ . Then choose  $N$  points on  $\partial\tilde{\Omega}$  listed as  $\tilde{\mathbf{x}}_1, \tilde{\mathbf{x}}_2, \dots, \tilde{\mathbf{x}}_N$ , and form

$$u_N(\mathbf{c}, \mathbf{d}, \{\tilde{\mathbf{x}}_k\}; \mathbf{x}) = \sum_{k=1}^N [c_k \Gamma_1(\mathbf{x}, \tilde{\mathbf{x}}_k) + d_k \Gamma_2(\mathbf{x}, \tilde{\mathbf{x}}_k)], \quad \mathbf{x} \in \bar{\Omega}. \quad (4.6)$$

Choose  $N_1$  points  $\mathbf{x}_1, \mathbf{x}_2, \dots, \mathbf{x}_{N_1}$ , on  $\partial\Omega_1$ , and  $N_2$  points  $\mathbf{x}_{N_1+1}, \mathbf{x}_{N_1+2}, \dots, \mathbf{x}_N$ , with  $N = N_1 + N_2$ , on  $\partial\Omega_2$  and set up a system

$$\begin{aligned} u_N(\mathbf{c}, \mathbf{d}, \{\tilde{\mathbf{x}}_k\}; \mathbf{x}_m) &= f_1(\mathbf{x}_m), & \Delta u_N(\mathbf{c}, \mathbf{d}, \{\tilde{\mathbf{x}}_k\}; \mathbf{x}_m) &= f_2(\mathbf{x}_m), & 1 \leq m \leq N_1, \\ \frac{\partial u_N}{\partial \mathbf{n}}(\mathbf{c}, \mathbf{d}, \{\tilde{\mathbf{x}}_k\}; \mathbf{x}_m) &= g_1(\mathbf{x}_m), & \frac{\partial \Delta u_N}{\partial \mathbf{n}}(\mathbf{c}, \mathbf{d}, \{\tilde{\mathbf{x}}_k\}; \mathbf{x}_m) &= g_2(\mathbf{x}_m), & N_1 + 1 \leq m \leq N, \end{aligned}$$

which leads to the following system

$$\begin{bmatrix} A_{11} & A_{12} \\ A_{21} & A_{22} \end{bmatrix} \begin{bmatrix} \mathbf{c} \\ \mathbf{d} \end{bmatrix} = \begin{bmatrix} \mathbf{f} \\ \mathbf{g} \end{bmatrix}, \quad (4.7)$$

where  $A_{ij}$  for  $i, j = 1, 2$  are given by

$$\begin{aligned} A_{11} &= \begin{bmatrix} \Gamma_1(\mathbf{x}_1, \tilde{\mathbf{x}}_1) & \Gamma_1(\mathbf{x}_1, \tilde{\mathbf{x}}_2) & \dots & \Gamma_1(\mathbf{x}_1, \tilde{\mathbf{x}}_N) \\ \Gamma_1(\mathbf{x}_2, \tilde{\mathbf{x}}_1) & \Gamma_1(\mathbf{x}_2, \tilde{\mathbf{x}}_2) & \dots & \Gamma_1(\mathbf{x}_2, \tilde{\mathbf{x}}_N) \\ \vdots & \vdots & \ddots & \vdots \\ \Gamma_1(\mathbf{x}_{N_1}, \tilde{\mathbf{x}}_1) & \Gamma_1(\mathbf{x}_{N_1}, \tilde{\mathbf{x}}_2) & \dots & \Gamma_1(\mathbf{x}_{N_1}, \tilde{\mathbf{x}}_N) \\ \Delta\Gamma_1(\mathbf{x}_1, \tilde{\mathbf{x}}_1) & \Delta\Gamma_1(\mathbf{x}_1, \tilde{\mathbf{x}}_2) & \dots & \Delta\Gamma_1(\mathbf{x}_1, \tilde{\mathbf{x}}_N) \\ \Delta\Gamma_1(\mathbf{x}_2, \tilde{\mathbf{x}}_1) & \Delta\Gamma_1(\mathbf{x}_2, \tilde{\mathbf{x}}_2) & \dots & \Delta\Gamma_1(\mathbf{x}_2, \tilde{\mathbf{x}}_N) \\ \vdots & \vdots & \ddots & \vdots \\ \Delta\Gamma_1(\mathbf{x}_{N_1}, \tilde{\mathbf{x}}_1) & \Delta\Gamma_1(\mathbf{x}_{N_1}, \tilde{\mathbf{x}}_2) & \dots & \Delta\Gamma_1(\mathbf{x}_{N_1}, \tilde{\mathbf{x}}_N) \end{bmatrix}, \\ A_{12} &= \begin{bmatrix} \Gamma_2(\mathbf{x}_1, \tilde{\mathbf{x}}_1) & \Gamma_2(\mathbf{x}_1, \tilde{\mathbf{x}}_2) & \dots & \Gamma_2(\mathbf{x}_1, \tilde{\mathbf{x}}_N) \\ \Gamma_2(\mathbf{x}_2, \tilde{\mathbf{x}}_1) & \Gamma_2(\mathbf{x}_2, \tilde{\mathbf{x}}_2) & \dots & \Gamma_2(\mathbf{x}_2, \tilde{\mathbf{x}}_N) \\ \vdots & \vdots & \ddots & \vdots \\ \Gamma_2(\mathbf{x}_{N_1}, \tilde{\mathbf{x}}_1) & \Gamma_2(\mathbf{x}_{N_1}, \tilde{\mathbf{x}}_2) & \dots & \Gamma_2(\mathbf{x}_{N_1}, \tilde{\mathbf{x}}_N) \\ \Delta\Gamma_2(\mathbf{x}_1, \tilde{\mathbf{x}}_1) & \Delta\Gamma_2(\mathbf{x}_1, \tilde{\mathbf{x}}_2) & \dots & \Delta\Gamma_2(\mathbf{x}_1, \tilde{\mathbf{x}}_N) \\ \Delta\Gamma_2(\mathbf{x}_2, \tilde{\mathbf{x}}_1) & \Delta\Gamma_2(\mathbf{x}_2, \tilde{\mathbf{x}}_2) & \dots & \Delta\Gamma_2(\mathbf{x}_2, \tilde{\mathbf{x}}_N) \\ \vdots & \vdots & \ddots & \vdots \\ \Delta\Gamma_2(\mathbf{x}_{N_1}, \tilde{\mathbf{x}}_1) & \Delta\Gamma_2(\mathbf{x}_{N_1}, \tilde{\mathbf{x}}_2) & \dots & \Delta\Gamma_2(\mathbf{x}_{N_1}, \tilde{\mathbf{x}}_N) \end{bmatrix}, \end{aligned}$$

$$A_{21} = \begin{bmatrix} \frac{\partial \Gamma_1}{\partial \mathbf{n}}(\mathbf{x}_{N_1+1}, \tilde{\mathbf{x}}_1) & \frac{\partial \Gamma_1}{\partial \mathbf{n}}(\mathbf{x}_{N_1+1}, \tilde{\mathbf{x}}_2) & \cdots & \frac{\partial \Gamma_1}{\partial \mathbf{n}}(\mathbf{x}_{N_1+1}, \tilde{\mathbf{x}}_N) \\ \frac{\partial \Gamma_1}{\partial \mathbf{n}}(\mathbf{x}_{N_1+2}, \tilde{\mathbf{x}}_1) & \frac{\partial \Gamma_1}{\partial \mathbf{n}}(\mathbf{x}_{N_1+2}, \tilde{\mathbf{x}}_2) & \cdots & \frac{\partial \Gamma_1}{\partial \mathbf{n}}(\mathbf{x}_{N_1+2}, \tilde{\mathbf{x}}_N) \\ \vdots & \vdots & \ddots & \vdots \\ \frac{\partial \Gamma_1}{\partial \mathbf{n}}(\mathbf{x}_N, \tilde{\mathbf{x}}_1) & \frac{\partial \Gamma_1}{\partial \mathbf{n}}(\mathbf{x}_N, \tilde{\mathbf{x}}_2) & \cdots & \frac{\partial \Gamma_1}{\partial \mathbf{n}}(\mathbf{x}_N, \tilde{\mathbf{x}}_N) \\ \frac{\partial \Delta \Gamma_1}{\partial \mathbf{n}}(\mathbf{x}_{N_1+1}, \tilde{\mathbf{x}}_1) & \frac{\partial \Delta \Gamma_1}{\partial \mathbf{n}}(\mathbf{x}_{N_1+1}, \tilde{\mathbf{x}}_2) & \cdots & \frac{\partial \Delta \Gamma_1}{\partial \mathbf{n}}(\mathbf{x}_{N_1+1}, \tilde{\mathbf{x}}_N) \\ \frac{\partial \Delta \Gamma_1}{\partial \mathbf{n}}(\mathbf{x}_{N_1+2}, \tilde{\mathbf{x}}_1) & \frac{\partial \Delta \Gamma_1}{\partial \mathbf{n}}(\mathbf{x}_{N_1+2}, \tilde{\mathbf{x}}_2) & \cdots & \frac{\partial \Delta \Gamma_1}{\partial \mathbf{n}}(\mathbf{x}_{N_1+2}, \tilde{\mathbf{x}}_N) \\ \vdots & \vdots & \ddots & \vdots \\ \frac{\partial \Delta \Gamma_1}{\partial \mathbf{n}}(\mathbf{x}_N, \tilde{\mathbf{x}}_1) & \frac{\partial \Delta \Gamma_1}{\partial \mathbf{n}}(\mathbf{x}_N, \tilde{\mathbf{x}}_2) & \cdots & \frac{\partial \Delta \Gamma_1}{\partial \mathbf{n}}(\mathbf{x}_N, \tilde{\mathbf{x}}_N) \end{bmatrix},$$

$$A_{22} = \begin{bmatrix} \frac{\partial \Gamma_2}{\partial \mathbf{n}}(\mathbf{x}_{N_1+1}, \tilde{\mathbf{x}}_1) & \frac{\partial \Gamma_2}{\partial \mathbf{n}}(\mathbf{x}_{N_1+1}, \tilde{\mathbf{x}}_2) & \cdots & \frac{\partial \Gamma_2}{\partial \mathbf{n}}(\mathbf{x}_{N_1+1}, \tilde{\mathbf{x}}_N) \\ \frac{\partial \Gamma_2}{\partial \mathbf{n}}(\mathbf{x}_{N_1+2}, \tilde{\mathbf{x}}_1) & \frac{\partial \Gamma_2}{\partial \mathbf{n}}(\mathbf{x}_{N_1+2}, \tilde{\mathbf{x}}_2) & \cdots & \frac{\partial \Gamma_2}{\partial \mathbf{n}}(\mathbf{x}_{N_1+2}, \tilde{\mathbf{x}}_N) \\ \vdots & \vdots & \ddots & \vdots \\ \frac{\partial \Gamma_2}{\partial \mathbf{n}}(\mathbf{x}_N, \tilde{\mathbf{x}}_1) & \frac{\partial \Gamma_2}{\partial \mathbf{n}}(\mathbf{x}_N, \tilde{\mathbf{x}}_2) & \cdots & \frac{\partial \Gamma_2}{\partial \mathbf{n}}(\mathbf{x}_N, \tilde{\mathbf{x}}_N) \\ \frac{\partial \Delta \Gamma_2}{\partial \mathbf{n}}(\mathbf{x}_{N_1+1}, \tilde{\mathbf{x}}_1) & \frac{\partial \Delta \Gamma_2}{\partial \mathbf{n}}(\mathbf{x}_{N_1+1}, \tilde{\mathbf{x}}_2) & \cdots & \frac{\partial \Delta \Gamma_2}{\partial \mathbf{n}}(\mathbf{x}_{N_1+1}, \tilde{\mathbf{x}}_N) \\ \frac{\partial \Delta \Gamma_2}{\partial \mathbf{n}}(\mathbf{x}_{N_1+2}, \tilde{\mathbf{x}}_1) & \frac{\partial \Delta \Gamma_2}{\partial \mathbf{n}}(\mathbf{x}_{N_1+2}, \tilde{\mathbf{x}}_2) & \cdots & \frac{\partial \Delta \Gamma_2}{\partial \mathbf{n}}(\mathbf{x}_{N_1+2}, \tilde{\mathbf{x}}_N) \\ \vdots & \vdots & \ddots & \vdots \\ \frac{\partial \Delta \Gamma_2}{\partial \mathbf{n}}(\mathbf{x}_N, \tilde{\mathbf{x}}_1) & \frac{\partial \Delta \Gamma_2}{\partial \mathbf{n}}(\mathbf{x}_N, \tilde{\mathbf{x}}_2) & \cdots & \frac{\partial \Delta \Gamma_2}{\partial \mathbf{n}}(\mathbf{x}_N, \tilde{\mathbf{x}}_N) \end{bmatrix}.$$

The vectors  $\mathbf{f} = [f_{11}, \dots, f_{1N_1}, f_{21}, \dots, f_{2N_1}]^T \in \mathbb{R}^{2N_1 \times 1}$  and  $\mathbf{g} = [g_{1N_1+1}, \dots, g_{1N}, g_{2N_1+1}, \dots, g_{2N}]^T \in \mathbb{R}^{2N_2 \times 1}$  are formed by

$$f_{1k} = f_1(\mathbf{x}_k), \quad f_{2k} = f_2(\mathbf{x}_k), \quad 1 \leq k \leq N_1,$$

$$g_{1k} = g_1(\mathbf{x}_k), \quad g_{2k} = g_2(\mathbf{x}_k), \quad N_1 + 1 \leq k \leq N,$$

and the vector of unknown coefficients in (4.7),

$$\mathbf{c} = [c_1, c_2, \dots, c_N]^T,$$

$$\mathbf{d} = [d_1, d_2, \dots, d_N]^T.$$

Once the matrix in (4.7) is invertible, the unknown coefficients  $\mathbf{x}^* = [\mathbf{c}, \mathbf{d}]^T$  can be determined and  $u_N(\mathbf{x})$  in (4.6) is considered as an approximate solution of the biharmonic

problem (4.1)-(4.3). Or we may choose or determine the unknown coefficients  $\mathbf{x}^*$  to be the solution of the following minimization problem

$$\min_{\mathbf{x}^* \in \mathbb{R}^{2N}} \|\mathbf{A}\mathbf{x}^* - \mathbf{b}\|, \quad (4.8)$$

as discussed before, by using the singular value decomposition of a matrix or regularization method.

## 4.2 Numerical Examples by using MFS

**Example 4.1.** Consider the boundary problem for the biharmonic equation

$$\begin{aligned} \Delta^2 u(x, y) &= 0 & (x, y) \in \Omega, \\ u(x, y) &= x^4 - y^4 \quad \text{and} \quad \Delta u(x, y) = 12x^2 - 12y^2 & (x, y) \in \partial\Omega_1, \\ \frac{\partial u}{\partial \mathbf{n}}(x, y) &= 4x^4 - 4y^4 \quad \text{and} \quad \frac{\partial \Delta u}{\partial \mathbf{n}}(x, y) = 24x^2 - 24y^2 & (x, y) \in \partial\Omega_2, \end{aligned}$$

where  $\Omega = \{(x, y) : x^2 + y^2 \leq 1\}$  is the unit disc and  $\partial\Omega = \partial\Omega_1 \cup \partial\Omega_2$  such that  $\partial\Omega_1 = \{(x, y) : x = \cos(t), y = \sin(t), 0 \leq t < \pi\}$  and  $\partial\Omega_2 = \{(x, y) : x = \cos(t), y = \sin(t), \pi \leq t < 2\pi\}$ .

The exact solution of the above problem is  $u_{exact} = x^4 - y^4$ . We use a fictitious domain

$\tilde{\Omega} = \{(x, y) : x = a \cos t, y = b \sin(t + \sin t), 0 \leq t \leq 2\pi\}$ , where  $\mathbf{a} = 3, 3, 4, 4$  and

$\mathbf{b} = 3, 4, 4, 5$ , respectively. We choose  $\tilde{\mathbf{x}}_k = (a \cos \frac{2\pi k}{N}, b \sin(\frac{2\pi k}{N} + \sin \frac{2\pi k}{N}))$ ,  $0 \leq k \leq$

$N - 1$  on  $\partial\tilde{\Omega}$ . Then in order to resolve the difficulty due to the unstable result, we apply

the TSVD with singular value tolerances,  $\epsilon = \{10^{-3}, 10^{-5}, 10^{-7}\}$ , respectively to obtain the

approximate solution through (4.4)-(4.7). To estimate the maximum error, we use points

$\mathbf{z}_{k,m} = (r_k \cos \frac{2\pi m}{M_k}, r_k \sin \frac{2\pi m}{M_k})$ , in  $\Omega$ , where  $r_k = \frac{k}{M}$ ,  $M_k = kM$ ,  $1 \leq m \leq M_k$ ,  $1 \leq k \leq$

$M$ , and  $\mathbf{z}_k = (\cos \frac{\pi k}{N_1}, \sin \frac{\pi k}{N_1})$ ,  $0 \leq k \leq N_1 - 1$ , on  $\partial\Omega_1$  and  $\mathbf{z}_k = (\cos(\pi + \frac{\pi k}{N_2}), \sin(\pi + \frac{\pi k}{N_2}))$ ,  $0 \leq k \leq N_2 - 1$ , on  $\partial\Omega_2$  to get the numerical estimate for

$$\max_{k,m} |u_{exact}(\mathbf{z}_{k,m}) - u_N(\mathbf{z}_{k,m})|.$$

Then our numerical approximation errors are presented in the following table with various  $a$ ,  $b$ , and  $N$ :

Figure 4.1: Choose collocation points in  $\bar{\Omega} = \Omega \cup \partial\Omega$  where  $\partial\Omega = \partial\Omega_1 \cup \partial\Omega_2$ , and  $N = 20$  source points on the  $\partial\tilde{\Omega} = \{(x, y) : x = 3 \cos t, y = 3 \sin(t + \sin t), 0 \leq t < 2\pi\}$

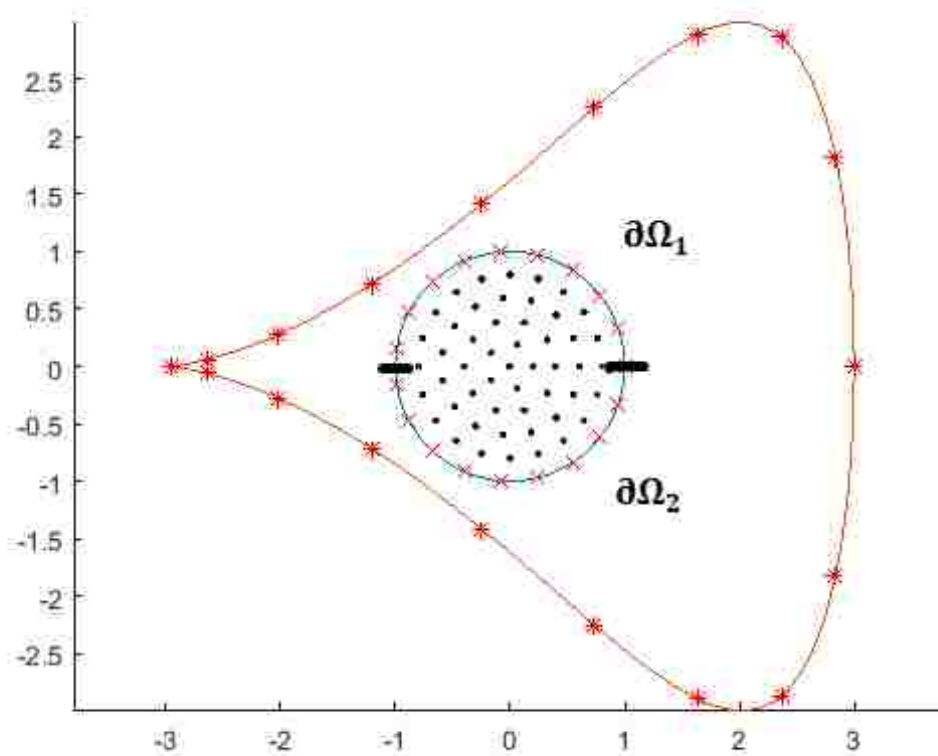
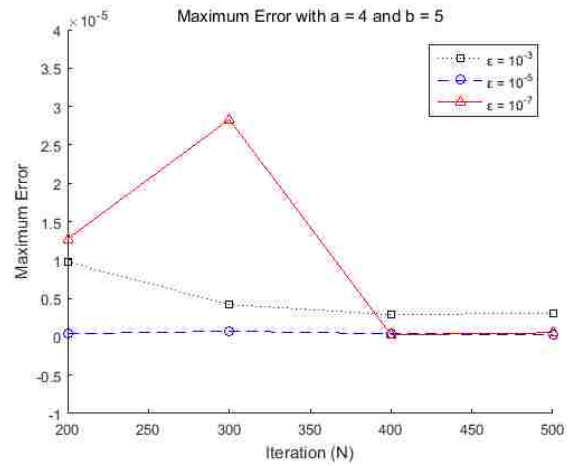
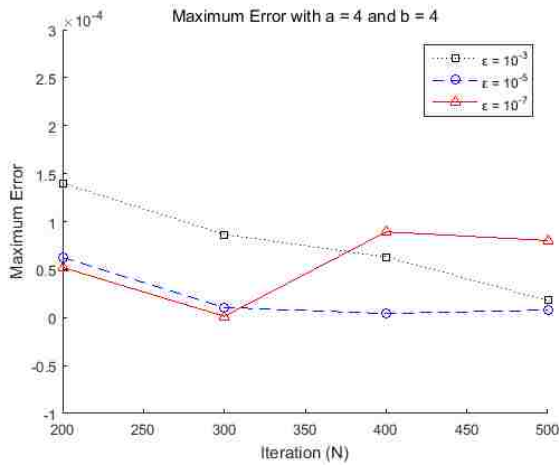
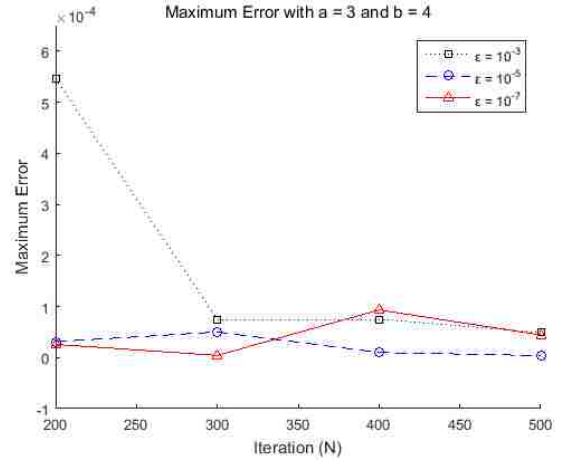
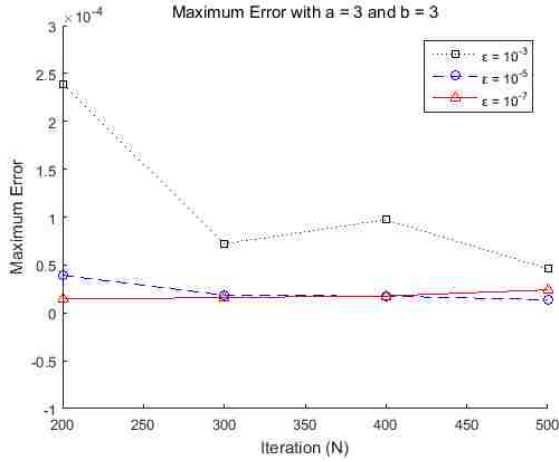


Table 4.1: Maximum Error  $\|u_{exact} - u_N\|_{C(\bar{\Omega})}$ 

	$N_1 = 100$ $N_2 = 100$ $N = 200$	$N_1 = 150$ $N_2 = 150$ $N = 300$	$N_1 = 200$ $N_2 = 200$ $N = 400$	$N_1 = 250$ $N_2 = 250$ $N = 500$
$a = 3, b = 3$ $\epsilon = 10^{-3}$	2.3886e-04 (k = 73)	7.2239e-05 (k = 88)	9.7180e-05 (k = 99)	4.6016e-05 (k = 108)
$a = 3, b = 3$ $\epsilon = 10^{-5}$	3.9144e-05 (k = 79)	1.8477e-05 (k = 95)	1.7482e-05 (k = 107)	1.3794e-05 (k = 120)
$a = 3, b = 3$ $\epsilon = 10^{-7}$	1.4286e-05 (k = 87)	1.5980e-05 (k = 102)	1.7683e-05 (k = 117)	2.4028e-05 (k = 129)
$a = 3, b = 4$ $\epsilon = 10^{-3}$	5.4638e-04 (k = 67)	7.4690e-05 (k = 79)	7.4902e-05 (k = 88)	4.9360e-05 (k = 96)
$a = 3, b = 4$ $\epsilon = 10^{-5}$	3.1126e-05 (k = 74)	5.0089e-05 (k = 86)	9.9726e-06 (k = 96)	3.7933e-06 (k = 106)
$a = 3, b = 4$ $\epsilon = 10^{-7}$	2.5734e-05 (k = 80)	4.2955e-06 (k = 93)	9.3278e-05 (k = 103)	4.4248e-05 (k = 113)
$a = 4, b = 4$ $\epsilon = 10^{-3}$	1.4012e-04 (k = 63)	8.6581e-05 (k = 71)	6.3257e-05 (k = 79)	1.7787e-05 (k = 86)
$a = 4, b = 4$ $\epsilon = 10^{-5}$	6.2605e-05 (k = 67)	1.0525e-05 (k = 78)	4.2323e-06 (k = 87)	7.7189e-06 (k = 93)
$a = 4, b = 4$ $\epsilon = 10^{-7}$	5.2175e-05 (k = 74)	1.2660e-06 (k = 85)	8.9303e-05 (k = 94)	8.0271e-05 (k = 100)
$a = 4, b = 5$ $\epsilon = 10^{-3}$	9.7287e-06 (k = 57)	4.2001e-06 (k = 66)	2.8641e-06 (k = 70)	3.1107e-06 (k = 72)
$a = 4, b = 5$ $\epsilon = 10^{-5}$	3.9192e-07 (k = 63)	7.2941e-07 (k = 71)	3.8620e-07 (k = 78)	2.9312e-07 (k = 81)
$a = 4, b = 5$ $\epsilon = 10^{-7}$	1.2734e-05 (k = 67)	2.8318e-05 (k = 78)	2.4865e-07 (k = 86)	5.2336e-07 (k = 88)

Figure 4.2: Maximum errors in a domain  $\bar{\Omega}$  with singular value tolerances,  $\epsilon = 10^{-3}$  ( $\square$ ),  $\epsilon = 10^{-5}$  ( $\circ$ ),  $\epsilon = 10^{-7}$  ( $\triangle$ ), respectively



**Example 4.2.** Consider the boundary problem for the biharmonic equation

$$\Delta^2 u(x, y) = 0 \quad (x, y) \in \Omega,$$

$$u(x, y) = e^x \cos(y) + e^y \sin(x) + x^3 - 2y^3 \quad \text{and}$$

$$\Delta u(x, y) = 6x - 12y \quad (x, y) \in \partial\Omega,$$

where  $\Omega = \{(x, y) : -2 \leq x \leq -1, -1 \leq y \leq 1, \text{ or } -1 \leq x \leq 0, -1 \leq y \leq 0\}$  is the L-shaped domain. The exact solution of the above problem is  $u_{exact} = e^x \cos(y) + e^y \sin(x) + x^3 - 2y^3$ . We use a fictitious domain  $\tilde{\Omega} = \{(x, y) : x = a \sin t, y = b \cos(t + \cos t), 0 \leq t \leq 2\pi\}$ , where  $a = 3, 4$  and  $b = 3, 4$ , respectively. We choose  $\tilde{\mathbf{x}}_{\mathbf{k}} = (a \sin \frac{2\pi k}{N}, b \cos(\frac{2\pi k}{N} + \cos \frac{2\pi k}{N}))$ ,  $0 \leq k \leq N - 1$  on  $\partial\tilde{\Omega}$ . Then the varying number of collocation points on  $\partial\Omega$  and source points on  $\partial\tilde{\Omega}$  cause the ill-condition system (4.7) and hence in order to resolve the unstable results, we use the Tikhonov regularization with regularization parameters,  $\mu = \{10^{-3}, 10^{-5}, 10^{-7}\}$ , respectively to obtain the approximate solution through (4.4)-(4.7). To estimate the maximum error, we use points  $\mathbf{z}_{k,m} = (\frac{k}{M}, \frac{m}{M})$ ,  $-2M \leq k \leq -M$  and  $-M \leq m \leq M$  or  $-M \leq k \leq 0$  and  $-M \leq m \leq 0$  with  $M = 100$  in  $\bar{\Omega} = \Omega \cup \partial\Omega$  to get the numerical infinity norm in Example 4.1. Then our numerical approximation errors are presented in the following table with various  $a$ ,  $b$ , and  $N$ :

Figure 4.3: Choose collocation points on the  $\bar{\Omega} = \Omega \cup \partial\Omega$  and  $N = 20$  source points on the  $\partial\Omega = \{(x, y) : x = a \sin t, y = b \cos(t + \cos t), 0 \leq t < 2\pi\}$

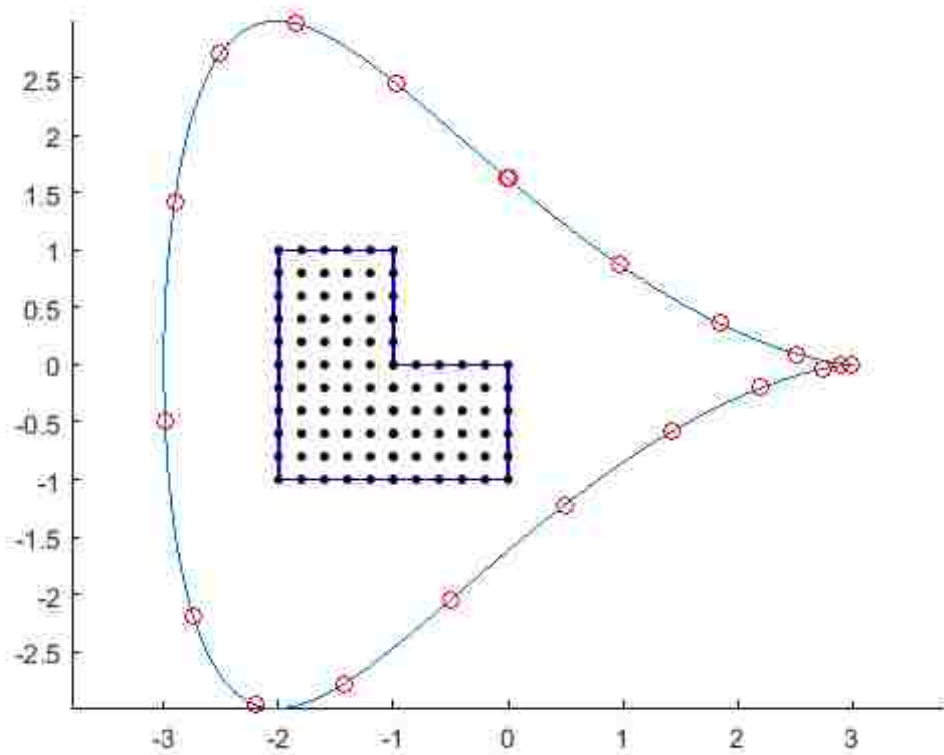
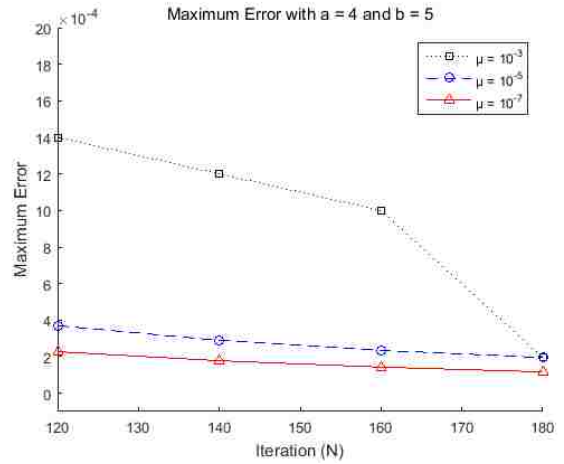
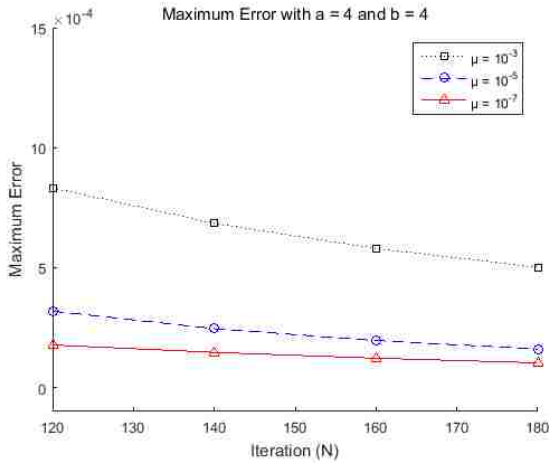
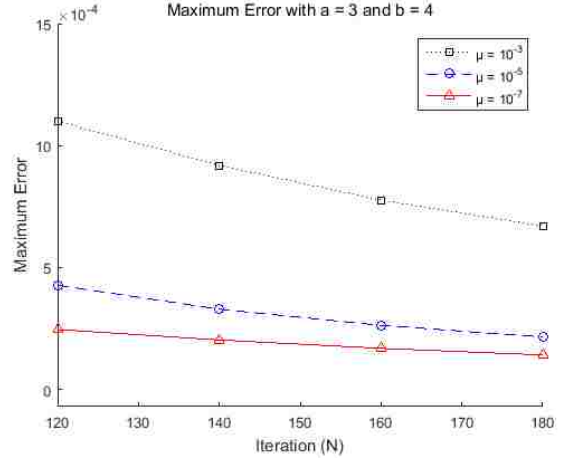
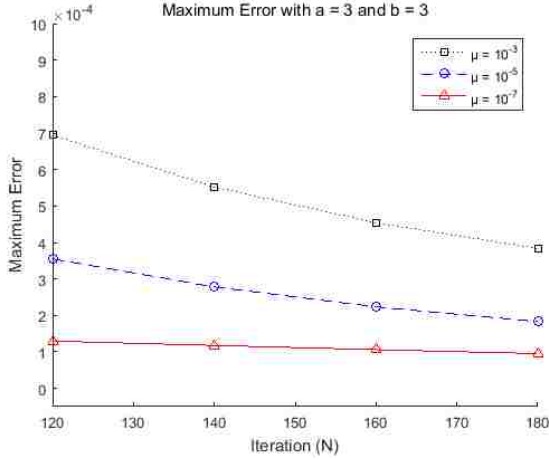




Table 4.2: Maximum Error  $\|u_{exact} - u_N\|_{C(\bar{\Omega})}$

	N = 120	N = 140	N = 160	N = 180
$a = 3, b = 3, \mu = 10^{-3}$	6.9399e-04	5.5198e-04	4.5417e-04	3.8337e-04
$a = 3, b = 3, \mu = 10^{-5}$	3.5497e-04	2.7811e-04	2.2341e-04	1.8332e-04
$a = 3, b = 3, \mu = 10^{-7}$	1.2972e-04	1.1770e-04	1.0616e-04	9.5411e-05
$a = 3, b = 4, \mu = 10^{-3}$	0.0011	9.1833e-04	7.7623e-04	6.7057e-04
$a = 3, b = 4, \mu = 10^{-5}$	4.2704e-04	3.2949e-04	2.6295e-04	2.1550e-04
$a = 3, b = 4, \mu = 10^{-7}$	2.4625e-04	2.0316e-04	1.6886e-04	1.4171e-04
$a = 4, b = 4, \mu = 10^{-3}$	8.3193e-04	6.8431e-04	5.7938e-04	5.0126e-04
$a = 4, b = 4, \mu = 10^{-5}$	3.1836e-04	2.4537e-04	1.9577e-04	1.6047e-04
$a = 4, b = 4, \mu = 10^{-7}$	1.7726e-04	1.4655e-04	1.2221e-04	1.0291e-04
$a = 4, b = 5, \mu = 10^{-3}$	0.0014	0.0012	0.0010	8.8411e-04
$a = 4, b = 5, \mu = 10^{-5}$	3.6978e-04	2.8939e-04	2.3456e-04	1.9530e-04
$a = 4, b = 5, \mu = 10^{-7}$	2.2710e-04	1.7807e-04	1.4279e-04	1.1681e-04

Figure 4.4: Maximum errors in a domain  $\bar{\Omega}$  with regularization parameters,  $\mu = 10^{-3}$  ( $\square$ ),  $\mu = 10^{-5}$  ( $\circ$ ),  $\mu = 10^{-7}$  ( $\triangle$ ), respectively



**Example 4.3.** Consider the boundary problem for the biharmonic equation

$$\Delta^2 u(x, y, z) = 0 \quad (x, y, z) \in \Omega,$$

$$u(x, y, z) = 5xe^{2y} \cos(2z) + x^3 - y^3 + 3z^3$$

and

$$\Delta u(x, y, z) = 6x - 6y + 18z, \quad (x, y, z) \in \partial\Omega,$$

where  $\Omega = \{(x, y, z) : -1 \leq x, y, z \leq 1\}$  is the cube. The exact solution of the above problem is  $u_{exact} = 5xe^{2y} \cos(2z) + x^3 - y^3 + 3z^3$ . We use a bumpy spherical fictitious domain  $\tilde{\Omega} = \{(x, y, z) : \rho \sin(\theta) \cos(\phi), \rho \sin(\theta) \sin(\phi), \rho \cos(\theta), 0 \leq \theta \leq \pi, 0 \leq \phi \leq 2\pi\}$ , where  $\rho(\phi, \theta) = R + \frac{1}{6} \sin(6\phi) \sin(7\theta)$ ,  $R = 2, 3, 4, 5$ . We choose  $\tilde{\mathbf{x}}_{k,m} = (\rho \sin(\theta_k) \cos(\phi_{k,m}), \rho \sin(\theta_k) \sin(\phi_{k,m}), \rho \cos(\theta_k))$ , where  $\rho = R + \frac{1}{6} \sin(6\theta_k) \sin(7\phi_{k,m})$ ,  $R = 2, 3, 4, 5$ , and  $\theta_k = \frac{\pi(k+0.5)}{M_\theta}$ ,  $0 \leq k \leq M_\theta - 1$ , with  $M_\theta = \frac{\sqrt{\pi N}}{2r}$ , and  $\phi_{k,m} = \frac{2\pi m}{M_k}$ ,  $0 \leq m \leq M_k - 1$ , with  $M_k = \sqrt{\pi N \sin \theta_k}$ , on  $\partial\tilde{\Omega}$ . (see Figure 4.5). Then in order to resolve the difficulty due to the unstable result, we apply the TSVD with singular value tolerances,  $\epsilon = \{10^{-3}, 10^{-5}, 10^{-7}\}$ , respectively to obtain the approximate solution through (4.4)-(4.7). To estimate the maximum error, we use points  $\mathbf{z}_{k,l,m} = (\frac{k}{M}, \frac{l}{M}, \frac{m}{M})$ ,  $-M \leq k, l, m \leq M$ , with  $M = 10$  in  $\bar{\Omega} = \Omega \cup \partial\Omega$ , to get the numerical infinity norm in Example 4.1. Then our numerical approximation errors are presented in the following table with various R and N:

Figure 4.5: Choose collocation points on  $\bar{\Omega} = \Omega \cup \partial\Omega$  and  $N = 100$  source points on the bumpy spherical fictitious domain  $\partial\tilde{\Omega}$

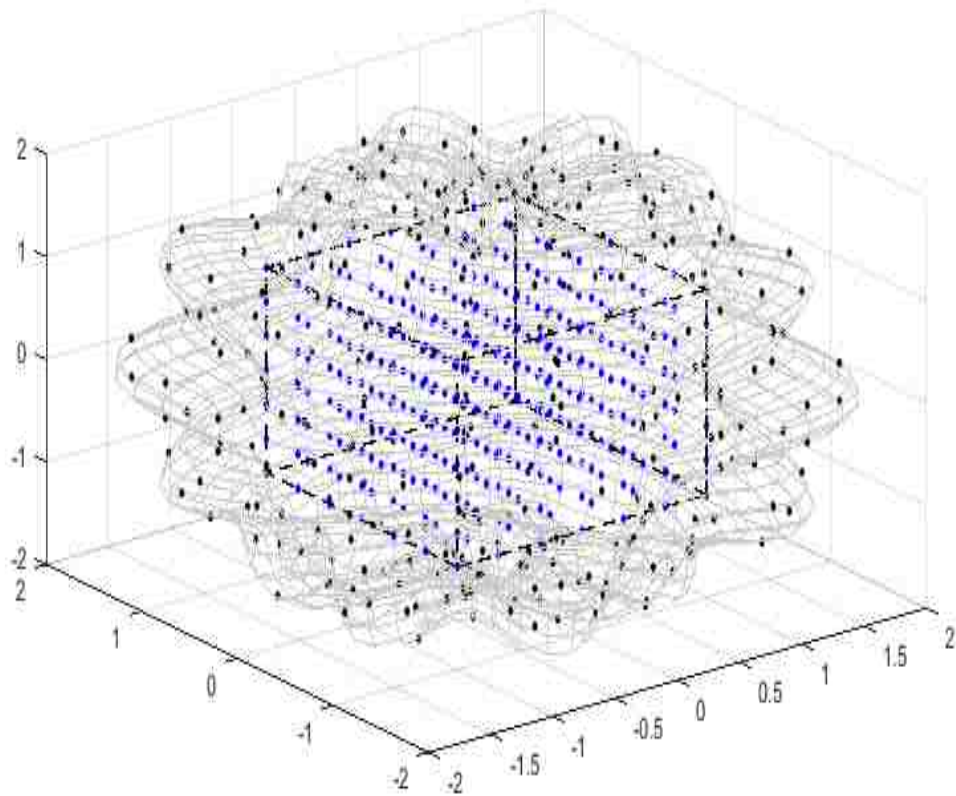
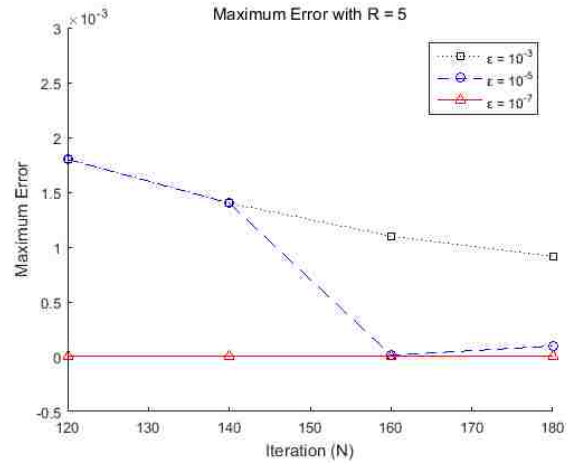
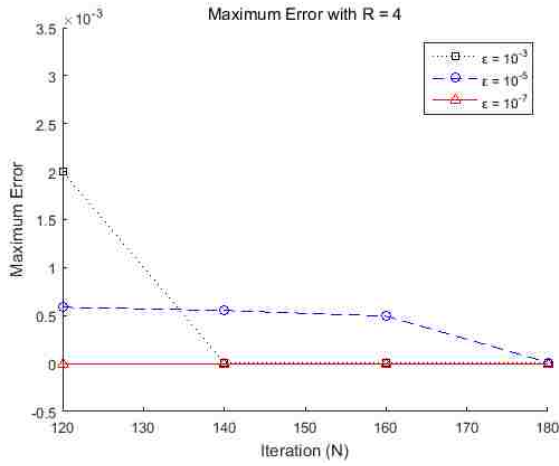
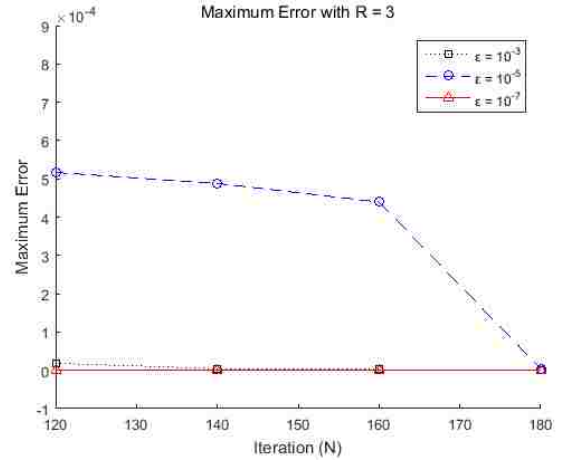
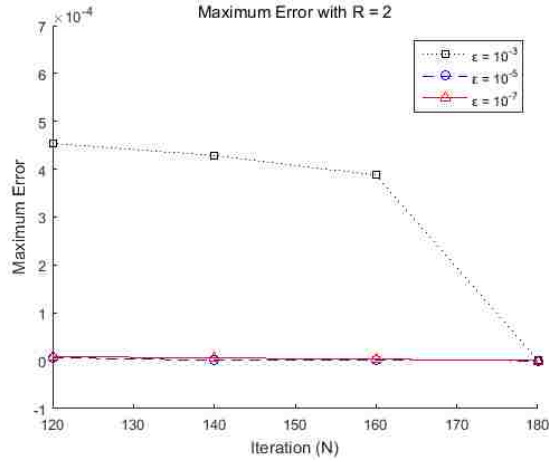


Table 4.3: Maximum Error  $\|u_{exact} - u_N\|_{C(\bar{\Omega})}$

	N = 120	N = 140	N = 160	N = 180
R = 2 $\epsilon = 10^{-3}$	4.5400e-04 (k = 8)	4.2848e-04 (k = 8)	3.8757e-04 (k = 8)	1.7225e-06 (k = 8)
R = 2 $\epsilon = 10^{-5}$	6.4147e-06 (k = 8)	9.2011e-07 (k = 9)	4.6282e-07 (k = 8)	2.5193e-07 (k = 8)
R = 2 $\epsilon = 10^{-7}$	8.6616e-06 (k = 8)	5.7495e-06 (k = 8)	3.2725e-06 (k = 8)	2.6196e-07 (k = 8)
R = 3 $\epsilon = 10^{-3}$	1.8411e-05 (k = 8)	4.0288e-06 (k = 8)	2.0628e-06 (k = 8)	1.2656e-06 (k = 8)
R = 3 $\epsilon = 10^{-5}$	5.1655e-04 (k = 7)	4.8796e-04 (k = 7)	4.3954e-04 (k = 7)	4.6735e-06 (k = 8)
R = 3 $\epsilon = 10^{-7}$	1.7755e-06 (k = 8)	1.1107e-06 (k = 8)	4.6440e-07 (k = 9)	2.1745e-07 (k = 9)
R = 4 $\epsilon = 10^{-3}$	0.0020 (k = 6)	8.2689e-06 (k = 7)	4.5682e-06 (k = 7)	2.8110e-06 (k = 7)
R = 4 $\epsilon = 10^{-5}$	5.8654e-04 (k = 7)	5.5266e-04 (k = 7)	4.9414e-04 (k = 8)	1.1976e-05 (k = 8)
R = 4 $\epsilon = 10^{-7}$	1.3015e-06 (k = 8)	8.9028e-07 (k = 8)	4.2401e-07 (k = 9)	2.2783e-07 (k = 9)
R = 5 $\epsilon = 10^{-3}$	0.0018 (k = 6)	0.0014 (k = 6)	0.0011 (k = 6)	9.1498e-04 (k = 7)
R = 5 $\epsilon = 10^{-5}$	0.0018 (k = 6)	0.0014 (k = 7)	1.1874e-05 (k = 7)	9.7606e-05 (k = 8)
R = 5 $\epsilon = 10^{-7}$	1.2177e-06 (k = 8)	1.3280e-06 (k = 8)	6.8098e-07 (k = 9)	3.8472e-07 (k = 9)

Figure 4.6: Maximum errors in a domain  $\bar{\Omega}$  with singular value tolerances,  $\epsilon = 10^{-3}$  ( $\square$ ),  $\epsilon = 10^{-5}$  ( $\circ$ ),  $\epsilon = 10^{-7}$  ( $\triangle$ ), respectively



### 4.3 Method of Particular Solutions (MPS) and DRM

First we describe the method of particular solutions to find an approximate solution of a biharmonic equation

$$\Delta^2 u(\mathbf{x}) = f(\mathbf{x}) \quad \text{in } \Omega. \quad (4.9)$$

For this purpose, we use a radial basis functions (RBF)

$$\phi(\mathbf{x}) = \phi(\|\mathbf{x}\|),$$

where  $\phi(\cdot)$  is a univariate function. Then we approximate  $f(x)$  by the collocation method. To be specific, we choose  $\mathbf{x}_1, \mathbf{x}_2, \dots, \mathbf{x}_M$  in  $\Omega$ , (see Figure 2.1) and consider a linear combination of  $\phi(\|\mathbf{x} - \mathbf{x}_k\|)$ ,  $1 \leq k \leq M$ , or

$$\sum_{k=1}^M c_k \phi(\|\mathbf{x} - \mathbf{x}_k\|),$$

where  $c_k$ ,  $1 \leq k \leq M$ , so chosen that

$$\sum_{k=1}^M c_k \phi(\|\mathbf{x}_m - \mathbf{x}_k\|) = f(\mathbf{x}_m), \quad 1 \leq m \leq M.$$

The above equation yields

$$\begin{bmatrix} \phi(0) & \dots & \phi(\|\mathbf{x}_1 - \mathbf{x}_M\|) \\ \vdots & \ddots & \vdots \\ \phi(\|\mathbf{x}_M - \mathbf{x}_1\|) & \dots & \phi(0) \end{bmatrix} \begin{bmatrix} c_1 \\ \vdots \\ c_M \end{bmatrix} = \begin{bmatrix} f(\mathbf{x}_1) \\ \vdots \\ f(\mathbf{x}_M) \end{bmatrix}. \quad (4.10)$$

It is known in [25] that for Gaussian  $e^{-c\|\mathbf{x}\|^2}$ , or multiquadratic  $\sqrt{\|\mathbf{x}\|^2 + c^2}$ , where  $c > 0$  is a constant, the above coefficient matrix is always invertible. Hence  $\{c_k\}_{k=1}^M$  can be found. However, the above matrix may not be invertible for other RBFs, e.g.  $\phi(\mathbf{x}) = \|\mathbf{x}\|^2 \ln \|\mathbf{x}\|$ , thin plate splines.

Suppose that  $\{c_k\}_{k=1}^M$  is determined (e.g. using  $e^{-c\|\mathbf{x}\|^2}$  or  $\sqrt{\|\mathbf{x}\|^2 + c^2}$ ). Then

$$\sum_{k=1}^M c_k \phi(\|\mathbf{x} - \mathbf{x}_k\|)$$

is considered as an approximation of  $f(\mathbf{x})$ , and hence we turn to study the following biharmonic equation

$$\Delta^2 u(\mathbf{x}) = \sum_{k=1}^M c_k \phi(\|\mathbf{x} - \mathbf{x}_k\|), \quad \mathbf{x} \in \Omega.$$

If  $\psi$  is a RBF solution of  $\Delta^2 \psi(\|\mathbf{x}\|) = \phi(\|\mathbf{x}\|)$ , then

$$u(\mathbf{x}) = \sum_{k=1}^M c_k \psi(\|\mathbf{x} - \mathbf{x}_k\|)$$

is an approximate solution of the biharmonic equation (4.9).

Using Lemma 2.1 in section 2.3, the radially particular solutions of biharmonic equations,  $\Delta^2 \psi(r) = \phi(r)$ , are also derived in [17], given by

$$\begin{aligned} \psi(r) &= \frac{1}{4} r^2 (\ln r - 1) \int_0^r t \phi(t) dt - \frac{1}{4} \int_0^r t^3 (\ln t - 1) \phi(t) dt \\ &\quad + \frac{1}{4} \ln r \int_0^r t^3 \phi(t) dt - \frac{1}{4} r^2 \int_0^r t \phi(t) \ln t dt \\ &\quad + Ar^2 \ln r + Br^2 + C \ln r + D \end{aligned} \quad (4.11)$$

in  $\mathbb{R}^2$ , and

$$\begin{aligned} \psi(r) &= -\frac{r}{2} \int_0^r t^2 \phi(t) dt + \frac{1}{2} \int_0^r t^3 \phi(t) dt \\ &\quad - \frac{1}{6r} \int_0^r t^4 \phi(t) dt + \frac{r^2}{6} \int_0^r t \phi(t) dt \\ &\quad + Ar + Br^2 + \frac{C}{r} + D, \end{aligned} \quad (4.12)$$

in  $\mathbb{R}^3$ , where we may choose  $A = B = C = D = 0$ .



Correspondingly the approximate particular solutions of (4.9) are given in [17] by

$$\begin{aligned}
u_p(\mathbf{x}) &= \frac{1}{n^{2(1-\gamma)}} \sum_{\mathbf{j} \in I_n(\Omega_\delta)} f\left(\frac{\mathbf{j}}{n}\right) n^{-4\gamma} \\
&\times \left[ \frac{1}{4} (n^\gamma \|\mathbf{x} - \mathbf{j}/n\|)^2 (\ln(n^\gamma \|\mathbf{x} - \mathbf{j}/n\|) - 1) \int_0^{n^\gamma \|\mathbf{x} - \mathbf{j}/n\|} t \phi(t) dt \right. \\
&- \frac{1}{4} \int_0^{n^\gamma \|\mathbf{x} - \mathbf{j}/n\|} t^3 (\ln t - 1) \phi(t) dt + \frac{1}{4} \ln(n^\gamma \|\mathbf{x} - \mathbf{j}/n\|) \int_0^{n^\gamma \|\mathbf{x} - \mathbf{j}/n\|} t^3 \phi(t) dt \\
&\left. - \frac{1}{4} (n^\gamma \|\mathbf{x} - \mathbf{j}/n\|)^2 \int_0^{n^\gamma \|\mathbf{x} - \mathbf{j}/n\|} t \phi(t) \ln t dt \right]
\end{aligned} \tag{4.13}$$

in  $\mathbb{R}^2$ , and

$$\begin{aligned}
u_p(\mathbf{x}) &= \frac{1}{n^{3(1-\gamma)}} \sum_{\mathbf{j} \in I_n(\Omega_\delta)} f\left(\frac{\mathbf{j}}{n}\right) n^{-4\gamma} \\
&\times \left[ -\frac{n^\gamma \|\mathbf{x} - \mathbf{j}/n\|}{2} \int_0^{n^\gamma \|\mathbf{x} - \mathbf{j}/n\|} t^2 \phi(t) dt + \frac{1}{2} \int_0^{n^\gamma \|\mathbf{x} - \mathbf{j}/n\|} t^3 \phi(t) dt \right. \\
&- \frac{1}{6 n^\gamma \|\mathbf{x} - \mathbf{j}/n\|} \int_0^{n^\gamma \|\mathbf{x} - \mathbf{j}/n\|} t^4 \phi(t) dt \\
&\left. + \frac{(n^\gamma \|\mathbf{x} - \mathbf{j}/n\|)^2}{6} \int_0^{n^\gamma \|\mathbf{x} - \mathbf{j}/n\|} t \phi(t) dt \right]
\end{aligned} \tag{4.14}$$

in  $\mathbb{R}^3$ .

Now for a Dirichlet problem of biharmonic equations

$$\Delta^2 u(\mathbf{x}) = f(\mathbf{x}), \quad \mathbf{x} \in \Omega, \tag{4.15}$$

$$u(\mathbf{x}) = h(\mathbf{x}), \quad \mathbf{x} \in \partial\Omega, \tag{4.16}$$

first we use the MPS to get an approximate solution of biharmonic equations. Namely, choose a RBF  $\phi(r)$ . Then we get an approximate solution  $u_p$  of  $\Delta^2 u(\mathbf{x}) = f(\mathbf{x})$ , as discussed above in (4.9). Next we consider the Dirichlet boundary problem of the Laplace equation

$$\Delta^2 u(\mathbf{x}) = 0, \quad \mathbf{x} \in \Omega, \tag{4.17}$$

$$u(\mathbf{x}) = h(\mathbf{x}) - u_p(\mathbf{x}), \quad \mathbf{x} \in \partial\Omega. \tag{4.18}$$

The MFS can be applied to obtain an approximate solution  $u_N$  of (4.16)-(4.17). Then

$$u_A(\mathbf{x}) = u_N(\mathbf{x}) + u_p(\mathbf{x}).$$

is considered as an approximate solution of (4.14)-(4.15). Such a combination of MPS and MFS is called the dual reciprocity method (DRM).

## 4.4 Numerical Examples by MFS and Collocation Methods

**Example 4.4.** Consider the boundary problem for the biharmonic equation

$$\Delta^2 u(x, y) = 25 e^{2x} \sin(3y), \quad (x, y) \in \Omega,$$

$$u(x, y) = e^{2x} \sin(3y) \quad \text{and} \quad \Delta u(x, y) = -5 e^{2x} \sin(3y), \quad (x, y) \in \partial\Omega,$$

where  $\Omega = \{(x, y) : -1 \leq x \leq 1, \text{ or } -1 \leq y \leq 1\}$  is the square. The exact solution of the above problem is  $u_{exact} = e^{2x} \sin(3y)$ . Choose a Gaussian radial basis function (RBF)  $\phi(r) = e^{-2r^2}$  where  $r = \|x\|$ . We use a fictitious domain  $\tilde{\Omega} = \{(x, y) : x = a \cos^3(t), y = b \sin^3(t), 0 \leq t \leq 2\pi\}$ , where  $a = 4, 4, 5, 5$  and  $b = 4, 5, 5, 6$ , respectively. We choose  $\tilde{\mathbf{x}}_k = (a \cos^3(\frac{2\pi k}{N}), b \sin^3(\frac{2\pi k}{N}))$ ,  $0 \leq k \leq N - 1$ , on  $\partial\tilde{\Omega}$ . Then in order to resolve the difficulty due to the unstable result, we apply the TSVD with singular value tolerances,  $\epsilon = \{10^{-3}, 10^{-5}, 10^{-7}\}$ , respectively, to obtain the approximate solution through (4.4)-(4.7). To estimate the maximum error, we use points  $\mathbf{z}_{k,m} = (\frac{k}{M}, \frac{m}{M})$ ,  $-M \leq k \leq M$  and  $-M \leq m \leq M$ , with  $M = 100$  in  $\bar{\Omega} = \Omega \cup \partial\Omega$  to get the numerical estimate (see Figure 4.7) for

$$\max_{\bar{\Omega}} |u_{exact}(\mathbf{z}_{k,m}) - u_A(\mathbf{z}_{k,m})|.$$

Then our numerical approximation errors are presented in the following table with various  $a$ ,  $b$ , and  $N$ :

Figure 4.7: Choose collocation points in  $\bar{\Omega} = \Omega \cup \partial\Omega$  and  $N = 20$  source points on the  $\partial\tilde{\Omega} = \{(x, y) : x = 4 \cos^3(t), y = 4 \sin^3(t), 0 \leq t < 2\pi\}$

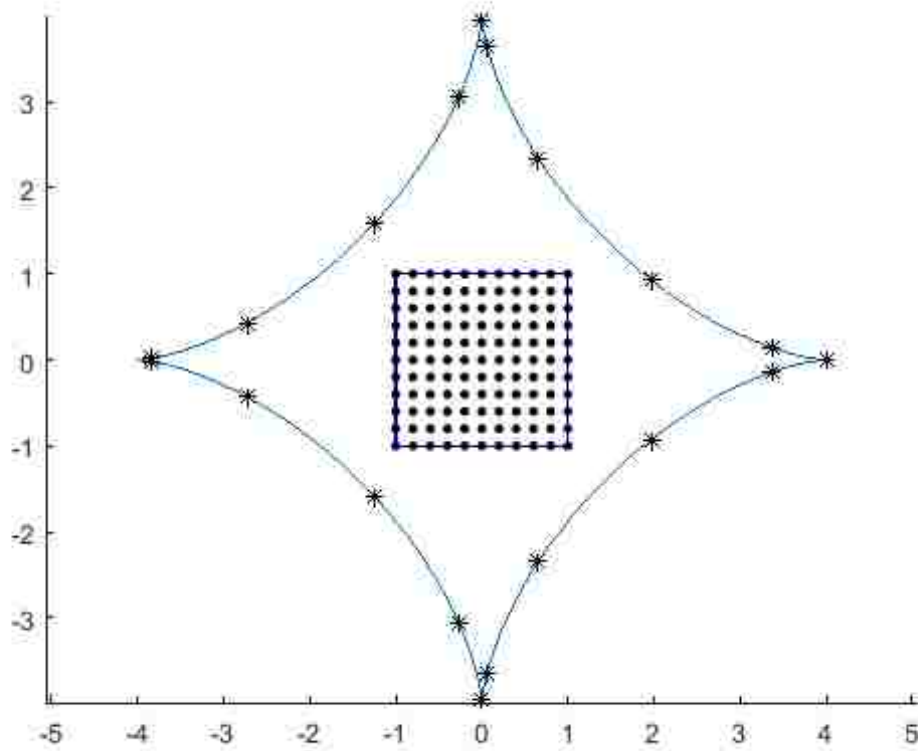
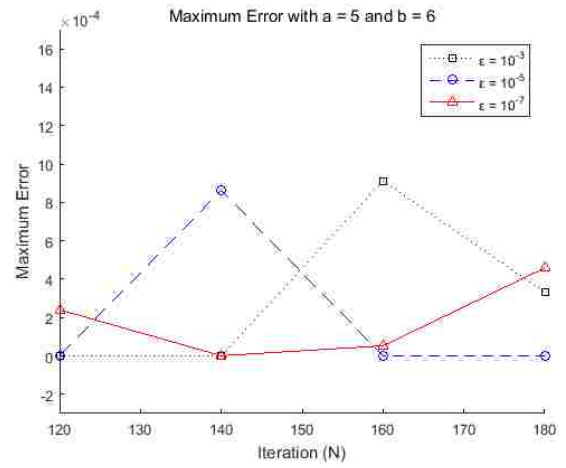
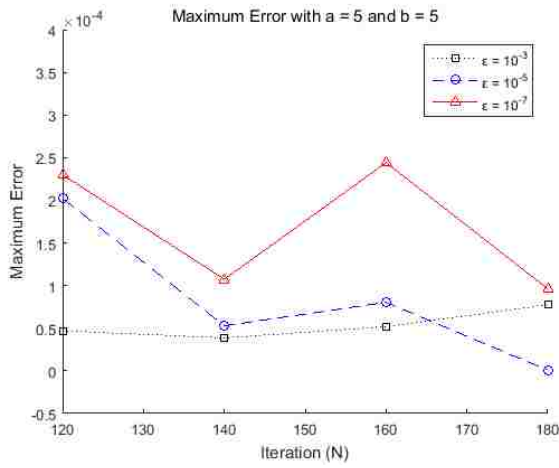
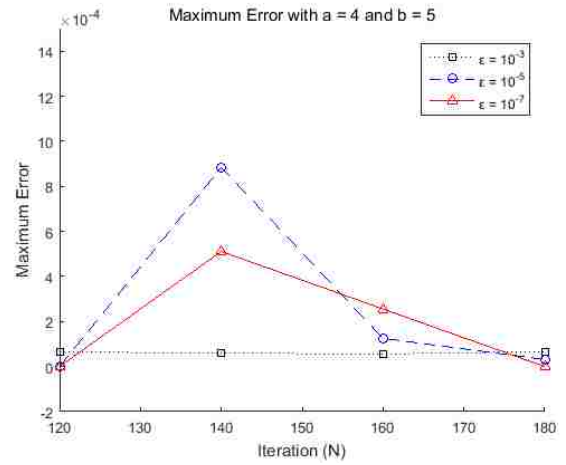
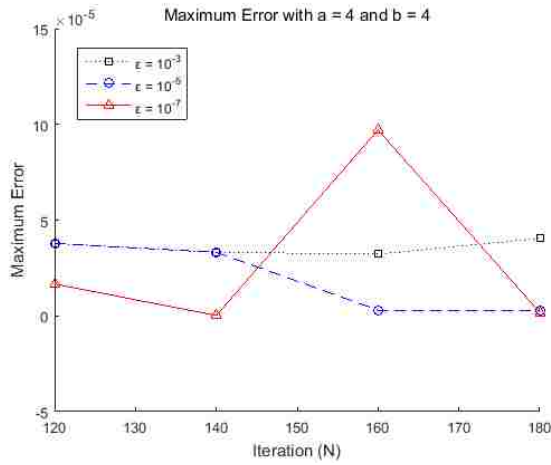


Table 4.4: Maximum Error  $\|u_{exact} - u_A\|_{C(\bar{\Omega})}$  with the Gaussian RBF  $\phi(r) = e^{-2r^2}$

	N = 120	N = 140	N = 160	N = 180
a = 4, b = 4 $\epsilon = 10^{-3}$	3.7851e-05 (k = 17)	3.3175e-05 (k = 17)	3.2297e-05 (k = 17)	4.0468e-05 (k = 17)
a = 4, b = 4 $\epsilon = 10^{-5}$	3.7851e-05 (k = 17)	3.3175e-05 (k = 17)	3.0143e-06 (k = 18)	2.7825e-06 (k = 18)
a = 4, b = 4 $\epsilon = 10^{-7}$	1.6667e-05 (k = 19)	1.8069e-07 (k = 19)	9.7123e-05 (k = 19)	1.8055e-06 (k = 19)
a = 4, b = 5 $\epsilon = 10^{-3}$	6.5255e-05 (k = 17)	5.9290e-05 (k = 17)	5.5789e-05 (k = 17)	6.6515e-05 (k = 17)
a = 4, b = 5 $\epsilon = 10^{-5}$	3.1297e-07 (k = 19)	8.8396e-04 (k = 19)	1.2537e-04 (k = 19)	3.1376e-05 (k = 19)
a = 4, b = 5 $\epsilon = 10^{-7}$	5.3866e-07 (k = 20)	5.1116e-04 (k = 20)	2.5542e-04 (k = 20)	2.8819e-07 (k = 20)
a = 5, b = 5 $\epsilon = 10^{-3}$	4.6969e-05 (k = 17)	3.8649e-05 (k = 17)	5.1966e-05 (k = 17)	7.7667e-05 (k = 17)
a = 5, b = 5 $\epsilon = 10^{-5}$	2.0206e-04 (k = 19)	5.2882e-05 (k = 19)	8.0295e-05 (k = 19)	9.1467e-07 (k = 19)
a = 5, b = 5 $\epsilon = 10^{-7}$	2.3002e-04 (k = 20)	1.0738e-04 (k = 20)	2.4418e-04 (k = 20)	9.6331e-05 (k = 20)
a = 5, b = 6 $\epsilon = 10^{-3}$	1.1638e-06 (k = 18)	7.1239e-07 (k = 18)	9.1190e-04 (k = 18)	3.3249e-04 (k = 18)
a = 5, b = 6 $\epsilon = 10^{-5}$	2.1900e-06 (k = 19)	8.6323e-04 (k = 19)	6.1059e-07 (k = 19)	1.1316e-06 (k = 19)
a = 5, b = 6 $\epsilon = 10^{-7}$	2.4044e-04 (k = 21)	1.2093e-06 (k = 21)	5.2768e-05 (k = 21)	4.5847e-04 (k = 21)

Figure 4.8: Maximum errors in a domain  $\bar{\Omega}$  with singular value tolerances,  $\epsilon = 10^{-3}$  ( $\square$ ),  $\epsilon = 10^{-5}$  ( $\circ$ ),  $\epsilon = 10^{-7}$  ( $\triangle$ ), respectively



**Example 4.5.** Consider the boundary problem for the biharmonic equation

$$\Delta^2 u(x, y) = (8x - 12y) \cos(x + y) - 8 \sin(x + y), \quad (x, y) \in \Omega,$$

$$u(x, y) = (2x - 3y) \cos(x + y),$$

and

$$\Delta u(x, y) = 2 \sin(x + y) - (4x - 6y) \cos(x + y), \quad (x, y) \in \partial\Omega,$$

where  $\Omega = \{(x, y) : -1 \leq x \leq 0, -1 \leq y \leq 1, \text{ or } 0 \leq x \leq 1, -1 \leq y \leq 0\}$  is the L-shaped domain. The exact solution of the above problem is  $u_{exact} = (2x - 3y) \cos(x + y)$ . Choose a Gaussian RBF  $\phi(r) = e^{-3r^2}$  where  $r = \|x\|$ . We use a fictitious domain  $\tilde{\Omega} = \{(x, y) : x = a \cos t, y = b \sin(t + \cos t), 0 \leq t \leq 2\pi\}$ , where  $a = 3, 4$  and  $b = 3, 4$ , respectively. We choose  $\tilde{\mathbf{x}}_k = (a \cos \frac{2\pi k}{N}, b \sin(\frac{2\pi k}{N} + \cos \frac{2\pi k}{N}))$ ,  $0 \leq k \leq N-1$ , on  $\partial\tilde{\Omega}$ . The large number of collocation points on  $\partial\Omega$  and source points on  $\partial\tilde{\Omega}$  cause the ill-condition system (4.7). In order to resolve the unstable results, we use the Tikhonov regularization with regularization parameters,  $\mu = \{10^{-1}, 10^{-3}, 10^{-5}\}$ , respectively, to obtain the approximate solution through (4.4)-(4.7). To estimate the maximum error, we use points  $\mathbf{z}_{k,m} = (\frac{k}{M}, \frac{m}{M})$ ,  $-2M \leq k \leq -M$  and  $-M \leq m \leq M$  or  $-M \leq k \leq 0$  and  $-M \leq m \leq 0$  with  $M = 100$  in  $\bar{\Omega} = \Omega \cup \partial\Omega$  to get the numerical infinity norm in Example 4.1. Then our numerical approximation errors are presented in the following table with various  $a$ ,  $b$ , and  $N$ :

Figure 4.9: Choose collocation points on the  $\bar{\Omega} = \Omega \cup \partial\Omega$  and  $N = 20$  source points on the  $\partial\tilde{\Omega} = \{(x, y) : x = a \sin t, y = b \cos(t + \cos t), 0 \leq t < 2\pi\}$

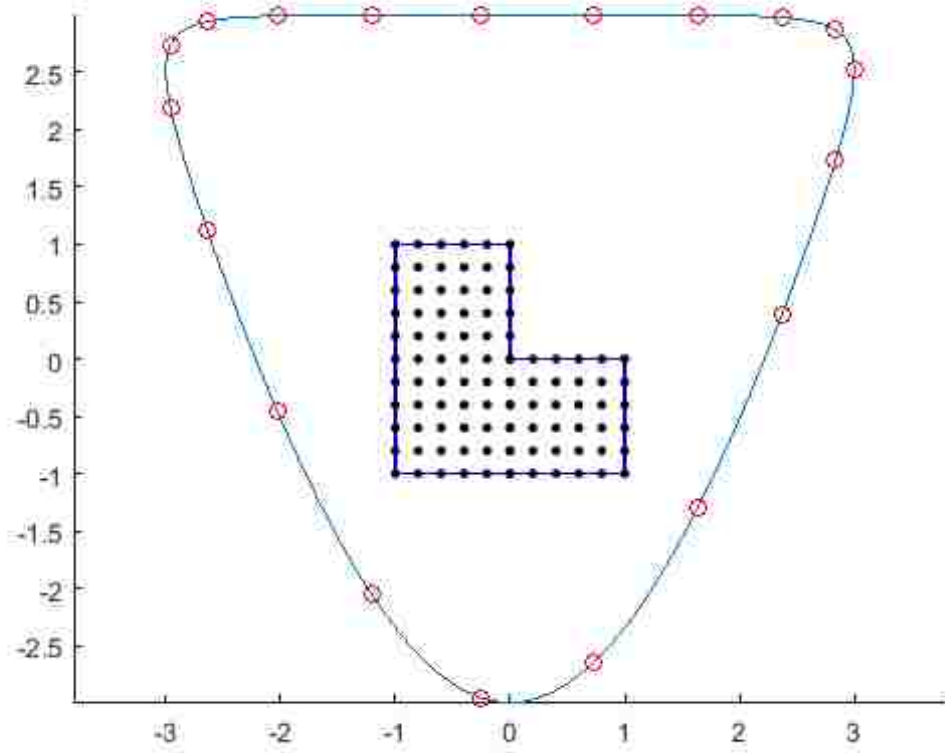
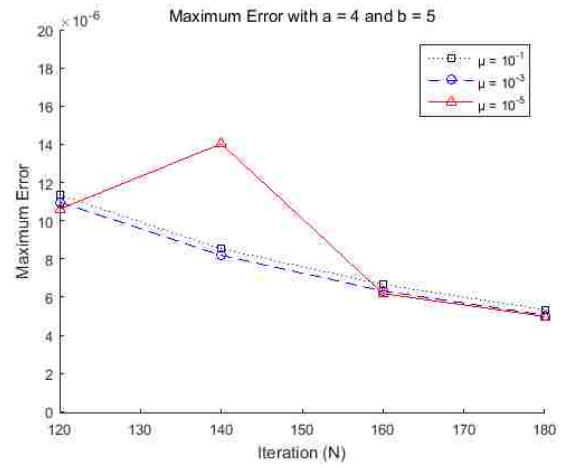
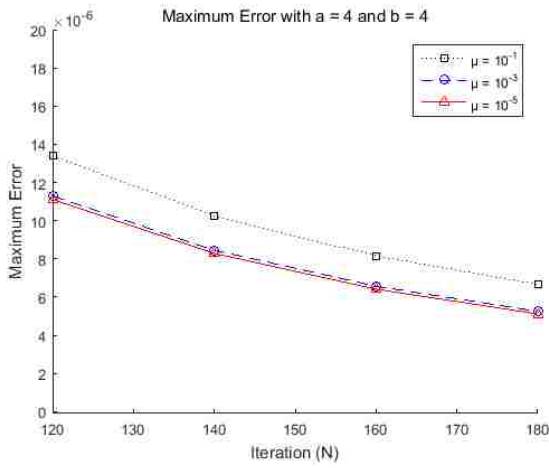
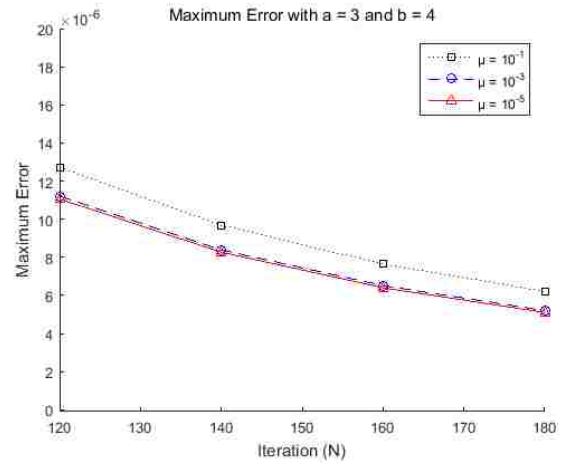
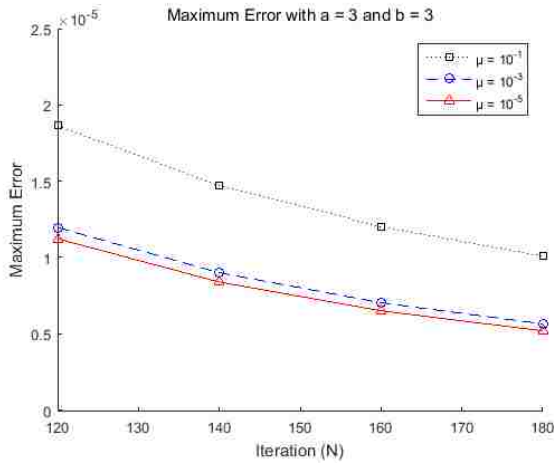


Table 4.5: Maximum Error  $\|u_{exact} - u_N\|_{C(\bar{\Omega})}$  with the Gaussian RBF  $\phi(r) = e^{-3r^2}$

	N = 120	N = 140	N = 160	N = 180
a = 3, b = 3, $\mu = 10^{-1}$	1.8636e-05	1.4715e-05	1.2024e-05	1.0085e-05
a = 3, b = 3, $\mu = 10^{-3}$	1.1963e-05	9.0015e-06	7.0304e-06	5.6517e-06
a = 3, b = 3, $\mu = 10^{-5}$	1.1228e-05	8.3920e-06	6.5086e-06	5.1946e-06
a = 3, b = 4, $\mu = 10^{-1}$	1.2719e-05	9.6801e-06	7.6437e-06	6.2096e-06
a = 3, b = 4, $\mu = 10^{-3}$	1.1208e-05	8.3868e-06	6.5124e-06	5.2044e-06
a = 3, b = 4, $\mu = 10^{-5}$	1.1059e-05	8.2653e-06	6.4006e-06	5.1039e-06
a = 4, b = 4, $\mu = 10^{-1}$	1.3396e-05	1.0261e-05	8.1525e-06	6.6624e-06
a = 4, b = 4, $\mu = 10^{-3}$	1.1283e-05	8.4488e-06	6.5661e-06	5.2524e-06
a = 4, b = 4, $\mu = 10^{-5}$	1.1107e-05	8.2831e-06	6.4119e-06	5.1141e-06
a = 4, b = 5, $\mu = 10^{-1}$	1.1339e-05	8.5269e-06	6.6504e-06	5.3387e-06
a = 4, b = 5, $\mu = 10^{-3}$	1.0975e-05	8.1814e-06	6.3170e-06	5.0529e-06
a = 4, b = 5, $\mu = 10^{-5}$	1.0605e-05	1.4025e-05	6.1833e-06	4.9843e-06



Figure 4.10: Maximum errors in a domain  $\bar{\Omega}$  with regularization parameters,  $\mu = 10^{-1}$  ( $\square$ ),  $\mu = 10^{-3}$  ( $\circ$ ),  $\mu = 10^{-5}$  ( $\triangle$ ), respectively



**Example 4.6.** Consider the boundary problem for the biharmonic equation

$$\Delta^2 u(x, y, z) = 4e^{2x} \sin(y + z), \quad (x, y, z) \in \Omega,$$

$$u(x, y, z) = e^{2x} \sin(y + z),$$

and

$$\Delta u(x, y, z) = 2e^{2x} \sin(y + z), \quad (x, y, z) \in \partial\Omega,$$

where  $\Omega = \{(x, y, z) : -1 \leq x, y, z \leq 1\}$  is the cube. The exact solution of the above problem is  $u_{exact} = e^{2x} \sin(y + z)$ . Choose a Gaussian RBF  $\phi(r) = e^{-3r^2}$  where  $r = \|x\|$ . We use an ellipsoid fictitious domain  $\tilde{\Omega} = \{(x, y, z) : \frac{x^2}{a^2} + \frac{y^2}{b^2} + \frac{z^2}{c^2} \leq 1\}$ , where  $a = 4, 5, 6, 7$ ,  $b = 3, 4, 5, 6$ , and  $c = 3, 4, 5, 6$ . We choose  $\tilde{\mathbf{x}}_{\mathbf{k}, \mathbf{m}} = (a \sin \theta_k \cos \phi_{k,m}, b \sin \theta_k \sin \phi_{k,m}, c \cos \phi_{k,m})$ , where  $a = 4, 5, 6, 7$ ,  $b = 3, 4, 5, 6$ , and  $c = 3, 4, 5, 6$  and  $\theta_k = \frac{\pi(k+0.5)}{M_\theta}$ ,  $0 \leq k \leq M_\theta - 1$ , with  $M_\theta = \frac{\sqrt{\pi N}}{2r}$ , and  $\phi_{k,m} = \frac{2\pi m}{M_k}$ ,  $0 \leq m \leq M_k - 1$ , with  $M_k = \sqrt{\pi N \sin \theta_k}$ , on  $\partial\tilde{\Omega}$ , (see Figure 4.11). We use the Tikhonov regularization with regularization parameters,  $\mu = \{10^{-1}, 10^{-3}, 10^{-5}\}$ , respectively, to obtain the approximate solution through (4.4)-(4.7). To estimate the maximum error, we use points  $\mathbf{z}_{k,l,m} = (\frac{k}{M}, \frac{l}{M}, \frac{m}{M})$ ,  $-M \leq k, l, m \leq M$ , with  $M = 10$  in  $\bar{\Omega} = \Omega \cup \partial\Omega$ , to get the numerical infinity norm in Example 4.1. Then our numerical approximation errors are presented in the following table with various  $a, b, c$ , and  $N$ :

Figure 4.11: Choose collocation points on  $\bar{\Omega} = \Omega \cup \partial\Omega$  and  $N = 100$  source points on the ellipsoid fictitious domain  $\partial\tilde{\Omega}$  with  $a = 5$ ,  $b = 3$ , and  $c = 3$

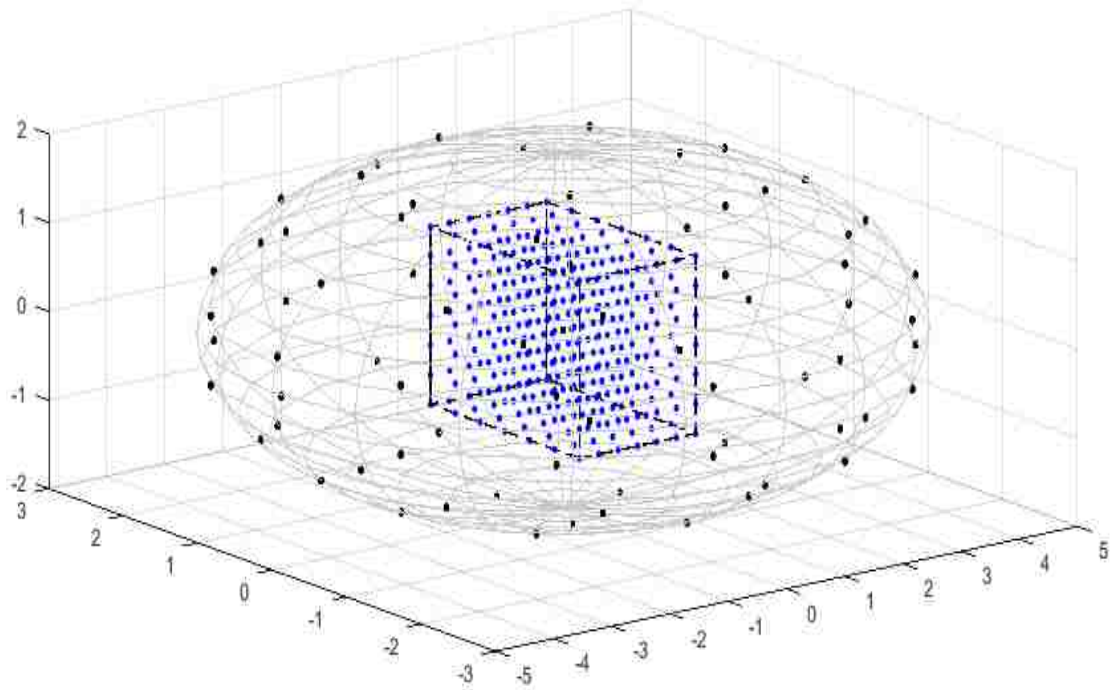
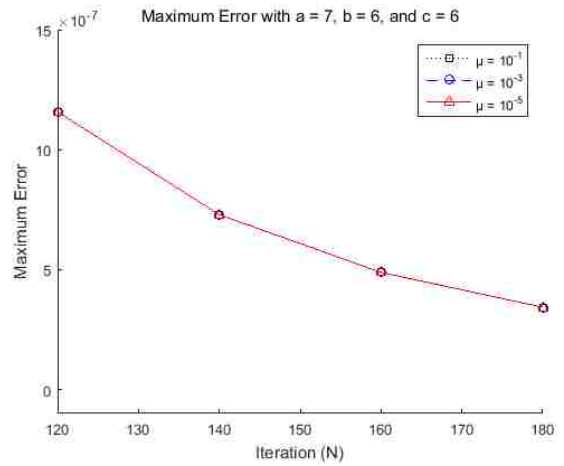
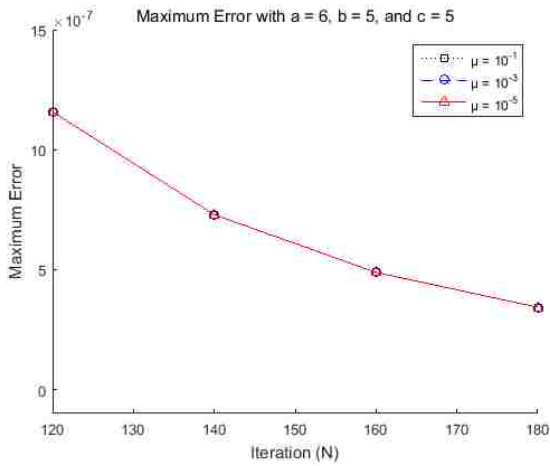
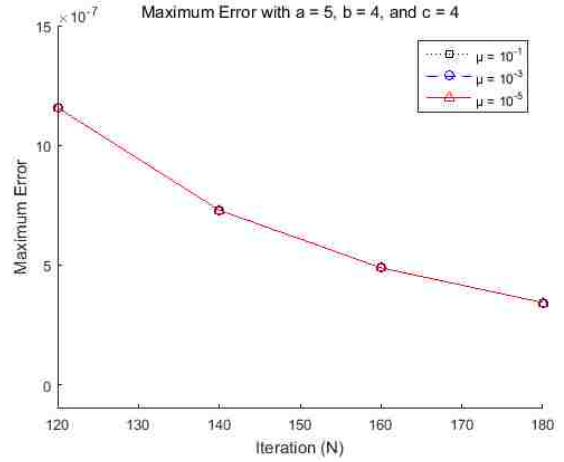
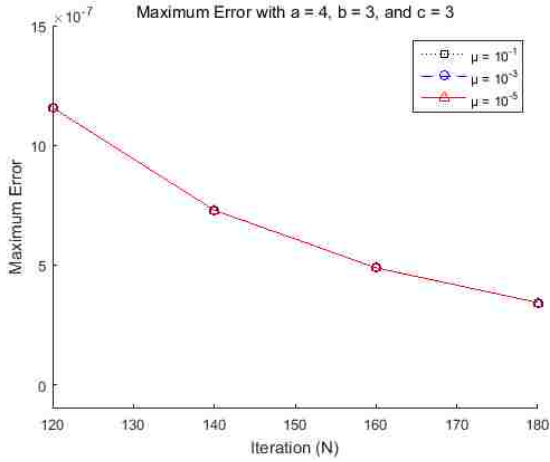


Table 4.6: Maximum Error  $\|u_{exact} - u_N\|_{C(\bar{\Omega})}$  with the Gaussian RBF  $\phi(r) = e^{-3r^2}$

	N = 120	N = 140	N = 160	N = 180
a = 4, b = 3, c = 3, $\mu = 10^{-1}$	1.1574e-06	7.2886e-07	4.8828e-07	3.4294e-07
a = 4, b = 3, c = 3, $\mu = 10^{-3}$	1.1574e-06	7.2886e-07	4.8828e-07	3.4294e-07
a = 4, b = 3, c = 3, $\mu = 10^{-5}$	1.1574e-06	7.2886e-07	4.8828e-07	3.4294e-07
a = 5, b = 4, c = 4, $\mu = 10^{-1}$	1.1574e-06	7.2886e-07	4.8828e-07	3.4294e-07
a = 5, b = 4, c = 4, $\mu = 10^{-3}$	1.1574e-06	7.2886e-07	4.8828e-07	3.4294e-07
a = 5, b = 4, c = 4, $\mu = 10^{-5}$	1.1574e-06	7.2886e-07	4.8828e-07	3.4294e-07
a = 6, b = 5, c = 5, $\mu = 10^{-1}$	1.1574e-06	7.2886e-07	4.8828e-07	3.4294e-07
a = 6, b = 5, c = 5, $\mu = 10^{-3}$	1.1574e-06	7.2886e-07	4.8828e-07	3.4294e-07
a = 6, b = 5, c = 5, $\mu = 10^{-5}$	1.1574e-06	7.2886e-07	4.8828e-07	3.4294e-07
a = 7, b = 6, c = 6, $\mu = 10^{-1}$	1.1574e-06	7.2886e-07	4.8828e-07	3.4294e-07
a = 7, b = 6, c = 6, $\mu = 10^{-3}$	1.1574e-06	7.2886e-07	4.8828e-07	3.4294e-07
a = 7, b = 6, c = 6, $\mu = 10^{-5}$	1.1574e-06	7.2886e-07	4.8828e-07	3.4294e-07

Figure 4.12: Maximum errors in domain  $\bar{\Omega}$  with singular value tolerances,  $\epsilon = 10^{-1}$  ( $\square$ ),  $\epsilon = 10^{-3}$  ( $\circ$ ),  $\epsilon = 10^{-5}$  ( $\triangle$ ), respectively



## 4.5 Numerical Examples by Approximate Particular Solutions

In this section, we use the approximate particular solutions described in section 4.3 with MFS to present some numerical examples.

**Example 4.7.** Consider the boundary problem for the biharmonic equation

$$\begin{aligned}\Delta^2 u(x, y) &= 8(2x^4 + 12x^2 + 3)e^{2y}, & (x, y) \in \Omega, \\ u(x, y) &= x^4 e^{2y} \quad \text{and} \quad \Delta u(x, y) = 4x^2(x^2 + 3)e^{2y}, & (x, y) \in \partial\Omega,\end{aligned}$$

where  $\Omega = \{(x, y) : -2 \leq x \leq -1, -1 \leq y \leq 1, \text{ or } -1 \leq x \leq 0, 0 \leq y \leq 1\}$  is the  $\Gamma$ -shaped domain. The exact solution of the above problem is  $u_{exact} = x^4 e^{2y}$ . Choose three different radial basis functions in Example 2.4:

- (a)  $\phi(r^2) = \frac{c}{\pi} e^{-cr^2}$ , where  $r = \|\mathbf{x}\|$  and  $c = 1, 3, 5$ , respectively,
- (b)  $\phi(r^2) = \begin{cases} (c+1)(1-r^2)^c/\pi, & 0 \leq r \leq 1, \\ 0, & r > 1, \end{cases}$  for  $c = 3, 4, 5$ , respectively,
- (c)  $\phi(r^2) = \frac{c-1}{\pi(r^2+1)^c}$ , for  $c = 3, 4, 5$ , respectively,

and we use a fictitious domain  $\tilde{\Omega} = \{(x, y) : x = a \sin(t), y = b \cos(t + \cos(t)), 0 \leq t \leq 2\pi\}$ , where  $a = 3, 3, 4, 4$  and  $b = 3, 4, 4, 5$ , respectively. We choose  $\tilde{\mathbf{x}}_{\mathbf{k}} = (a \sin(\frac{2\pi k}{N}), b \cos(\frac{2\pi k}{N} + \cos(\frac{2\pi k}{N})))$ ,  $0 \leq k \leq N-1$ , on  $\partial\tilde{\Omega}$ . To estimate the maximum error, we use points  $\mathbf{z}_{k,m} = (\frac{k}{M}, \frac{m}{M})$ ,  $-2M \leq k \leq -M$  and  $-M \leq m \leq M$  or  $-M \leq k \leq 0$  and  $0 \leq m \leq M$  with  $M = 100$  in  $\bar{\Omega} = \Omega \cup \partial\Omega$  to get the numerical estimate (see Figure 4.13) for

$$\max_{k,m} |u_{exact}(\mathbf{z}_{k,m}) - u_A(\mathbf{z}_{k,m})|.$$

Then our numerical approximation errors are presented in the following table with various  $a$ ,  $b$ , and  $N$ :

Figure 4.13: Choose collocation points in  $\bar{\Omega} = \Omega \cup \partial\Omega$  and  $N = 20$  source points on the  $\partial\Omega = \{(x, y) : x = 3 \sin(t), y = 3 \cos(t + \cos(t)), 0 \leq t \leq 2\pi\}$

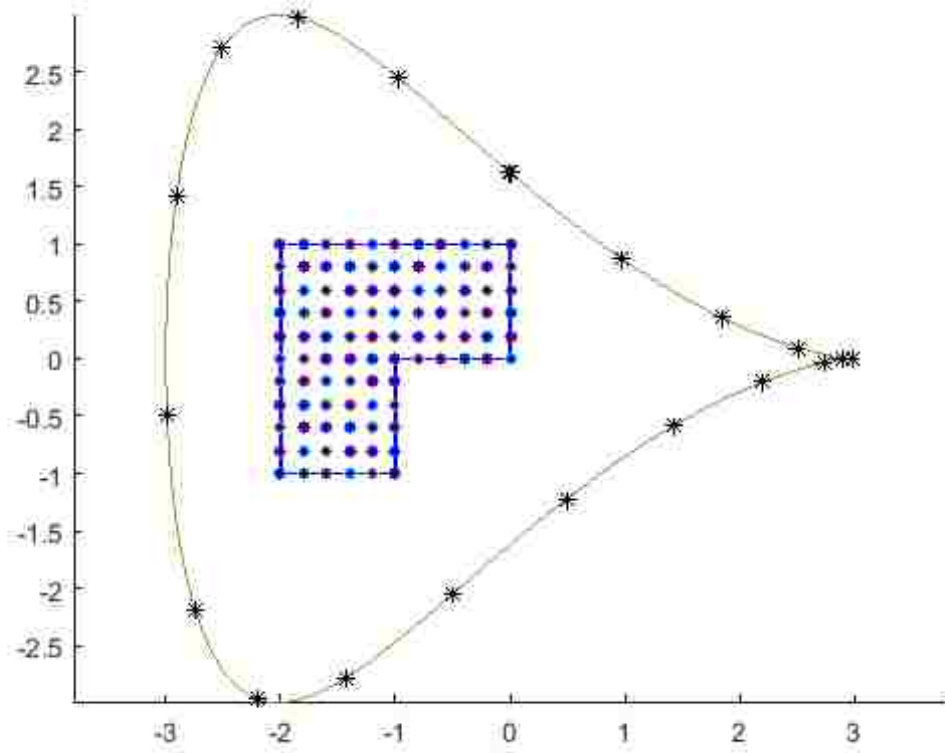


Table 4.7: Maximum Error  $\|u_{exact} - u_A\|_{C(\bar{\Omega})}$  with (a) the Gaussian RBFs  $\phi(r^2) = \frac{c}{\pi} e^{-cr^2}$

	N = 20	N = 30	N = 40	N = 50
a = 3, b = 3, c = 1	0.0019	0.0024	0.0050	0.0027
a = 3, b = 3, c = 3	0.0029	0.0028	0.0032	0.0030
a = 3, b = 3, c = 5	0.0029	0.0033	0.0027	0.0030
a = 3, b = 4, c = 1	0.0026	0.0019	0.0026	0.0195
a = 3, b = 4, c = 3	0.0023	0.0030	0.0041	0.0038
a = 3, b = 4, c = 5	0.0037	0.0026	0.0041	0.0433
a = 4, b = 4, c = 1	0.0025	0.0030	0.0029	0.0033
a = 4, b = 4, c = 3	0.0037	0.0733	0.0039	0.0100
a = 4, b = 4, c = 5	0.0240	0.0035	0.0045	0.0079
a = 4, b = 5, c = 1	0.0028	0.0028	0.0038	0.0042
a = 4, b = 5, c = 3	0.0033	0.0039	0.0034	0.0042
a = 4, b = 5, c = 5	0.0039	0.0030	0.0064	0.0035



Figure 4.14: Maximum errors with  $c = 1$  ( $\square$ ),  $c = 3$  ( $\circ$ ),  $c = 5$  ( $\triangle$ ), respectively

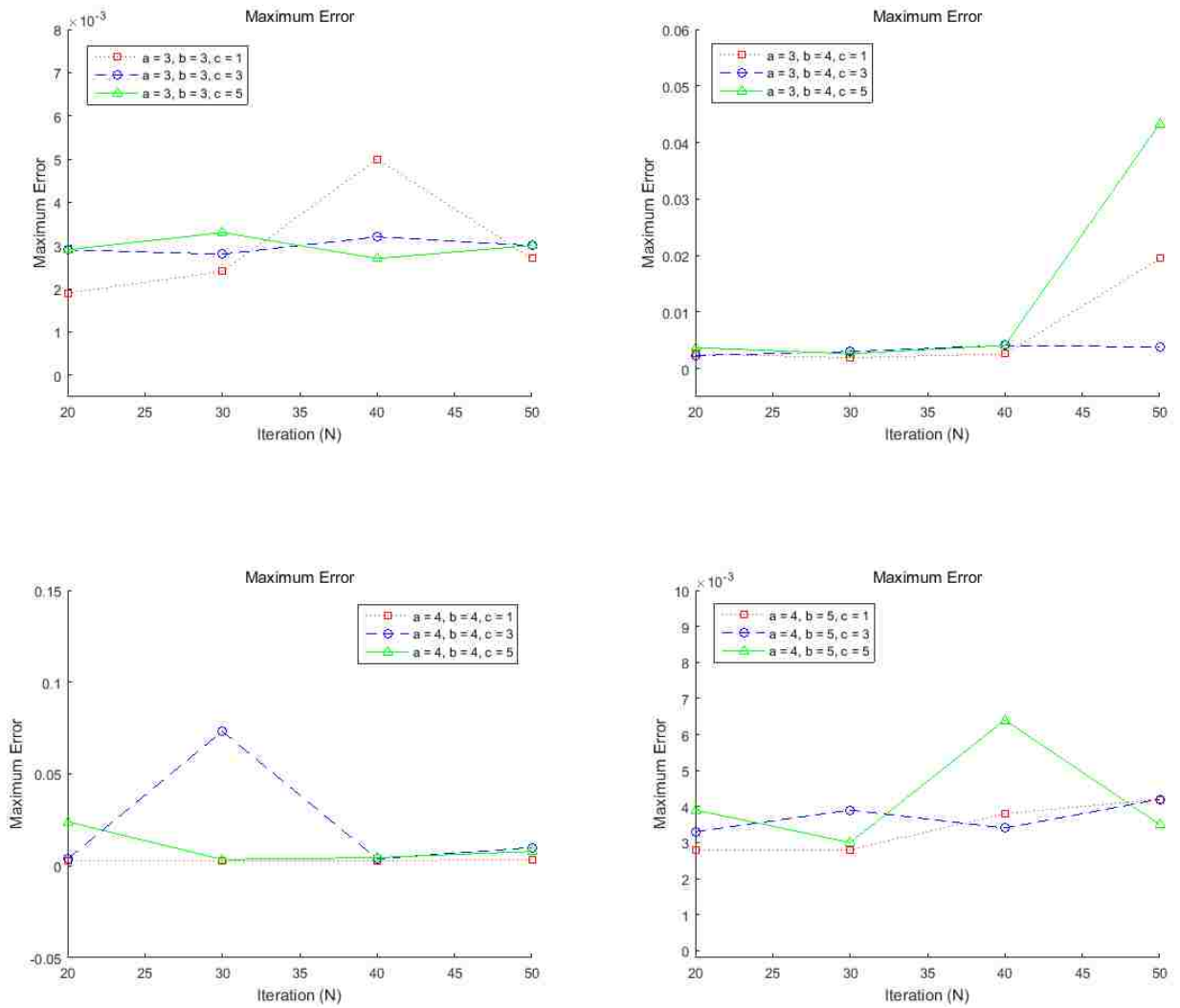


Table 4.8: Maximum Error  $\|u_{exact} - u_A\|_{C(\bar{\Omega})}$  with (b) the compactly supported RBFs  $\phi(r^2) = (c+1)(1-r^2)^c/\pi$ ,  $0 \leq r \leq 1$ , for  $c = 3, 4, 5$ .

	N = 20	N = 30	N = 40	N = 50
a = 3, b = 3, c = 3	6.9003e-08	4.2691e-07	4.7258e-07	4.2758e-07
a = 3, b = 3, c = 4	6.9003e-08	7.6326e-07	4.7258e-07	2.9567e-07
a = 3, b = 3, c = 5	8.7394e-07	3.2889e-07	1.1157e-06	5.1466e-07
a = 3, b = 4, c = 3	3.3888e-08	4.2691e-07	3.1600e-07	4.2758e-07
a = 3, b = 4, c = 4	3.3888e-08	7.6326e-07	8.1711e-08	2.9567e-07
a = 3, b = 4, c = 5	8.7394e-07	3.2889e-07	1.1157e-06	5.1466e-07
a = 4, b = 4, c = 3	3.3054e-08	4.2691e-07	3.1600e-07	4.2758e-07
a = 4, b = 4, c = 4	3.3054e-08	7.6326e-07	8.1711e-08	2.9567e-07
a = 4, b = 4, c = 5	8.7394e-07	3.2889e-07	1.1157e-06	5.1466e-07
a = 4, b = 5, c = 3	2.7810e-07	4.2691e-07	3.7688e-07	4.2758e-07
a = 4, b = 5, c = 4	2.7810e-07	7.6326e-07	3.7688e-07	2.9567e-07
a = 4, b = 5, c = 5	8.7394e-07	3.2889e-07	1.1157e-06	5.1466e-07

Figure 4.15: Maximum errors with  $c = 3$  ( $\square$ ),  $c = 4$  ( $\circ$ ),  $c = 5$  ( $\triangle$ ), respectively

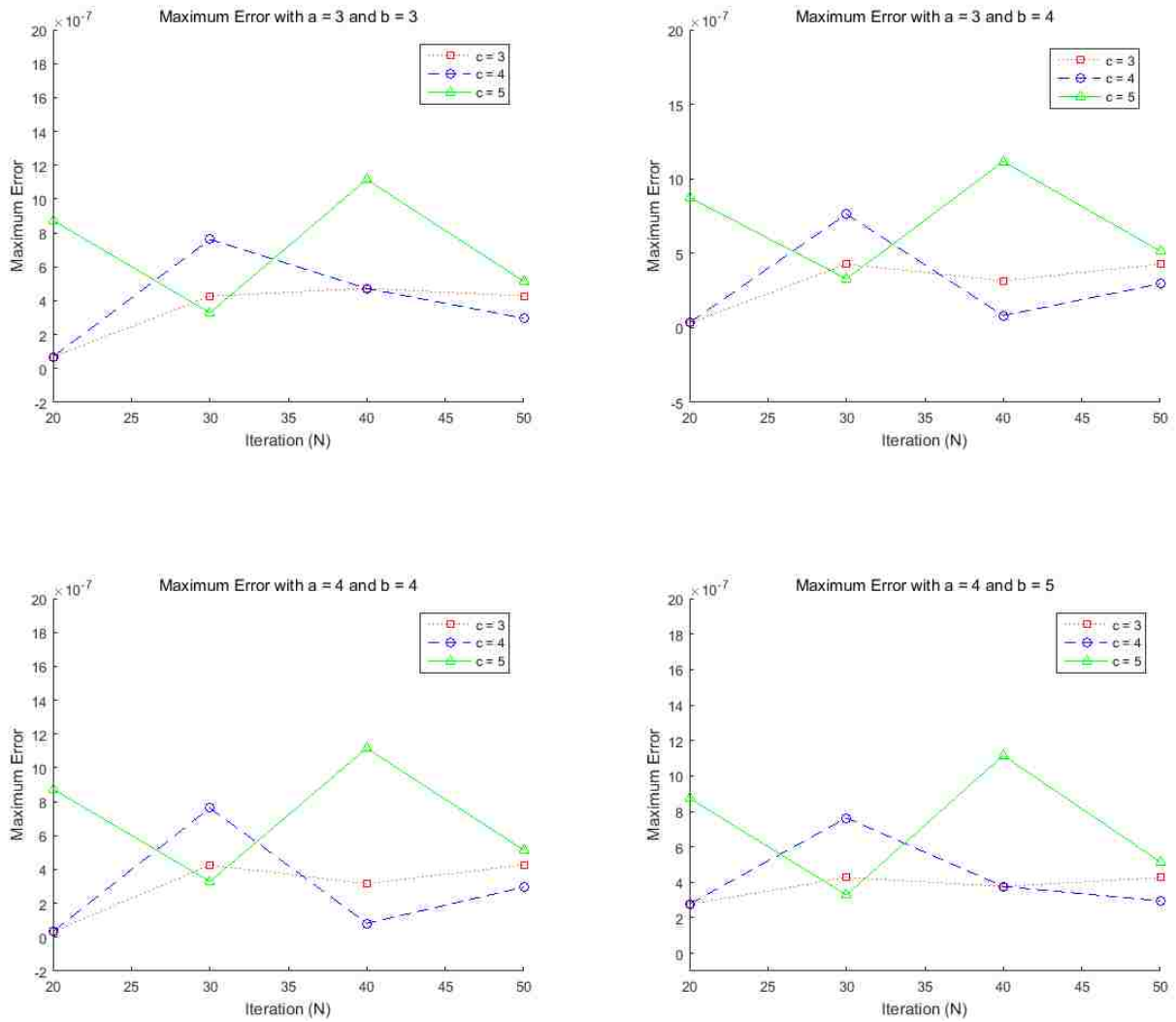
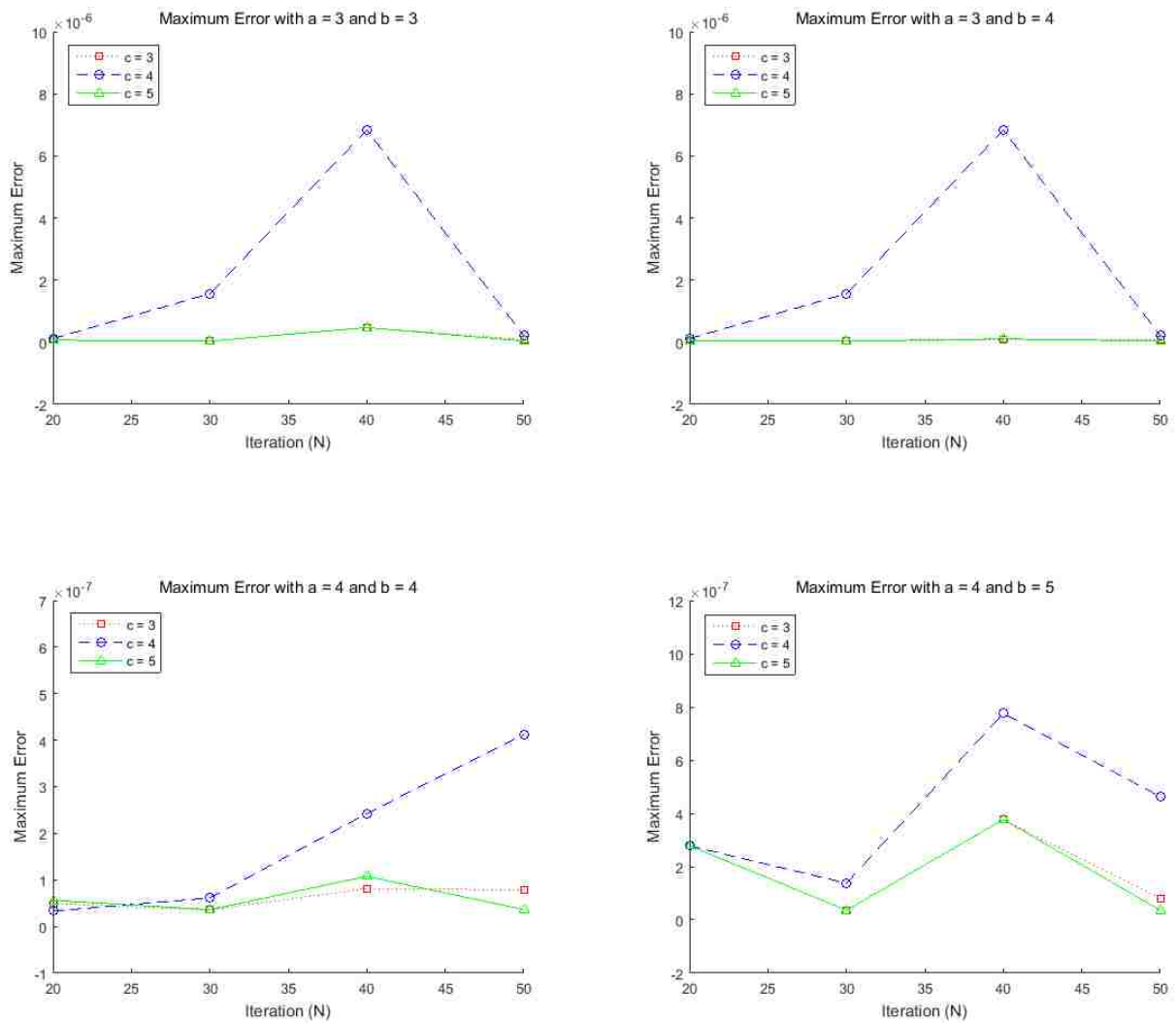


Table 4.9: Maximum Error  $\|u_{exact} - u_A\|_{C(\bar{\Omega})}$  with (c) the inverse multiquadratics RBFs  $\phi(r^2) = \frac{c-1}{\pi(r^2+1)^c}$ , for  $c = 3, 4, 5$ .

	N = 20	N = 30	N = 40	N = 50
a = 3, b = 3, c = 3	6.9003e-08	3.5952e-08	4.7258e-07	7.8516e-08
a = 3, b = 3, c = 4	1.1781e-07	1.5602e-06	6.8331e-06	2.0803e-07
a = 3, b = 3, c = 5	6.9003e-08	3.6095e-08	4.7258e-07	3.6344e-08
a = 3, b = 4, c = 3	4.8865e-08	3.5952e-08	8.1429e-08	7.8516e-08
a = 3, b = 4, c = 4	1.1781e-07	1.5602e-06	6.8331e-06	2.0803e-07
a = 3, b = 4, c = 5	5.6210e-08	3.6095e-08	1.0767e-07	3.6344e-08
a = 4, b = 4, c = 3	4.8865e-08	3.5952e-08	8.1429e-08	7.8516e-08
a = 4, b = 4, c = 4	3.3054e-08	6.1230e-08	2.4256e-07	4.1191e-07
a = 4, b = 4, c = 5	5.6210e-08	3.6095e-08	1.0767e-07	3.6344e-08
a = 4, b = 5, c = 3	2.7810e-07	3.5952e-08	3.7688e-07	7.8516e-08
a = 4, b = 5, c = 4	2.7810e-07	1.3770e-07	7.7597e-07	4.6340e-07
a = 4, b = 5, c = 5	2.7810e-07	3.6095e-08	3.7688e-07	3.6344e-08

Figure 4.16: Maximum errors with  $c = 3$  ( $\square$ ),  $c = 4$  ( $\circ$ ),  $c = 5$  ( $\triangle$ ), respectively



**Example 4.8.** Consider the boundary problem for the biharmonic equation

$$\Delta^2 u(x, y) = 25 e^{2x} \sin(3y), \quad (x, y) \in \Omega,$$

$$u(x, y) = e^{2x} \sin(3y) \quad \text{and} \quad \Delta u(x, y) = -5 e^{2x} \sin(3y), \quad (x, y) \in \partial\Omega,$$

where  $\Omega = \{(x, y) : -1 \leq x \leq 1, \text{ or } -1 \leq y \leq 1\}$  is the square. The exact solution of the above problem is  $u_{exact} = e^{2x} \sin(3y)$ . Choose three different radial basis functions in Example 4.7 and use an amoeba-like fictitious domain  $\tilde{\Omega} = \{(x, y) : x = r(t) \cos(t), y = r(t) \sin(t)\}$ , where  $r(t) = R e^{\sin(t)} \sin^2(2t) + R e^{\cos(t)} \cos^2(2t)$ ,  $0 \leq t < 2\pi$ ,  $R = 3, 5$ , respectively. We choose  $\tilde{\mathbf{x}}_{\mathbf{k}} = ((R e^{\sin(\frac{2\pi k}{N})} \sin^2(2\frac{2\pi k}{N}) + R e^{\cos(\frac{2\pi k}{N})} \cos^2(2\frac{2\pi k}{N})) \cos(\frac{2\pi k}{N}), (R e^{\sin(\frac{2\pi k}{N})} \sin^2(2\frac{2\pi k}{N}) + R e^{\cos(\frac{2\pi k}{N})} \cos^2(2\frac{2\pi k}{N})) \sin(\frac{2\pi k}{N}))$ ,  $0 \leq t < 2\pi$ ,  $0 \leq k \leq N - 1$  on  $\partial\tilde{\Omega}$ . To estimate the maximum error, we use points  $\mathbf{z}_{k,m} = (\frac{k}{M}, \frac{m}{M})$ ,  $0 \leq k \leq M$  and  $0 \leq m \leq M$  with  $M = 100$  in  $\bar{\Omega} = \Omega \cup \partial\Omega$  to get the numerical infinity norm in Example 4.7. Then our numerical approximation errors are presented in the following table with various R, c, and N:

Figure 4.17: Choose collocation points on the  $\bar{\Omega} = \Omega \cup \partial\Omega$  and  $N = 20$  source points on the amoeba-like fictitious domain  $\partial\tilde{\Omega}$

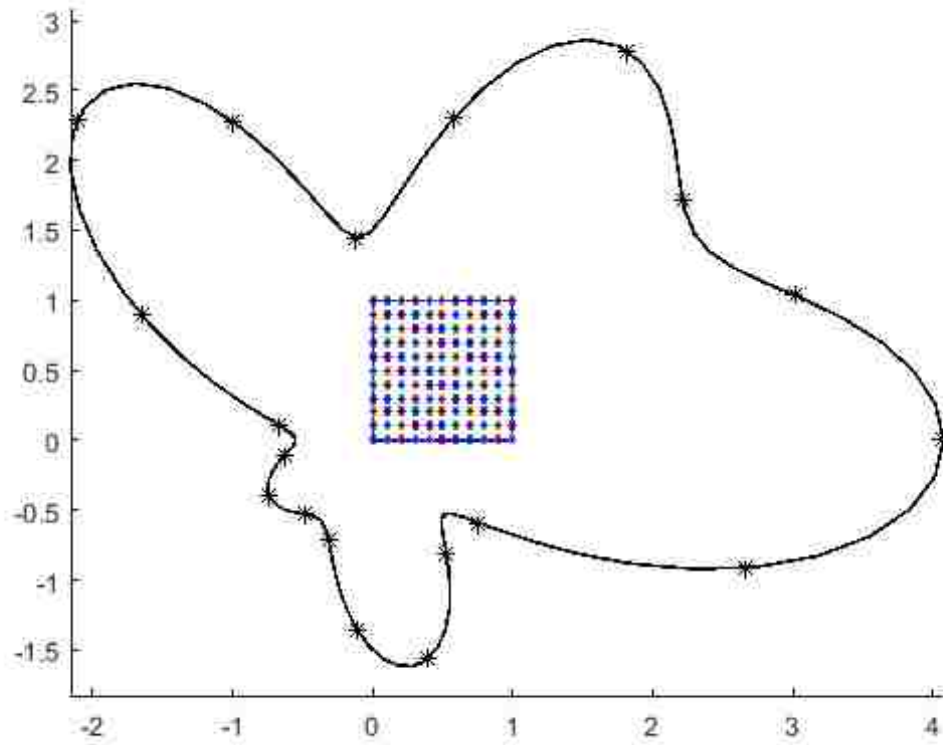


Table 4.10: Maximum Error  $\|u_{exact} - u_A\|_{C(\bar{\Omega})}$  with (a) the Gaussian RBFs  $\phi(r^2) = \frac{c}{\pi} e^{-cr^2}$

	N = 20	N = 30	N = 40	N = 50
R = 3, c = 1	3.5172e-07	1.6777e-06	8.8683e-06	8.3699e-07
R = 3, c = 3	2.3647e-05	1.6777e-06	8.8683e-06	1.9180e-05
R = 3, c = 5	3.5172e-07	1.1419e-04	8.8683e-06	4.9673e-06
R = 5, c = 1	2.4589e-04	2.6321e-05	1.4816e-05	1.1964e-05
R = 5, c = 3	2.4589e-04	2.6321e-05	1.4816e-05	1.9180e-05
R = 5, c = 5	2.4589e-04	1.1419e-04	1.4816e-05	1.1964e-05

Figure 4.18: Maximum errors with  $c = 1$  ( $\square$ ),  $c = 3$  ( $\circ$ ),  $c = 5$  ( $\triangle$ ), respectively

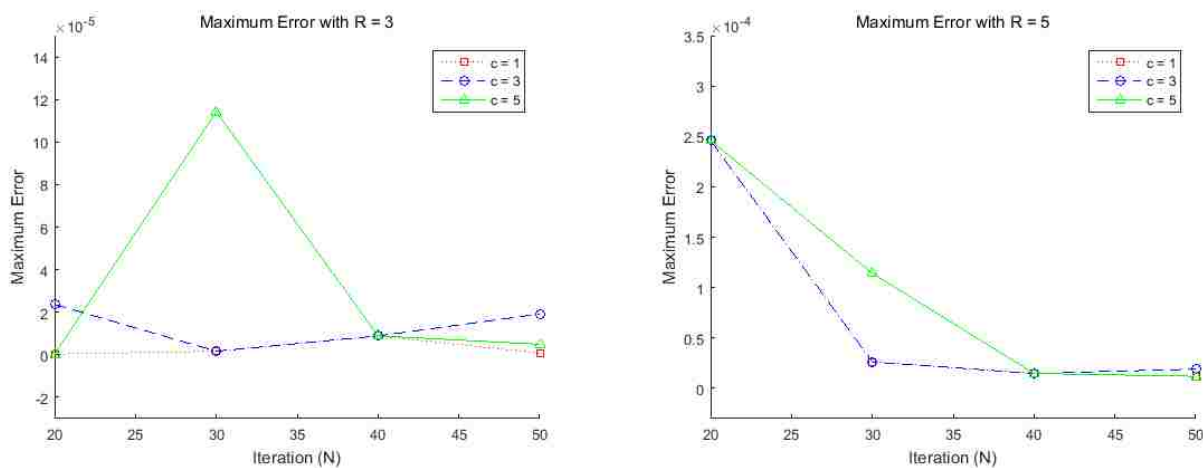




Table 4.11: Maximum Error  $\|u_{exact} - u_A\|_{C(\bar{\Omega})}$  with (b) the compactly supported RBFs  $\phi(r^2) = (c + 1)(1 - r^2)^c/\pi, 0 \leq r \leq 1$ , for  $c = 3, 4, 5$ .

	N = 20	N = 30	N = 40	N = 50
R = 3, c = 3	1.1219e-05	1.1142e-05	1.1797e-05	2.1115e-04
R = 3, c = 4	1.8310e-06	1.6644e-05	1.3619e-05	2.0901e-05
R = 3, c = 5	5.8106e-05	1.3606e-05	5.1823e-05	7.0469e-05
R = 5, c = 3	1.1219e-05	1.1142e-05	1.1797e-05	2.1115e-04
R = 5, c = 4	1.8310e-06	1.6644e-05	1.3619e-05	2.0901e-05
R = 5, c = 5	5.8106e-05	1.3606e-05	5.1823e-05	7.0469e-05

Figure 4.19: Maximum errors with  $c = 3$  ( $\square$ ),  $c = 4$  ( $\circ$ ),  $c = 5$  ( $\triangle$ ), respectively

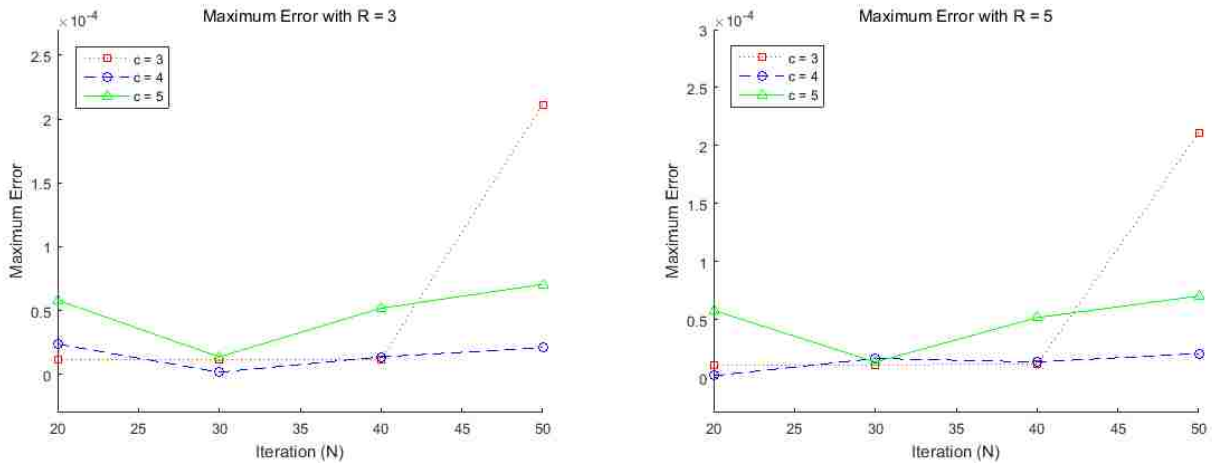
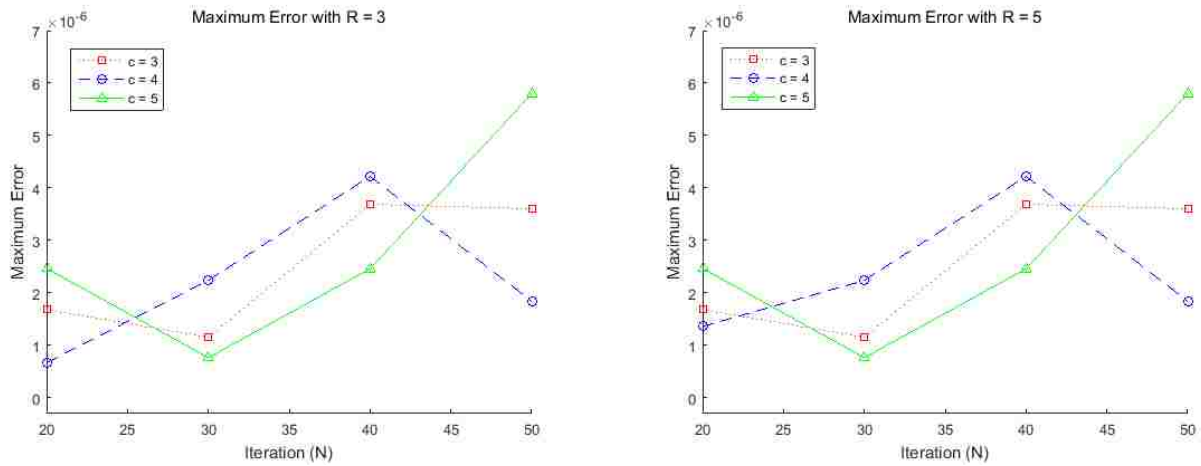


Table 4.12: Maximum Error  $\|u_{exact} - u_A\|_{C(\bar{\Omega})}$  with (c) the inverse multiquadratics RBFs  $\phi(r^2) = \frac{c-1}{\pi(r^2+1)^c}$ , for  $c = 3, 4, 5$ .

	N = 20	N = 30	N = 40	N = 50
R = 3, c = 3	1.6800e-06	1.1556e-06	3.6894e-06	3.6035e-06
R = 3, c = 4	6.7088e-07	2.2396e-06	4.2230e-06	1.8409e-06
R = 3, c = 5	2.4687e-06	7.6650e-07	2.4588e-06	5.7989e-06
R = 5, c = 3	1.6800e-06	1.1556e-06	3.6894e-06	3.6035e-06
R = 5, c = 4	1.3610e-06	2.2396e-06	4.2230e-06	1.8409e-06
R = 5, c = 5	2.4687e-06	7.6650e-07	2.4588e-06	5.7989e-06

Figure 4.20: Maximum errors with  $c = 3$  ( $\square$ ),  $c = 4$  ( $\circ$ ),  $c = 5$  ( $\triangle$ ), respectively



**Example 4.9.** Consider the boundary problem for the biharmonic equation

$$\Delta^2 u(x, y, z) = (125 x^2 - 100) e^{2y} \cos(3z), \quad (x, y, z) \in \Omega,$$

$$u(x, y, z) = 5 x^2 e^{2y} \cos(3z),$$

and

$$\Delta u(x, y, z) = (10 - 25 x^2) e^{2y} \cos(3z), \quad (x, y, z) \in \partial\Omega,$$

where  $\Omega = \{(x, y, z) : -1 \leq x, y, z \leq 1\}$  is the cube. The exact solution of the above problem is  $u_{exact} = 5 x^2 e^{2y} \cos(3z)$ . Choose three different radial basis functions in Example 2.4:

$$(a) \phi(r^2) = \frac{c}{\pi} e^{-cr^2}, \text{ where } r = \|\mathbf{x}\| \text{ and } c = 1, 3, 5, \text{ respectively,}$$

$$(b) \phi(r^2) = \begin{cases} ((2c+3)!!)(1-r^2)^c/(4\pi(2c)!!), & 0 \leq r \leq 1, \\ 0, & r > 1, \end{cases} \text{ for } c = 3, 4, 5, \text{ respectively,}$$

$$(c) \phi(r^2) = \frac{1}{2\pi^2} \frac{(2c-2)!!}{(2c-5)!!} \frac{1}{(r^2+1)^c}, \text{ for } c = 3, 4, 5, \text{ respectively,}$$

where  $n!! = 1 \cdot 3 \cdots n$ , if  $n$  is an odd number or  $2 \cdot 4 \cdots n$ , if  $n$  is an even number, and

we use a bumpy spherical fictitious domain  $\tilde{\Omega} = \{(x, y, z) : \rho \sin(\theta) \cos(\phi), \rho \sin(\theta) \sin(\phi), \rho \cos(\theta), 0 \leq \theta \leq \pi, 0 \leq \phi \leq 2\pi\}$ , where  $\rho(\phi, \theta) = R + \frac{1}{6} \sin(6\phi) \sin(7\theta)$ ,  $R = 3, 5$ .

We choose  $\tilde{\mathbf{x}}_{k,m} = (\rho \sin(\theta_k) \cos(\phi_{k,m}), \rho \sin(\theta_k) \sin(\phi_{k,m}), \rho \cos(\theta_k))$ , where  $\rho = R + \frac{1}{6} \sin(6\theta_k) \sin(7\phi_{k,m})$ ,  $R = 3, 5$ , and  $\theta_k = \frac{\pi(k+0.5)}{M_\theta}$ ,  $0 \leq k \leq M_\theta - 1$ , with  $M_\theta =$

$\frac{\sqrt{\pi N}}{2r}$ , and  $\phi_{k,m} = \frac{2\pi m}{M_k}$ ,  $0 \leq m \leq M_k - 1$ , with  $M_k = \sqrt{\pi N \sin \theta_k}$ , on  $\partial\tilde{\Omega}$ . To estimate

the maximum error, we use points  $\mathbf{z}_{k,l,m} = (\frac{k}{M}, \frac{l}{M}, \frac{m}{M})$ ,  $-M \leq k, l, m \leq M$ , with  $M =$

40 in  $\bar{\Omega} = \Omega \cup \partial\Omega$ , to get the numerical infinity norm in example 4.7. Then our numerical

approximation errors are presented in the following table with various  $R, c, M$ , and  $N$ :

Figure 4.21: Choose collocation points on  $\bar{\Omega} = \Omega \cup \partial\Omega$  and  $N = 100$  source points on the bumpy spherical fictitious domain  $\partial\tilde{\Omega}$  with  $R = 3, 5$

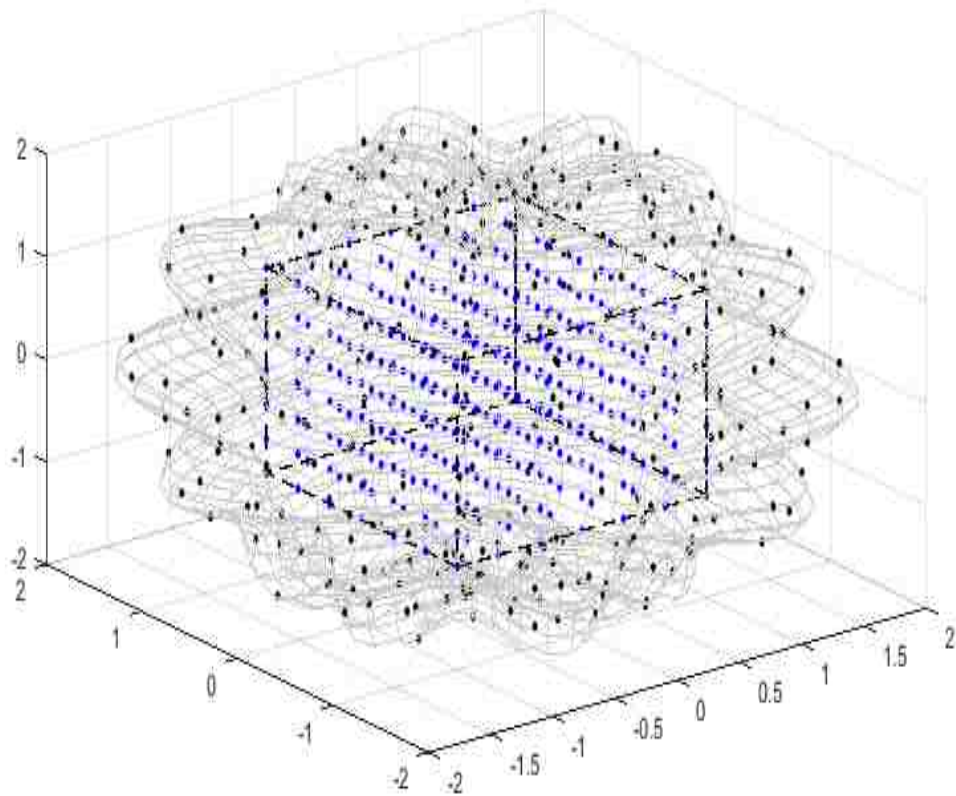


Table 4.13: Maximum Error  $\|u_{exact} - u_A\|_{C(\bar{\Omega})}$  with (a) the Gaussian RBFs  $\phi(r^2) = \frac{c}{\pi} e^{-cr^2}$  for  $c=1, 3, 5$ .

	M = 10 N = 100	M = 12 N = 100	M = 14 N = 100	M = 16 N = 100
R = 3, c = 1	4.3048e-08	5.4483e-08	6.5633e-08	7.8721e-08
R = 3, c = 3	4.3048e-08	5.4483e-08	6.5633e-08	7.8721e-08
R = 3, c = 5	4.3048e-08	5.4483e-08	6.5633e-08	7.8721e-08
R = 5, c = 1	8.0743e-11	3.6721e-09	7.5417e-09	1.2528e-08
R = 5, c = 3	8.0743e-11	3.6721e-09	7.5417e-09	1.2528e-08
R = 5, c = 5	8.0743e-11	3.6721e-09	7.5417e-09	1.2528e-08

Figure 4.22: Maximum errors on a bumpy spherical fictitious domain  $\tilde{\Omega} = \{(x, y, z) : \rho \sin(\theta) \cos(\phi), \rho \sin(\theta) \sin(\phi), \rho \cos(\phi), 0 \leq \theta \leq 2\pi, 0 \leq \phi \leq \pi\}$ , where  $\rho(\theta, \phi) = R + \frac{1}{6} \sin(6\theta) \sin(7\phi)$  with  $R = 3, 5$  and  $c = 1, (\square), c = 3, (\circ), c = 5, (\triangle)$ , respectively

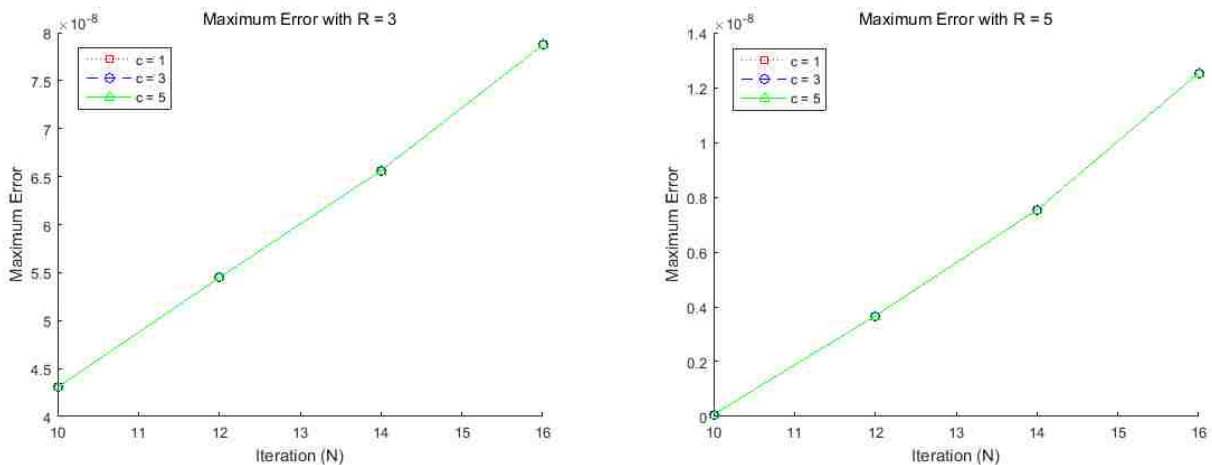


Table 4.14: Maximum Error  $\|u_{exact} - u_A\|_{C(\bar{\Omega})}$  with (b) the compactly supported RBFs  $\phi(r^2) = ((2c + 3)!!)(1 - r^2)^c / (4\pi(2c)!!)$ ,  $0 \leq r \leq 1$ , or  $0$ ,  $r > 1$  for  $c = 3, 4, 5$ .

	M = 10 N = 100	M = 12 N = 100	M = 14 N = 100	M = 16 N = 100
R = 3, c = 3	4.3585e-16	5.7381e-15	2.3102e-16	1.5529e-15
R = 3, c = 4	1.0274e-15	8.4308e-16	1.2149e-15	2.6908e-15
R = 3, c = 5	2.2253e-16	5.0871e-16	1.0637e-15	9.5410e-17
R = 5, c = 3	4.3585e-16	5.7381e-15	2.3102e-16	1.5529e-15
R = 5, c = 4	1.0274e-15	8.4308e-16	1.2149e-15	2.6908e-15
R = 5, c = 5	2.2253e-16	5.0871e-16	1.0637e-15	9.5410e-17

Figure 4.23: Maximum errors on a bumpy spherical fictitious domain  $\tilde{\Omega} = \{(x, y, z) : \rho \sin(\theta) \cos(\phi), \rho \sin(\theta) \sin(\phi), \rho \cos(\phi), 0 \leq \theta \leq 2\pi, 0 \leq \phi \leq \pi\}$ , where  $\rho(\theta, \phi) = R + \frac{1}{6} \sin(6\theta) \sin(7\phi)$  with  $R = 3, 5$  and  $c = 3$ , ( $\square$ ),  $c = 4$ , ( $\circ$ ),  $c = 5$ , ( $\triangle$ ), respectively

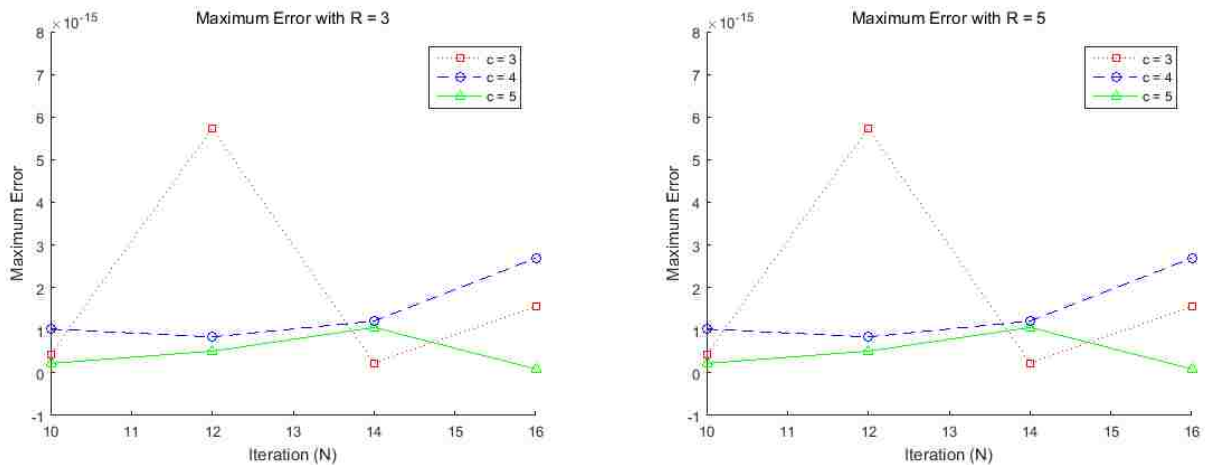
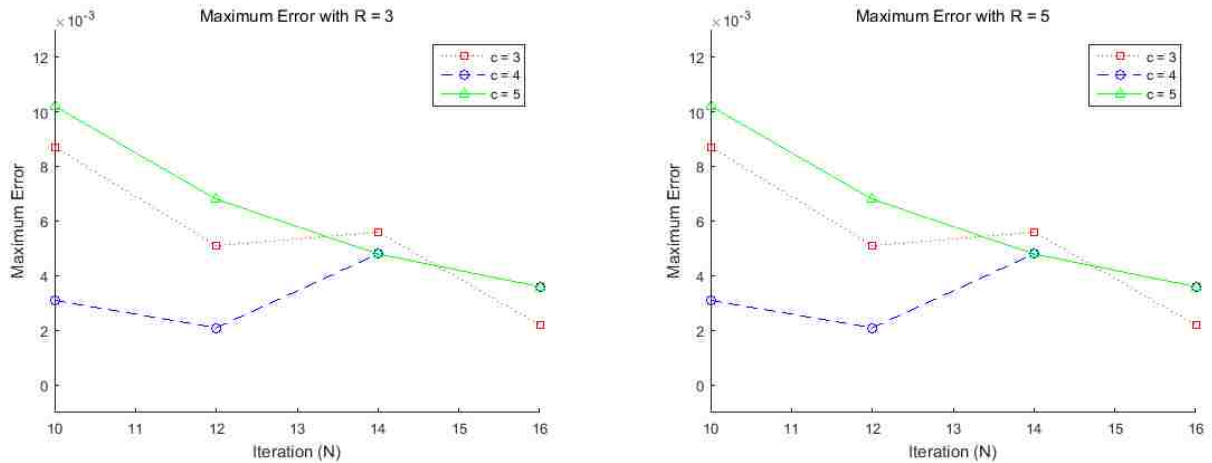


Table 4.15: Maximum Error  $\|u_{exact} - u_A\|_{C(\bar{\Omega})}$  with (c) the inverse multiquadratics RBFs  $\phi(r^2) = \frac{1}{2\pi^2} \frac{(2c-2)!!}{(2c-5)!!} \frac{1}{(r^2+1)^c}$ , for  $c = 3, 4, 5$ .

	M = 10 N = 100	M = 12 N = 100	M = 14 N = 100	M = 16 N = 100
R = 3, c = 3	0.0087	0.0051	0.0056	0.0022
R = 3, c = 4	0.0031	0.0021	0.0048	0.0036
R = 3, c = 5	0.0102	0.0068	0.0048	0.0036
R = 5, c = 3	0.0087	0.0051	0.0056	0.0022
R = 5, c = 4	0.0031	0.0021	0.0048	0.0036
R = 5, c = 5	0.0102	0.0068	0.0048	0.0036

Figure 4.24: Maximum errors on a bumpy spherical fictitious domain  $\tilde{\Omega} = \{(x, y, z) : \rho \sin(\theta) \cos(\phi), \rho \sin(\theta) \sin(\phi), \rho \cos(\theta), 0 \leq \theta \leq 2\pi, 0 \leq \phi \leq \pi\}$ , where  $\rho(\theta, \phi) = R + \frac{1}{6} \sin(6\theta) \sin(7\phi)$  with  $R = 3, 5$  and  $c = 3, (\square), c = 4, (\circ), c = 5, (\triangle)$ , respectively



## BIBLIOGRAPHY

- [1] B. Bialecki and A. Karageorghis, Spectral Chebyshev Collocation for the Poisson and Biharmonic Equations, *SIAM J. Sci. Comput.*, **32**, No. 5, 2995-3019 (2010).
- [2] B. Bin-Mohsin, The method of fundamental solutions for Helmholtz-type problems, *The University of Leeds*, 10-13 (2013)
- [3] A. Bogomolny, *SIAM J. Numer. Anal.*, **22**, 644 (1985).
- [4] C.S. Chen and A. Karageorghis and Yan Li, On choosing the location of the sources in the MFS, *Numer. Algor.*, **72**, 107-130 (2016).
- [5] M. Deserno, How to generate equidistributed points on the surface of a sphere, *Carnegie Mellon University*, (2004)
- [6] G. Fairweather and A. Karageorghis and Y. Smyrlis, A matrix decomposition MFS algorithm for axisymmetric biharmonic problems, *Adv. Comput. Math.*, **23**, 55-71 (2005).
- [7] G. Fairweather and A. Karageorghis, The method of fundamental solutions for elliptic boundary value problems, *Adv. Comput. Math.*, **9**, 69-95 (1998).
- [8] M. Fuhry and L. Reichel, A new Tikhonov regularization Method, *Numer. Algor.*, **59**, 433-445 (2012).
- [9] M.A. Golberg and C.S. Chen, The method of fundamental solutions for potential Helmholtz and diffusion problems, *Comput. Mech. Publ.*, Southampton, 103-176 (1999).
- [10] M.A. Golberg, The method of fundamental solutions for Poisson's equation, *Engrg. Anal. Boundary Elem.*, **16**, 205-213 (1995).
- [11] I.S. Gradshteyn and I.M. Ryzhik, *Tables of Integrals Series and Products*, Academic Press, New York, (1965).
- [12] A. Karageorghis, The method of fundamental solutions for elliptic problems in circular domains with mixed boundary conditions, *Numer. Algor.*, **68**, 185-211 (2015).



- [13] A. Karageorghis, The method of fundamental solutions for the Numerical Solution of the Biharmonic Equation, *Comput. Physics*, **69**, 434-459 (1987).
- [14] T. Kitagawa, On the numerical stability of the method of fundamental solution applied to the Dirichlet problem, *Japan J. Appl. Math.*, **5**, 123-133 (1988).
- [15] Ming Li and C.S. Chen and A. Karageorghis, The MFS for the solution of harmonic boundary value problems with non-harmonic boundary conditions, *Comput. and Math. with Appl.*, **66**, 2400-2424 (2013).
- [16] X. Li, Radial basis approximation for Newtonian Potentials, *Adv. Comput. Math.*, **33**, 1-24 (2010).
- [17] X. Li, Radial basis approximation and its application to biharmonic equation, *Adv. Comput. Math.*, **32**, 275-302 (2010).
- [18] X. Li, Approximation of potential integral by radial bases for solutions of Helmholtz equation, *Adv. Comput. Math.*, **30**, 201-230 (2009).
- [19] X. Li, Rate of convergence of the method of fundamental solutions and hyperinterpolation for modified Helmholtz equations on the unit ball, *Adv. Comput. Math.*, **29**, 393-413 (2008).
- [20] X. Li, On the method of fundamental solutions in  $\mathcal{R}^2$ , *Comput. Sci.*, **4 (2)**, 567-586 (2007).
- [21] X. Li, Rate of approximation by the method of fundamental solutions for solving the Laplace equation on the unit sphere, *Journal of Information and Comput. Sci.*, **3 (2)**, 245-254 (2006).
- [22] X. Li, On solving boundary value problems of modified Helmholtz equations by plane wave functions, *Journal of Comput. and Appl. Math.*, **195**, 66-82 (2006).
- [23] X. Li, On convergence of the method of fundamental solutions for solving the Dirichlet problem of Poisson's equation, *Adv. Comput. Math.*, **23**, 265-277 (2005).
- [24] X. Li, Convergence of the method of fundamental solutions for solving the boundary value problem of the modified Helmholtz equation, *Appl. Math. and Comput.*, **159**, 113-125 (2004).

- [25] X. Li and M.A. Golberg, On the convergence of the dual reciprocity method for Poisson's equation, in: Transformation of Domain Effects to the Boundary, ed. Y.F. Rashed *WIT Press*, Southampton/Boston, 227-251 (2003).
- [26] Z.C. Li and M.G. Lee and J.Y. Chiang and Y.P. Liu, The Trefftz method using fundamental solutions for biharmonic equation, *Journal of Comput. and Appl. Math.*, **235**, 4350-4367 (2011).
- [27] L. Marin and D. Lesnic, The method of fundamental solutions for the Cauchy problem associated with two-dimensional Helmholtz-type equations, *Comput. Struct.*, **83**, 267-278 (2005).
- [28] L. Marin and D. Lesnic, The method of fundamental solutions for inverse boundary value problems associated with two-dimensional biharmonic equation, *Math. and Comput. Modelling*, **42**, 261-278 (2005).
- [29] C. Miranda, *Partial Differential Equations of Elliptic Type*, Springer, New York, (1970).
- [30] S. Murashima, Y. Nonaka, and H. Nieda, In Boundary Elements, *Proceedings of the Fifth International Conference*, Hiroshima, Japan, 1983, edited by C. A. Brebbia, T. Futagami, and M. Tanaka, Springer-Verlag, New York, 75 (1983).

# CURRICULUM VITAE

Graduate College  
University of Nevada, Las Vegas

Minhwa Choi  
choiminhwa131@gmail.com

## Degrees:

Bachelor of Engineering - Mechanical Engineering, 1997  
Myongji University, Republic of Korea

Master of Arts - Mathematics, 2003  
University of Missouri - St. Louis, U.S.A.

## Dissertation Title:

Meshless Methods for Numerically Solving Boundary Value Problems of  
Elliptic Type Partial Differential Equations

## Dissertation Examination Committee:

Chairperson, Xin Li, Ph.D.  
Committee Member, Rohan Dalpatadu, Ph.D.  
Committee Member, Douglas Burke, Ph.D.  
Graduate Faculty Representative, Woosoon Yim, Ph.D.